BACTERIOPHAGES ISOLATION FROM THE ENVIRONMENT AND THEIR ANTIMICROBIAL THERAPEUTIC POTENTIAL, VOLUME 2

EDITED BY: Robert Czajkowski and Krishna Mohan Poluri

PUBLISHED IN: Frontiers in Microbiology

frontiers Research Topics

ISSN 1664-8714
ISBN 978-2-88974-533-3
DOI 10.3389/978-2-88974-533-3

About Frontiers

Frontiers is more than just an open-access publisher of scholarly articles: it is a pioneering approach to the world of academia, radically improving the way scholarly research is managed. The grand vision of Frontiers is a world where all people have an equal opportunity to seek, share and generate knowledge. Frontiers provides immediate and permanent online open access to all its publications, but this alone is not enough to realize our grand goals.

Frontiers Journal Series

The Frontiers Journal Series is a multi-tier and interdisciplinary set of open-access, online journals, promising a paradigm shift from the current review, selection and dissemination processes in academic publishing. All Frontiers journals are driven by researchers for researchers; therefore, they constitute a service to the scholarly community. At the same time, the Frontiers Journal Series operates on a revolutionary invention, the tiered publishing system, initially addressing specific communities of scholars, and gradually climbing up to broader public understanding, thus serving the interests of the lay society, too.

Dedication to Quality

Each Frontiers article is a landmark of the highest quality, thanks to genuinely collaborative interactions between authors and review editors, who include some of the world's best academicians. Research must be certified by peers before entering a stream of knowledge that may eventually reach the public - and shape society; therefore, Frontiers only applies the most rigorous and unbiased reviews.
Frontiers revolutionizes research publishing by freely delivering the most outstanding research, evaluated with no bias from both the academic and social point of view. By applying the most advanced information technologies, Frontiers is catapulting scholarly publishing into a new generation.

What are Frontiers Research Topics?

Frontiers Research Topics are very popular trademarks of the Frontiers Journals Series: they are collections of at least ten articles, all centered on a particular subject. With their unique mix of varied contributions from Original Research to Review Articles, Frontiers Research Topics unify the most influential researchers, the latest key findings and historical advances in a hot research area! Find out more on how to host your own Frontiers Research Topic or contribute to one as an author by contacting the Frontiers Editorial Office: frontiersin.org/about/contact

BACTERIOPHAGES ISOLATION FROM THE ENVIRONMENT AND THEIR ANTIMICROBIAL THERAPEUTIC POTENTIAL, VOLUME 2

Topic Editors:
Robert Czajkowski, University of Gdansk, Poland
Krishna Mohan Poluri, Indian Institute of Technology Roorkee, India

Citation: Czajkowski, R., Poluri, K. M., eds. (2022). Bacteriophages Isolation From the Environment and Their Antimicrobial Therapeutic Potential, Volume 2. Lausanne: Frontiers Media SA. doi: 10.3389/978-2-88974-533-3

Table of Contents

frontiers in Microbiology

EDITORIAL
published: 26 January 2022
doi: 10.3389/fmicb.2022.847176

Editorial: Bacteriophages Isolation From the Environment and Their Antimicrobial Therapeutic Potential, Volume 2

Krishna Mohan Poluri[1]* *and Robert Czajkowski*[2]*

[1] Department of Biosciences and Bioengineering and Centre for Nanotechnology, Indian Institute of Technology Roorkee, Roorkee, India, [2] Laboratory of Biologically Active Compounds, Intercollegiate Faculty of Biotechnology, University of Gdansk and Medical University of Gdansk, University of Gdansk, Gdansk, Poland

Keywords: bacteriophage, phage therapy, multidrug-resistant bacteria, environmental phages, phage isolation, aquaculture

Editorial on the Research Topic

Bacteriophages Isolation From the Environment and Their Antimicrobial Therapeutic Potential, Volume 2

OPEN ACCESS

Edited and reviewed by:
Rustam Aminov,
University of Aberdeen,
United Kingdom

***Correspondence:**
Krishna Mohan Poluri
mohanpmk@gmail.com;
krishna.poluri@bt.iitr.ac.in
Robert Czajkowski
robert.czajkowski@ug.edu.pl

Specialty section:
This article was submitted to Antimicrobials, Resistance and Chemotherapy, a section of the journal Frontiers in Microbiology

Received: *01 January 2022*
Accepted: *04 January 2022*
Published: *26 January 2022*

Citation:
Poluri KM and Czajkowski R (2022) Editorial: Bacteriophages Isolation From the Environment and Their Antimicrobial Therapeutic Potential, Volume 2. Front. Microbiol. 13:847176. doi: 10.3389/fmicb.2022.847176

The emergence and spread of antibiotic-resistant bacteria was one of the leading global concerns of the last century (Zaman et al., 2017; Chokshi et al., 2019). Today, at the beginning of the twenty-first century, bacteria still hold accountability for preponderant infectious pathogenesis. In the war against them, nature has equipped us with bacterial viruses (named bacteriophages or phages) that dwell on bacteria and can readily kill them (Chibani-Chennoufi et al., 2004). With the advancements in science and medicine, humankind is thriving toward using, manipulating, and repurposing the bacteriophages as effective antibacterials (Burrowes et al., 2011; Chan et al., 2013).

However, the idea to use bacteriophages to combat bacterial infections is not entirely new (Wittebole et al., 2014). The first successful trials involving bacterial viruses against human and animal bacterial pathogens were done just after their initial discovery at the beginning of the twentieth century (Campbell, 2010). Unfortunately, these trials and treatments were virtually stopped when penicillin was successfully commercialized as the first antimicrobial (Gaynes, 2017).

The twenty-first century seems to be the opening of the second golden age of bacteriophages with the increasing number of new scientific publications on the topic as well as the expanding societal understanding and approval for the use of (alive) bacterial viruses to fight bacterial infections in medicine, veterinary, food microbiology and agriculture applications. This global rediscovery of bacteriophages is also reflected in this Research Topic.

One of the keystones to taking advantage of bacteriophages is identifying and thoroughly investigating them. The current thematic issue encloses several reports of isolation and characterization of lytic bacterial viruses to be used in medicine and veterinary. Khan et al. isolated an *Escherichia coli* C (phi x174 host) lytic phage named MSK and have exhaustively studied the genome of this novel phage. Authors have precisely distinguished 73 open reading frames (ORFs) having diverse functionalities, in which 46 of them showed marked similarity with the ORFs previously reported in Rtp group of bacteriophages. Belonging to the family of *Drexlerviridae*, MSK has exhibited potent lytic action against multidrug-resistant (MDR) *E. coli* and other pathogenic *E. coli*, *Pseudomonas syringae*, and *Salmonella anatum* strains. On similar lines, Xu et al. isolated another lytic bacteriophage from *Shigella flexneri*, named vB_ShiP-A7. This new member of *Podoviridae* rendered cogent antimicrobial effect against MDR strains of *Shigella flexneri* and *E. coli,*

as evidenced from the *in vivo* murine based studies. A new virulent bacteriophage of the *Myoviridae* family vB_EcoM_swi3 (swi3) from swine feces has been isolated and characterized by Sui et al. This bacteriophage is effective against infections caused by *Salmonella enteritidis* and pathogenic *E. coli,* as evidenced from both *in vitro* and *in vivo* studies. Gorodnichev et al. isolated and characterized three virulent phages: Dep622, vB_KpnM_Seu621, and KpS8, possessing narrow specificity toward MDR *Klebsiella pneumoniae* with K23 capsule type. From the analyzed phages, Dep622 specifically demonstrated polysaccharide depolymerase activity and successfully protected *Galleria mellonella* larvae infected with MDR *K. pneumoniae* strain.

Overuse and misuse of antibiotics may frequently lead to drug resistance in bacterial strains, and the common antibiotics are at the edge of failing. In such a scenario, bacteriophages may provide an attractive non-antibiotic approach to control pathogenic bacteria. Kortright et al. delineated the possibility of acquired cross-resistance in *E. coli* using two potential antibacterial agents- phage T6, phage U115 and an antibiotic albicidin. The study established that independent, selective resistance to any of these three antibacterial agents provided resistance to the other two. Whole-genome and targeted sequencing analysis of 29 samples showed that they all possess Tsx porin as a common point of interaction. In expounding the antimicrobial activity of bacteriophages, Yang et al. affirmed the efficiency of the KPP10 phage in treating *Pseudomonas aeruginosa* strain D4-induced pneumonia mouse models when administered intranasally. The model showed a significantly lower level of immunological indicators [TNFα, IL-1β, and IFN-γ] of infection without any lysis induced endotoxic shock.

Apart from humans, livestock and aquaculture are highly susceptible to bacterial infections and may act as symptomatic or asymptomatic carriers compromising human health. Most of these bacteria have become MDR due to extensive misuse of antibiotics in the feedstocks (Martin et al., 2015). It is believed that, at least to some extent and in some applications, antibiotics may be replaced by environmental-friendly alternatives: bacteriophages. Pelyuntha et al. has reported isolation and application of phage cocktail showing potential antimicrobial activity against *Salmonella* spp., sampled from broiler farms in Thailand. The cocktail derived from the three phages displaying the highest lytic ability was documented to markedly reduce the growth of *Salmonella* sp. collected from different sources over the country without any specific drug resistance pattern. Xie et al. sampled *Salmonella* sp. from beef hide and soil to analyze the antibacterial efficiency of four previously reported genetically diverse groups of bacteriophages against the tested bacterial strains. The individual phages showed comparable activity to the cocktail titer in liquid culture without significant phage-resistance activity. Tetens et al. reported the isolation and morphological characterization of 11 *Siphoviridae*-like phages along with three strains of their host, *Staphylococcus hyicus,* causing exudative epidermitis (EE) infection in piglet farms over Germany. Genome sequencing of the isolates identified a novel virulent phage, PITT-1 (PMBT8) and a novel temperate phage, PITT-5 (PMBT9). Further gene sequencing studies of the sampled host-bacterial strains revealed two toxin-encoding genes *exhA* and *exhC*, among which *exhC*-positive *S. hyicus* strains were found to be very mildly lysed by the majority of the lytic phages. Li et al. have isolated a novel bacteriophage BUCT549 infecting *Vibrio alginolyticus* from a seafood market sewage in China. *V. alginolyticus* is reported to cause food poisoning and septicemia in humans. Phylogenetic and transmission electron microscopic studies of BUCT549 reveal its kin association to the viral family *Siphoviridae*. Donati et al. investigated the efficacy of FpV4 and FPSV-D22, a dual-component phage mixture in controlling *Flavobacterium psychrophilum* infection triggered mortality of rainbow trout fry fish using oral, bath and injection-based administration approaches. This study documented the efficacy of the phage administration pathway in treating rainbow trout fry syndrome and endorsed the oral administration of the viral cocktail.

We believe that replacing antibiotics with bacteriophages in the various applications to prevent and treat bacterial infections in humans and animals will continue in the twenty-first century. In addition, with the use of genetically modified viruses, it will be possible to develop solutions to use them in personalized medicine.

Finally, we are sincerely thankful to all the authors for contributing to this Research Topic. We also would like to acknowledge the toiling and admirable work of the reviewers and their critical assessments of the reviewed manuscripts.

AUTHOR CONTRIBUTIONS

Both authors listed have made a substantial, direct, and intellectual contribution to the work and approved it for publication.

ACKNOWLEDGMENTS

KP acknowledge the support of grants GKC-01/2016-17/212/NMCG-Research from NMCG-MoWR, and CRG/2018/001329 from SERB-DST, Government of India. RC acknowledges the grant support of NCN OPUS 13 (2017/25/B/NZ9/00036) from the National Science Center, Poland (Narodowe Centrum Nauki, Polska). The authors thank G. Goutami Naidu, IIT-Roorkee, for the technical support during the manuscript preparation.

REFERENCES

Burrowes, B., Harper, D. R., Anderson, J., Mcconville, M., and Enright, M. C. (2011). Bacteriophage therapy: potential uses in the control of antibiotic-resistant pathogens. *Expert Rev. Anti. Infect. Ther.* 9, 775–785. doi: 10.1586/eri.11.90

Campbell, A. M. (2010). The legacy of 20th century phage research. *EcoSal. Plus* 4:2. doi: 10.1128/ecosal.1.2

Chan, B. K., Abedon, S. T., and Loc-Carrillo, C. (2013). Phage cocktails and the future of phage therapy. *Fut. Microbiol.* 8, 769–783. doi: 10.2217/fmb.13.47

Chibani-Chennoufi, S., Bruttin, A., Dillmann, M. L., and Brussow, H. (2004). Phage-host interaction: an ecological perspective. *J. Bacteriol.* 186, 3677–3686. doi: 10.1128/JB.186.12.3677-3686.2004

Chokshi, A., Sifri, Z., Cennimo, D., and Horng, H. (2019). Global Contributors to antibiotic resistance. *J. Glob. Infect. Dis.* 11, 36–42. doi: 10.4103/jgid.jgid_110_18

Gaynes, R. (2017). The discovery of penicillin-new insights after more than 75 years of clinical use. *Emerg. Infect. Dis.* 23, 849–853. doi: 10.3201/eid2305.161556

Martin, M. J., Thottathil, S. E., and Newman, T. B. (2015). Antibiotics overuse in animal agriculture: a call to action for health care providers. *Am. J. Public Health* 105, 2409–2410. doi: 10.2105/AJPH.2015.302870

Wittebole, X., De Roock, S., and Opal, S. M. (2014). A historical overview of bacteriophage therapy as an alternative to antibiotics for the treatment of bacterial pathogens. *Virulence* 5, 226–235. doi: 10.4161/viru.25991

Zaman, S. B., Hussain, M. A., Nye, R., Mehta, V., Mamun, K. T., and Hossain, N. (2017). A review on antibiotic resistance: alarm bells are ringing. *Cureus* 9:e1403. doi: 10.7759/cureus.1403

Conflict of Interest: The authors declare that the research was conducted in the absence of any commercial or financial relationships that could be construed as a potential conflict of interest.

Publisher's Note: All claims expressed in this article are solely those of the authors and do not necessarily represent those of their affiliated organizations, or those of the publisher, the editors and the reviewers. Any product that may be evaluated in this article, or claim that may be made by its manufacturer, is not guaranteed or endorsed by the publisher.

frontiers in Microbiology

ORIGINAL RESEARCH
published: 08 March 2021
doi: 10.3389/fmicb.2021.628309

Phage-Mediated Control of *Flavobacterium psychrophilum* in Aquaculture: *In vivo* Experiments to Compare Delivery Methods

Valentina Laura Donati[1], Inger Dalsgaard[1], Krister Sundell[2], Daniel Castillo[3], Mériem Er-Rafik[4], Jason Clark[5], Tom Wiklund[2], Mathias Middelboe[3] and Lone Madsen[1]*

[1] Unit for Fish and Shellfish Diseases, National Institute of Aquatic Resources, Technical University of Denmark, Kgs. Lyngby, Denmark, [2] Laboratory of Aquatic Pathobiology, Environmental and Marine Biology, Åbo Akademi University, Turku, Finland, [3] Marine Biological Section, Department of Biology, University of Copenhagen, Helsingør, Denmark, [4] National Centre for Nano Fabrication and Characterization, Technical University of Denmark, Kgs. Lyngby, Denmark, [5] Fixed Phage Ltd., Glasgow, United Kingdom

OPEN ACCESS

Edited by:
Robert Czajkowski, University of Gdańsk, Poland

Reviewed by:
Danish Javed Malik, Loughborough University, United Kingdom
Pilar García, Consejo Superior de Investigaciones Científicas (CSIC), Spain

***Correspondence:**
Valentina Laura Donati
valdo@aqua.dtu.dk

Specialty section:
This article was submitted to Antimicrobials, Resistance and Chemotherapy, a section of the journal Frontiers in Microbiology

Received: *11 November 2020*
Accepted: *15 February 2021*
Published: *08 March 2021*

Citation:
Donati VL, Dalsgaard I, Sundell K, Castillo D, Er-Rafik M, Clark J, Wiklund T, Middelboe M and Madsen L (2021) Phage-Mediated Control of Flavobacterium psychrophilum in Aquaculture: In vivo Experiments to Compare Delivery Methods. Front. Microbiol. 12:628309. doi: 10.3389/fmicb.2021.628309

Phage-based approaches have gained increasing interest as sustainable alternative strategies to antibiotic treatment or as prophylactic measures against disease outbreaks in aquaculture. The potential of three methods (oral, bath, and injection) for delivering a two-component phage mixture to rainbow trout fry for controlling *Flavobacterium psychrophilum* infections and reduce fish mortality was investigated using bacteriophages FpV4 and FPSV-D22. For the oral administration experiment, bacteriophages were applied on feed pellets by spraying (1.6×10^8 PFU g^{-1}) or by irreversible immobilization (8.3×10^7 PFU g^{-1}), using the corona discharge technology (Fixed Phage Ltd.). The fish showed normal growth for every group and no mortality was observed prior to infection as well as in control groups during the infection. Constant detection of phages in the intestine ($\sim 10^3$ PFU mg^{-1}) and more sporadic occurrence in kidney, spleen, and brain was observed. When fish were exposed to *F. psychrophilum,* no significant effect on fish survival, nor a direct impact on the number of phages in the sampled organs, were detected. Similarly, no significant increase in fish survival was detected when phages were delivered by bath (1st and 2nd bath: $\sim 10^6$ PFU ml^{-1}; 3rd bath: $\sim 10^5$ PFU ml^{-1}). However, when phages FpV4 and FPSV-D22 (1.7×10^8 PFU $fish^{-1}$) were administered by intraperitoneal injection 3 days after the bacterial challenge, the final percent survival observed in the group injected with bacteriophages FpV4 and FPSV-D22 (80.0%) was significantly higher than in the control group (56.7%). The work demonstrates the delivery of phages to fish organs by oral administration, but also suggests that higher phage dosages than the tested ones may be needed on feed pellets to offer fish an adequate protection against *F. psychrophilum* infections.

Keywords: *Flavobacterium psychrophilum*, rainbow trout fry syndrome (RTFS), rainbow trout fry (*Oncorhynchus mykiss*), phage-therapy, bacteriophages

INTRODUCTION

Phage therapy relies on the bactericidal activity of lytic bacteriophages (also called phages), which infect and kill specific bacterial hosts by lysing infected cells and releasing phage progeny to the environment [Twort, 1915; Roux, 2011; reviewed in Salmond and Fineran (2015); Dion et al. (2020)]. In the aquaculture sector, phage therapy efforts have targeted various pathogenic bacteria, such as *Vibrio spp., Aeromonas spp.*, *Flavobacterium spp.*, *Pseudomonas spp.*, and *Edwardsiella spp.* focusing, e.g., on the isolation and characterization of virulent phages (Kalatzis et al., 2016; Kazimierczak et al., 2019), cocktail formulations (Mateus et al., 2014; Duarte et al., 2018), dose and route of phage administration (Laanto et al., 2015; Almeida et al., 2019). However, despite the many benefits of phage therapy, various challenges have been faced such as the development of phage resistant bacteria, the inefficient delivery of phages in high dosages at the infection site, and the phage clearance activity from the organism mediated by the immune cells [reviewed in Culot et al. (2019); Kowalska et al. (2020)].

Flavobacterium psychrophilum (Borg, 1948; Bernardet et al., 1996) is the etiological agent of Rainbow Trout Fry Syndrome (RTFS, fry stage) (Lorenzen et al., 1991) and of Bacterial Coldwater Disease (BCWD, juvenile and adult fish) (Borg, 1960). Rainbow trout (*Oncorhynchus mykiss,* Walbaum) and coho salmon (*Oncorhynchus kisutch*) are the most susceptible salmonid species to this bacterium (Nematollahi et al., 2003). Despite a strong focus on preventive measures, for example good management practises and egg disinfection (Nematollahi et al., 2003; Madsen and Dalsgaard, 2008), antibiotics have been the most extensively used treatment for RTFS worldwide and resistance to their activity has been detected (Bruun et al., 2000, 2003; Schmidt et al., 2000; Izumi and Aranishi, 2004; Kum et al., 2008; Del Cerro et al., 2010; Sundell and Wiklund, 2011). With the isolation of bacteriophages infecting *F. psychrophilum* (Stenholm et al., 2008), the possibility of developing a sustainable alternative approach to the treatment of RTFS has gained more attention. Castillo et al. (2012) studied the application of phages in rainbow trout and Atlantic salmon delivering bacteriophages (10^9 PFU $fish^{-1}$) by intraperitoneal (IP) injection simultaneously to *F. psychrophilum* (10^8 CFU $fish^{-1}$). The authors were able to detect a reduction in mortality of fish treated with phages (Castillo et al., 2012). Subsequent studies on the dispersal and survival of *F. psychrophilum* phages in rainbow trout showed that infective *F. psychrophilum* phages were recovered from the internal organs of rainbow trout fry after administration by intraperitoneal injection (with and without the bacteria) (Madsen et al., 2013), by bath or via oral administration (oral intubation or by phage-coated feed) (Christiansen et al., 2014). However, in order to assess the potential of phage-based control of *F. psychrophilum* infections in rainbow trout, combined studies on phage delivery efficiency and fish mortality in challenge experiments are required.

Building on previous work (Madsen et al., 2013; Christiansen et al., 2014), this study brings new insights to the development of a bacteriophage-based treatment for *F. psychrophilum* infections in rainbow trout fry applicable in the field. The work includes oral administration of bacteriophages applied on feed pellets by spraying, or by irreversible immobilization, using corona discharge technology (Fixed Phage Ltd.) (Mattey, 2016, 2018). The immobilization stabilizes phages at room temperature, simplifying delivery and use of phage products (Mattey, 2016, 2018). The use of phage-treated feed could potentially be applied prophylactically in aquaculture facilities to prevent and control bacterial infections and mortalities caused by *F. psychrophilum*. Two additional delivery methods (by bath and by intraperitoneal injection) of the selected purified two-component mix of Danish bacteriophages with a wide host-range among virulent *F. psychrophilum* strains were also included in the study. The aim of the work was to (a) evaluate the effects of the oral administration of phages on healthy and infected fish comparing the two phage application methods on fish pellets (e.g., phage diffusion in internal organs) (Experiment A); (b) assess the effects on fish survival of the oral phage administration during *F. psychrophilum* infections (Experiment A) in comparison to when phages are delivered by repeated bath procedures and by intraperitoneal injection (Experiments B and C). The work demonstrates the delivery of phages to fish organs by oral administration, but also suggests that higher phage dosages than the tested ones may be needed on feed pellets to offer fish an adequate protection against *F. psychrophilum* infections for the application in the field.

MATERIALS AND METHODS

Bacterial Strain

Flavobacterium psychrophilum 950106-1/1, a well-characterized Danish strain isolated in 1995 from rainbow trout in a freshwater farm, was selected for the experiments (serotype Fd, virulent) (Madsen and Dalsgaard, 1999, 2000; Dalsgaard and Madsen, 2000; Sundell et al., 2019). *Flavobacterium psychrophilum* FPS-S6, a Swedish strain isolated in 2017 from rainbow trout (serotype Th, virulent), was utilized for the propagation of phage FPSV-D22 since it was the most efficient host for producing high phage titers (Sundell et al., 2019). The bacteria were stored at −80°C in tryptone yeast extract salts medium [TYES: 0.4% tryptone, 0.04% yeast extract, 0.05% $CaCl_2 \times 2H_2O$, 0.05% $MgSO_4 \times 7H_2O$ (pH 7.2)] (Holt et al., 1993) and glycerol (15–20%). For bacteriophage detection and quantification, *F. psychrophilum* 950106-1/1 was inoculated from a −80°C stock into 5 ml TYES broth (referred as TYES-B), incubated at 15°C at 100 rpm for 48–72 h and then streaked on TYES agar (TYES-B with 1.1% agar, referred as TYES-A). After 3–4 days at 15°C, single colonies were picked and inoculated in TYES-B for 48 h. For challenge experiments, *F. psychrophilum* 950106-1/1 was prepared and infection challenge performed as described by Madsen and Dalsgaard (1999). Intraperitoneal (IP) injection was selected as infection method due to its reproducibility when it comes to experimental *F. psychrophilum* infections in rainbow trout (Madsen and Dalsgaard, 1999). According to the established infection dose, appropriate dilutions of the 48-h culture were performed prior to IP injection and CFU were counted before and after infection.

Bacteriophages

Bacteriophages FpV4 and FPSV-D22 were used in these experiments (**Supplementary Table 1**). FpV4 (lytic phage belonging to *Podoviridae* family, 90 kb genome) was isolated in 2005 from water with feces samples (Stenholm et al., 2008; Castillo and Middelboe, 2016) and FPSV-D22 (lytic phage belonging to *Siphoviridae* family), isolated in 2017 from fish tissue samples collected at Danish freshwater farms of rainbow trout (Sundell et al., 2019). Both phages were characterized to have a broad host range among *F. psychrophilum* strains [(Stenholm et al., 2008; Castillo et al., 2014) and unpublished data]. High titer solutions of FpV4 and FPSV-D22 were purified and stored in SM buffer [8 mM $MgSO_4$, 50 mM Tris–Cl (pH 7.5), 99 mM NaCl, 0.01% gelatin] and glycerol (15%) at −80°C (Stenholm et al., 2008; Sundell et al., 2019). The bacteriophages were observed by transmission electron microscopy (TEM) after negative staining with uranyl acetate (**Supplementary Table 1**). To make these observations, 5 μl of the phage solution were deposited onto a freshly glow discharged carbon-covered grid. The bacteriophage solution was left for 2 min and the grid was negatively stained with 5 μl uranyl acetate (2% in water) for another minute and finally dried using a filter paper. The grids were observed at 200 kV with a Tecnai G2 (FEI) microscope. Images were acquired with a camera Ultrascan US1000 (Gatan). The concentration of phages FpV4 and FPSV-D22 was 10^9 PFU ml^{-1} in SM buffer with 0.01% gelatin.

Preparation and Purification of High-Titer Phage Solutions

Based on previous challenge experiments (data not published and Christiansen, 2014), where we detected an early onset of mortality in fish exposed to crude lysates of phages, we decided to PEG purify phage solutions in order to decrease the concentration of compounds that could be toxic for the fish. Gram negative bacteria produce endotoxins which might induce allergic reactions (Kowalska et al., 2020). For the fish experiments, 1 L of bacterial cultures (OD 600 nm = 0.2) were separately infected with the phages FPSV-D22 and FpV4 at MOI = 1 (*F. psychrophilum* FPS-S6 and 950106-1/1, respectively) and incubated for ∼3 days. The lysed bacterial cultures were centrifuged (9000 × *g*, 10 min, 4°C) and filtered through a 0.2 μm-pore size sterile filter. Then, the phage stocks FPSV-D22 (5.0×10^9 PFU ml^{-1}) and FpV4 (3.0×10^9 PFU ml^{-1}) were concentrated by adding poly-ethylene glycol 8000 (PEG-8000) and Sodium Chloride (final concentration 10% w/v and 1 M, respectively), followed by incubation at 4°C for 24 h. Subsequently, phage solutions were centrifuged (10,000 × *g*, 30 min, 4°C) and the phage pellet was resuspended in 200 mL of SM buffer (Castillo et al., 2019).

Fish (Experiment A and B)

Rainbow trout eyed eggs were purchased at a Danish commercial fish farm (officially registered free of bacterial kidney disease and viral diseases as IPN, VHS and IHN). Eggs were disinfected with a iodine-based solution [100 ppm active iodine; 1% Actomar K30 (Desag AF, Uster, Switzerland)], hatched and fish grown at the Unit for Fish and Shellfish Diseases (National Institute of Aquatic Resources, Kgs. Lyngby, Denmark). Fish were initially raised in a recirculation system. When the desired size and weight were reached, fish were transferred to a specific laboratory area used for experimental challenges (flow-through system) and divided randomly in 8-L tanks, each with its own inlet/outlet for water and air-supply. Water temperature was constantly maintained at 13°C.

Fish (Experiment C)

Rainbow trout fry (1–2 g) were purchased from a commercial fish farm in Finland and kept and reared at the fish facilities of Åbo Akademi University (Turku, Finland) in tanks with flow through of dechlorinated tap water (∼12°C) and continuous aeration.

Experiment A: Delivery of Phages by Phage-Sprayed and Phage-Immobilized Feed

Preparation of Phage Feed

Feed pellets (0.8 mm, BIOMAR A/S, Denmark) from the same batch were treated (by spraying or immobilization) with FpV4/FPSV-D22-cocktail [total phage concentration of $3.3 \times 10^9 \pm 6.1 \times 10^8$ PFU ml^{-1} (SD, $n = 3$)], which was prepared mixing 1:1 PEG-purified solutions of FpV4 (1.2×10^9 PFU ml^{-1}) and of FPSV-D22 (4.9×10^9 PFU ml^{-1}). In the case of phage-sprayed feed, 30 ml of PEG-purified phage preparation containing FpV4 and FPSV-D22 were applied per 100 g of feed pellets with the use of a spray-bottle as previously described (Christiansen et al., 2014). The process was performed in a flow bench where the feed pellets were left to dry. Fixed Phage Ltd. produced phage-immobilized feed applying 20 ml of PEG-purified phage preparation per 100 g (Mattey, 2016, 2018). Phage-feed pellets were stored at 5°C before use in the experiments.

Detection and Quantification of Bacteriophages on Feed

To verify the presence of bacteriophages on feed, the classical method for phage detection was utilized. Three-hundred microliters of a 48-h old *F. psychrophilum* broth culture (in exponential phase) were mixed with 4 ml of TYES soft agar (0.4% agar) and poured into a TYES-A plate (Stenholm et al., 2008; Madsen et al., 2013). For qualitative detection, feed pellets were spread on the bacterial lawn and plates were incubated at 15°C for 3–4 days. Phages on feed pellets were quantified according to Christiansen et al. (2014) with some modifications. Three replicates of 0.1 g of feed and 2 ml of SM buffer were prepared in 2 ml sterile micro tubes (SARSTEDT AG & Co. KG, Germany) for each feed type. A sterile 5 mm steel bead (Qiagen, Germany) was added to each micro tube and samples were homogenized with a Qiagen TissueLyser II (1 min at 20 Hz; Qiagen, Germany). After storage for 1 h at 5°C, samples were transferred to 15 ml sterile Falcon tubes containing 3 ml of sterile SM buffer and vortexed. Phages were quantified by spotting 5 μl of serial 10-fold dilutions (180 μl of SM buffer and 20 μl of sample) of the homogenized

solutions in triplicates on a bacterial lawn (TYES soft agar with 48-h old *F. psychrophilum* culture). Plates were incubated at 15°C for 3–4 days and single plaques were then counted in the preferred dilution to estimate the phage titer per gram of feed pellets (Clokie and Kropinski, 2009; Madsen et al., 2013; Christiansen et al., 2014).

Set Up and Infection Method

The first investigated method of phage treatment was through phage application on feed pellets (by spraying or by using the Fixed Phage Ltd. immobilization technique) (**Table 1** and **Figure 1A**). Rainbow trout fry of 1–2 g were randomly subdivided in 12 × 8 L-aquaria (∼50 fish/aquarium). Fish in four aquaria were fed with phage-sprayed feed; fish in other four aquaria with phage-immobilized feed and fish in the remaining aquaria with control (untreated) feed. All groups were fed at 2% of fish weight per day during the experiment. After a 12-day prophylactic treatment period, fish in three of the four aquaria per feed-type group were exposed to the bacterial pathogen, *F. psychrophilum* 950106-1/1, by IP injection (50 μl, 1×10^4 CFU fish^{-1}). Fish in the remaining three aquaria (one aquarium per diet group) were injected with sterile TYES-B (as controls for the infection). Prior to IP injection, fish were anesthetized with 3-aminobenzoic acid ethyl ester (MS-222, Sigma catalog number A-5040). For each feed-type group, two of the infected aquaria were utilized to follow mortality of fish and the two remaining (one infected with the bacterium and one non-infected) were used for live fish sampling during the experiment. Dead and moribund fish were weighed, their length measured, and bacteriological examination of spleen, kidney and brain performed. If possible, internal organs were also collected and stored for phage detection/quantification. During the experiment, several parameters were considered to evaluate the fish health status: feed intake and swimming activity (behavioral observations); fin condition, presence of wounds and coloration (darkening) (external appearance); growth and abnormal mortality (production parameters) (Segner et al., 2019).

Fish Sampling

Five fish from each sampling aquaria were sampled randomly at 1, 4, 8, 11, 19, 33, and 56 days post infection. Additionally, five fish were collected from the sampling aquaria not infected with *F. psychrophilum* 1 day before the bacterial challenge. During sampling days, fish were euthanized with an overdose of MS-222. Weight and length of each fish were measured and bacteriological examination of spleen, kidney, and brain performed. To assess the spread of phages in fish, internal organs (spleen, kidney, brain, and the anterior part of the intestine) were collected in pre-weighted 1.5 ml sterile micro tubes (SARSTEDT AG & Co. KG, Germany) containing 300 μl of SM buffer. After the sampling, micro tubes containing fish organs were re-weighted to determine the weight of the organs and 5 μl of chloroform were added under a fume hood to kill any possible bacteria present in the samples. The used phages are not sensitive to chloroform. Fish were not fed for 24 h before sampling.

Bacteriological Examination

Using 1 μl sterile inoculation loops, samples from spleen, kidney, and brain were collected for each sampled and moribund/dead fish and streaked on TYES-A. Agar plates were incubated at 15°C from 4 to 5 days up to 4 weeks and *F. psychrophilum* yellow colonies were identified. Randomly chosen yellow colonies were analyzed by MALDI-TOF (Bruker) to confirm that *F. psychrophilum* was the re-isolated bacteria.

Bacteriophage Detection and Quantification

Phage detection in the sampled organs was performed as previously described (Madsen et al., 2013; Christiansen et al., 2014). Briefly, chloroform-fixed fish samples were homogenized by vortexing for 20 s and centrifuged for 10 s at 10,000 RPM at 5°C (1 min for intestine samples) to separate chloroform to the bottom of the tube. A spot test method was then performed (Stenholm et al., 2008; Clokie and Kropinski, 2009). For quantification of plaque forming units, 5 μl of undiluted sample were spotted on a freshly prepared bacterial lawn (as described above)in triplicate and incubated at 15°C for 3–4 days. Spots that presented single plaques (from 1 to 30) were counted and the titer of phages per milligram of tissue quantified. In the case of confluent or semi-confluent clearing areas, samples were 10-fold diluted (180 μl of SM buffer and 20 μl of sample) in triplicate and spotted on a bacterial lawn. Plates were incubated at 15°C for 3–4 days, single plaques counted from the preferred dilution and the titer of phages was estimated.

Experiment B: Delivery of Phages by Bath

Rainbow trout fry of 2–3 g were randomly subdivided in 4 × 8 L-aquaria (∼30 fish/aquarium) (**Table 1** and **Figure 1B**). Fish were fed with commercial feed pellets (0.8 mm, BIOMAR A/S, Denmark) at 2% of fish weight per day during the experiment. Fish in the four aquaria were exposed to the bacterial pathogen, *F. psychrophilum* 950106-1/1, by IP injection (50 μl, 1×10^5 CFU fish^{-1}). Based on the results of Experiment A, we decided to increase the infection dose 10 times with the aim of increasing the probability of that bacteria and phages would come into contact with each other. Prior to IP injection, fish were anesthetized with MS-222. The FpV4/FPSV-D22-mix [total phage concentration of $3.3 \times 10^9 \pm 6.1 \times 10^8$ PFU ml^{-1} (SD, $n = 3$)] was prepared by mixing 1:1 PEG-purified solutions of FpV4 (1.2×10^9 PFU ml^{-1}) and of FPSV-D22 (4.9×10^9 PFU ml^{-1}). At 48 h post infection, the water in the aquaria was removed and replaced with 2 L of cold tap water containing PEG-purified FpV4 and FPSV-D22 (2 ml of phage mix in 2 L of water – estimated concentration of $3.3 \times 10^6 \pm 6.1 \times 10^5$ PFU ml^{-1}) in two aquaria and 2 L of cold tap water without bacteriophages in the other two aquaria. Fish were bathed in the phage solution for 1 h and 30 min and subsequently, aquaria were filled up and the flow-through water system was re-established. The same procedure was performed 1 week after the first phage bath. One week after the second phage bath, phages were directly administered to the selected aquaria (2 ml of phage mix in 8 L of water – estimated concentration of $8.3 \times 10^5 \pm 1.5 \times 10^5$ PFU ml^{-1}) and the water flow

TABLE 1 | Overview of the studied experimental delivery methods.

Exp.	Phage delivery method	Administered phage titer	Administration time	Fish		Bacterial infection dose (IP*) (CFU $fish^{-1}$)
				Weight (g)	Total n. (n. per replicate)	
A	Phage-sprayed feed	$1.6 \times 10^8 \pm 2.5 \times 10^7$ PFU g^{-1} [b]	Continuous feeding started 12 days before IP*	1.9 (±0.7)[c]	895 (55 ± 4)[d]	1.0×10^4
	Phage-immobilized feed	$8.3 \times 10^7 \pm 4.8 \times 10^7$ PFU g^{-1}[b]				
	Control feed[a]	0 ± 0 PFU g^{-1}[b]				
B	Bath	I. $\sim 10^6$ PFU ml^{-1} II. $\sim 10^6$ PFU ml^{-1} III. $\sim 10^5$ PFU ml^{-1}	I. 48 h after IP* (1 h 30 min); II. One (1 h 30 min) and III. two weeks (3 h 30 min) after 1st bath	2–3	125 (31 ± 1)[d]	1.0×10^5
	Control bath	I. 0 PFU ml^{-1} II. 0 PFU ml^{-1} III. 0 PFU ml^{-1}				
C	IP injection	1.7×10^8 PFU $fish^{-1}$	3 days after IP*	∼7	120 (20 ± 0)[d]	1.7×10^7
	Control IP injection	0 PFU $fish^{-1}$				

**IP, bacterial intraperitoneal injection.*
[a]Non-treated commercial feed from the same batch as the phage-treated feed types.
[b]Average and standard deviation (n = 3).
[c]Average weight of fish sampled after 10 days of phage feed prophylaxis (standard deviation in the parenthesis; n = 15).
[d]Average number of fish per aquaria and standard deviation in the parenthesis.

stopped. After 3 h and 30 min, water flow was re-established. The four aquaria were utilized to follow mortality of fish. Dead and moribund fish were weighed, their length measured, and bacteriological examination of spleen, kidney and brain (as for Experiment A) was performed.

Experiment C: Delivery of Phages Through Intraperitoneal Injection

In experiment C, 120 rainbow trout (∼7 g) were randomly divided in 6 × 150 L-tanks (20 fish/aquarium) and fed with commercial feed pellets (1.2 mm, Rehuraisio, Finland) at 2% of fish weight per day (**Table 1** and **Figure 1C**). Fish in the six aquaria were anesthetized with benzocaine (10%) and exposed to *F. psychrophilum* 950106-1/1, by IP injection (100 µl, 1.7×10^7 CFU $fish^{-1}$). A higher bacterial dose, compared to the previous experiments, was chosen because of the larger fish size. According to Madsen and Dalsgaard (1999), fingerlings have to be challenged with the IP method with an infection dose of 10^7 CFU $fish^{-1}$ or higher to induce mortalities. At 3 days post infection (dpi), fish in three tanks were exposed to PEG-purified bacteriophages FpV4 and FPSV-D22 by IP injection (100 µl, 1.7×10^8 PFU $fish^{-1}$). Prior to phage exposure, PEG-purified FpV4 (1.2×10^9 PFU ml^{-1}) and FPSV-D22 (2.2×10^9 PFU ml^{-1}) solutions were mixed 1:1. Fish in the other three tanks were IP injected with sterile SM buffer as controls. Fish mortality was recorded for 21 dpi and, during this period, dead and moribund fish were removed, weighed and bacteriological examination of spleen and kidney performed. A subset of samples were analyzed and verified as *F. psychrophilum* by PCR (Toyama et al., 1994). To ensure delivery of phages in the fish internal organs by this method, fifteen additional rainbow trout were placed in a 150-L aquarium and injected with bacteriophages alone (100 µl, 1.7×10^8 PFU $fish^{-1}$). At 4 and 34 days after exposure, spleen and kidney of five fish were sampled and analyzed for phage detection as described in Experiment A.

Statistical Analysis

Phage quantification and survival data were analyzed using GraphPad Prism version 8.4.0 for Windows, GraphPad Software, San Diego, CA, United States, www.graphpad.com. For linear regression analysis of phage concentration detected in sampled organs over time, values were first log transformed. In the Kaplan-Meier survival analysis, data from replicate aquaria were merged together [the difference in survival between replicates was ≤20% (Amend, 1981; Midtlyng, 2016)] and comparison of survival curves was performed with the Log-rank (Mantel–Cox) test and the Gehan-Breslow-Wilcoxon test.

RESULTS

Phage Delivery by Feed Pellets: Phage-Immobilized and Phage-Sprayed Feed (Experiment A)

In order to evaluate the potential protection conferred by the phage cocktail targeting *F. psychrophilum*, rainbow trout fry (1.5–2 g) were fed either with phage-immobilized ($8.3 \times 10^7 \pm 2.5 \times 10^7$ PFU g^{-1}) or phage-sprayed ($1.6 \times 10^8 \pm 4.8 \times 10^7$ PFU g^{-1}) feed at 2% of their body weight for 12 days before bacterial challenge (**Table 1**, **Figure 1A** and **Supplementary Figures 1A,B**). Fish growth, abnormal mortalities, feed intake, swimming activity, and external appearance (fin condition and coloration) were monitored

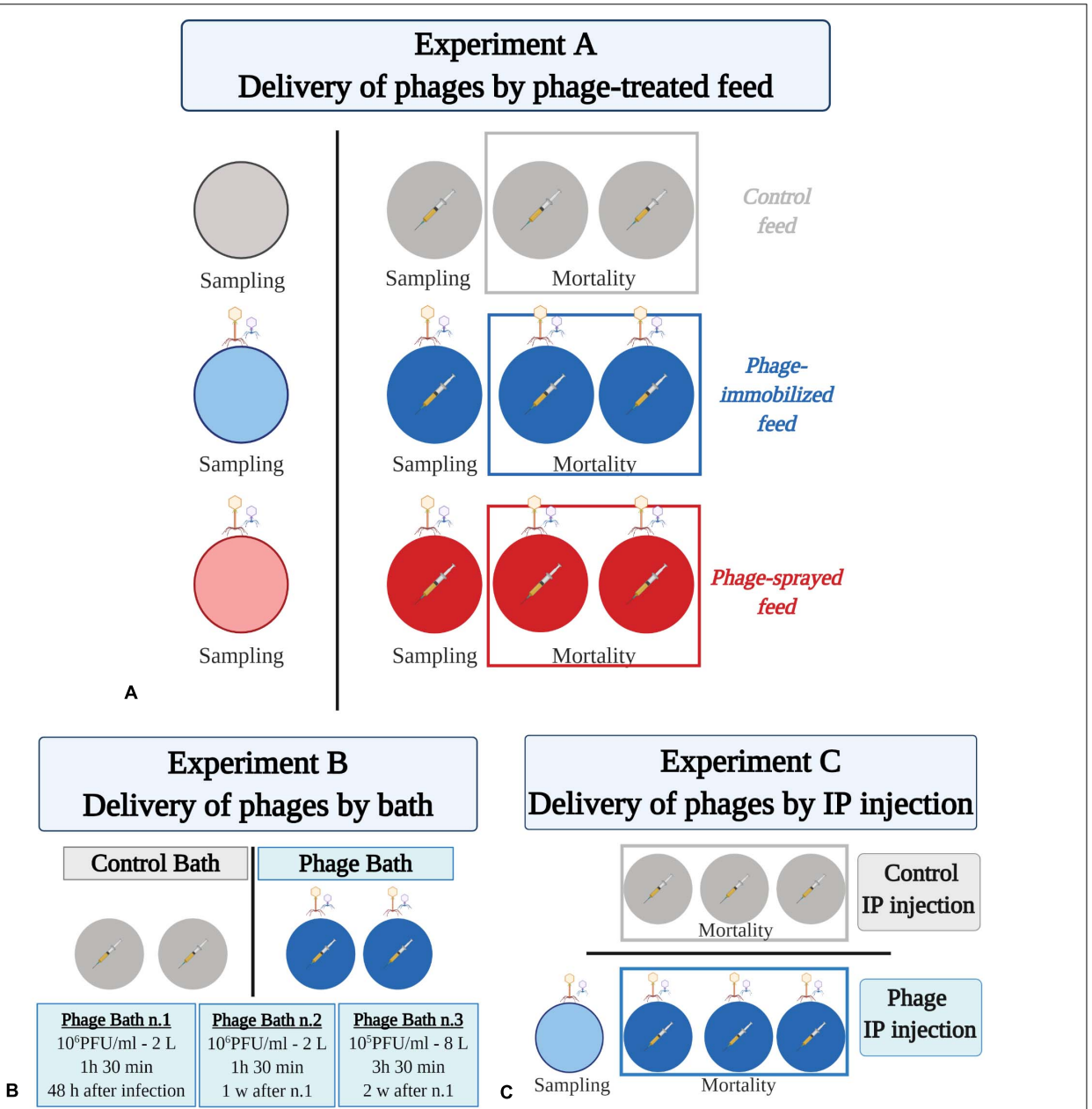

FIGURE 1 | Experimental fish trials to test phage delivery by feed **(A)**, by bath **(B)**, and by intraperitoneal injection **(C)**. **(A)** Eight hundred and ninety-five rainbow trout fry were divided randomly in 12 aquaria (55 fish ± 4) which are represented by colored circles. Fish were fed at 2% of their body weight with either control feed (in gray), phage-immobilized (in blue), or phage-sprayed (in red) feed. Bacteriophage drawings indicate FpV4 and FPSV-D22, which were administered to fish by feed. For each group, three of the four aquaria were challenged with *F. psychrophilum* (1×10^4 CFU fish^{-1}; indicated by a syringe with yellow content because of the coloration of the bacteria). Fish in the fourth aquarium were injected with sterile TYES-B as control for the infection. Two of the bacterial challenged aquaria per group were used to follow mortality. The remaining aquaria were dedicated to sampling (five fish at sampling point). **(B)** Hundred and twenty-five rainbow trout fry were divided in four aquaria (circles; 31 fish ± 1 per aquarium) and challenged with *F. psychrophilum* (1×10^5 CFU fish^{-1}; syringe with yellow content). Fish in two aquaria were exposed to three rounds of FpV4 and FPSV-D22 phages bath (blue circles; indicated by bacteriophage drawings). Mortality was followed w = week. **(C)** Hundred and twenty rainbow trout (7 g), divided in six aquaria (circles, 20 fish ± 0 per aquarium), were IP challenged with *F. psychrophilum* (1.7×10^7 CFU fish^{-1}; syringe with yellow content). Three days later, fish in three aquaria were exposed to phages FpV4 and FPSV-D22 by IP injection (blue circles; indicated by bacteriophage drawings). This aquaria were used to follow mortality. One additional aquarium was included for few sampling where fish were only exposed to the two component phage mix (light blue circle; 15 fish). Created with BioRender.com (the figure was exported under a paid subscription).

during the experiment. Positive growth was detected for all groups (**Supplementary Figure 1C** and **Supplementary Table 2**) and no mortalities were observed prior to infection. The addition of phages in either way did not seem to change the taste of the feed for the fish and the fish ate the amount of feed that they were offered (fish not challenged with the bacterium and

prior to infection in all groups). Other visual signs of disease conditions, such as destroyed fins, lethargic swimming, color changes, and skin ulceration were not seen prior to infection and in non-challenged groups.

Efficiency of Phage Delivery: Percentage of Isolation of *F. psychrophilum* and Its Phages in Fish Organs

The qualitative detection of bacteriophages in intestine, kidney, spleen, and brain of fish fed with phage immobilized feed, phage sprayed feed, and control feed verified the presence of bacteriophages in treated fish and thereby the delivery of phages through the feed pellets before any manipulation (IP injection with either *F. psychrophilum* or sterile TYES-B) (**Figure 2**). The results showed that phages were present in the intestine (100% of sampled fish) and in the internal organs of the fish prior to bacterial challenge (100%, 20%, and 40% of kidney, spleen and brain of sampled fish fed with phage-sprayed feed, respectively; 80%, 40%, and 20% of kidney, spleen, and brain of sampled fish fed with phage-immobilized feed, respectively) (**Figures 2**, **3**). Subsequently, we observed the constant presence of bacteriophages in intestines of fish fed with phage-treated feeds during the experiment with more variable occurrence of phages in the other tested organs (**Figure 2**).

In fish fed with phage-immobilized feed and not exposed to *F. psychrophilum*, bacteriophages were detected in 80% of kidney samples before day 8 and in 40–60% after 8 days post infection (dpi) (**Figure 3A**). Except for fish sampled 8 dpi, fish challenged with *F. psychrophilum* and fed with phage-immobilized feed (**Figure 3A**) showed a lower percentage of phages in the fish kidney compared to the controls (0–40% at 1, 4, and 11 dpi; frequency of re-isolation of bacterium = 20–60% until 11 dpi). Subsequently, no bacteria were re-isolated from fish kidney and the frequency of isolation of phages changed from 0% at 19 dpi to 80 and 60% at 33 and 56 dpi, respectively. For spleen samples, we were able to detect phages in 40–60% of fish not challenged with *F. psychrophilum* until 4 dpi and subsequently the percentage of detection dropped to 0–20% (**Figure 3B**). When fish were also exposed to the bacterium, the percentage of phage detection in spleen was between 20 and 60% until 11 dpi, while *F. psychrophilum* was re-isolated from 40 to 60% of the sampled spleens (**Figure 3B**). Subsequently, no bacteria were re-isolated and phages were detected in 0–20% of the spleen samples. A lower frequency of phage detection was measured in the brain of fish fed with phage-immobilized feed, whether or not fish were challenged with *F. psychrophilum* (between 0 and 20% except for 11 and 33 dpi where 60 and 40% of sampled brains were positive for phages in non-challenged fish, **Figure 3C**). *F. psychrophilum* was re-isolated only from the brain of one fish sampled 11 dpi.

Fish fed with phage-sprayed feed (negative to *F. psychrophilum)* were characterized by a consistent phage detection in fish kidney (60–100%; **Figure 3A**), an increase of the frequency of phage isolation in spleen samples from 20 to 60% during the experiment (**Figure 3B**) and more variable measurements in the fish brain (20–60%; **Figure 3C**). When fish were exposed to *F. psychrophilum* (**Figures 3A,B**), we observed a decrease in phage detection in kidney and spleen samples from 80 to 20% from 1 dpi to 19 and 33 dpi. Subsequently, the frequency of phage detection was increased to 80% for kidney samples (56 dpi) and to 60% for spleen samples (56 dpi). A similar pattern was observed for brain samples (**Figure 3C**) where our measurements showed an initial decrease in phage detection (from 40 to 20%) with a higher detection frequency at 56 dpi. (60%). For *F. psychrophilum*, we detected high frequencies in spleen and kidney (80% for spleen samples and 60% of kidney samples) in the first days after the bacterial challenge, which decreased during the experiment. In brain samples, *F. psychrophilum* was detected at 8 and 11 dpi (40% of sampled fish).

In fish fed with control feed, the frequency of isolation of the bacteria in kidney samples (**Figure 3A**) shifted from 20% at 1 and 4 dpi to 80, 40, and 20% at 8, 11, and 19 dpi, respectively. *F. psychrophilum* was re-isolated from 40% of spleen samples until 8 dpi and to 20% at 11 and 19 dpi (**Figure 3B**). *F. psychrophilum* was only detected in the brain of one fish at 8, 11, and 19 dpi (**Figure 3C**). No phages were detected in fish fed with control feed and no *F. psychrophilum* was re-isolated from fish that served as negative control for the infection fed in any of the three feed groups (IP with sterile TYES-B) (**Figure 3**).

Efficiency of Phage Delivery in Fish Organs: Quantification

After 12 days of phage prophylactic administration, the concentration of phages detected in the intestine of fish was $2.2 \times 10^3 \pm 1.7 \times 10^3$ PFU mg^{-1} and $1.2 \times 10^3 \pm 1.0 \times 10^3$ PFU mg^{-1} (day −1) in fish fed with phage-immobilized and phage-sprayed feed, respectively, and these concentrations were maintained over time when fish were not challenged with the bacterium (**Figures 4A,B**). In fish exposed to *F. psychrophilum*, the intestinal phage concentration was also maintained in fish fed with phage-immobilized feed even if we observed a larger variation (SD) among the biological replicates 11 dpi ($1.7 \times 10^3 \pm 1.7 \times 10^3$ PFU mg^{-1}) (**Figure 4A**). A different situation was observed in challenged fish fed with phage-sprayed feed where a decrease in the intestinal phage concentration was detected in the first 8 days after the bacterial challenge. Indeed, the titer of phages per mg of intestine decreased from $9.1 \times 10^2 \pm 5.2 \times 10^2$ PFU mg^{-1} measured at 1 dpi to $2.6 \times 10^2 \pm 3.5 \times 10^2$ PFU mg^{-1} 8 dpi. Subsequently, the number of phages detected in the intestines started to rise even if a large variation among the sampled fish was detected at 11 and 19 dpi. Thirty-three days after the infection the intestinal phage titer raised to $1.0 \times 10^3 \pm 1.2 \times 10^3$ PFU mg^{-1} (**Figure 4B**).

Bacteriophages were detected in the kidney of 57.5% and 75.0% of non-challenged sampled fish and of 42.9% and 51.4% of challenged sampled fish fed with phage-immobilized and phage-sprayed feed, respectively (**Figure 3**). In fish fed with phage-immobilized feed (**Figure 4C**), the titer of phages in the kidney was $\sim 10^1$ PFU mg^{-1} 1 day before the infection and at 1 and 4 dpi. The titer per mg of kidney decreased in the following days reaching its lowest point at 33 dpi (0.5 ± 0.8 PFU mg^{-1}). At the end of the experiment, the concentration of phages in the kidney was restored to $1.4 \times 10^1 \pm 2.1 \times 10^1$ PFU mg^{-1} (56 dpi). When fish fed with phage-immobilized feed were challenged with the bacterium, the concentration of phages in kidney

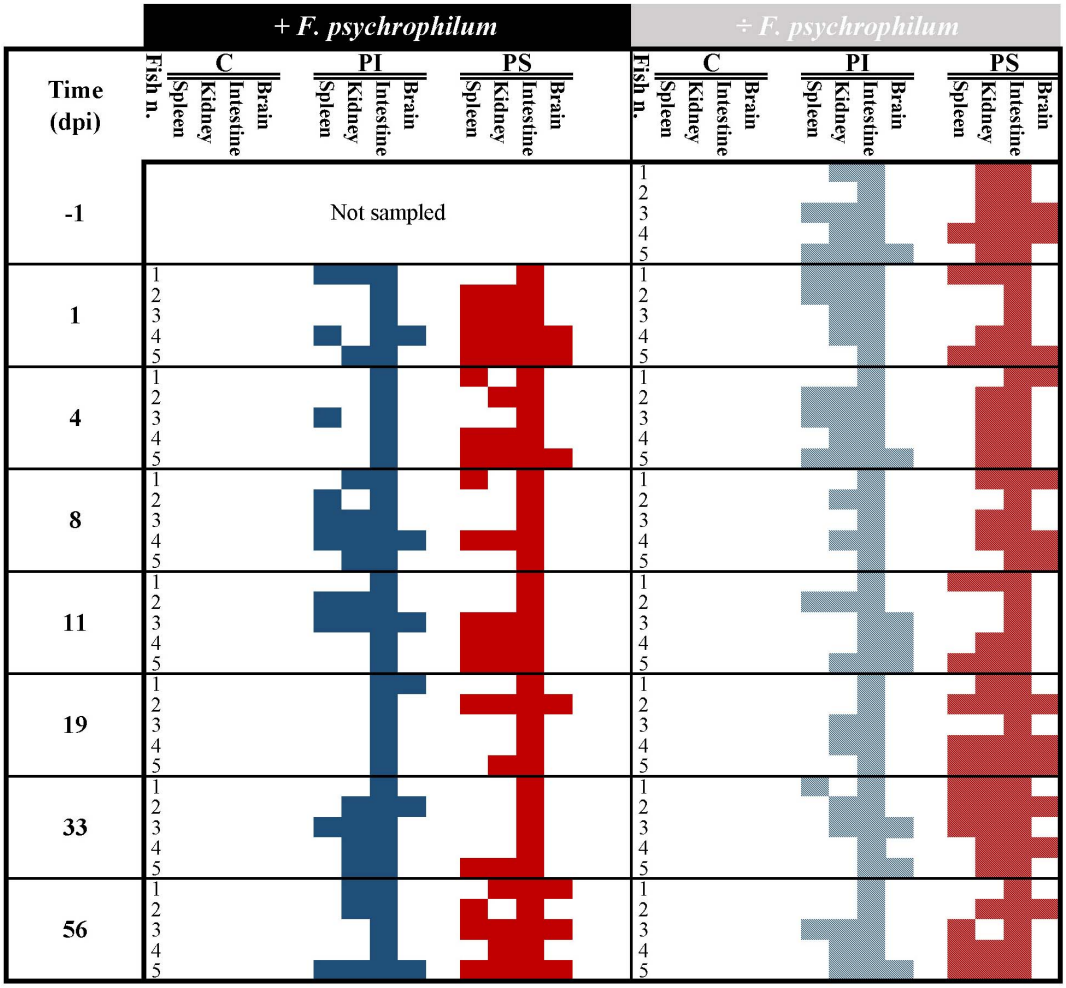

FIGURE 2 | Experiment A. Qualitative detection of bacteriophages in fish organs (spleen, kidney, intestine, and brain) over time in fish fed with phage-immobilized (PI), phage-sprayed (PS), and control (C) feed. Blue and red colors indicate the presence of phages in organs of fish fed with phage-immobilized and phage-sprayed feed, respectively, challenged with *F. psychrophilum* (full color, no pattern) or not (pattern, striped). Absence of phages in the tested organ is indicated by white/blank. Positive detection = presence of one or more plaques in at least one of the technical triplicates. At each sampling point, five fish were sampled in each group except 1 day before the infection where samples were collected only from groups not supposed to be challenged with *F. psychrophilum*. dpi, days post infection.

samples over time was on average similar to the non-challenged fish (the lowest concentration, 4.3 ± 9.7 PFU mg^{-1}, was detected 1 dpi and the highest, $3.5 \times 10^1 \pm 4.1 \times 10^1$ PFU mg^{-1}, 8 dpi). For fish fed with phage-sprayed (**Figure 4D**), the concentration of phages in the kidney was constant over time with values as $1.7 \times 10^1 \pm 1.9 \times 10^1$ PFU mg^{-1} (1 day before challenge) and $1.3 \times 10^1 \pm 1.5 \times 10^1$ PFU mg^{-1} (19 dpi). In case of bacterial challenge, the overall concentration of phages per mg of kidney decreased 10 times compared to non-challenged fish (e.g., 2.8 ± 4.7 PFU mg^{-1} detected 11 dpi) except for the initial high phage concentration detected 1 dpi ($6.4 \times 10^1 \pm 7.3 \times 10^1$ PFU mg^{-1}).

Bacteriophages were detected in the spleen of 25.0% and 35.0% of non-challenged sampled fish and of 28.6% and 48.6% of challenged sampled fish fed with phage-immobilized and phage-sprayed feed, respectively (**Figure 3**). Quantifying the number of phages per mg of spleen in fish fed with phage-immobilized feed (**Figure 4E**), we observed a decrease from $3.8 \times 10^1 \pm 5.8 \times 10^1$ PFU mg^{-1} detected 1 day before the bacterial challenge to 0.5 ± 1.1 PFU mg^{-1} and 0.3 ± 0.8 PFU mg^{-1} measured 33 and 56 dpi, respectively. In fish challenged with the bacteria, the number of phages detected over time was stable with values between $2.9 \times 10^1 \pm 4.1 \times 10^1$ PFU mg^{-1} (8 dpi) and 1.1 ± 2.3 PFU mg^{-1} (19 dpi). In fish fed with phage-sprayed feed (**Figure 4F**), the concentration of phages per mg of spleen was $1.2 \times 10^2 \pm 1.3 \times 10^2$ PFU mg^{-1} (+ *F. psychrophilum*) and $1.4 \times 10^1 \pm 1.9 \times 10^1$ PFU mg^{-1} (÷ *F. psychrophilum*) measured 1 day post infection, and 1.8 ± 3.2 PFU mg^{-1} (+ *F. psychrophilum*) and 2.9 ± 4.6 PFU mg^{-1} (÷ *F. psychrophilum*) 56 dpi.

The number of phages per mg of brain was also quantified (**Figures 4G,H**), although the percentage of detection

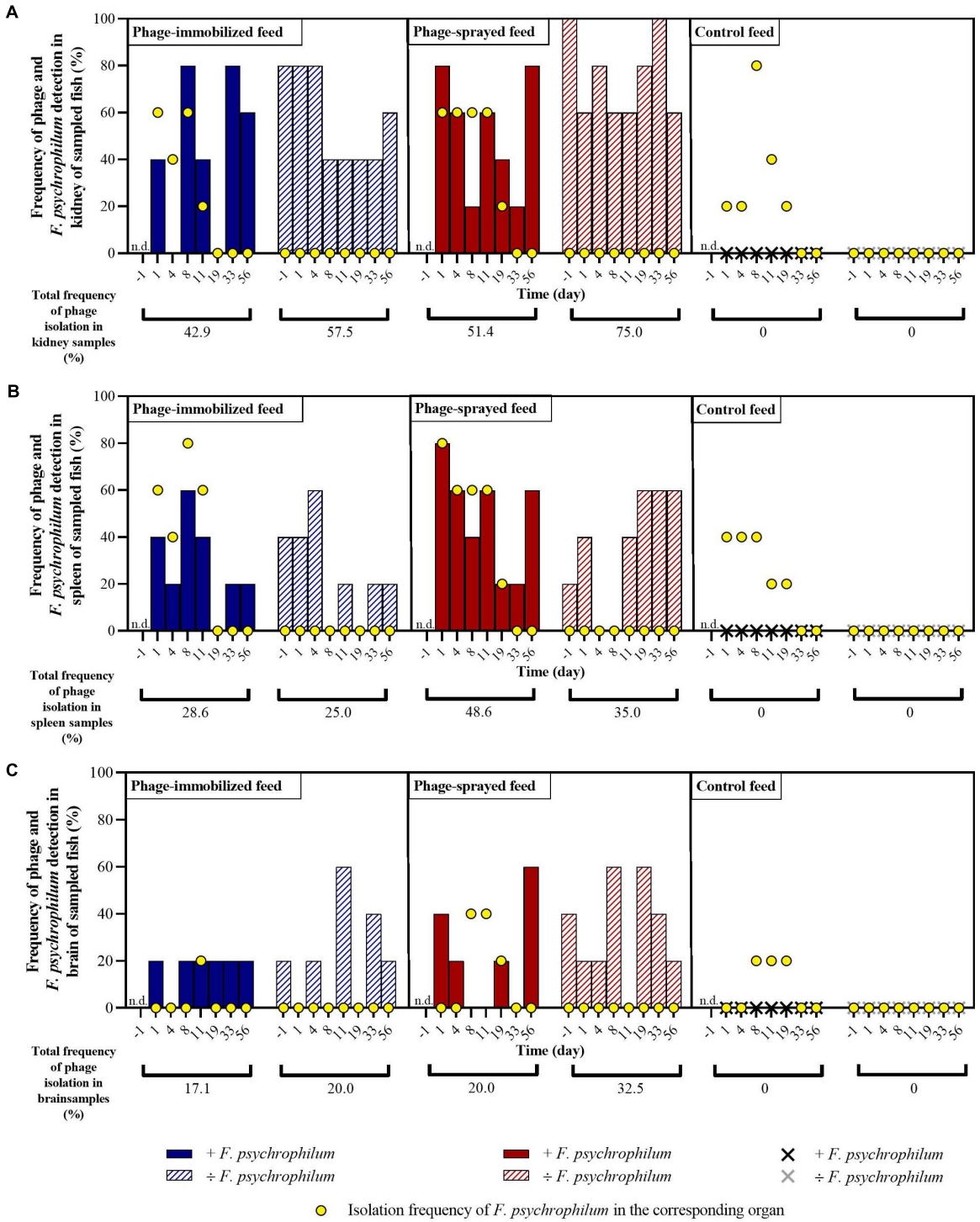

FIGURE 3 | Experiment A. Frequency of detection of bacteriophages and of isolation of *F. psychrophilum* in kidney **(A)**, spleen **(B)**, and brain **(C)** of sampled fish in the different groups over time. No phages were detected in internal organs of fish fed with control feed. Five fish were sampled at each sampling point per group. n.d., not determined. For each organ of each feed group, the total percentage of phages isolation over time is calculated with and without *F. psychrophilum*.

over time was low (20.0% and 32.5% of non-challenged sampled fish and 17.1% and 20.0% of challenged sampled fish fed with phage-immobilized and phage-sprayed feed, respectively – **Figure 3**). In fish fed with phage-immobilized feed (**Figure 4G**), the concentration of phages per mg of brain was 0.9 ± 1.9 PFU mg^{-1} (+ *F. psychrophilum*) and

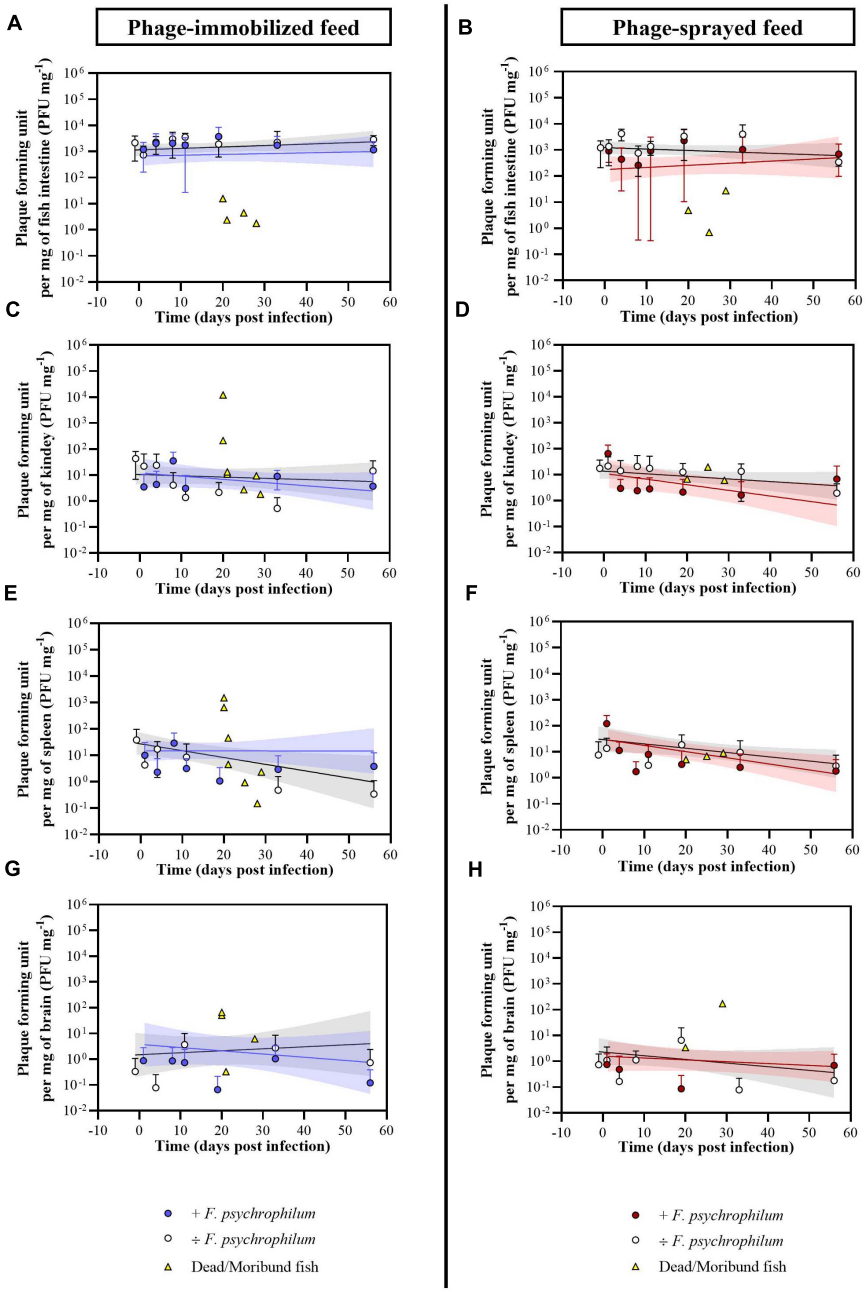

FIGURE 4 | Experiment A. Quantification of bacteriophages FpV4 and FPSV-D22 in intestine **(A,B)**, kidney **(C,D)**, spleen **(E,F)**, and brain **(G,H)** of fish fed with phage-immobilized **(A,C,E,G)** and phage-sprayed **(B,D,F,H)** feed. Values represent the average of five biological replicates per time point and error bars the standard deviation. Concentration of phages in the organs of dead fish (dead because of *F. psychrophilum* infection) is included in the graphs for the corresponding organ and feed type (each symbol in yellow represents a single fish). Simple linear regression lines were calculated from the log-transformed PFU over time and 95% confidence bands are also presented.

0.0 ± 0.0 PFU mg^{-1} (÷ *F. psychrophilum*) measured 1 day post infection, and 0.1 ± 0.3 PFU mg^{-1} (+ *F. psychrophilum*) and 0.7 ± 1.6 PFU mg^{-1} (÷ *F. psychrophilum*) 56 dpi. In **Figure 4H**, the quantification of phages in the brain of fish fed with phage-sprayed feed is presented. We detected 0.8 ± 1.2 PFU mg^{-1} (+ *F. psychrophilum*) and 1.1 ± 2.4 PFU mg^{-1} (÷ *F. psychrophilum*) measured 1 day post infection, and 0.7 ± 1.2 PFU mg^{-1} (+ *F. psychrophilum*) and 0.2 ± 0.4 PFU mg^{-1} (÷ *F. psychrophilum*) 56 dpi. The phage propagation rates in fish organs over time, calculated from linear regression analysis, are presented in **Supplementary Table 3**.

Eight and four randomly chosen dead fish were sampled for phage analysis in the groups fed with phage-immobilized and phage-sprayed feed, respectively (**Figure 4** and **Supplementary Table 4**). For fish fed with phage-immobilized feed, phage concentration was between 0.0 and 15.6 PFU mg^{-1} in the intestine, 0.0 and 45.3 PFU mg^{-1} in the spleen, 0.0 and 13.3 PFU mg^{-1} in the kidney, and 0.0 and 65.9 PFU mg^{-1} in the brain. Only two fish (n. 1 and n. 2; **Supplementary Table 4**) showed a higher concentration of phages in kidney and spleen compared to the others (1.2×10^4 and 210.5 PFU mg^{-1} in kidney samples; 1.3×10^3 and 641.9 PFU mg^{-1} in spleen samples). A similar situation was observed for fish fed with phage-sprayed feed where we detected between 0.0 and 27.5 PFU mg^{-1} of intestine, 0.0 and 74.2 PFU mg^{-1} of spleen, 0.0 and 77.8 PFU mg^{-1} of kidney, and 0.0 and 170.8 PFU mg^{-1} of brain. In the control feed group, only one dead fish was sampled for phage analysis and no phages could be detected.

Effect of Phage Delivery on Fish Survival (Experiments A, B and C)

To evaluate the protective effect of bacteriophages and to compare the three phage delivery methods, survival of fish was quantified over time in the three experiments (see experimental set-up in **Figure 1** and **Table 1**). In Experiment A where phages were delivered via the feed, fish mortality started around 10 days post infection (dpi) for the three feed-type groups and it was followed until 56 dpi. The final percent survival for fish fed with phage-sprayed, phage-immobilized and control feed was 75.6%, 80.1%, and 76.8%, respectively (**Figure 5A**), with no significant differences among the curves. No mortality was observed in the non-challenged groups of fish fed with the three feed types. When phages FpV4 and FPSV-D22 were administered by bath (Experiment B – **Figure 5B**), the final percent survival was 45.3% in the phage bath group and 42.6% in the control group (no significant difference). When phages FpV4 and FPSV-D22 were administered by intraperitoneal injection 3 days after the bacterial challenge (Experiment C), the final percent survival observed in the control group (56.7%) was significantly lower than the survival of the group injected with bacteriophages FpV4 and FPSV-D22 (80.0%) (**Figure 5C**).

To confirm the presence of phages delivered by IP injection (Experiment C), five fish were sampled in the control aquaria (only phages) 4 and 34 days after the injection. Four days after IP injection, the concentration of phages detected in the spleen and kidney was 3.3 ± 1.5 and 8.2 ± 3.0 PFU mg^{-1}, respectively. Thirty-four days post inoculation, phages were detected in the kidney of two fish (0.03 and 0.06 PFU mg^{-1}).

DISCUSSION

Phage-therapy has gained increased attention in aquaculture as a sustainable alternative strategy to antibiotic treatment or as a prophylactic measure against disease outbreaks. In our study, we investigated the potential of different methods for delivering a two-component phage mixture to rainbow trout fry to control *F. psychrophilum* infections and to reduce fish mortality.

Phage Delivery by Feed Pellets in Aquaculture

Oral administration of phages for systemic circulation in fish using phage-immobilized (produced by corona discharge technology patented by Fixed Phage Ltd. – final concentration of 8.3×10^7 PFU g^{-1} of feed pellets) and phage-sprayed in-house feed pellets (1.6×10^8 PFU g^{-1}) provided a constant delivery of phages to the fish, without a negative effect on fish health or growth. The higher phage density in the internal organs obtained using the phage-sprayed feed compared to the one obtained in fish fed with phage-immobilized feed may partly reflect the higher phage concentration on the manually sprayed feed. However, differences in the orientation of phages on the feed pellets and their detachment and infectivity after the corona discharge and spray treatment, respectively, might also affect the efficiency of delivery. Leppänen et al. (2019) recently showed that the antimicrobial efficiency was higher for detached phages compared to the attached ones and that covalently bound phages on carboxylate-treated gold had the lowest infectivity even if this surface was characterized by the highest number of attached phages. The authors suggest that the lost infectivity of covalently bound phages might have been caused by chemical interactions or the improper orientation of the phages on the surface (Leppänen et al., 2019). In our study, it does not seem that the covalently bound phages on feed pellets by the corona discharge method are characterized by a lower infectivity compared to phages applied using a spraying approach, as indicated by a very similar and stable phage number in the fish intestine when fed with the two phage-feed types. It is not clear if the lower phage translocation efficiency in the internal organs in fish fed with phage-immobilized feed compared with the phage-sprayed feed is due to a tighter binding of the phages to the feed pellets, or a lower number of phages attached to the pellets. Nevertheless, the application of phages on feed pellets by the corona discharge method reduces the time for feed preparation (compared to spraying procedures) and enables the stable immobilization of bacteriophages.

The stable concentration of phages detected in the gut after feeding with phage coated pellets indicated a positive gut transit of the selected phages in the gastrointestinal environment, as described previously (Christiansen et al., 2014). However, the detection of phages in the internal organs (spleen, kidney, and brain) was not always possible, suggesting inefficient phage penetration from the gastrointestinal tract into the systemic circulation. In a systematic analysis of 144 relevant human and animal experiments, the oral administration route was described as the least effective among the tested methods in delivering active phages that penetrate into the circulatory system (Dąbrowska, 2019) presumably by the transcytosis mechanism (Barr, 2017; Nguyen et al., 2017). Indeed, even if bacteriophages can be isolated in feces/intestine indicating a positive gut transit, it is not always possible to isolate them from blood/internal organs. However, the dose of administration can significantly contribute

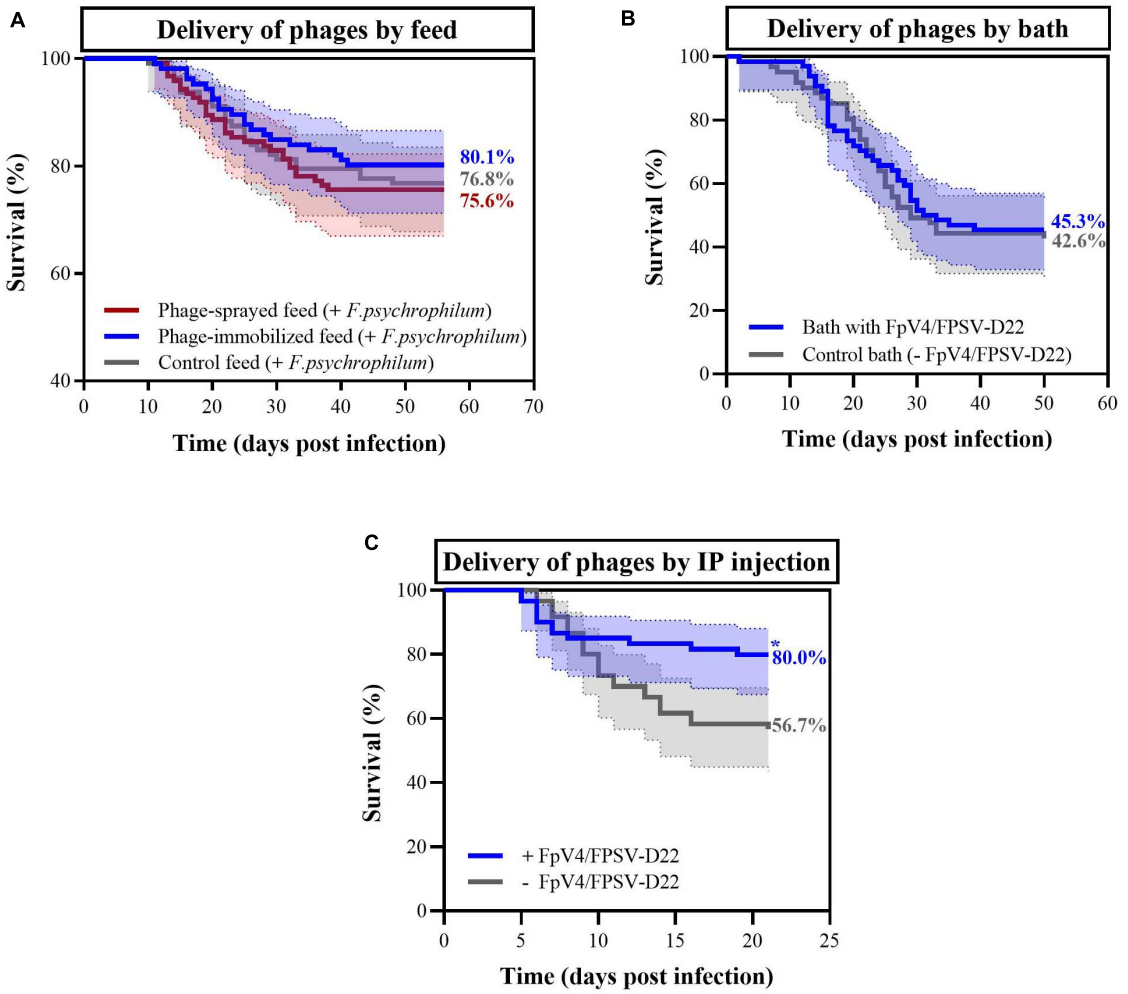

FIGURE 5 | Percent survival observed in rainbow trout fry exposed to *F. psychrophilum* and bacteriophages in the three experiments. In **(A)**, survival of fish fed with phage-immobilized feed (blue), phage-sprayed feed (red) feed and control feed (gray) are displayed (Experiment A). No mortality was observed in the control aquaria (data not shown). In **(B)**, survival of fish bathed in phage solution (blue) and in control bath (gray) in Experiment B. In **(C)**, bacteriophages were delivered with IP injections 3 days after the bacterial challenge (blue) while phage control fish were injected with sterile SM buffer (gray) (Experiment C). In all three experiments, moribund and dead fish were positive to *F. psychrophilum*. Final percent survival are presented for each curve in the figures. * = the curves are significantly different. 95% confidence interval is presented for each curve.

to phage ability to pass to the systemic circulation (Dąbrowska, 2019). Thus, a key step in delivering phages via feed is the application of very high initial titers. In a recent study, the delivery of *Edwardsiella tarda* phage ETP-1 bio-encapsulated in *Artemia* nauplii (enriched *Artemia* at 10^{11} PFU ml^{-1}) could provide phages with a concentration of 10^4–10^6 PFU mg^{-1} of tissue 10 days after the start of the phage feeding in gut, kidney, spleen and liver of zebrafish (Nikapitiya et al., 2020). Interestingly, it seemed that phage penetration from the gut into the circulatory system was very efficient and only a 10-fold phage decay was observed between the gut and the kidney at the time points examined.

The pH in the gut environment may affect the stability and infectivity of phages as discussed by Madsen et al. (2013) and Christiansen et al. (2014). *In vitro* experiments have shown that the stability of *F. psychrophilum* phages FpV4 and FpV9 were lost completely at pH 3 and in part reduced (a 10 fold reduction over 90 days) at pH 4.5 (Madsen et al., 2013). These pH values resemble the stomach environment (Bucking and Wood, 2009). FpV9 remained stable at pH 6 and 7.5 (typical of intestine environment) (Bucking and Wood, 2009; Madsen et al., 2013). In our experiment, phages were administered together with the feed, thus the stomach pH would likely have been around 4.9 (Bucking and Wood, 2009; Madsen et al., 2013), potentially causing a minor loss in the amount of infective phages in the stomach. However, other factors like the presence of macromolecules or the bacterial microflora in the gut may potentially protect the phages *in vivo* (Dąbrowska, 2019).

Phage decay in the circulatory system has mainly been attributed to the activity of the innate and the adaptive immune

systems, with lymphoid organs considered as the main players in phage clearance and de-activation by phagocytosis [reviewed by Dąbrowska (2019); Van Belleghem et al. (2019)]. In fish, the main non-mucosal lymphoid organs are the thymus, the kidney (in adult fish mainly the head kidney or *pronephros*) and the spleen (Secombes and Wang, 2012). In our Experiment A, we detected a stable concentration of infective phages ($\sim 10^1$ PFU mg^{-1}) in the kidney of 57.5 and 75.0% of fish fed with phage-immobilized and phage-sprayed feed, respectively (fish were sampled 24 h after feeding; non-infected fish). These results are in line with previous reported delivery efficiencies using oral intubation (Christiansen et al., 2014) and intraperitoneal injection (Madsen et al., 2013) of *F. psychrophilum* phages in rainbow trout fry, where 75% (24 h after delivery) and 100% (up to 72 h after delivery) of sampled fish showed presence of infective phages in the kidney, respectively (Madsen et al., 2013; Christiansen et al., 2014). The constant detection of infective phages in kidney of fry exposed to the treatment may reflect the role of this well-perfused organ in phage clearance from blood in fish (meaning that phages may be constantly delivered but do not accumulate over time because neutralized), unlike in mammals, where the kidneys have different functions and do not seem to be involved in phage clearance (Dąbrowska, 2019).

The lower detection frequency of active phages in spleen samples compared to intestine and kidney samples, i.e., phage detection in 25 and 35% of spleen of fish fed with phage-immobilized and phage-sprayed feed, respectively (non-infected fish) was also in agreement with previous findings of 100–1000 fold decrease in phage concentration from intestine to spleen (Christiansen et al., 2014). In addition, the concentration of phages in the spleen appeared to decrease by 10 fold over time (non-infected fish). It is not clear if this is a result of the in-activation of phages in the spleen, or a consequence of the relatively low phage dose delivered. The spleen, a main secondary lymphoid organ (in fish and in mammals) and a reservoir of disease in fish (Secombes and Wang, 2012), has been suggested to play an important role in phage clearance (Dąbrowska, 2019). Previous experiments in rainbow trout (5 g) where bacteriophages were administered by oral intubation (100 μl of 1×10^8 PFU ml^{-1}) showed a complete disappearance of viable phages from the spleen 27 h after phage exposure (Christiansen et al., 2014). Similar results were obtained in mice after the administration of a vibriophage (oral gavage; 100 μl of 1×10^8 PFU ml^{-1}), which showed a very high concentration of infective phages in spleen 6 h after the administration, which then decreased over time reaching 10^1 PFU mg^{-1} of tissue at 24 h (Jaiswal et al., 2014). Other studies, however, have demonstrated the presence of active phages in the spleen for a few days after exposure. However, it is unclear how quickly the phages are inactivated (Dąbrowska, 2019).

The detection of phages in 20.0% and in 32.5% of brain samples of fish fed with phage-immobilized and phage-sprayed feed, respectively, documented that phages FpV4 and FPSV-D22 are likely able to cross the blood-brain barrier. However, the simultaneous collection of blood during brain sampling procedures cannot be excluded. Since the dose and the delivery route have been identified as major conditions influencing the diffusion of phages in the brain (Dąbrowska, 2019), we also believe that the low percentage of detection is linked to the relatively low phage dose administered by feed pellets.

Phage Delivery Methods and Fish Survival During *F. psychrophilum* Infection

The first indication that the constant delivery of phage FpV9 through feed (1.5×10^8 PFU g^{-1}) could provide a decrease in rainbow trout fry (2.5 g) mortality affected by *F. psychrophilum* was provided by Christiansen (2014) (final cumulative mortality of 40% against 53% of control fish). In our Experiment A, we did not observe a similar outcome when phages were delivered orally (phage-sprayed feed: 1.6×10^8 PFU g^{-1}; phage-immobilized feed: 8.3×10^7 PFU g^{-1}). The lack of a significant beneficial effect on fish survival after bacterial challenge, may reflect a low phage density and a reduced phage-pathogen encounter rate in the infected organs. Similar results were obtained when phages were delivered by bath.

Intraperitoneal injection of bacteriophages has been suggested to be the best route of administration providing a fast and efficient delivery, and is recommended for systemic or localized infections (Dąbrowska, 2019). Phages spread very rapidly in the organs of the fish when delivered with this method but they can also quickly disappear when their target bacteria are not present (IP injection of FpV9 – 10^7 PFU $fish^{-1}$) (Madsen et al., 2013). Previous experiments demonstrated the potential of using *F. psychrophilum* phages to treat RTFS administered by IP injection (phage 1H and 6H delivered together with *F. psychrophilum*) (Castillo et al., 2012). In our Experiment C, phages delivered in high concentrations (1.7×10^8 PFU $fish^{-1}$) by intraperitoneal injection 3 days after bacterial challenge were able to combat the bacterial infection and reduce mortality. These results support the utilization of the selected phages to control *F. psychrophilum* when delivered in high dosages. Further, delivering both the pathogen and phages by IP injection likely increases the probability of phage-pathogen encounter in the intraperitoneal cavity.

Phage-therapy may be more effective on acute than on chronic infections, as the application of an adequate dose of the right phage/phages during early stages of a bacterial infection (during log-phase growth and before the establishment of biofilm), should efficiently eliminate the pathogen [D'Hérrelle and Smith, 1930; discussed and reviewed by Abedon (2014)]. Thus, the state and abundance of the bacteria in the body is important to ensure phage-host interaction and phage proliferation in the infected organs. For our experiments, we selected the intraperitoneal injection of *F. psychrophilum* as reproducible infection method, although it is considered relatively harsh for the fish and distant from how it would happen in an aquaculture environment (Madsen and Dalsgaard, 1999). With this method, the injected bacteria spread rapidly in the fish organs (peritoneal

cavity, spleen, kidney, and brain) in the first 4 days after the infection procedure (Madsen et al., 2013). As expected, we were able to detect *F. psychrophilum* in the internal organs of the fish 1 dpi but no difference in the development of the infection in the three feed-groups was observed (Experiment A). Similar results were obtained by Madsen et al. (2013) where the simultaneous IP injection of phage FpV9 did not reduce the occurrence of *F. psychrophilum* in the organs. When looking at the concentration of phages, we detected a large variation in intestinal phage concentration among sampled fish in the first 10–20 dpi, which was more prominent in fish fed phage-sprayed feed. This might be the result of the bacterial infection, since the reduced feed intake is one of the clinical signs of infected/diseased fish (Nematollahi et al., 2003). The lower concentration of phages detected in the intestine of dead/moribund fish supports this hypothesis. As observed by Madsen et al. (2013), no increase in phage concentration in the kidney in the presence of *F. psychrophilum* was observed. Only few dead fish showed a higher phage concentration indicating phage proliferation in the organ. A similar situation was observed for spleen samples. More markedly for fish fed with phage-sprayed feed, the overall frequency of phage detection was higher when the bacterium was present (48.6% against 35% of control fish). We believe that the undetected phage proliferation in organs containing the bacterium may be a consequence of the relatively low concentration of phages obtained *in situ* by the administration of phage-treated feed pellets (in experiment A). To conclude, our understanding of phage replication *in situ* is limited and so, one should focus on optimizing the delivery of high densities of phages with the aim of maximizing phage concentrations at the site of infection, without relying on the self-replicating properties of the phage (Abedon and Thomas-Abedon, 2010; Abedon, 2014). In addition, the role of poorly mixed environments (biofilm) for phage-host encounter in fish organs should be better understood (Abedon and Thomas-Abedon, 2010; Abedon, 2014).

Finally, when comparing our results on fish survival, it is important to mention that the fish used in Experiment A and B were at the fry stage (2–3 g), whereas larger fish (fingerlings, ∼7 g) were used in experiment C. This is important as higher mortalities from *F. psychrophilum* infections are generally observed in fry population (80%) than larger fish (fingerlings and bigger; 20%) during disease outbreaks in fish farms (Lorenzen, 1994). Differences in fish size and immune status between experiments (Madsen and Dalsgaard, 1999) thus likely explain why the final mean mortality in the fingerlings in Experiment C was lower than for fish in Experiment B, in control groups, despite that they were challenged with the highest bacterial dose.

CONCLUSION AND FUTURE PERSPECTIVES

Even though phage therapy seems very attractive and straightforward, it presents various drawbacks/challenges. In our experiments, we believe that the delivery of bacteriophages applied by Fixed Phage Ltd. technology on feed pellets represents an effective method of delivering a product in the intestine with a feasible application in the field. It also reduces the time-consuming tasks of spraying and drying feed pellets. We believe that the inefficient delivery of phages to the internal organs (i.e., the high loss of infective phages during the delivery process across the intestinal barrier as well as the potential too low phage concentration applied in feed and bath experiments) was the reason for the lack of a beneficial effect on survival of fish challenged with *F. psychrophilum*. The significant increase in fish survival upon IP administration supports the hypothesis that the delivery of higher dosages of phages at the infection site could positively contribute to fish health/recovery, and emphasizes the need for applying higher concentrations of phages on the feed to account of the loss of infective phages during the delivery process. Based on preliminary experiments, we have indications that increasing the number of phages per gram of feed also increases the re-isolation percentage of phages from the fish organs. We therefore think that it is reasonable to suggest that increasing the phage concentration on the feed will lead to increased phage densities in the target organs. However, establishing the relationship between phage doses on the feed and the subsequent concentration in the organs upon delivery is, however, an important next step in the development and optimization of the feed-based delivery.

DATA AVAILABILITY STATEMENT

The original contributions presented in the study are included in the article/**Supplementary Material**, further inquiries can be directed to the corresponding author.

ETHICS STATEMENT

The animal study was reviewed and approved by the Animal Experiments Inspectorate of Denmark (Dyreforsøgstilsynet, permission n. 2013-15-2934-00976 until 07-10-2019 and n. 2019-15-0201-00159 from 08-10-2019) (Experiments A and B) and by the National Animal Experiment Board (Eläinkoelautakunta, ELLA) (personal license, under project ESAVI/4225/04.10.07/2017) (Experiment C).

AUTHOR CONTRIBUTIONS

VD: planning and execution of experiments A and B including phage-sprayed feed preparation, fish sampling and phage analysis in fish organs, data preparation and analysis, and writing of the manuscript. ID: planning, execution and supervision of experiments A and B, data interpretation, and manuscript preparation. KS and TW: planning and execution of experiment C and contribution to manuscript preparation. DC: production of PEG-purified phage solutions applied on feed pellets and contribution to manuscript preparation. ME-R: TEM imaging of bacteriophages FpV4 and FPSV-D22 and contribution to manuscript preparation. JC: production of

phage-immobilized feed and contribution to manuscript preparation. MM: data interpretation, manuscript preparation, and funding acquisition. LM: planning, execution and supervision of fish experiments A and B, data interpretation, and manuscript preparation. All authors have read and approved the final version of the manuscript.

FUNDING

This work resulted from the BONUS FLAVOPHAGE project supported by BONUS (Art 185), funded jointly by the EU, Innovation Fund Denmark and Academy of Finland.

ACKNOWLEDGMENTS

The authors would like to thank Kári Karbech Mouritsen for his excellent technical support during fish experimental trials and fish samplings as well as the fish caretakers of the Blue Unit at the Technical University of Denmark.

SUPPLEMENTARY MATERIAL

The Supplementary Material for this article can be found online at: https://www.frontiersin.org/articles/10.3389/fmicb.2021.628309/full#supplementary-material

REFERENCES

Abedon, S. T. (2014). Phage therapy: eco-physiological pharmacology. *Scientifica* 2014:581639. doi: 10.1155/2014/581639

Abedon, S. T., and Thomas-Abedon, C. (2010). Phage therapy pharmacology. *Curr. Pharm. Biotechnol.* 11, 28–47. doi: 10.2174/138920110790725410

Almeida, G. M. F., Mäkelä, K., Laanto, E., Pulkkinen, J., Vielma, J., and Sundberg, L. R. (2019). The fate of bacteriophages in recirculating aquaculture systems (RAS)— towards developing phage therapy for RAS. *Antibiotics* 8:192. doi: 10.3390/antibiotics8040192

Amend, D. F. (1981). Potency testing of fish vaccines. *Develop. Biol. Standard* 49, 447–454.

Barr, J. J. (2017). A bacteriophages journey through the human body. *Immunol. Rev.* 279, 106–122. doi: 10.1111/imr.12565

Bernardet, J. F., Segers, P., Vancanneyt, M., Berthe, F., Kersters, K., and Vandamme, P. (1996). Cutting a gordian knot: emended classification and description of the genus *Flavobacterium*, emended description of the family *Flavobacteriaceae*, and proposal of *Flavobacterium hydatis* nom. nov. (basonym, *Cytophaga aquatilis* Strohl and Tait 1978). *Int. J. Syst. Bacteriol.* 46, 128–148. doi: 10.1099/00207713-46-1-128

Borg, A. F. (1948). *Studies on Myxobacteria Associated with Diseases in Salmonid Fishes*. Ph. D. Thesis, University of Washington, Seattle, WA.

Borg, A. F. (1960). Studies on myxobacteria associated with diseases in salmonid fishes. *Wildlife Dis. Ser.* 8, 1–85.

Bruun, M. S., Madsen, L., and Dalsgaard, I. (2003). Efficiency of oxytetracycline treatment in rainbow trout experimentally infected with *Flavobacterium psychrophilum* strains having different *in vitro* antibiotic susceptibilities. *Aquaculture* 215, 11–20. doi: 10.1016/S0044-8486(01)00897-3

Bruun, M. S., Schmidt, A. S., Madsen, L., and Dalsgaard, I. (2000). Antimicrobial resistance patterns in Danish isolates of *Flavobacterium psychrophilum*. *Aquaculture* 187, 201–212. doi: 10.1016/S0044-8486(00)00310-0

Bucking, C., and Wood, C. M. (2009). The effect of postprandial changes in pH along the gastrointestinal tract on the distribution of ions between the solid and fluid phases of chyme in rainbow trout. *Aquac. Nutr.* 15, 282–296. doi: 10.1111/j.1365-2095.2008.00593.x

Castillo, D., Andersen, N., Kalatzis, P. G., and Middelboe, M. (2019). Large phenotypic and genetic diversity of prophages induced from the fish pathogen *Vibrio anguillarum*. *Viruses* 11:983. doi: 10.3390/v11110983

Castillo, D., Christiansen, R. H., Espejo, R., and Middelboe, M. (2014). Diversity and geographical distribution of *Flavobacterium psychrophilum* isolates and their phages: patterns of susceptibility to phage infection and phage host range. *Microb. Ecol.* 67, 748–757. doi: 10.1007/s00248-014-0375-8

Castillo, D., Higuera, G., Villa, M., Middelboe, M., Dalsgaard, I., Madsen, L., et al. (2012). Diversity of *Flavobacterium psychrophilum* and the potential use of its phages for protection against bacterial cold water disease in salmonids. *J. Fish Dis.* 35, 193–201. doi: 10.1111/j.1365-2761.2011.01336.x

Castillo, D., and Middelboe, M. (2016). Genomic diversity of bacteriophages infecting the fish pathogen *Flavobacterium psychrophilum*. *FEMS Microbiol. Lett.* 363:fnw272. doi: 10.1093/femsle/fnw272

Christiansen, R. H. (2014). *Phage-Host Interactions in Flavobacterium Psychrophilum and the Potential for Phage Therapy in Aquaculture*. Ph. D. Thesis, University of Copenhagen, Copenhagen.

Christiansen, R. H., Dalsgaard, I., Middelboe, M., Lauritsen, A. H., and Madsen, L. (2014). Detection and quantification of *Flavobacterium psychrophilum*-specific bacteriophages *in vivo* in rainbow trout upon oral administration: implications for disease control in aquaculture. *Appl. Environ. Microbiol.* 80, 7683–7693. doi: 10.1128/AEM.02386-14

Clokie, M. R. J., and Kropinski, A. M. (eds) (2009). *Bacteriophages. Methods and Protocols. Volume 1: Isolation, Characterization, and Interactions*. Totowa, NJ: Humana Press. doi: 10.1007/978-1-60327-164-6

Culot, A., Grosset, N., and Gautier, M. (2019). Overcoming the challenges of phage therapy for industrial aquaculture: a review. *Aquaculture* 513:734423. doi: 10.1016/j.aquaculture.2019.734423

Dąbrowska, K. (2019). Phage therapy: what factors shape phage pharmacokinetics and bioavailability? Systematic and critical review. *Med. Res. Rev.* 39, 2000–2025. doi: 10.1002/med.21572

Dalsgaard, I., and Madsen, L. (2000). Bacterial pathogens in rainbow trout, *Oncorhynchus mykiss* (Walbaum), reared at Danish freshwater farms. *J. Fish Dis.* 23, 199–209. doi: 10.1046/j.1365-2761.2000.00242.x

Del Cerro, A., Márquez, I., and Prieto, J. M. (2010). Genetic diversity and antimicrobial resistance of *Flavobacterium psychrophilum* isolated from cultured rainbow trout, *Onchorynchus mykiss* (Walbaum), in Spain. *J. Fish Dis.* 33, 285–291. doi: 10.1111/j.1365-2761.2009.01120.x

D'Hérrelle, F., and Smith, G. H. (1930). *The Bacteriophage and Its Clinical Application*. Springfield, I11: Charles C. Thomas.

Dion, M. B., Oechslin, F., and Moineau, S. (2020). Phage diversity, genomics and phylogeny. *Nat. Rev. Microbiol.* 18, 125–138. doi: 10.1038/s41579-019-0311-5

Duarte, J., Pereira, C., Moreirinha, C., Salvio, R., Lopes, A., Wang, D., et al. (2018). New insights on phage efficacy to control *Aeromonas salmonicida* in aquaculture systems: an *in vitro* preliminary study. *Aquaculture* 495, 970–982. doi: 10.1016/j.aquaculture.2018.07.002

Holt, R. A., Rohovec, J. S., and Fryer, J. L. (1993). "Bacterial cold-water disease," in *Bacterial Diseases of Fish*, eds N. R. Inglis, V. Roberts, and R. J. Bromage (Sydney, NSW: Halsted Press), 3–22.

Izumi, S., and Aranishi, F. (2004). Relationship between *gyr*A mutations and quinolone resistance in *Flavobacterium psychrophilum* isolates. *Appl. Environ. Microbiol.* 70, 3968–3972. doi: 10.1128/AEM.70.7.3968-3972.2004

Jaiswal, A., Koley, H., Mitra, S., Saha, D. R., and Sarkar, B. (2014). Comparative analysis of different oral approaches to treat *Vibrio cholerae* infection in adult mice. *Int. J. Med. Microbiol.* 304, 422–430. doi: 10.1016/j.ijmm.2014.02.007

Kalatzis, P. G., Bastías, R., Kokkari, C., and Katharios, P. (2016). Isolation and characterization of two lytic bacteriophages, φSt2 and φGrn1; phage therapy application for biological control of *Vibrio alginolyticus* in aquaculture live feeds. *PLoS One* 11:e0151101. doi: 10.1371/journal.pone.0151101

Kazimierczak, J., Wójcik, E. A., Witaszewska, J., Guziński, A., Górecka, E., Stańczyk, M., et al. (2019). Complete genome sequences of *Aeromonas* and *Pseudomonas* phages as a supportive tool for development of antibacterial treatment in aquaculture. *Virol. J.* 16:4. doi: 10.1186/s12985-018-1113-5

Kowalska, J. D., Kazimierczak, J., Sowińska, P. M., Wójcik, E. A., Siwicki, A. K., and Dastych, J. (2020). Growing trend of fighting infections in aquaculture environment—opportunities and challenges of phage therapy. *Antibiotics* 9:301. doi: 10.3390/antibiotics9060301

Kum, C., Kirkan, S., Sekkin, S., Akar, F., and Boyacioglu, M. (2008). Comparison of *in vitro* antimicrobial susceptibility in *Flavobacterium psychrophilum* isolated from rainbow trout fry. *J. Aquat. Anim. Health* 20, 245–251. doi: 10.1577/H07-040.1

Laanto, E., Bamford, J. K. H., Ravantti, J. J., and Sundberg, L. R. (2015). The use of phage FCL-2 as an alternative to chemotherapy against columnaris disease in aquaculture. *Front. Microbiol.* 6:829. doi: 10.3389/fmicb.2015.00829

Leppänen, M., Maasilta, I. J., and Sundberg, L. R. (2019). Antibacterial efficiency of surface-immobilized *Flavobacterium*-infecting bacteriophage. *ACS Appl. Bio Mater.* 2, 4720–4727. doi: 10.1021/acsabm.9b00242

Lorenzen, E. (1994). *Studies on Flexibacter Psychrophilus in Relation to Rainbow Trout Fry Syndrome (RTFS)*. Ph. D. Thesis, National Veterinary Laboratory & Royal Veterinary and Agricultural University, Århus.

Lorenzen, E., Dalsgaard, I., From, J., Hansen, E. M., Hørlyck, V., Korsholm, H., et al. (1991). Preliminary investigation of fry mortality syndrome in rainbow trout. *Bull. Eur. Ass. Fish Pathol.* 11, 77–79.

Madsen, L., Bertelsen, S. K., Dalsgaard, I., and Middelboe, M. (2013). Dispersal and survival of *Flavobacterium psychrophilum* phages *in vivo* in rainbow trout and *in vitro* under laboratory conditions: implications for their use in phage therapy. *Appl. Environ. Microbiol.* 79, 4853–4861. doi: 10.1128/AEM.00509-13

Madsen, L., and Dalsgaard, I. (1999). Reproducible methods for experimental infection with *Flavobacterium psychrophilum* in rainbow trout *Oncorhynchus mykiss*. *Dis. Aquat. Organ.* 36, 169–176. doi: 10.3354/dao036169

Madsen, L., and Dalsgaard, I. (2000). Comparative studies of Danish *Flavobacterium psychrophilum* isolates: ribotypes, plasmid profiles, serotypes and virulence. *J. Fish Dis.* 23, 211–218. doi: 10.1046/j.1365-2761.2000.00240.x

Madsen, L., and Dalsgaard, I. (2008). Water recirculation and good management: potential methods to avoid disease outbreaks with *Flavobacterium psychrophilum*. *J. Fish Dis.* 31, 799–810. doi: 10.1111/j.1365-2761.2008.00971.x

Mateus, L., Costa, L., Silva, Y. J., Pereira, C., Cunha, A., and Almeida, A. (2014). Efficiency of phage cocktails in the inactivation of *Vibrio* in aquaculture. *Aquaculture* 42, 167–173. doi: 10.1016/j.aquaculture.2014.01.001

Mattey, M. (2016). Treatement of Bacterial Infections in Aquaculture. International Patent Application no. PCT/EP2016/058809. Geneva: World Intellectual Property Organization.

Mattey, M. (2018). Treatment of Bacterial Infections in Aquaculture. U.S. Patent Application no. 15/567,825. Washigton, DC: U.S. Patent and Trademark Office.

Midtlyng, P. J. (2016). "Chapter 6. Methods for measuring efficacy, safety and potency of fish vaccines," in *Fish Vaccines*, ed. A. Adams (Basel: Springer Basel), 119–141. doi: 10.1007/978-3-0348-0980-1

Nematollahi, A., Decostere, A., Pasmans, F., and Haesebrouck, F. (2003). *Flavobacterium psychrophilum* infections in salmonid fish. *J. Fish Dis.* 26, 563–574. doi: 10.1046/j.1365-2761.2003.00488.x

Nguyen, S., Baker, K., Padman, B. S., Patwa, R., Dunstan, R. A., Weston, T. A., et al. (2017). Bacteriophage transcytosis provides a meachanism to cross epithelial cell layers. *mBio* 8:e01874–17. doi: 10.1128/mBio.01874-17

Nikapitiya, C., Dananjaya, S. H. S., Edirisinghe, S. L., Chandrarathna, H. P. S. U., and Lee, J. (2020). Development of phage delivery by bioencapsulation of *Artemia* nauplii with *Edwardsiella tarda* phage (ETP-1). *Braz. J. Microbiol.* 51:2153–2162. doi: 10.1007/s42770-020-00324-y

Roux, M. (2011). On an invisible microbe antagonistic to dysentery bacilli . Note by M. F. d'Herelle, presented by M. Roux. Comptes rendus academie des sciences 1917; 165:373–5. *Bacteriophage* 1, 3–5. doi: 10.4161/bact.1.1.14941

Salmond, G. P. C., and Fineran, P. C. (2015). A century of the phage: past, present and future. *Nat. Rev. Microbiol.* 13, 777–786. doi: 10.1038/nrmicro3564

Schmidt, A. S., Bruun, M. S., Dalsgaard, I., Pedersen, K., and Larsen, J. L. (2000). Occurrence of antimicrobial resistance in fish-pathogenic and environmental bacteria associated with four Danish rainbow trout farms. *Appl. Environ. Microbiol.* 66, 4908–4915. doi: 10.1128/AEM.66.11.4908-4915.2000

Secombes, C. J., and Wang, T. (2012). "The innate and adaptive immune system of fish," in *Infectious Disease in Aquaculture*, ed. A. Brian (Cambridge: Woodhead Publishing Limited), 3–68. doi: 10.1533/9780857095732.1.3

Segner, H., Reiser, S., Ruane, N., Rösch, R., Steinhagen, D., and Vehanen, T. (2019). *Welfare of Fishes in Aquaculture. FAO Fisheries and Aquaculture Circular No. C1189*. Budapest: FAO.

Stenholm, A. R., Dalsgaard, I., and Middelboe, M. (2008). Isolation and characterization of bacteriophages infecting the fish pathogen *Flavobacterium psychrophilum*. *Appl. Environ. Microbiol.* 74, 4070–4078. doi: 10.1128/AEM.00428-08

Sundell, K., Landor, L., Nicolas, P., Jørgensen, J., Castillo, D., Middelboe, M., et al. (2019). Phenotypic and genetic predictors of pathogenicity and virulence in *Flavobacterium psychrophilum*. *Front. Microbiol.* 10:1711. doi: 10.3389/fmicb.2019.01711

Sundell, K., and Wiklund, T. (2011). Effect of biofilm formation on antimicrobial tolerance of *Flavobacterium psychrophilum*. *J. Fish Dis.* 34, 373–383. doi: 10.1111/j.1365-2761.2011.01250.x

Toyama, T., Kita-Tsukamoto, K., and Wakabayashi, H. (1994). Identification of *Cytophage psychrophila* by PCR targeted 16S ribosomal RNA. *Fish Pathol.* 29, 271–275. doi: 10.3147/jsfp.29.271

Twort, F. W. (1915). An investigation on the nature of ultra-microscopic viruses. *Lancet* 186, 1241–1243. doi: 10.1016/S0140-6736(01)20383-3

Van Belleghem, J. D., Dąbrowska, K., Vaneechoutte, M., Barr, J. J., and Bollyky, P. L. (2019). Interactions between bacteriophage, bacteria, and the mammalian immune system. *Viruses* 11:10. doi: 10.3390/v11010010

Conflict of Interest: JC was employed by the company Fixed Phage Ltd. (Glasgow, United Kingdom).

The remaining authors declare that the research was conducted in the absence of any commercial or financial relationships that could be construed as a potential conflict of interest.

frontiers in Microbiology

ORIGINAL RESEARCH
published: 28 May 2021
doi: 10.3389/fmicb.2021.662461

Isolation and Characterization of Potential *Salmonella* Phages Targeting Multidrug-Resistant and Major Serovars of *Salmonella* Derived From Broiler Production Chain in Thailand

*Wattana Pelyuntha[1], Ruttayaporn Ngasaman[2], Mingkwan Yingkajorn[3], Kridda Chukiatsiri[4], Soottawat Benjakul[5] and Kitiya Vongkamjan[1,5,6]**

[1] Faculty of Agro-Industry, Prince of Songkla University, Songkhla, Thailand, [2] Faculty of Veterinary Science, Prince of Songkla University, Songkhla, Thailand, [3] Division of Pathology, Faculty of Medicine, Prince of Songkla University, Songkhla, Thailand, [4] Faculty of Animal Science and Technology, Maejo University, Chiang Mai, Thailand, [5] International Center of Excellence in Seafood Science and Innovation, Faculty of Agro-Industry, Prince of Songkla University, Songkhla, Thailand, [6] Department of Biotechnology, Faculty of Agro-Industry, Kasetsart University, Bangkok, Thailand

Salmonella is a major foodborne pathogen that causes foodborne disease in humans through consumption of contaminated foods, especially those of animal origin. Multiple *Salmonella* strains are antibiotic-resistant due to the common use of antibiotics in farm animals, including broiler farms. In this study, an alternative strategy using phage-based treatment was evaluated against *Salmonella* isolated from the broiler production. The prevalence of *Salmonella* spp. showed up to 46.2 and 44.4% in bedding samples from the broiler farms located in eastern and southern Thailand, respectively. Overall, 21 samples (36.2%) were positive for *Salmonella* and eight serovars were recovered from cloacal swabs, bedding materials (rice husk), and boot swabs collected from five farms. Up to 20 *Salmonella* phages were isolated from seven water samples from wastewater treatment ponds, a river, and a natural reservoir in Songkhla province. Isolated phages were investigated, as well as their lysis ability on eight target *Salmonella* serovars derived from broiler farms, five foodborne outbreak-related serovars, and 10 multidrug-resistant (MDR) serovars. All phages showed a strong lytic ability against five serovars of *Salmonella* derived from broiler farms including Kentucky, Saintpaul, Schwarzengrund, Corvalis, and Typhimurium; three foodborne outbreak serovars including Enteritidis, Typhimurium, and Virchow; and eight MDR serovars including Agona, Albany, Give, Kentucky, Typhimurium, Schwarzengrund, Singapore, and Weltevreden. Three phages with the highest lysis potential including vB_SenS_WP109, vB_SenS_WP110, and vB_SenP_WP128 were selected for a phage cocktail preparation. Overall, a phage

OPEN ACCESS

Edited by:
Robert Czajkowski, University of Gdańsk, Poland

Reviewed by:
Juhee Ahn, Kangwon National University, South Korea
Dacil Rivera, Andres Bello University, Chile

***Correspondence:**
Kitiya Vongkamjan
kitiyavongkamjan.a@ku.th;
kitiya.v@psu.ac.th

Specialty section:
This article was submitted to Antimicrobials, Resistance and Chemotherapy, a section of the journal Frontiers in Microbiology

Received: *01 February 2021*
Accepted: *09 April 2021*
Published: *28 May 2021*

Citation:
Pelyuntha W, Ngasaman R, Yingkajorn M, Chukiatsiri K, Benjakul S and Vongkamjan K (2021) Isolation and Characterization of Potential Salmonella Phages Targeting Multidrug-Resistant and Major Serovars of Salmonella Derived From Broiler Production Chain in Thailand. Front. Microbiol. 12:662461. doi: 10.3389/fmicb.2021.662461

cocktail could reduce *Salmonella* counts by 2.2–2.8 log units at 6 h of treatment. Moreover, *Salmonella* did not develop a resistant pattern after being treated with a phage cocktail. Findings here suggest that a phage cocktail is an effective biocontrol to combat *Salmonella* derived from broiler production chain, other serovars linked to foodborne outbreaks, and MDR serovars.

Keywords: animal farm, antibiotic resistance, biocontrol, broiler, phage cocktail, *Salmonella*, phage lysis, phage therapy

INTRODUCTION

Salmonellosis is one of the most common foodborne infections worldwide caused by consumption of contaminated foods with *Salmonella* spp. and becoming an important public health concern (Eng et al., 2015). Poultry meat and its products have served as major sources of *Salmonella* spp., which have caused human and animal diseases as well as economic losses to the poultry industry (Barbour et al., 2015). In Thailand, *Salmonella* contamination in broilers and poultry meat has been previously reported (Sripaurya et al., 2019). Although *Salmonella* contamination in broiler farms (at the beginning of the poultry production chain) is commonly reported, Dookeran et al. (2012) observed that broiler carcass contamination with *Salmonella* spp. increased during transportation from the farm to the processing plant, during processing, and at retail outlets.

For the poultry industry, controlling the presence of *Salmonella* is crucial for food safety as well as for preventing the spread of antimicrobial resistance (Pulido-Landínez, 2019). Antimicrobial agents are widely used for growth promotion or treatment purposes (World Health Organization (WHO), 2018), which can lead to the occurrence of antimicrobial-resistant strains in broilers and broiler meat. These will link to a potential source for transmission to human since antibiotic-resistant *Salmonella* isolated at the farm level may spread to humans through direct contact or contaminated meat (Dolejska et al., 2013). Overall, antimicrobial-resistant *Salmonella* strains are frequently encountered worldwide and the proportion of antimicrobial-resistant dramatically increased over the past decade (World Health Organization (WHO), 2018). To decrease the risk factors that are related to *Salmonella* contamination in poultry meat production, the steps of *Salmonella* elimination from poultry cultivation to processing and handling (from farm to table) are necessary (Vandeplas et al., 2010; Alum et al., 2016).

Bacteriophages (phages) are viruses of bacteria and not harmful to humans and animals. Phages have been used to treat bacterial infection caused by MDR microorganisms and treat against several foodborne pathogens (Goodridge and Bisha, 2011; Dy et al., 2018) with a strong bactericidal effect and high specificity. Phage has become an attractive approach to combat *Salmonella* in broilers or broiler meat due to its high specificity and effortless in administration or application (Lim et al., 2012; Nabil et al., 2018). In addition, several previous studies have confirmed that a phage cocktail composed of several phages was more effective in controlling *Salmonella* spp. than one phage alone (Goodridge, 2010; Hooton et al., 2011; Chan and Abedon, 2012; Chan et al., 2013; Clavijo et al., 2019; Petsong et al., 2019). However, since levels of antimicrobial resistance were generally high in *Salmonella* spp. isolated from broilers, it is therefore necessary to investigate the effectiveness of phages and a developed phage cocktail against MDR *Salmonella* strains derived from broiler production chain, including broiler farms, slaughterhouses, and retail stores at the wet market.

Therefore, this study aims to evaluate the effective control strategy for *Salmonella* that were detected in broiler farms using phage cocktail. Environmental samples and cloacal swabs were screened for the occurrence of *Salmonella* in broiler farms from eastern and southern Thailand. Information from this study on the lysis ability of phages against *Salmonella* derived from broiler farms, MDR-*Salmonella* strains, and those major serovars linked to foodborne outbreaks will be useful for further phage selection and consideration of using phages as a potential biocontrol to improve food safety along broiler production or in poultry meat processing.

MATERIALS AND METHODS

Broiler Farms and Sampling Location

Five broiler farms located in the eastern (n = 2) and southern (n = 3) areas of Thailand were included in this study. Broiler farms in this study are large flocks with over 20,000 birds. All farms are enclosed, located far away from human communities, natural reservoirs, and main roads, in a wide-open space. All farms have generally high infrastructure, high sanitary and hygienic conditions, and adequate biosecurity measures in controlling stray animals, rodents, reptiles, and amphibians. Waste and by-products are usually removed from a farm without contaminating the environment. In some farms, bedding materials are dried up and packaged within broiler houses before sold as manure.

Collection of Samples

For two farms located in the east of Thailand, bedding materials composed of dried husk were collected by pooling sample (100 g) from four sections of a given pen on days 0, 2, 4, 6, 8, 9, 10, 15, 16, 20, 22, 23, 27, 31, 37, 39, and 42 of poultry cultivation. A total of 26 bedding samples were collected from farm A and farm B (**Table 1**). For three farms located in the south of Thailand, seven bedding samples were collected from farm C (n = 2), farm D (n = 2), and farm E (n = 3). Each sample was collected by pooling sample (100 g) from four sections of a given pen. Cloacal swabs were collected from farm C (n = 5), farm D

TABLE 1 | Distribution of *Salmonella* spp. in broiler farms.

Farm	No. of positive samples/No. of collected samples[a] (%)			
	Bedding	Cloacal swab	Boot swab	Total
Eastern Farms				
Farm A	5/5	nc	nc	5/5 (100)
Farm B	7/21	nc	nc	7/21 (33.3)
Total	12/26 (46.2)	0	0	12/26 (46.2)
Southern Farms				
Farm C	2/3	3/5	2/2	7/10 (70)
Farm D	1/4	0/6	0/2	1/12 (8.3)
Farm E	1/2	0/5	0/3	1/10 (10)
Total	4/9 (44.4)	3/16 (18.8)	2/7 (28.6)	9/32 (28.1)

[a]*nc refers to no samples collected.*

(n = 6), and farm E (n = 5). Each cloacal sample was collected by swabbing 10 chickens with individual cotton stick, pooled as one sample, and transferred to a sterile zip-lock bag. Boot cover swab samples were collected from farm C (n = 5), farm D (n = 6), and farm E (n = 5). Each boot cover swab sample was collected by wearing boot covers and walking up and down each of the four sections of a given pen. All samples were kept with sterile plastic bags and stored in an icebox (4°C) during transportation to the laboratory for analysis.

Salmonella Isolation and Confirmation

Collected samples were processed for *Salmonella* isolation following the protocol of Biomérieux company that was modified from ISO 6579:2002. Briefly, an approximately 25 g of bedding sample was enriched with 225 ml of buffered peptone water (BPW) (#421121, Biomérieux, Marcy l'Étoile, France) supplemented with Salmonella Supplement Tablet (#421202, Biomérieux, Marcy l'Étoile, France). For cloacal swabs and boot cover swabs, 90 ml of BPW supplemented with Salmonella Supplement Tablet was added to each sample. All samples were incubated at 41.5°C for 18 h. A loopful of each enriched sample was streaked on SALMA plate (#418247, Biomérieux, Marcy l'Étoile, France) and incubated at 37°C for 24 h. A pink to purple typical colony on the plate was observed and re-streaked on tryptic soy agar (TSA) plate to obtain a pure culture for further confirmation. *Salmonella* isolates were kept in 15% glycerol at -80°C for further analysis. Colonies of *Salmonella* were selected for serotyping by the agglutination latex test by a commercial service company (S. A. P. Laboratory Co., Ltd., Bangkok, Thailand).

Bacteriophage Isolation, Purification, and Lysate Preparation

Wastewater samples from a wastewater treatment station of Prince of Songkla University hospital were collected for phage isolation. These include three samples of aerated wastewater treatment ponds (A1, A2, and A3) and two samples of sediment wastewater treatment pond (S1 and S2). Approximately 100 ml of each sample was kept in a sterile bottle and stored in an icebox (4°C) during transportation to the laboratory for analysis. One sample from a river (R) and another from a natural reservoir (NR) in Songkhla province were collected using sterile bottles and kept in an icebox during transportation to the laboratory. *Salmonella* phages were isolated using enrichment isolation with a multi-strain of *Salmonella* mixture obtained from broiler farms (**Table 2**) and from our laboratory collection (*S.* Agona H2-016 and *S.* Anatum A4-525). Enrichment and isolation steps were performed following a standard protocol from our laboratory (Petsong et al., 2019). Plaques were observed on each host lawn. A single plaque was chosen for purification for three passages with a specific host that showed a positive result, using a double-layer agar technique. Isolated plaque from the third purification passage was used to prepare 10-fold serial dilutions in SM buffer. Appropriate dilutions were used to prepare the overlay with the given host to yield the semi-confluent lysis and then harvest with 5 ml of SM buffer followed by centrifugation at 6000 rpm for 15 min at 4°C. The supernatant was filtrated through 0.20-μm syringe filters, and phage lysates were kept at 4°C. The phage titer was determined by counting plaques present on each plate of a given dilution (Petsong et al., 2019).

Host Range Determination

Lysis ability for each phage was determined by a spot test on the bacterial lawn of a given *Salmonella* strain from broiler farms in this study, foodborne outbreak-linked *Salmonella* (*S.* Enteritidis S5-371, *S.* Hadar PPI-013, *S.* Infantis S5-506, *S.* Typhimurium S5-370, and *S.* Virchow H2-117), and the MDR-*Salmonella* strains listed in **Supplementary Table 1**. All selected MDR strains were previously isolated from several types of samples collected from the broiler production chain such as chicken meat stalls located in wet markets, slaughterhouses, commercial farms, and free range farms. All MDR isolates and their antibiotic resistance profiles were consequently investigated using a standard agar disk diffusion assay according to the Clinical and Laboratory Standard Institute guidelines (Clinical and Laboratory Standard Institute (CLSI), 2015; Sripaurya et al., 2019). Collection of *Salmonella* strains was kept at the Faculty of Agro-Industry, Prince of Songkla University. Lysis ability of isolated phages was determined by spotting 10 μl of each phage lysate (8 log PFU/ml) on the bacterial host lawn. Two independent replicates were performed. Phage lysis patterns were determined after 18–24 h of incubation at 37°C (Petsong et al., 2019).

Efficiency of Plating

Three phage isolates with the highest % of lytic ability (see in **Table 3**) were selected for the assessment of efficiency of plating (EOP), following the protocol of Vongkamjan et al. (2017). Three phages were tested three times independently using four dilutions (3–6 log PFU/ml) against 24 different *Salmonella* isolates (eight serovars derived from broiler farms, five foodborne outbreak-related serovars, and 10 MDR serovars) and one of original strain for phage isolation. The EOP was calculated using the given formula:

EOP = average PFU on target bacteria/average PFU on host bacteria

Efficiency of plating was classified as "High production" when the ratio was 0.5 or more. An EOP of 0.1 or higher, but below

TABLE 2 | Serovars of *Salmonella* derived from broiler farms.

Farm (no. of positive samples)	Type of sample	Serovar[a]	Code name
Eastern Farms			
Farm A (5)	Bedding	Schwarzengrund*#	H2
		Saintpaul*#	H13
		Albany*#	H32
		Kentucky*#	S1H28
		Kentucky	S2H28
Farm B (7)	Bedding	Mbandaka*#	H17D2
		Mbandaka	H1D8
		Mbandaka	H5D42
		Agona	H5D42
		Agona*#	H3D6
		Agona	H16D20
		Agona	H14D23
		Kentucky	H9D9
Southern Farms			
Farm C (7)	Bedding	Typhimurium	F1-W1-S1
		Typhimurium	F1-W1-S3
	Cloacal swab	Typhimurium*#	F1-W1-C2
		Typhimurium	F1-W1-C3
		Typhimurium	F1-W1-C4
	Boot swab	Typhimurium	F1-W1-B1
		Typhimurium	F1-W1-B2
Farm D (1)	Bedding	Agona#	F2-W3-S3
Farm E (1)	Bedding	Corvalis*#	F3-W5-S2

[a]*Serovars with (*) indicate serovars used for phage enrichment and isolation. Serovars with (#) indicate serovars used for host range determination.*

0.5, was considered as "Medium production" efficiency, and that between 0.001 and 0.1 was considered as "Low production" efficiency. An EOP of 0.001 or below and when any dilutions did not result in any plaque formation were classified as inefficient (Mirzaei and Nilsson, 2015; Manohar et al., 2019).

Transmission Electron Microscopy Analysis

Selected phages were identified as the morphology by transmission electron microscopy (TEM) analysis. Grid samples were prepared using a given phage lysate (8 log PFU/ml) following a protocol of Vongkamjan et al. (2012). Uranyl acetate (1%) was used for negative staining. The imaging was acquired with TEM model JEM-2010 (JEOL Ltd., Tokyo, Japan) at 160 kV and an instrumental magnification of 100,000× at Scientific Equipment Center, Prince of Songkla University, Hat Yai, Thailand.

Development and Efficacy Evaluation of a Phage Cocktail

Three different phages with the highest lytic activity were mixed together in equal proportions (a ratio of 1:1:1) to obtain a phage cocktail stock at a concentration of 8 log PFU/ml. Selected phages used for phage cocktail development were chosen based on the highest % total lysis ability along with their lysis profile patterns against the strains derived from broiler farms and foodborne outbreak-related and MDR isolates. A developed phage cocktail was evaluated for its effectiveness on five strains linked to foodborne outbreaks and eight other strains presenting major serovars derived from broiler farms in Thailand (marked with * in **Table 2**). A 20-ml suspension of a given strain (2 log CFU/ml) was mixed with 20 ml of a phage cocktail (final concentration of 5 and 7 log PFU/ml) at the ratio of 1:1 by volume [multiplicity of infection (MOI) 1000 and 100,000] and incubated at 37°C in a shaking incubator at 220 rpm for 18 h (Petsong et al., 2019). The culture broth was sampled every 6-h intervals for 18 h. Samples were serially 10-fold diluted with phosphate buffer saline (PBS) to obtain the appropriate dilution. Each dilution (0.1 ml) was spread on TSA plates. All plates were incubated at 37°C for 24–48 h. The culture of each *Salmonella* without a phage cocktail was served as control. All the tests were run in triplicate (Petsong et al., 2019). The presence and absence of *Salmonella* in the treatments and control were also confirmed by modified ISO 6579: 2002 following the protocol of Biomérieux company as previously described and re-streaked on Xylose Lysine Decarboxylase agar. The amount of phage during this assay was only monitored in the treatment of *S.* Enteritidis and *S.* Typhimurium as representatives by sampling the culture broth every 6-h intervals for 18 h. The culture broth was centrifuged at 6500 rpm for 15 min at 4°C and filtrated through 0.20-μm syringe filters. A number of phage was determined by counting plaques present on each plate of a given dilution as previously described.

In addition, the effectiveness of single phage treatment was also evaluated using *S.* Enteritidis S5-371 and *S.* Typhimurium S5-370 to compare the result with those of cocktail. A 20-ml *Salmonella* suspension (initial 3 log CFU/ml) was mixed with 20 ml of each phage or phage cocktail at a final concentration of 5 log PFU/ml (MOI 100). A number of viable *Salmonella* were examined as previously described.

Evaluation of Phage-Resistant Development in *Salmonella* After Treatment With a Phage Cocktail

The change of *Salmonella* resistance phenotype after treatment with a cocktail was investigated by a spot test. *S.* Enteritidis S5-371 and *S.* Typhimurium S5-370 were used as representatives for all strains of *Salmonella* included in this study. The culture of a given *Salmonella* strain (5 log CFU/ml) was mixed with a phage cocktail (final concentration of 7 log PFU/ml) and incubated at 37°C in a shaking incubator at 220 rpm for 18 h. A loopful of culture was streaked on the TSA plate to obtain a single colony. A single colony was grown in TSB overnight as previously described. Each overnight culture was used to prepare a double layer plate for a spot test with a phage cocktail upon serial dilutions. Overnight culture was subsequently used for phage cocktail treatment in the second and third passage following the same protocol of the first passage to evaluate the phage resistance following the protocols of Petsong et al. (2019).

TABLE 3 | Lysis profiles of isolated *Salmonella* phages from various sources.

Descriptions	***Salmonella* phages (WP)**									
	64	65	66	70	73	74	75.1	75.2	79.1	79.2
Host of isolation (refer to **Table 2**)	H2	H2	H2	H2	H13	H13	H13	H13	H13	H13
Source of isolation	A1	A2	S1	R	A1	A2	S1	S1	R	R
Plaque morphotype (mm)	0.5	0.5	0.5	0.5	0.5	0.5	1.0	0.5	1.0	0.5
Lysis profile (%)										
Eastern broiler farm isolates	66.7	66.7	66.7	66.7	50.0	50.0	50.0	50.0	50.0	50.0
Agona H3D6	+	+	+	+	–	–	–	–	–	–
Albany H32	–	–	–	–	–	–	–	–	–	–
Kentucky S1H28	+	+	+	+	+	+	+	+	+	+
Mbandaka H17D2	–	–	–	–	–	–	–	–	–	–
Saintpaul H13	+	+	+	+	+	+	+	+	+	+
Schwarzengrund H2	+	+	+	+	+	+	+	+	+	+
Southern broiler farm isolates	66.7	66.7	66.7	66.7	66.7	66.7	66.7	66.7	66.7	66.7
Agona F2-W3-S3	–	–	–	–	–	–	–	–	–	–
Corvalis F3-W5-S2	+	+	+	+	+	+	+	+	+	+
Typhimurium F1-W1-C2	+	+	+	+	+	+	+	+	+	+
Foodborne outbreak-related isolates	60.0	60.0	60.0	60.0	60.0	60.0	60.0	60.0	60.0	60.0
Enteritidis S5-371	+	+	+	+	+	+	+	+	+	+
Hadar PPI-013	–	–	–	–	–	–	–	–	–	–
Infantis S5-506	–	–	–	–	–	–	–	–	–	–
Typhimurium S5-370	+	+	+	+	+	+	+	+	+	+
Virchow H2-117	+	+	+	+	+	+	+	+	+	+
MDR isolates	81.8	81.8	81.8	81.8	81.8	81.8	81.8	77.3	81.8	81.8
Agona 223SL	+	+	+	+	+	+	+	–	+	+
Albany 198SL	+	+	+	+	+	+	+	+	+	+
Corvalis 069SL	–	–	–	–	–	–	–	–	–	–
Give 188SL	+	+	+	+	+	+	+	+	+	+
Kentucky 180SL	+	+	+	+	+	+	+	+	+	+
Kentucky 210SL	–	–	–	–	–	–	–	–	–	–
Kentucky 222SL	+	+	+	+	+	+	+	+	+	+
Kentucky 245SL	+	+	+	+	+	+	+	+	+	+
Kentucky 256SL	+	+	+	+	+	+	+	+	+	+
Mbandaka 034SL	–	–	–	–	–	–	–	–	–	–
Typhimurium 032SL	+	+	+	+	+	+	+	+	+	+
Typhimurium 205SL	+	+	+	+	+	+	+	+	+	+
Typhimurium 206SL	–	–	–	–	–	–	–	–	–	–
Schwarzengrund 086SL	+	+	+	+	+	+	+	+	+	+
Schwarzengrund 248SL	+	+	+	+	+	+	+	+	+	+
Schwarzengrund 252SL	+	+	+	+	+	+	+	+	+	+
Schwarzengrund 253SL	+	+	+	+	+	+	+	+	+	+
Singapore 154SL	+	+	+	+	+	+	+	+	+	+
Singapore 170SL	+	+	+	+	+	+	+	+	+	+
Singapore 174SL	+	+	+	+	+	+	+	+	+	+
Weltevreden 001SL	+	+	+	+	+	+	+	+	+	+
Weltevreden 013SL	+	+	+	+	+	+	+	+	+	+
% Total lysis ability	75.0	75.0	75.0	75.0	72.2	72.2	72.2	69.4	72.2	72.2

(Continued)

TABLE 3 | Continued

Descriptions	***Salmonella* phages (WP)**									
	109*	110*	111	118	119	120	121	122	126	128*
Host of isolation (refer to **Table 2**)	S1H28	S1H28	S1H28	A4-525	A4-525	A4-525	A4-525	A4-525	A4-525	H2-016
Source of isolation	A1	A2	S1	A1	A2	S1	S2	A3	NR	A2
Plaque morphotype (mm)	0.5	0.1	0.1	1.0	1.0	1.0	0.3	0.3	0.1	2.0
Lysis profile (%)										
Eastern broiler farm isolates	83.3	83.3	50.0	50.0	50.0	50.0	50.0	50.0	50.0	66.7
Agona H3D6	+	+	−	−	−	−	−	−	−	−
Albany H32	+	+	−	−	−	−	−	−	−	−
Kentucky S1H28	+	+	+	+	+	+	+	+	+	+
Mbandaka H17D2	−	−	−	−	−	−	−	−	−	+
Saintpaul H13	+	+	+	+	+	+	+	+	+	+
Schwarzengrund H2	+	+	+	+	+	+	+	+	+	+
Southern broiler farm isolates	66.7	66.7	66.7	66.7	66.7	66.7	66.7	66.7	66.7	66.7
Agona F2-W3-S3	−	−	−	−	−	−	−	−	−	−
Corvalis F3-W5-S2	+	+	+	+	+	+	+	+	+	+
Typhimurium F1-W1-C2	+	+	+	+	+	+	+	+	+	+
Foodborne outbreak-related isolates	100.0	80.0	80.0	60.0	60.0	60.0	60.0	60.0	60.0	80.0
Enteritidis S5-371	+	+	+	+	+	+	+	+	+	+
Hadar PPI-013	+	+	+	−	−	−	−	−	−	−
Infantis S5-506	+	−	−	−	−	−	−	−	−	+
Typhimurium S5-370	+	+	+	+	+	+	+	+	+	+
Virchow H2-117	+	+	+	+	+	+	+	+	+	+
MDR isolates	90.9	95.5	81.8	81.8	81.8	81.8	77.3	81.8	81.8	81.8
Agona 223SL	+	+	+	+	+	+	−	+	+	+
Albany 198SL	+	+	+	+	+	+	+	+	+	+
Corvalis 069SL	−	+	−	−	−	−	−	−	−	−
Give 188SL	+	+	+	+	+	+	+	+	+	+
Kentucky 180SL	+	+	+	+	+	+	+	+	+	+
Kentucky 210SL	+	+	−	−	−	−	−	−	−	−
Kentucky 222SL	+	+	+	+	+	+	+	+	+	+
Kentucky 245SL	+	+	+	+	+	+	+	+	+	+
Kentucky 256SL	+	+	+	+	+	+	+	+	+	+
Mbandaka 034SL	−	−	−	−	−	−	−	−	−	−
Typhimurium 032SL	+	+	+	+	+	+	+	+	+	+
Typhimurium 205SL	+	+	+	+	+	+	+	+	+	+
Typhimurium 206SL	+	+	−	−	−	−	−	−	−	−
Schwarzengrund 086SL	+	+	+	+	+	+	+	+	+	+
Schwarzengrund 248SL	+	+	+	+	+	+	+	+	+	+

(Continued)

TABLE 3 | Continued

Descriptions	*Salmonella* phages (WP)									
	109*	110*	111	118	119	120	121	122	126	128*
Schwarzengrund 252SL	+	+	+	+	+	+	+	+	+	+
Schwarzengrund 253SL	+	+	+	+	+	+	+	+	+	+
Singapore 154SL	+	+	+	+	+	+	+	+	+	+
Singapore 170SL	+	+	+	+	+	+	+	+	+	+
Singapore 174SL	+	+	+	+	+	+	+	+	+	+
Weltevreden 001SL	+	+	+	+	+	+	+	+	+	+
Weltevreden 013SL	+	+	+	+	+	+	+	+	+	+
% Total lysis ability	88.9	88.9	75.0	72.2	72.2	72.2	69.4	72.2	72.2	77.8

The asterisk (*) indicates phages that were used in the phage cocktail development.
A1, A2, and A3: water samples collected from aerated wastewater treatment ponds collected on March 28, 2019, September 17, 2019, and October 26, 2019, respectively. S1 and S2: water samples collected from sediment wastewater treatment ponds collected on March 28, 2019 and September 17, 2019, respectively. NR: water sample from natural reservoir, R: water sample from river in Songkhla province.
Lysis ability: + represents lysis and − represents no lysis.

Statistical Analysis

Statistical analysis was performed using SPSS (Version 22.0) of Windows statistics software (SPSS Inc., Chicago, IL, United States). Data of *Salmonella* reduction during incubation period were subjected to analysis of variance followed by Tukey's range test. A significant difference between the control and the phage cocktail treatments was calculated using the independent-samples *t* test. A difference was considered statistically significant at $p < 0.05$.

RESULTS

Overall Prevalence and Serovar Diversity of *Salmonella* spp. in Broiler Farms

Salmonella spp. were detected in 46.2 and 28.1% of samples collected from two broiler farms in eastern Thailand and three broiler farms in southern Thailand, respectively (**Table 1**). Bedding showed a typical source for *Salmonella* spp. in all farms sampled. Although only one sample type was collected in eastern farms due to contamination issue, all three sample types were collected in southern farms with only farm C showing *Salmonella* positive in three sample types (70% of samples collected).

Eastern farms showed higher diversity of *Salmonella* serovars from bedding samples than those from southern farms (**Table 2**). *Salmonella* detected from five positive samples from farm A presented four serovars including Schwarzengrund, Saintpaul, Albany, and Kentucky. Seven positive samples from farm B showed three serovars including Mbandaka, Agona, and Kentucky. Serovar Typhimurium was the only serovar detected in bedding, cloacal swab, and boot swab samples from farm C. Two positive bedding samples from farm D and farm E showed two distinct serovars, Agona and Corvalis.

Phage Lysis Ability

Overall, 20 phages recovered from the collected water samples showed various plaque morphotypes, ranging from as tiny as 0.1 mm to a large plaque size as 2.0 mm (**Table 3**). Most phages isolated here (18 phages) showed similar lysis ability covering over 15 serovars from various sources. These presented

TABLE 4 | Efficiency of plating (EOP) of selected phages on bacterial hosts.

Salmonella	Efficiency of plating (EOP)*		
	WP109	**WP110**	**WP128**
Agona H3D6	<0.001	<0.001	<0.001
Albany H32	<0.001	0.20 ± 0.00	<0.001
Kentucky S1H28	**1.00**	**1.00**	0.002 ± 0.00
Mbandaka H17D2	<0.001	<0.001	<0.001
Saintpaul H13	3.48 ± 0.74	1.00 ± 0.57	0.01 ± 0.00
Schwarzengrund H2	1.92 ± 0.11	0.43 ± 0.24	0.01 ± 0.00
Typhimurium F1-W1-C2	0.004 ± 0.00	0.002 ± 0.00	0.01 ± 0.00
Corvalis F3-W5-S2	0.004 ± 0.00	0.01 ± 0.00	<0.001
Enteritidis S5-371	8.90 ± 2.40	5.20 ± 1.13	0.02 ± 0.00
Hadar PPI-013	0.02 ± 0.00	0.008 ± 0.00	<0.001
Infantis S5-506	0.004 ± 0.00	<0.001	<0.001
Typhimurium S5-370	0.10 ± 0.03	0.01 ± 0.00	<0.001
Virchow H2-117	0.004 ± 0.00	0.02 ± 0.00	<0.001
Agona 223SL	0.004 ± 0.00	0.18 ± 0.00	1.31 ± 0.25
Albany 198SL	1.80 ± 0.28	1.42 ± 0.25	0.01 ± 0.00
Corvalis 069SL	<0.001	0.002 ± 0.00	<0.001
Give 188SL	0.45 ± 0.26	0.15 ± 0.07	<0.001
Kentucky 180SL	0.45 ± 0.26	2.90 ± 0.56	0.004 ± 0.00
Mbandaka 034SL	<0.001	<0.001	<0.001
Typhimurium 032SL	0.04 ± 0.01	0.07 ± 0.01	0.011 ± 0.001
Schwarzengrund 086SL	5.20 ± 0.00	0.40 ± 0.07	0.009 ± 0.00
Singapore 154SL	0.004 ± 0.00	0.002 ± 0.00	<0.001
Weltevreden 001SL	0.48 ± 0.08	0.14 ± 0.08	0.003 ± 0.00
Agona H2-016	0.26 ± 0.04	1.90 ± 0.14	**1.00**

**All values provided are expressed as mean ± standard deviation in triplicate. EOP values were classified as high production (EOP > 0.5), medium production (0.1 < EOP < 0.5), low production (0.001 < EOP < 0.1), and inefficient production (EOP < 0.001). The original strain of isolation has an EOP value of 1.0 and is shown in boldface (S. Kentucky H1S28 for WP109 and WP110, and S. Agona H2-016 for WP128).*

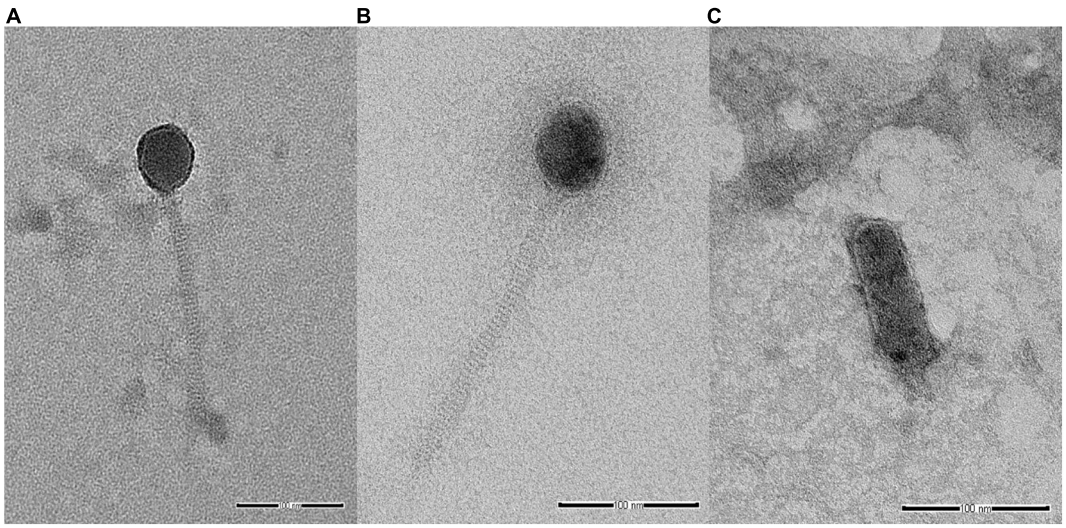

FIGURE 1 | Transmission electron microscopy analysis of *Salmonella* phages. **(A)** vB_SenS_WP109, **(B)** vB_SenS_WP110, and **(C)** vB_SenP_WP128 at a magnification of 100,000×. Bar, 100 nm.

69.4–88.9% lysis ability on 36 different *Salmonella* isolates. In addition, two phages (WP109 and WP110) showed considerably strong lysis ability covering over 14 serovars from various sources and representing 88.9% lysis ability on 36 different *Salmonella* isolates.

All 20 phages showed strong lysis on the isolates presenting five major serovars, including Kentucky, Saintpaul, and Schwarzengrund from eastern farms and Corvalis and Typhimurium from southern farms. A few phages could lyse isolates of serovars Agona, Albany, and Mbandaka derived from broiler farms in this study. Only six phages (30%) could lyse *S.* Agona H3D6 isolated from bedding of farm B whereas no phage could lyse *S.* Agona F2-W3-S3 isolated from bedding of farm D (southern farm). Two phages (WP109 and WP110) showed strong lysis on *S.* Albany H32 isolated from bedding of farm A. The only phage WP128 showed strong lysis on *S.* Mbandaka H17D2 isolated from bedding of farm B.

All 20 phages showed strong lysis on the three reference serovars that were foodborne outbreak-related (Enteritidis, Typhimurium, and Virchow). *S.* Hadar PPI-013 was susceptible to lysis by phage WP109, WP110, and WP111 whereas serovar Infantis S5-506 was susceptible to lysis by two phages WP109 and WP128. Most phages isolated here showed strong lysis against MDR strains (10 serovars) representing 77.3–95.5% lysis ability on 22 different *Salmonella* isolates. Among 10 serovars of the MDR strains tested, only serovar Mbandaka showed to be resistant to all phages. One tetracycline-resistant strain, *S.* Corvalis 069SL, was susceptible to lysis by only phage WP110, whereas serovars Kentucky (210SL) and Typhimurium (206SL) were susceptible to lysis by two phages WP109 and WP110.

Efficiency of Plating

The EOP assay reveals that phage WP109 showed high EOP on 6 of 24 isolates of *Salmonella* tested, medium EOP on 5 isolates, low EOP on 8 isolates, and an inefficient EOP on 5 isolates. Phage WP110 showed a high EOP on 6 isolates, medium EOP on 6 isolates, low EOP on 7 isolates, and an inefficient EOP on 4 isolates. Phage WP128 only showed high EOP against *S.* Agona H2-016, the original host and *S.* Agona 223SL. Interestingly, this phage could not produce a medium productive infection despite showing a high percentage of low EOP (10/24) and inefficient EOP (12/24) as shown in **Table 4**.

TEM Analysis

Analysis of selected *Salmonella* phages using TEM allowed the morphological classification of phages into viral order and family. *Salmonella* phages WP109 and WP110 were classified into the order *Caudovirales*, and family *Siphoviridae*. Phage WP109 showed icosahedral-shaped head with a size of 54.2 nm × 53.1 nm and a tail length of 182.1 nm (**Figure 1A**). Phage WP110 showed a head size of 59.8 nm × 55.3 mm and a tail length of 214.2 nm (**Figure 1B**). Phage WP128 was assigned to order *Caudovirales* and family *Podoviridae* with the C3 morphotype as shown in **Figure 1C**. This phage had an elongated head with a size of 96.9 nm × 32.2 nm and a short tail length of 19.2 nm.

Evaluation of Phage Cocktail Efficiency Targeting *Salmonella in vitro*

To evaluate the efficiency of a phage cocktail on *Salmonella* growth, the number of *Salmonella* in the presence and absence of a phage cocktail was counted every 6-h interval for 18 h. As shown in **Table 5**, a phage-treated treatment could significantly reduce the cell number by 100% (2 log units) for strains *S.* Enteritis S5-371, *S.* Virchow H2-117, *S.* Schwarzengrund H2, *S.* Saintpaul H13, *S.* Kentucky S1H28, *S.* Typhimurium F1-W1-C2, and *S.* Corvalis F3-W5-S2 during 6 to 18 h in a phage cocktail treatment at MOI of 1000. In the treatment of

TABLE 5 | Efficacy evaluation of a phage cocktail on diverse *Salmonella* serovars.

Salmonella	Time (h)	Bacterial count[A] (log CFU/ml)			%Reduction at MOI 1000	%Reduction at MOI 100000
		Control	Cocktail at MOI 1000	Cocktail at MOI 100000		
Agona H3D6	0	2.8 ± 0.2^{a}	2.6 ± 0.1^{a}	2.8 ± 0.2^{a}	–	–
	6	6.1 ± 0.1^{b}	5.8 ± 0.4^{b}	5.7 ± 0.4^{b}	16.3 ± 1.0	6.8 ± 0.5
	12	8.0 ± 0.0^{c}	7.4 ± 0.1^{c}	$6.5 \pm 0.2^{c*}$	7.4 ± 1.3	19.2 ± 2.7
	18	8.2 ± 0.2^{c}	8.4 ± 0.2^{c}	8.0 ± 0.1^{d}	0	1.8 ± 0.1
Albany H32	0	2.3 ± 0.1^{a}	2.3 ± 0.4^{a}	2.7 ± 0.3^{a}	–	–
	6	6.9 ± 0.1^{b}	$5.9 \pm 0.1^{b*}$	$6.1 \pm 0.1^{b*}$	14.6 ± 1.3	11.4 ± 2.3
	12	8.1 ± 0.1^{c}	$7.3 \pm 0.0^{b*}$	8.0 ± 0.0^{c}	10.2 ± 0.9	2.0 ± 0.7
	18	8.4 ± 0.0^{d}	8.2 ± 0.1^{c}	$8.0 \pm 0.1^{c*}$	2.9 ± 1.3	5.5 ± 1.5
Kentucky S1H28	0	2.4 ± 0.6^{a}	2.3 ± 0.2	2.2 ± 0.2	–	–
	6	7.2 ± 0.3^{b}	nd	nd	100	100
	12	8.3 ± 0.1^{c}	nd	nd	100	100
	18	8.1 ± 0.0^{c}	nd	nd	100	100
Mbandaka H17D2	0	2.4 ± 0.1^{a}	2.6 ± 0.2^{a}	2.5 ± 0.2^{a}	–	–
	6	6.7 ± 0.1^{b}	6.6 ± 0.1^{b}	6.6 ± 0.2^{b}	1.4 ± 0.2	2.4 ± 0.3
	12	8.3 ± 0.0^{c}	8.4 ± 0.3^{c}	8.3 ± 0.1^{c}	0	0
	18	8.1 ± 0.1^{c}	9.5 ± 0.0^{d}	8.2 ± 0.0^{c}	0	0
Saintpaul H13	0	2.1 ± 0.1^{a}	2.2 ± 0.2	2.4 ± 0.4	–	–
	6	6.5 ± 0.2^{b}	nd	nd	100	100
	12	8.4 ± 0.1^{c}	nd	nd	100	100
	18	8.4 ± 0.1^{c}	nd	nd	100	100
Schwarzengrund H2	0	2.3 ± 0.3^{a}	2.4 ± 0.3	2.4 ± 0.4	–	–
	6	6.4 ± 0.1^{b}	nd	nd	100	100
	12	8.3 ± 0.1^{c}	nd	nd	100	100
	18	8.3 ± 0.1^{c}	nd	nd	100	100
Typhimurium F1-W1-C2	0	2.9 ± 0.5^{a}	2.3 ± 0.1	2.6 ± 0.1	–	–
	6	6.4 ± 0.3^{b}	nd	nd	100	100
	12	8.2 ± 0.0^{c}	nd	nd	100	100
	18	8.3 ± 0.0^{d}	nd	nd	100	100
Corvalis F3-W5-S2	0	2.3 ± 0.0^{a}	2.3 ± 0.2	2.3 ± 0.0	–	–
	6	6.7 ± 0.2^{b}	nd	nd	100	100
	12	8.3 ± 0.1^{c}	nd	nd	100	100
	18	8.5 ± 0.2^{d}	nd	nd	100	100
Enteritidis S5-371	0	2.4 ± 0.3^{a}	2.4 ± 0.2	2.4 ± 0.3	–	–
	6	6.9 ± 0.1^{b}	nd	nd	100	100
	12	8.3 ± 0.1^{c}	nd	nd	100	100
	18	8.3 ± 0.1^{c}	nd	nd	100	100
Hadar PPI-013	0	2.9 ± 0.2^{a}	2.9 ± 0.2^{a}	2.7 ± 0.3	–	–
	6	6.5 ± 0.8^{b}	$3.4 \pm 0.2^{a*}$	nd	47.1 ± 5.0	100
	12	8.2 ± 0.1^{c}	$3.6 \pm 0.1^{a*}$	nd	55.9 ± 1.8	100
	18	8.5 ± 0.2^{c}	9.1 ± 0.1^{b}	nd	0	100
Infantis S5-506	0	2.4 ± 0.2^{a}	2.6 ± 0.1^{a}	2.2 ± 0.0^{a}	–	–
	6	6.8 ± 0.2^{b}	6.7 ± 0.2^{b}	$5.5 \pm 0.1^{b*}$	0.6 ± 0.1	18.4 ± 3.0
	12	8.2 ± 0.0^{c}	7.5 ± 0.4^{b}	$6.8 \pm 0.1^{c*}$	9.1 ± 0.9	16.6 ± 0.9
	18	8.3 ± 0.3^{c}	9.3 ± 0.1^{c}	8.0 ± 0.1^{d}	0	3.3 ± 0.8
Typhimurium S5-370	0	2.3 ± 0.3^{a}	2.4 ± 0.3^{a}	2.3 ± 0.1	–	–
	6	6.4 ± 0.1^{b}	$2.3 \pm 0.2^{a*}$	nd	66.0 ± 2.2	100
	12	8.3 ± 0.1^{c}	$4.6 \pm 0.0^{b*}$	nd	45.0 ± 0.3	100
	18	8.3 ± 0.1^{c}	$7.3 \pm 0.0^{c*}$	nd	12 ± 0.1	100
Virchow H2-117	0	2.6 ± 0.1^{a}	2.7 ± 0.1	2.7 ± 0.0	–	–
	6	6.9 ± 0.0^{b}	nd	nd	100	100
	12	8.3 ± 0.0^{c}	nd	nd	100	100
	18	8.4 ± 0.1^{c}	nd	nd	100	100

[A] *All values provided are expressed as mean ± standard deviation in triplicate.*

The lowercase letters for control or phage treatment and those connected by different letters are significantly different ($p < 0.05$) whereas the asterisk (*) indicates the significant difference ($p < 0.05$) of bacterial counts between control and the phage treatment at the same time. "nd" refers to no bacterial count detected. The percentage of bacterial reduction at 0 h was normalized to 0.0.

higher MOI at 100,000, significant reduction of the cell number (100% reduction; 2 log units) was also observed for strains *S.* Typhimurium S5-370 and *S.* Hadar PPI-013. However, a phage cocktail incompletely reduced the population of *S.* Albany H32, *S.* Mbandaka H17D2, and *S.* Agona H3D6 derived from eastern broiler farm, and *S.* Infantis S5-506, the foodborne-outbreak isolate as observed by a reduction of only 0.1–0.3 and 0.1–1.3 log units after 6 h of treatment at MOI 1000 and 100,000, respectively.

The amount of phage during the assay was also monitored as shown in **Figures 2**, **3**. The results indicated that the number of phages slightly increased in the treatment of *S.* Enteritidis at both MOIs (5.6–6.7 PFU/ml at MOI 1000 and 7.0–7.5 at MOI 100,000) but without significant difference at each sampling time ($p > 0.05$) as shown in **Figure 2**. In the treatment of *S.* Typhimurium, the number of phages significantly increased at MOI 1000 ($p < 0.05$) (5.0–7.1 log PFU/ml) whereas no significant difference was observed at MOI 100,000 (6.9–7.2 log PFU/ml) (**Figure 3**).

The study of bacterial inactivation by each of the three single phages was performed. The significant difference was observed in each single phage and a phage cocktail at 6 h ($p < 0.05$) for both *Salmonella*. The significant reduction of *Salmonella* cells was observed in the treatment of phage WP109 or phage WP128, and phage cocktail at 12 and 18 h ($p < 0.05$) when compared to the control. However, phage WP110 could reduce the number of both *Salmonella* at 12 and 18 h but there was no significant difference ($p > 0.05$). Importantly, phage cocktail showed higher reduction of *Salmonella* counts than other single phage treatments at the end of study as shown in **Figures 4**, **5**.

Evaluation of Phage-Resistance Development in *Salmonella* After Treatment With a Phage Cocktail

After treatment with a phage cocktail, *S.* Enteritis and *S.* Typhimurium culture were re-tested with the same phage cocktail for three passages. Compared to the control culture, which had no prior phage cocktail treatment, the phage-treated *Salmonella* culture showed the same lysis ability with a phage cocktail for both serovars and for three passages (**Table 6**).

DISCUSSION

Several studies have been reported showing that samples such as bedding materials, feed, water, cloacal swab, boot swab, dust, and even litter collected from several regions of commercial poultry farms worldwide are important sources of *Salmonella* spp. (Mueller-Doblies et al., 2009; Djeffal et al., 2018; Eguale, 2018; Dagnew et al., 2020). Various contamination rates with *Salmonella* were observed, for example, in European countries; 68 of 4331 samples (1.57%) were collected from poultry farms in the region of Pomerania, Warmia, and Mazury of Northern Poland during 2014 to 2016 (Witkowska et al., 2018). In African countries, 370 samples (14.1%) including dust, litter, feces, feed, and water samples collected from 228 poultry farms in different regions of Nigeria showed a positive result for *Salmonella* isolation (Fagbamila et al., 2017), and 4.7% of collected samples (pooled fresh fecal dropping) from 48 examined poultry farms in Ethiopia from July 2013 to January 2014 were also positive for *Salmonella* (Eguale, 2018).

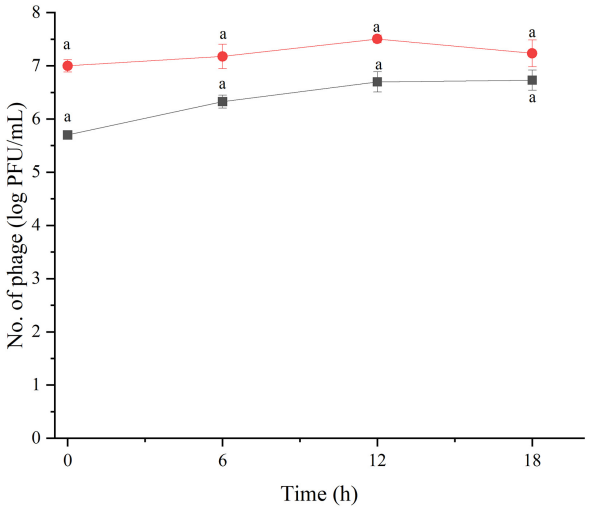

FIGURE 2 | The number of phage concentration during efficacy evaluation of a phage cocktail on *Salmonella* Enteritidis. MOI100 (black square and line) and MOI 100000 (red circle and line). All values provided are expressed as mean ± standard deviation in triplicate. The lowercase letters connected by the different letters are significantly different ($p < 0.05$).

The colonization of *Salmonella* at the farm level has been considered as the most high-risk factor for the human food chain. It is linked with the contamination of poultry products and causes the possible outbreak of human salmonellosis. In the present study, 21 of 58 samples (36.20%) from five examined poultry farms were contaminated by *Salmonella*. The prevalence of *Salmonella* spp. observed here was higher than the above reports (Ziyate et al., 2016; Fagbamila et al., 2017; Eguale, 2018). The possible reason could be due to differences in farm management and practices as all examined farms were large-scale commercial poultry farms that hold more than 20,000 chickens per cultivation. Furthermore, the accumulation of this pathogen in bedding materials by excreting this pathogen through the feces of chickens without any changing materials is also an important factor (Nair and Johny, 2019), thus showing as *Salmonella*-positive in bedding samples from all examined farms.

Many serovars of *Salmonella*, especially the non-typhoidal *Salmonella*, have been found among poultry farms in several parts of the world, which can lead to contamination in poultry products such as fresh meat and raw eggs (Kumar et al., 2019). For example, the dominant serovar of *Salmonella* distributed in poultry farms in Ethiopia was *S.* Saintpaul (76.92%), followed by *S.* Typhimurium (11.53%), *S.* Kentucky (7.69%), and *S.* Haifa (3.85%) (Eguale, 2018). *S.* Kentucky was frequently isolated from poultry farms in Nigeria and Bangladesh (Barua et al., 2012; Fagbamila et al., 2017), while seven different serovars were distributed in laying hen farms in Morocco as follows: *S.* Enteritidis (37.5%), *S.* Kentucky (31.3%), *S.* Infantis (10.9%), *S.* Typhimurium (6.24%), *S.* Thompson (6.2%), *S.* Agona (4.7%), and *S.* Amsterdam (3.1%) (Ziyate et al., 2016). In Thailand, *S.* Corvalis (37.8%), *S.* Albany (24.3%), and *S.* Enteritidis (24.3%)

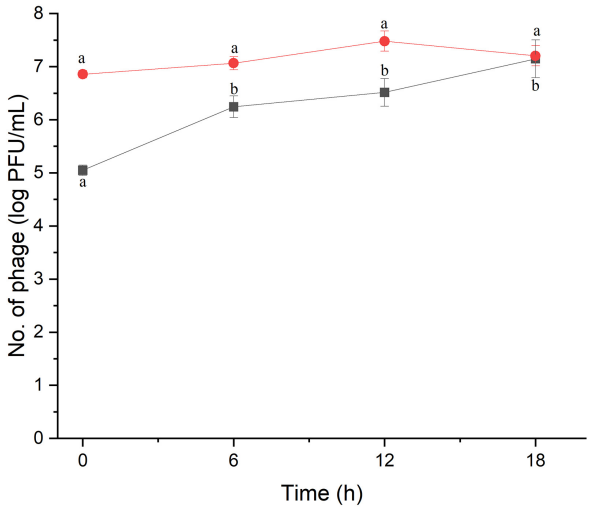

FIGURE 3 | The number of phage concentration during efficacy evaluation of a phage cocktail on *Salmonella* Typhimurium. MOI 1000 (black square and line) and MOI 100000 (red circle and line). All values provided are expressed as mean ± standard deviation in triplicate. The lowercase letters connected by the different letters are significantly different ($p < 0.05$).

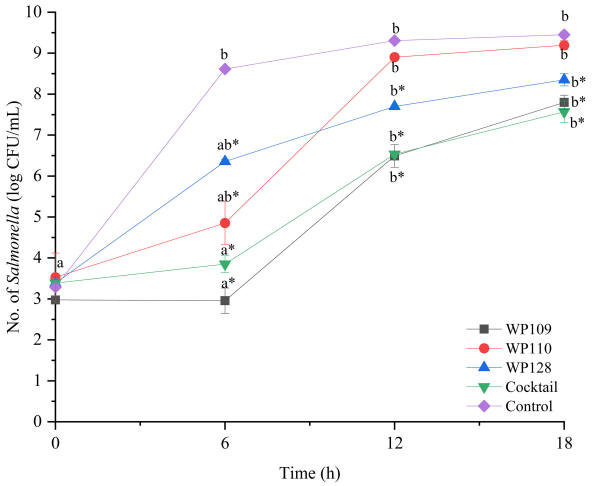

FIGURE 4 | The number of viable *Salmonella* Enteritidis count when treated with a phage cocktail (5 log PFU/ml) with the beginning of bacterial concentration by 3 log CFU/ml (MOI 100). All values provided are expressed as mean ± standard deviation in triplicate. The lowercase letters for control or phage treatment and those connected by the different letters are significantly different ($p < 0.05$) whereas the *asterisk* (*) indicates the significant difference ($p < 0.05$) of bacterial counts between control and the phage treatment at the same time.

are the most serovars isolated from broiler farms in Chiang Mai province (Lampang et al., 2014). *S.* Kentucky (22.94%) and *S.* Give (20.18%) were also found as the most serovars in local slaughterhouses in nine provinces of central Thailand between April and July 2018 (Phongaran et al., 2019). Similar to the previous reports, *S.* Agona, *S.* Kentucky, *S.* Mbandaka, and *S.* Typhimurium observed in this study were the major serovars among samples collected from poultry farms, while *S.* Albany, *S.* Schwarzengrund, *S.* Corvalis, and *S.* Saintpaul presented as minor serovars.

A number of *Salmonella* phages could be isolated from various water sources in this study, suggesting that water and/or wastewater are common sources of *Salmonella* phages as previously reported by several studies (Sundar et al., 2009; Rattanachaikunsopon and Phumkhachorn, 2012; Yildirim et al., 2018; Petsong et al., 2019). Previous studies have shown the usefulness of phage therapy using phages with a board-lysis ability, including those five *Salmonella* phages (phiSE) isolated from chicken feces that could lyse six important serovars tested including Abony, Enteritidis, Gallinarum, Pullorum, Typhi, and Typhimurium (Hungaro et al., 2013). *Salmonella* phages STm101 and STm118 isolated from Thai poultry farms could also infect eight different *Salmonella* serovars (infected 50% of tested isolates) (Phothaworn et al., 2019). In addition, MDR isolates have been critical for animal farms. Previous studies have focused on using phages to target MDR isolates such as seven virulent *Salmonella* phages (SPFM) that could infect 100% of MDR-*Salmonella* isolated from pigs in the United Kingdom (Thanki et al., 2019) whereas other six *Salmonella* phages could lyse clinically isolated and ciprofloxacin-induced antibiotic-resistant *S.* Typhimurium (Jung et al., 2017). In the current study, 20 isolated phages showed strong lysis patterns against serovars

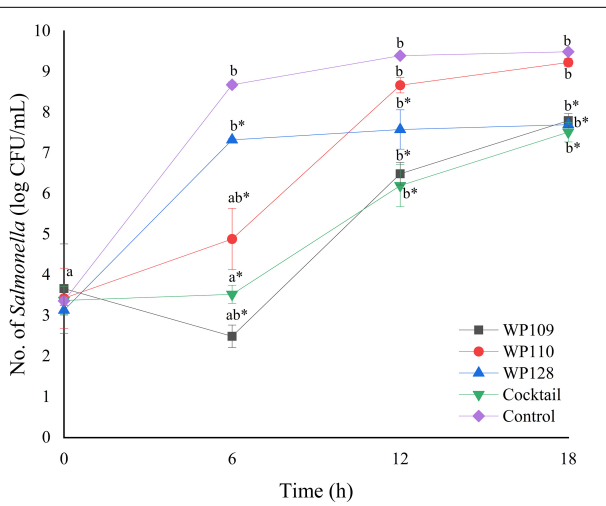

FIGURE 5 | The number of viable *Salmonella* Typhimurium count when treated with a phage cocktail (5 log PFU/ml) with the beginning of bacterial concentration by 3 log CFU/ml (MOI 100). All values provided are expressed as mean ± standard deviation in triplicate. The lowercase letters for control or phage treatment and those connected by the different letters are significantly different ($p < 0.05$) whereas the *asterisk* (*) indicates the significant difference ($p < 0.05$) of bacterial counts between control and the phage treatment at the same time.

from broiler farms, serovars with food-linked illness, and MDR strains, suggesting that their lytic activities are advantageous in combating *Salmonella* prevalent in the broiler production chain and preventing MDR spread through the food chain.

Phages with a board-host lysis ability are able to eliminate certain hosts due to their high specificity. The EOP assay

TABLE 6 | Re-challenge of *S.* Enteritidis and *S.* Typhimurium upon phage treatment by a phage cocktail.

Treatments	Lysis ability[a] of cocktail (Phage titer log PFU/ml)											
	Passages											
	1				2				3			
	7	6	5	4	7	6	5	4	7	6	5	4
Control *S.* Enteritidis	+++	++	++	+	++	++	+	−	++	++	+	−
Cocktail-treated *S.* Enteritidis	+++	++	++	++	++	++	+	−	++	++	+	−
Control *S.* Typhimurium	++	+	+	−	+++	++	+	−	+++	++	+	−
Cocktail-treated *S.* Typhimurium	+++	++	+	+	++	++	+	−	+++	++	+	−

[a]*Lysis ability: +++ indicates strong lysis; ++ indicates medium lysis; + indicates weak lysis; − indicates no lysis. Control is culture without prior phage cocktail treatment.*

confirmed that individual phages included in a phage cocktail showed high productive infection against most isolates of *Salmonella* from diverse sources in this study. The EOP assay has been widely used for phage efficacy evaluation (Mirzaei and Nilsson, 2015; Manohar et al., 2019). In this study, single phage treatments could reduce *Salmonella* counts. However, the phage cocktail showed higher reduction of *Salmonella* counts than other single phage treatments. The combination of several phages in treatment as a phage cocktail is usually preferred and used for treating the bacterial co-infections and can expand their lytic activity as previous reported by others (Goodridge, 2010; Hooton et al., 2011; Chan and Abedon, 2012; Rattanachaikunsopon and Phumkhachorn, 2012; Chan et al., 2013). In addition, a single phage can increase the chance of phage resistance in bacteria compared to phage cocktail treatment. This is because the bacteria might resist one type of phage in cocktail but is still susceptible to others as previously reported by others (Rohde et al., 2018; Yang et al., 2020). In a previous work, the *in vitro* study showed that a phage cocktail made of KP4, KP5, and KP50 could decrease the number of *S.* Enteritidis and *S.* Typhimurium by 4 log CFU/ml after 4 h of treatment (Petsong et al., 2019). SalmoLyse, the cocktail of six *Salmonella* phages, at concentration levels of 8 log PFU/ml or greater, was able to inactivate 90% of *S.* Typhimurium growth after 1 h of incubation (Heyse et al., 2015). In the current study, our newly developed phage cocktail could reduce the number of tested *Salmonella* serovars derived from foodborne outbreak-related and animal farm origin as indicated by the highest reduction by 100% after 6 h of treatment with MOI 1000 and 100,000. On the other hand, some isolates including *S.* Albany H32, *S.* Mbandaka H17D2, *S.* Agona H3D6, and *S.* Infantis S5-506 seem to be resilient to phage cocktail treatment since these isolates were susceptible to only one or two phages composed in this cocktail despite the fact that each isolate was treated with low MOI. However, phage cocktail could reduce the number of these isolate counts, but there was no significant difference ($p > 0.05$). The amount of phages during phage cocktail efficiency assay might correlate with the number of viable *Salmonella* count (**Table 5**). In the treatment of *S.* Enteritidis, both MOIs could reduce the number of *Salmonella* by 100% reduction at 6 h. This is why the number of phage was not rapidly produced. In contrast to the treatment of *S.* Enteritidis at MOI 1000, this MOI could not completely reduce the number of *Salmonella* during assay. This is why the number of phages was significantly increased. At MOI 100,000, the number of phages remained in the concentration between 6.9 and 7.2 log PFU/ml, and this result is concordant to the 100% reduction of bacteria at 6 h.

In addition, phage cocktail did not change *Salmonella* phenotypic characteristics through resistant patterns after treatment with this phage cocktail, indicating that no mutation was observed. Therefore, the use of this phage cocktail could be specific for controlling *Salmonella* distributed/contaminated in the broiler production chain and MDR *Salmonella*.

CONCLUSION

Multiple *Salmonella* serovars have been prevalent in broiler farms from eastern and southern Thailand. The collected data could be used as an effective tool to explore the alternative strategy to combat *Salmonella* contamination and/or infection in broiler production chain. In addition, the overuse of antibiotics during broiler production can impact the development of resistance in bacteria and subsequently pose a serious threat to humans through the food production chain. Phages should be an attractive strategy as indicated by their specific lysis ability on the *Salmonella* hosts. Hence, *Salmonella* phages isolated in this study were tested against *Salmonella* hosts that may cause potential food safety issues in the broiler production chain. Overall, these phages showed strong lysis on the MDR strains, indicating potential phage control application to prevent the spread of MDR strains in the broiler production chain. Our study showed that a newly developed phage cocktail can decrease and/or eliminate *Salmonella* spp. *in vitro*. However, the efficiency of this cocktail application on a large scale should be undertaken in the further work. The real impact of utilization of phage cocktail as a biocontrol agent on poultry meat production and for preventing the spread of MDR through food production chain needs to be evaluated.

DATA AVAILABILITY STATEMENT

The raw data supporting the conclusions of this article will be made available by the authors, without undue reservation.

AUTHOR CONTRIBUTIONS

All authors conceived and designed the experiments and approved the final draft of the manuscript. WP executed the lab experiments, analyzed the data, and prepared the manuscript. KV is the principal investigator of the project who was responsible for preparation of project proposal, procuring funding, resource allocation, and managing human resource along with RN, MY, KC, and SB.

FUNDING

This study received funding from the Agricultural Research Development Agency (ARDA), Thailand (grant number: CRP6305031030) (to KV). The funder was not involved in the study design; collection, analysis, and interpretation of data; the writing of this article; or the decision to submit it for publication.

ACKNOWLEDGMENTS

This research was supported by the Postdoctoral Fellowship from Prince of Songkla University (to WP) and TRF distinguish professor grant (to SB).

SUPPLEMENTARY MATERIAL

The Supplementary Material for this article can be found online at: https://www.frontiersin.org/articles/10.3389/fmicb.2021.662461/full#supplementary-material

Supplementary Table 1 | Antibiotic-resistant *Salmonella* used in host range determination.

REFERENCES

Alum, E. A., Urom, S. M. O. C., and Ben, C. M. A. (2016). Microbiological contamination of food: the mechanisms, impacts and prevention. *Int. J. Sci. Technol. Res.* 5, 65–78.

Barbour, E. K., Ayyash, D. B., Alturkistni, W., Alyahiby, A., Yaghmoor, S., Iyer, A., et al. (2015). Impact of sporadic reporting of poultry *Salmonella* serovars from selected developing countries. *J. Infect. Dev. Ctries.* 9, 1–7. doi: 10.3855/jidc.5065

Barua, H., Biswas, P. K., Olsen, K. E., and Christensen, J. P. (2012). Prevalence and characterization of motile *Salmonella* in commercial layer poultry farms in Bangladesh. *PLoS One* 7:e35914. doi: 10.1371/journal.pone.0035914

Chan, B. K., and Abedon, S. T. (2012). Phage therapy pharmacology: phage cocktails. *Adv. Appl. Microbiol.* 78, 1–23. doi: 10.1016/B978-0-12-394805-2.00001-4

Chan, B. K., Abedon, S. T., and Loc-Carrillo, C. (2013). Phage cocktails and the future of phage therapy. *Future Microbiol.* 8, 769–783. doi: 10.2217/fmb.13.47

Clavijo, V., Baquero, D., Hernandez, S., Farfan, J. C., Arias, J., Arévalo, A., et al. (2019). Phage cocktail SalmoFREE® reduces *Salmonella* on a commercial broiler farm. *Poult. Sci.* 98, 5054–5063. doi: 10.3382/ps/pez251

Clinical and Laboratory Standard Institute (CLSI) (2015). *Performance Standards and Antimicrobial Susceptibility Testing: 25th Informational Supplement. CLSI Document M100-S25*. Wayne, PA: CLSI.

Dagnew, B., Alemayehu, H., Medhin, G., and Eguale, T. (2020). Prevalence and antimicrobial susceptibility of *Salmonella* in poultry farms and in-contact humans in Adama and Modjo towns, Ethiopia. *MicrobiologyOpen* 9:e1067. doi: 10.1002/mbo3.1067

Djeffal, S., Mamache, B., Elgroud, R., Hireche, S., and Bouaziz, O. (2018). Prevalence and risk factors for *Salmonella* spp. contamination in broiler chicken farms and slaughterhouses in the northeast of Algeria. *Vet. World* 11, 1102–1108. doi: 10.14202/vetworld.2018.1102-1108

Dolejska, M., Villa, L., Hasman, H., Hansen, L., and Carattoli, A. (2013). Characterization of IncN plasmids carrying bla$_{CTX-M-1}$ and qnr genes in *Escherichia coli* and *Salmonella* from animals, the environment and humans. *J. Antimicrob. Chemother.* 68, 333–339. doi: 10.1093/jac/dks387

Dookeran, M. M., Baccus-Taylor, G. S. H., Akingbala, J. O., Tameru, B., and Lammerding, A. M. (2012). Assessing thermal inactivation of *Salmonella* on cooked broiler chicken carcasses in Trinidad and Tobago. *Open Conf. Proc. J.* 3, 12–19. doi: 10.2174/2210289201203020012

Dy, R. L., Rigano, L. A., and Fineran, P. C. (2018). Phage-based biocontrol strategies and their application in agriculture and aquaculture. *Biochem. Soc. Trans.* 46, 1605–1613. doi: 10.1042/BST20180178

Eguale, T. (2018). Non-typhoidal *Salmonella* serovars in poultry farms in central Ethiopia: prevalence and antimicrobial resistance. *BMC Vet. Res.* 14:217. doi: 10.1186/s12917-018-1539-4

Eng, S. K., Pusparajah, P., Ab Mutalib, N. S., Ser, H. L., Chan, K. G., and Lee, L. H. (2015). *Salmonella*: a review on pathogenesis, epidemiology and antibiotic resistance. *Front. Life Sci.* 8:284–293. doi: 10.1080/21553769.2015.1051243

Fagbamila, I. O., Barco, L., Mancin, M., Kwaga, J., Ngulukun, S. S., Zavagnin, P., et al. (2017). *Salmonella* serovars and their distribution in Nigerian commercial chicken layer farms. *PLoS One* 12:e0173097. doi: 10.1371/journal.pone.0173097

Goodridge, L. D. (2010). Designing phage therapeutics. *Curr. Pharm. Biotechnol.* 11, 15–27. doi: 10.2174/138920110790725348

Goodridge, L. D., and Bisha, B. (2011). Phage-based biocontrol strategies to reduce foodborne pathogens in foods. *Bacteriophage* 1, 130–137. doi: 10.4161/bact.1.3.17629

Heyse, S., Hanna, L. F., Woolston, J., Sulakvelidze, A., and Charbonneau, D. (2015). Bacteriophage cocktail for biocontrol of *Salmonella* in dried pet food. *J. Food Prot.* 78, 97–103. doi: 10.4315/0362-028X.JFP-14-041

Hooton, S. P., Atterbury, R. J., and Connerton, I. F. (2011). Application of a bacteriophage cocktail to reduce *Salmonella typhimurium* U288 contamination on pig skin. *Int. J. Food Microbiol.* 151, 157–163. doi: 10.1016/j.ijfoodmicro.2011.08.015

Hungaro, H. M., Mendonça, R. C. S., Gouvêa, D. M., Vanetti, M. C. D., and de Oliveira Pinto, C. L. (2013). Use of bacteriophages to reduce *Salmonella* in chicken skin in comparison with chemical agents. *Food Res. Int.* 52, 75–81. doi: 10.1016/j.foodres.2013.02.032

Jung, L. S., Ding, T., and Ahn, J. (2017). Evaluation of lytic bacteriophages for control of multidrug-resistant *Salmonella typhimurium*. *Ann. Clin. Microbiol. Antimicrob.* 16:66. doi: 10.1186/s12941-017-0237-6

Kumar, Y., Singh, V., Kumar, G., Gupta, N. K., and Tahlan, A. K. (2019). Serovar diversity of *Salmonella* among poultry. *Indian J. Med. Res.* 150, 92–95. doi: 10.4103/ijmr.IJMR_1798_17

Lampang, K. N., Chailangkarn, S., and Padungtod, P. (2014). Prevalence and antimicrobial resistance of *Salmonella* serovars in chicken farm, Chiang Mai and Lamphun province, Northern of Thailand. *Chiang Mai Vet. J.* 12, 85–93.

Lim, T. H., Kim, M. S., Lee, D. H., Lee, Y. N., Park, J. K., Youn, H. N., et al. (2012). Use of bacteriophage for biological control of *Salmonella enteritidis* infection in chicken. *Res. Vet. Sci.* 93, 1173–1178. doi: 10.1016/j.rvsc.2012.06.004

Manohar, P., Tamhankar, A. J., Lundborg, C. S., and Nachimuthu, R. (2019). Therapeutic characterization and efficacy of bacteriophage cocktails infecting *Escherichia coli*, *Klebsiella pneumoniae*, and *Enterobacter* species. *Front. Microbiol.* 10:574. doi: 10.3389/fmicb.2019.00574

Mirzaei, M. K., and Nilsson, A. S. (2015). Isolation of phages for phage therapy: a comparison of spot tests and efficiency of plating analyses for determination

of host range and efficacy. *PLoS One* 10:e0118557. doi: 10.1371/journal.pone.0118557

Mueller-Doblies, D., Sayers, A. R., Carrique-Mas, J. J., and Davies, R. H. (2009). Comparison of sampling methods to detect *Salmonella* infection of turkey flocks. *J. Appl. Microbiol.* 107, 635–645. doi: 10.1111/j.1365-2672.2009.04230.x

Nabil, N. M., Tawakol, M. M., and Hassan, H. M. (2018). Assessing the impact of bacteriophages in the treatment of *Salmonella* in broiler chickens. *Infect. Ecol. Epidemiol.* 8:1539056. doi: 10.1080/20008686.2018.1539056

Nair, D. V., and Johny, A. K. (2019). "*Salmonella* in poultry meat production," in *Food Safety in Poultry Meat Production*, eds K. Venkitanarayanan, S. ThakurSteven, and S. C. Ricke (Berlin: Springer Nature), 1–24.

Petsong, K., Benjakul, S., Chaturongakul, S., Switt, A. I. M., and Vongkamjan, K. (2019). Lysis profiles of *Salmonella* phages on *Salmonella* isolates from various sources and efficiency of a phage cocktail against *S. enteritidis* and *S. typhimurium*. *Microorganisms* 7:100. doi: 10.3390/microorganisms7040100

Phongaran, D., Khang-Air, S., and Angkititrakul, S. (2019). Molecular epidemiology and antimicrobial resistance of *Salmonella* isolates from broilers and pigs in Thailand. *Vet. World* 12, 1311–1318. doi: 10.14202/vetworld.2019.1311-1318

Phothaworn, P., Dunne, M., Supokaivanich, R., Ong, C., Lim, J., Taharnklaew, R., et al. (2019). Characterization of flagellotropic, Chi-Like *Salmonella* phages isolated from Thai poultry farms. *Viruses* 11:520. doi: 10.3390/v11060520

Pulido-Landínez, M. (2019). Food safety-*Salmonella* update in broilers. *Anim. Feed Sci. Technol.* 250, 53–58. doi: 10.1016/j.anifeedsci.2019.01.008

Rattanachaikunsopon, P., and Phumkhachorn, P. (2012). "Bacteriophage PPST1 isolated from hospital wastewater, a potential therapeutic agent against drug resistant *Salmonella enterica* subsp. enterica serovar typhi," in *Salmonella: Distribution, Adaptation, Control Measures and Molecular Technologies*, eds B. Annous and J. Gurtler (London: IntechOpen), 159–172.

Rohde, C., Resch, G., Pirnay, J. P., Blasdel, B. G., Debarbieux, L., Gelman, D., et al. (2018). Expert opinion on three phage therapy related topics: bacterial phage resistance, phage training and prophages in bacterial production strains. *Viruses* 10:178. doi: 10.3390/v10040178

Sripaurya, B., Ngasaman, R., Benjakul, S., and Vongkamjan, K. (2019). Virulence genes and antibiotic resistance of *Salmonella* recovered from a wet market in Thailand. *J. Food Safe* 39:e12601. doi: 10.1111/jfs.12601

Sundar, M. M., Nagananda, G. S., Das, A., Bhattacharya, S., and Suryan, S. (2009). Isolation of host-speci?c bacteriophages from sewage against human pathogens. *Asian J. Biotechnol.* 1, 163–170. doi: 10.3923/ajbkr.2009.163.170

Thanki, A. M., Brown, N., Millard, A. D., and Clokie, M. R. (2019). Genomic characterisation of jumbo *Salmonella* phages that effectively target UK pig-associated *Salmonella* serotypes. *Front. Microbiol.* 10:1491. doi: 10.3389/fmicb.2019.01491

Vandeplas, S., Dauphin, R. D., Beckers, Y., Thonart, P., and Thewis, A. (2010). *Salmonella* in chicken: current and developing strategies to reduce contamination at farm level. *J. Food Prot.* 73, 774–785. doi: 10.4315/0362-028x-73.4.774

Vongkamjan, K., Benjakul, S., Vu, H. T. K., and Vuddhakul, V. (2017). Longitudinal monitoring of *Listeria monocytogenes* and *Listeria* phages in seafood processing environments in Thailand. *Food Microbiol.* 66, 11–19. doi: 10.1016/j.fm.2017.03.014

Vongkamjan, K., Switt, A. M., den Bakker, H. C., Fortes, E. D., and Wiedmann, M. (2012). Silage collected from dairy farms harbors an abundance of Listeriaphages with considerable host range and genome size diversity. *Appl. Environ. Microbiol.* 78, 8666–8675. doi: 10.1128/AEM.01859-12

Witkowska, D., Kuncewicz, M., Żebrowska, J. P., Sobczak, J., and Sowińska, J. (2018). Prevalence of *Salmonella* spp. in broiler chicken flocks in northern Poland in 2014–2016. *Ann. Agric. Environ. Med.* 25, 693–697. doi: 10.26444/aaem/99528

World Health Organization (WHO) (2018). *Salmonella* (non-Typhoidal). Available online at: https://www.who.int/en/news-room/fact-sheets/detail/salmonella-(non-typhoidal) (Accessed September 14, 2020)

Yang, Y., Shen, W., Zhong, Q., Chen, Q., He, X., Baker, J. L., et al. (2020). Development of a bacteriophage cocktail to constrain the emergence of phage-resistant *Pseudomonas aeruginosa*. *Front. Microbiol.* 11:327. doi: 10.3389/fmicb.2020.00327

Yildirim, Z., Sakın, T., and Çoban, F. (2018). Isolation of lytic bacteriophages infecting *Salmonella typhimurium* and *Salmonella enteritidis*. *Acta Biol. Hung.* 69, 350–369. doi: 10.1556/018.68.2018.3.10

Ziyate, N., Karraouan, B., Kadiri, A., Darkaoui, S., Soulaymani, A., and Bouchrif, B. (2016). Prevalence and antimicrobial resistance of *Salmonella* isolates in Moroccan laying hens farms. *J. Appl. Poult. Res.* 25, 539–546. doi: 10.3382/japr/pfw03

Conflict of Interest: The authors declare that the research was conducted in the absence of any commercial or financial relationships that could be construed as a potential conflict of interest.

frontiers in Microbiology

ORIGINAL RESEARCH
published: 17 June 2021
doi: 10.3389/fmicb.2021.668319

Characterization and Genomic Analysis of BUCT549, a Novel Bacteriophage Infecting *Vibrio alginolyticus* With Flagella as Receptor

Jing Li[1†], Fengjuan Tian[1†], Yunjia Hu[1†], Wei Lin[1], Yujie Liu[1], Feiyang Zhao[2], Huiying Ren[2], Qiang Pan[2], Taoxing Shi[3] and Yigang Tong[1]**

[1] College of Life Science and Technology, Beijing University of Chemical Technology, Beijing, China, [2] Qingdao Phagepharm Bio-tech Co., Ltd., Shandong, China, [3] Academy of Military Medical Sciences, Beijing, China

OPEN ACCESS

Edited by:
Robert Czajkowski,
University of Gdańsk, Poland

Reviewed by:
Konstantin Anatolievich Miroshnikov,
Institute of Bioorganic Chemistry (RAS), Russia
Jens Andre Hammerl,
Bundesinstitut für Risikobewertung, Germany

***Correspondence:**
Taoxing Shi
shitaoxing@sina.com
Yigang Tong
tong.yigang@gmail.com

[†] These authors have contributed equally to this work

Specialty section:
This article was submitted to Virology, a section of the journal Frontiers in Microbiology

Received: 16 February 2021
Accepted: 14 May 2021
Published: 17 June 2021

Citation:
Li J, Tian F, Hu Y, Lin W, Liu Y, Zhao F, Ren H, Pan Q, Shi T and Tong Y (2021) Characterization and Genomic Analysis of BUCT549, a Novel Bacteriophage Infecting Vibrio alginolyticus With Flagella as Receptor. Front. Microbiol. 12:668319. doi: 10.3389/fmicb.2021.668319

Vibrio alginolyticus is one of the most important of pathogens that can infect humans and a variety of aquatic animals, and it can cause food poisoning and septicemia in humans. Widely used antibiotics are gradually losing their usefulness, and phages are gaining more attention as new antibacterial strategies. To have more potential strategies for controlling pathogenic bacteria, we isolated a novel *V. alginolyticus* phage BUCT549 from seafood market sewage. It was classified as a new member of the family *Siphoviridae* by transmission electron microscopy and a phylogenetic tree. We propose creating a new genus for BUCT549 based on the intergenomic similarities (maximum is 56%) obtained from VIRIDIC calculations. Phage BUCT549 could be used for phage therapy due to its stability in a wide pH (3.0–11.0) range and high-temperature (up to 60°C) environment. It had a latent period of 30–40 min and a burst size of 141 PFU/infected bacterium. In the phylogenetic tree based on a terminase large subunit, BUCT549 was closely related to eight *Vibrio* phages with different species of host. Meanwhile, our experiments proved that BUCT549 has the ability to infect a strain of *Vibrio parahaemolyticus*. A coevolution experiment determined that three strains of tolerant *V. alginolyticus* evaded phage infestation by mutating the MSHA-related membrane protein expression genes, which caused the loss of flagellum. This research on novel phage identification and the mechanism of infestation will help phages to become an integral part of the strategy for biological control agents.

Keywords: *vibrio alginolyticus*, bacteriophage, receptor, MSHA protein, genome analysis

INTRODUCTION

V. alginolyticus is a pathogenic bacterium common in oceans and lakes, and it is prone to causing outbreaks of *Vibrio* diseases in fish, shrimp, shellfish, and other farmed animals in the aquaculture industry. Accidentally ingested *V. alginolyticus* can easily cause septicemia and other extra-intestinal infections in humans (Altekruse et al., 2000; Horseman and Surani, 2011; Mohamad et al., 2019). The frequent use of antibiotics has led to an increase of resistance strains

of *V. alginolyticus*, which puts more pressure on the pathogenic bacteria in the economics and medical fields. *V. alginolyticus* has been the third most common *Vibrio* species in human disease reports for many years (Jacobs Slifka et al., 2017). In recent years, there has been an upward trend in the incidence of water pollution and food poisoning caused by *V. alginolyticus*. It worth paying more attention to *V. alginolyticus*, and it is urgent to develop alternative approaches of antibiotics to control these pathogens (Newton et al., 2012; Osunla and Okoh, 2017).

Bacteriophages, the most abundant organisms on Earth, can be found in all corners in worldwide distribution. They are gradually being developed as an alternative to antibiotics for the treatment of various bacterial infections. Phages in the ocean have an important role in carbon and energy cycling (Suttle, 2007). Compared with antibiotics, phages have many advantages, such as high specificity, obvious antibacterial effect, and simple isolation and preparation, and they are gradually being applied in the farming and medical industries. Here, we isolated a *V. alginolyticus* from farmed sick shrimp and obtained a novel *V. alginolyticus* phage designated as BUCT549 (GenBank accession no. MT735629.1) from the sewage in a nearby seafood market. Phage BUCT549 has the ability to infect both *V. alginolyticus* and *V. parahaemolyticus*. In this study, we identified its biological and genomic characteristics and screened the tolerant bacteria by coculture of phage and bacteria to promote coevolution. Furthermore, we identity that the host receptor of phage BUCT549 was an MSHA type transmembrane protein, which provides more basis for the subsequent use of the phage to control *Vibrio* hazards.

MATERIALS AND METHODS

Isolated and Identification of Bacterial Pathogens

V. alginolyticus was isolated as a host from diseased shrimp in a farm in 2019 (Qingdao, Shandong, China) and cultured at 37°C using 2216E plates (2216E agar, Solarbio). The bacterial species of the host was identified by 16S universal primers (16S-F-5′-AACTGGAGGAAGGTGGGGAT-3′, and 16S-R-5′-AGGAGGTGATCCAACCGCA-3′) and Sanger sequencing.

Isolation and Purification of BUCT549

Sewage from a seafood market in Qingdao was centrifuged at 10,000 × g for 10 min, and the supernatant was filtered through a 0.22-μm syringe filter, 50 μL of filtrate was mixed with 5 mL of log phase (OD_{600}≈0.5) *V. alginolyticus* culture, incubated overnight at 37°C and 220 rpm. The culture solution was centrifuged at 8,000 × g for 10 min, and the supernatant filtered through a 0.22-μm filter to obtain a phage stock solution. The filtrate was applied to make double-layer plates and cultured at 37°C until translucent individual plaques appeared. A single plaque was picked and added to 5 mL of 2216E liquid medium containing 100 μL of *V. alginolyticus* inoculum and cultured at 37°C for 6 h. The phage was obtained again by centrifugation, filtration, dilution, and plating. This step of phage purification was repeated three times.

High-Throughput Genome Sequencing of Phage BUCT549

Phage genomic DNA was extracted using a modified phenol-chloroform extraction protocol (Li et al., 2019). A 2 × 300 nt paired-end DNA library was prepared with the NEBNext® UltraTM II DNA Library Prep Kit for Illumina following the manufacturer's protocol[1]. Briefly, 150 ng of DNA were dissolved in deionized water to a final volume of 50 μL and disrupted to 300-bp fragments using a Bioruptor UCD-200TS ultrasound system. Then, the fragmented DNAs were end-repaired and adaptor ligated using NEBNext Ultra II End Prep Enzyme and Ligation Master Mix, respectively. Next, the adaptor-ligated DNA was selected and cleaned using EBNext Sample Purification Beads. Finally, the adaptor-ligated DNA was subjected to PCR amplification, and the PCR products were cleaned using EBNext Sample Purification Beads. High-throughput sequencing of the DNA was performed on an Illumina MiSeq instrument (San Diego, CA, United States).

Transmission Electron Microscopy (TEM)

Phage particles were centrifuged at 13,000 × g for 2 h and then purified by sucrose density gradient centrifugation to visualize phage morphology by TEM (Chen et al., 2018). A 20-μL aliquot of phage suspension was incubated on a carbon-coated copper grid for 15 min and then dried using filter paper. The copper grid covering the phages was then stained with 2% (w/v) phosphotungstic acid (pH7.0) for 2 min. Finally, phage morphology was examined at 80 kV using a JEM-1200EX transmission electron microscope (Jeol Ltd., Tokyo, Japan).

Multiplicity of Infection (MOI) and One-Step Growth Curves

The optimal MOI and one-step growth curves for isolated phages were determined using methods described previously (Xi et al., 2019). Briefly, phages were added to 5 mL of log-phase *V. alginolyticus* culture to achieve an MOI of 10, 1, 0.1, 0.01, 0.001, or 0.0001, and then incubated at 37°C, 220 rpm for 6 h. Culture supernatant was then filtered through a 0.22-μm filter, and the titer of the phage in the supernatant was measured using a double-layer agar plate method. Three replicates were conducted for determination. The MOI resulting in the highest phage titer was considered the optimal MOI of the phage.

The one-step growth curve of a phage reflects dynamic changes in the number of particles during phage replication. To obtain a one-step growth curve for BUCT549, phage suspension was added to 20 mL of log-phase *V. alginolyticus* culture at the optimal MOI and incubated at 37°C for 5 min. Then, the culture was centrifuged at 12,000 × g for 1 min and the supernatant discarded. The pellet was then washed twice with 2216E liquid medium and resuspended in 20 mL of 2216E liquid medium. The moment when the pellet was resuspended in medium was defined as time zero. Then, the resulting culture was transferred to a shaker and incubated at 37°C, 220 rpm for 3.5 h. Three

[1]https://international.neb.com/-/media/nebus/files/manuals/manuale6177-e7805.pdf

duplicate samples (100 μL) were collected every 20 min to determine the phage titer at different time points. Three replicates were conducted for determination. The one-step growth curve was obtained by plotting phage titer against time. The burst size was calculated by dividing the plateau phage titer by the initial phage titer.

Thermal and pH Stability

In the thermostability assay, the phage isolations were incubated at 40, 50, 60, and 70°C, and the aliquots were collected after 20, 40, and 60 min to be titered by the double-layer agar method. For the pH stability assay, samples of the isolated phage were mixed in a series of tubes containing 2216E liquid medium of different pH values [2–12, adjusted using NaOH (1 mol/L) or HCl (1 mol/L)], incubated for 1 h at 37°C, and then titered by the double-layer agar plate method.

Tolerant Bacteria Screening

Three independent cultures of *V. alginolyticus* in logarithmic phase were used to coculture with phage BUCT549, and after observing the reclouding of the culture, the surviving bacteria were used to delineate and pick single colonies for liquid culture, and tolerance to BUCT549 was confirmed after a spot assay and DAL assay. Bacteria nucleic acids were extracted using the Bacteria Genomic DNA Kit (cwbiotech) and the DNA library was prepared with the NEBNext® UltraTM II DNA Library Prep Kit for Illumina high-throughput genome sequencing.

Bioinformatics Analysis

Sequencing data were filtered using Trimmomatic v0.36 (Bolger et al., 2014) and assembled using SPAdes v3.13.0. Bacterial drug resistance genes are transmitted through ResFinder[2] (Bortolaia et al., 2020). Phage's tRNAs were detected using tRANscan-SE2[3] (Lowe and Eddy, 1997; Lowe and Chan, 2016); the virulence and pathogen genes carried by phages detected with VirulenceFinder[4] (Clausen et al., 2018) and PathogenFinder[5] (Cosentino et al., 2013). Rho—independent transcription terminators were projected by ARNold[6] (Gautheret and Lambert, 2001). Open reading frames (ORFs) were predicted with RAST[7] (Brettin et al., 2015). The ORFs were annotated using the BLASTp algorithm with the non-redundant (nr) protein database of the National Center for Biotechnology Information (NCBI)[8]. Phage homology calculations were performed using VIRIDIC[9] (Moraru et al., 2020). Use the SNP plugin in CLC Genomics Workbench 12.0 to find tolerant bacterial mutant loci, using clustalw[10] and ESPript[11] (Robert and Gouet, 2014) to determine mutant site translation. Comparative genomic analysis used Easyfig 2.2.3 (Sullivan et al., 2011). To determine the taxonomy of the isolated phages, phylogenetic analysis based on the terminase large subunit was carried out using software MEGA7 with the neighbor-joining method and 1,000 bootstrap replications and the tree optimized with Evolview (Subramanian et al., 2019). Shared gene analysis was performed using OrthoMCL (Chen et al., 2006), shared gene relationships were mapped using Cytoscape 3.7.1, and phage shared gene heat maps with BUCT549 were mapped using the R package pheatmap.

[2]https://cge.cbs.dtu.dk/services/ResFinder
[3]http://lowelab.ucsc.edu/cgi-bin/tRNAscan-SE2.cgi
[4]https://cge.cbs.dtu.dk/services/VirulenceFinder
[5]https://cge.cbs.dtu.dk/services/PathogenFinder
[6]http://rssf.i2bc.paris-saclay.fr/toolbox/arnold
[7]https://rast.nmpdr.org/rast.cgi
[8]https://www.ncbi.nlm.nih.gov
[9]http://rhea.icbm.uni-oldenburg.de/VIRIDIC/
[10]https://www.genome.jp/tools-bin/clustalw
[11]http://espript.ibcp.fr/ESPript/cgi-bin/ESPript.cgi

RESULTS AND DISCUSSION

Isolation and Identification of BUCT549 and Its Host

V. alginolyticus was isolated from the farmed shrimp with disease in Qingdao, China. We determined the antibiotic resistance of the bacterium from assembled NGS data by ResFinder. *V. alginolyticus* carries resistance genes for doxycycline [tet (35)], tetracycline [tet (34)] and tet [(35)], ampicillin (blaCARB-42), amoxicillin (blaCARB-42), and piperacillin (blaCARB-42), which may be the main reason for the failure to completely kill the bacteria during the culture process, thus causing diseases among shrimp. We used this bacterium as the host and collected the sewage from a nearby seafood market. Continuous purification using a double-layer agar plate finally yielded the lytic phage BUCT549, which can infect this *V. alginolyticus* strain. The results of TEM showed that phage BUCT549 was a typical phage of the family *Siphoviridae* within the *Caudovirales* order, which had an icosahedral head and a curved tail. The head diameter and tail length were approximately 186.1 ± 0.70 nm (n = 3) and 74.67 ± 0.41 nm (n = 3), respectively (**Figure 1**).

Biological Characterization of BUCT549

We determined the MOI of phage BUCT549 and found that the highest viral titer of it could reach 1.7×10^{10} pfu/mL when the MOI was equal to 0.1 (**Figure 2A**). The one-step growth curve

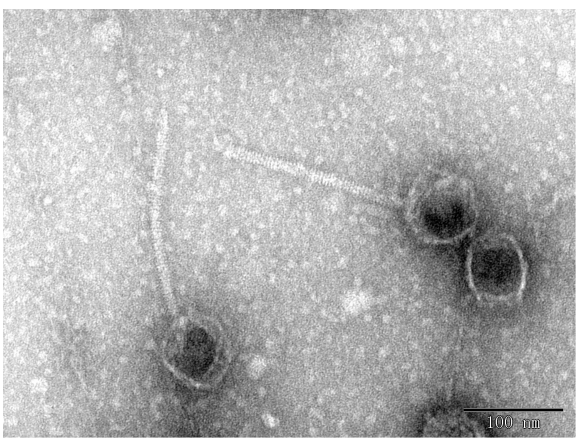

FIGURE 1 | Phage morphology observed using TEM.

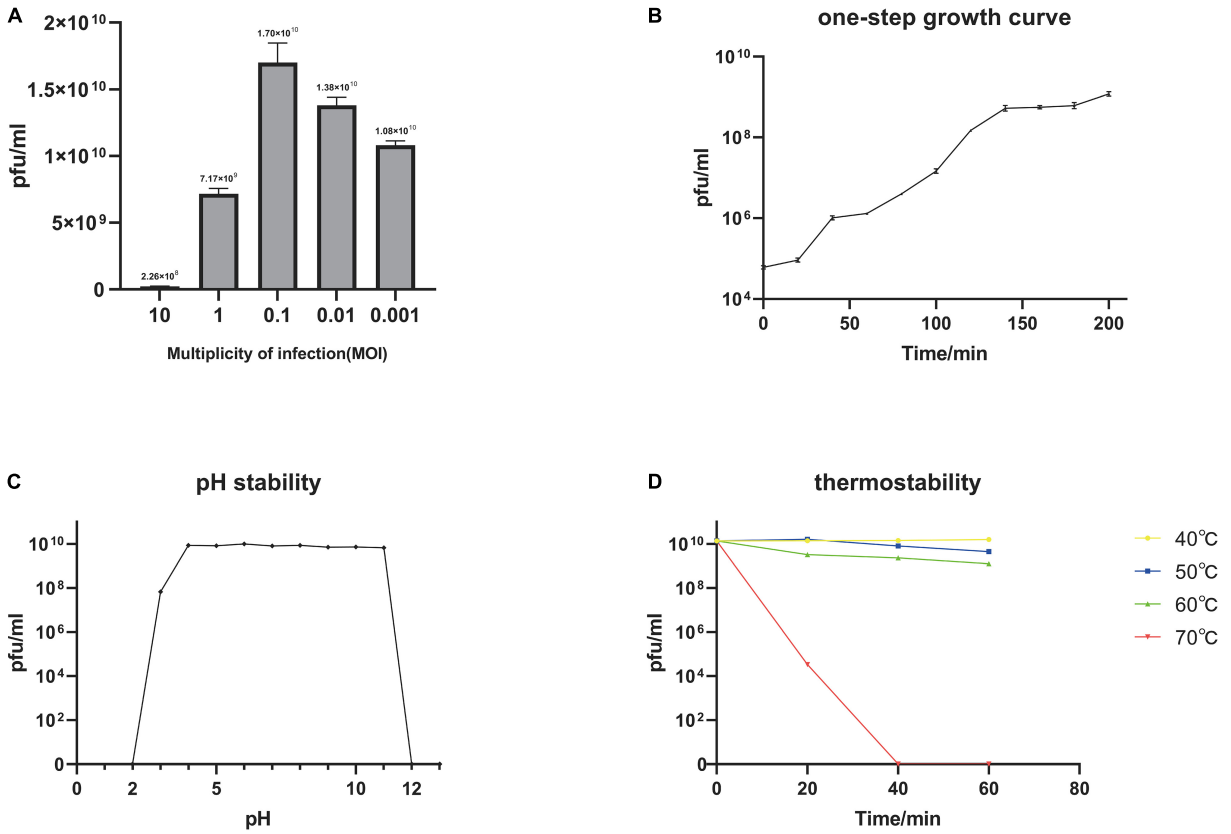

FIGURE 2 | Biological characterization of the phage BUCT549. **(A)** The MOI test of BUCT549. **(B)** The one-step growth curve of phage BUCT549, and data points show phage titers measured at 20-min intervals. **(C)** pH stability of BUCT549, and data points are phage titers measured after incubation of phage at different pH for 1 h. **(D)** Thermostability curve of BUCT549, and data points are phage titers measured after incubating the phage at different temperatures for 20, 40, and 60 min, respectively. All assays were performed in triplicate.

of phage BUCT549 was determined under the optimal MOI. The latent period was approximately 30–40 min, and the burst size was about 141 pfu/cell (**Figure 2B**). The burst size was defined as the ratio of the final number of free phage particles to the number of infected bacterial cells during the latent period.

Furthermore, we tested the stability of BUCT549, which showed that it was observably stable in lytic capacity between pH 3.0 and 11.0 by plaque counting (**Figure 2C**). During the temperature sensitivity assay, it was found that phage BUCT549 could be stable at 60°C for 1 h, and the activity of BUCT549 was not affected below 60°C (**Figure 2D**). The stability at room temperature or even at higher temperatures simplifies the conditions for phage storage or transport.

A double-layer agar plate test showed that phage BUCT549 could infect a strain of *V. parahaemolyticus* additionally. MLST typing was used to authenticate that this *V. parahaemolyticus* type is ST-772. The analysis of the NGS data of this *V. parahaemolyticus* revealed the presence of various resistance genes, such as streptomycin, sulfamethoxazole, ampicillin, and tetracycline. The ability of BUCT549 to infect resistant bacteria across species provides the possibility of its practical application, highlighting that it could be explored for phage therapies for infections of multiple drug-resistant *Vibrio* infections.

Coevolution Identifies the Phage BUCT549 Target Proteins

We determined the inhibition of *V. alginolyticus* growth by comparing the OD_{600} of *V. alginolyticus* with/without the addition of BUCT549. The *V. alginolyticus* was able to be kept at low levels for 120 min by BUCT549, but eventually it could survive with the existence of BUCT549 (**Figure 3**). To determine

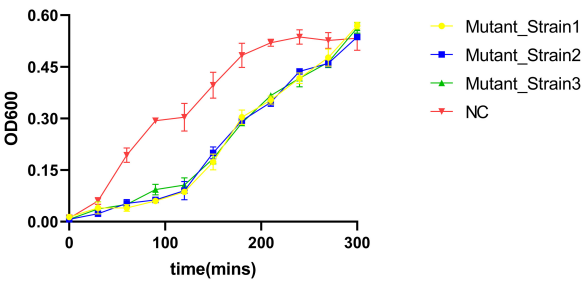

FIGURE 3 | *V. alginolyticus* kill curve. *V. alginolyticus* was incubated with/without the addition of the phage, and the curve was plotted by measuring *V. alginolyticus* OD600 at 30-min intervals.

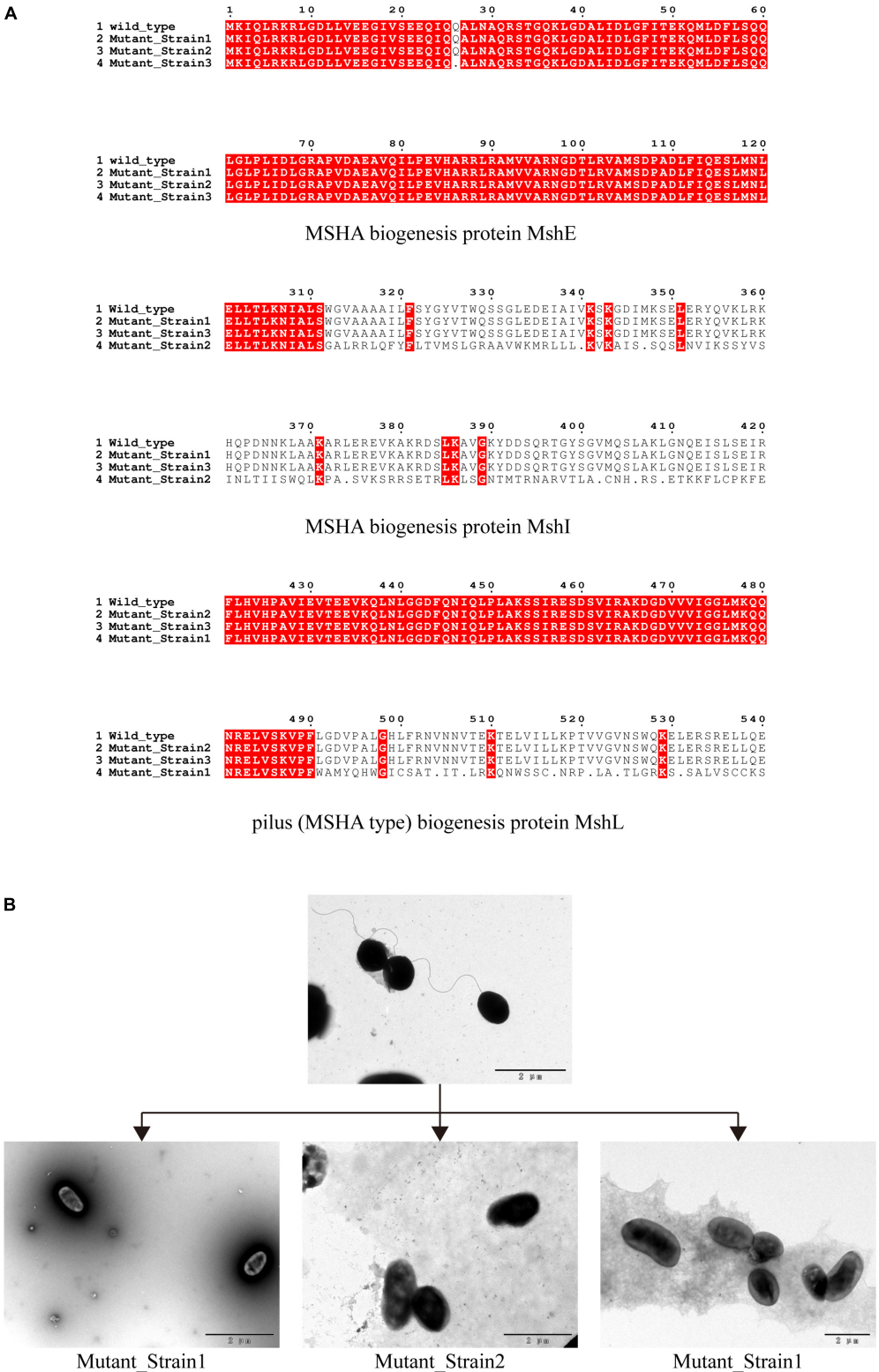

FIGURE 4 | Identification of phage recognition receptors based on coevolution. **(A)** Mutant strains tolerant to phage BUCT549, MSHA-like proteins affected by 100% mutated site. Mutant_Strain3 mutates at the 26th amino acid of MshE protein to produce a termination codon. Mutant_Strain2 has a deletion at amino acid 312 of the MshI protein, producing a stop codon at amino acid 340. Mutant_Strain1 has a deletion at amino acid 491 of the MshL protein, producing a stop codon at amino acid position 504. **(B)** Electron microscopic observation of the morphology of the host *V. alginolyticus* (with flagella) and three tolerate strains (without flagella).

the ability that *V. alginolyticus* escapes from BUCT549, we purified the single colonies of evolved *V. alginolyticus* from three groups that cocultured with BUCT549 independently. This stable evolution of resistance was confirmed by spot and DLA tests. It was determined that the three independently screened mutant strains could resist BUCT549. The three mutant strains (named Mutant_Strain1, Mutant_Strain2, and Mutant_Strain3) were subjected to NGS to identify the reasons for their acquisition of BUCT549 resistance. By comparison with sensitive strains using single nucleotide polymorphism (SNP) analysis in CLC software, we found 100% mutated sites in each of the tolerant strains. By comparison between these complete mutation sites, we found that all three independently generated mutant strains were mutated in proteins associated with the mannose-sensitive hemagglutinin MSHA biogenesis and caused various degrees of premature termination. Mutant_Strain3 mutates at the 26th amino acid of the MshE protein to produce a termination codon. Mutant_Strain2 has a deletion at amino acid 312 of the MshI protein, producing a stop codon at amino acid 340. Mutant_Strain1 has a deletion at amino acid 491 of the MshL protein, producing a stop codon at amino acid position 504 (**Figure 4A**). Besides this, the tolerant bacteria observed by electron microscopy did not have flagella present (**Figure 4B**). MSHA is a class of proteins associated with *Vibrio* movement and involved in biofilm formation (Utada et al., 2014). It is a potential settlement factor and protective antigen, affecting

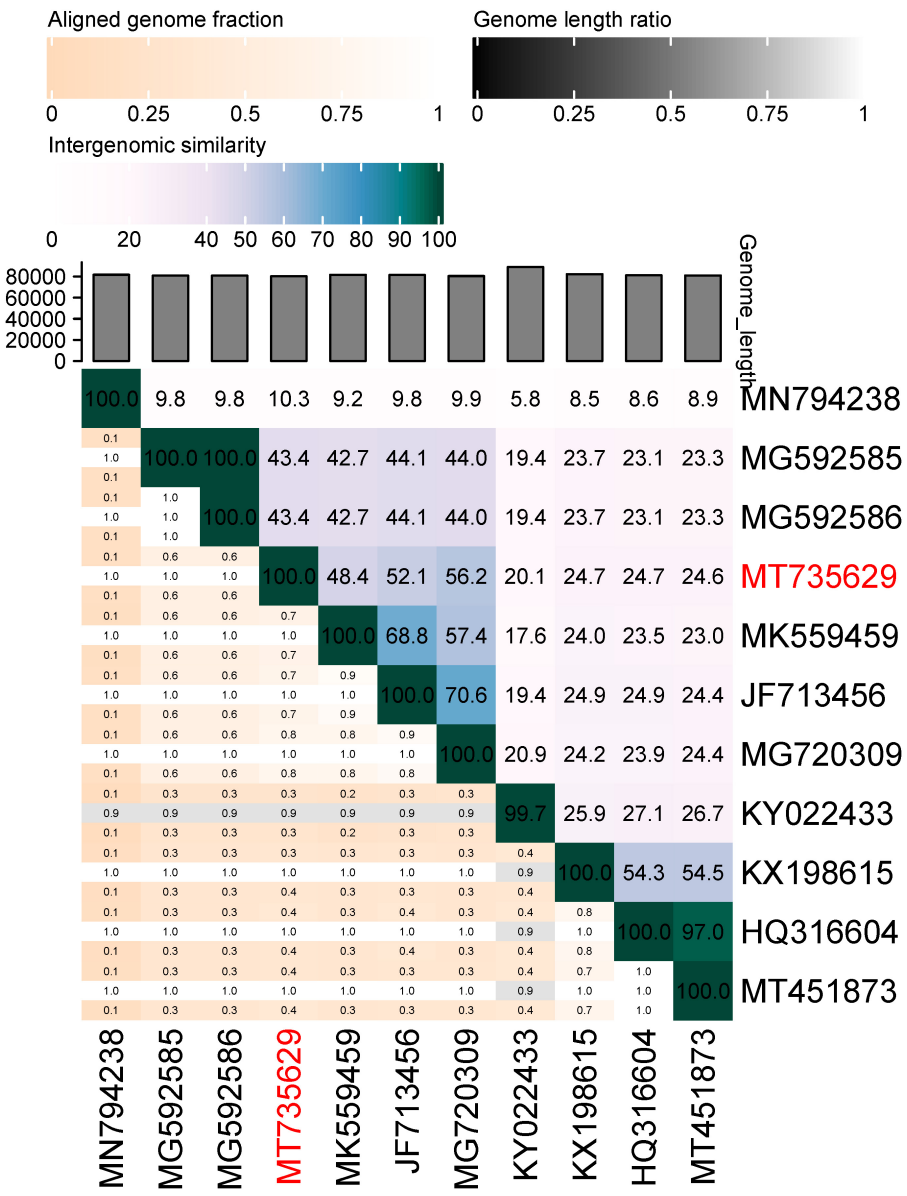

FIGURE 5 | Percentage sequence similarity between phages calculated using VIDIRIC. The horizontal and vertical coordinates indicate the corresponding phage Genebank number, and the phage in this study is marked in red font.

bacterial adhesion (Jonson et al., 1994). Studies report that it can be the receptor for *Vibrio cholerae* phage (Jouravleva et al., 1998; Campos et al., 2010). A large number of studies focus on *Vibrio cholerae*, but so far, this is the first reported infestation that *V. alginolyticus* phages could use flagella as a recognition receptor to infect. Our study suggests an evolutionary pathway for *Vibrio* to abandon some functions by MSHA protein mutation for escape phage.

Genomic Identification of the Phage BUCT549

The genome of BUCT549 was obtained using the Illumina sequencer platform, yielding 546,742 raw reads with an average length of 300 bp. By *de novo* assembly of these reads, a single contig of 80,294 bp in length and sequencing depth of 212 × was obtained with GC content of 45.54%. The genome of phage BUCT549 showed high sequence identity (76.32, 76.22, 75.27%) to the genomes of *Vibrio* phage 1 (GenBank: JF713456), *Vibrio* phage Ares1 (GenBank: MG720309) and *Vibrio* phage vB_VcaS_HC (GenBank:MK559459.1) with 37, 40, and 35% coverage, respectively. The low homology with known sequences showed that it is a novel discovered *V. alginolyticus* phage. We calculated the percentage of sequence similarity by VIRIDIC, resulting that the maximum similarity between BUCT549 and other known sequences is 56% (**Figure 5**), sufficient to qualify it as a new species. The International Committee on Taxonomy of Viruses (ICTV) describes a genus as a cohesive group of viruses sharing at least 60–70% nucleotide identity over the entire genome length (thresholds depending on the group of viruses) (Adriaenssens and Brister, 2017). Therefore, we are proposing to create a new genus in the *Siphoviridae* family to phage BUCT549.

ORF analysis of the phage using RAST determined that BUCT549 contains 119 predicted ORFs (**Figure 6**). In addition, we found 61 transcriptional terminators and no tRNA in BUCT549, indicating that BUCT549 is dependent on the host's replicative-translational machinery to complete its life activities. Phage BUCT549 did not carry any virulence or pathogenicity genes determined by VirulenceFinder and PathogenFinder, suggesting its potential application as an antibacterial and therapeutic agent. Using Blastp to annotate all ORFs, phage BUCT549 contains a large number of proteins of unknown

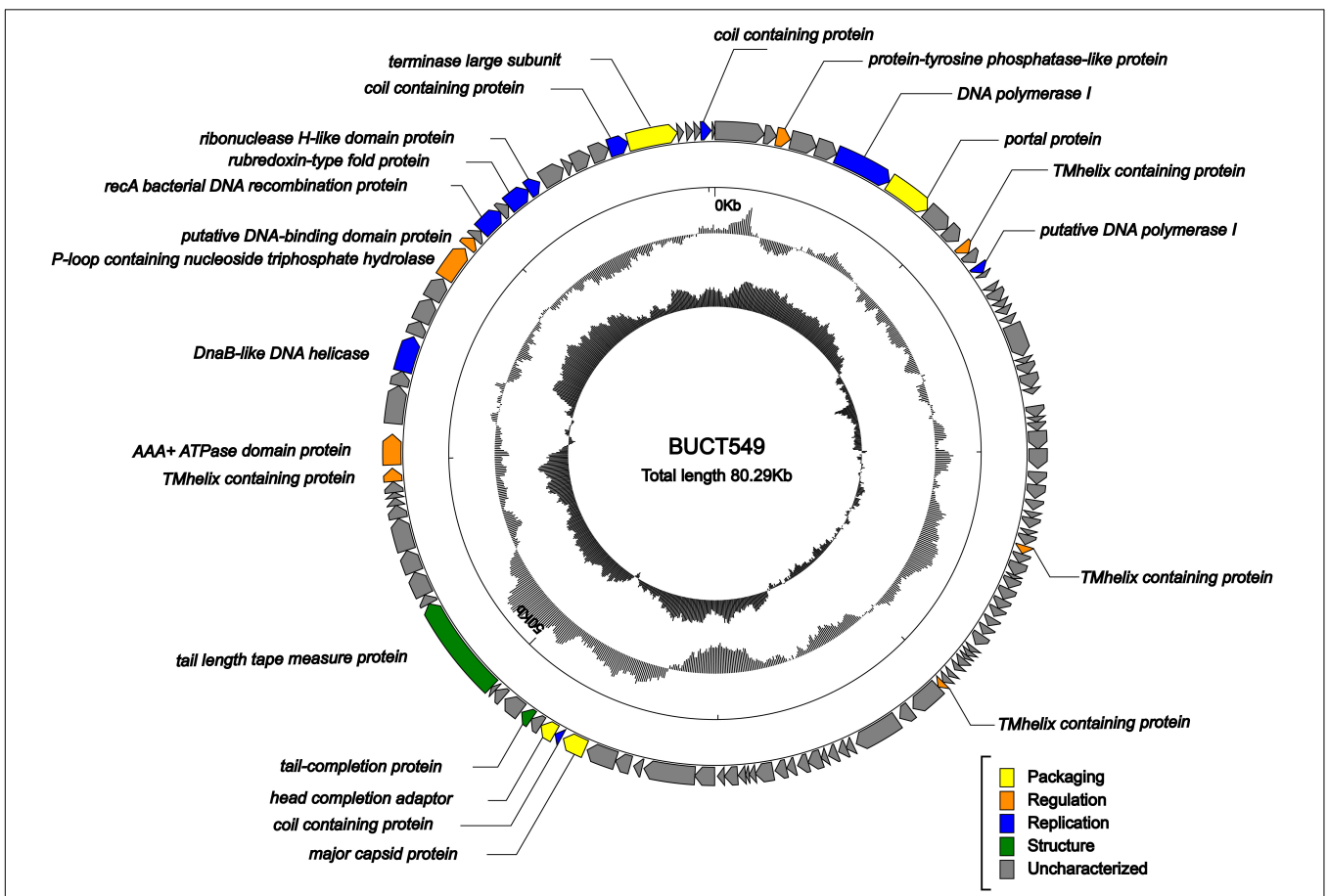

FIGURE 6 | Genome map of BUCT549. The outermost circle represents ORFs encoded in the genome with different colors representing different functions (clockwise arrow indicates the forward-reading frame, counterclockwise arrow indicates the reverse reading frame); the dark circles in the middle represent the GC content (outward indicates greater than the average GC content compared with the whole genome, and inward indicates the opposite); the innermost circle represents the GC skew (G–C/G + C. Outward indicates > 0 and inward indicates < 0).

function. Interestingly, we found that a lot of protein (81/119) annotation information for BUCT549 has similarity to *Vibrio* phage 1, which uses *Vibrio harveyi* as the host reported in 2012 (Khemayan et al., 2012). Using multiple-sequence alignment with *Vibrio* phage 1 and *Vibrio* phage Ares1, we found that BUCT549 was homologous to phage strains only in a relatively concentrated portion of the genome, and the homology coverage is less than 40% (**Figure 7**). A total of 18 proteins were successfully identified by protein profile, including portal protein, major capsid protein, head completion adaptor, tail length tape measure protein and other major structural proteins (**Supplementary Table 1**).

The phylogenetic tree was constructed using terminase large subunit of the phage, and some phages from the family *Myoviridae* and *Podoviridae* were selected as outgroups (**Figure 8**). BUCT549 was clustered with *Siphoviridae* phages, which is consistent with electron microscopy results. All the phages close to BUCT549 in the phylogenetic tree infect *Vibrio* bacteria, but they are quite different from each other (*Vibrio* phages are shown in the light green background and hosts are marked in the left). Phages under the same branch are able to infect *Vibrio harveyi* (*Vibrio* phage1 and *Vibrio* phage vb_VhaS-a), *Vibrio campbellii* (*Vibrio* phage vb_VcaS_HC), *Vibrio splendidus* (*Vibrio* phage 1.215.A. 10N.222.54.F7), *Vibrio cholerae* (*Vibrio* phage SIO-2), and *Vibrio natiegens* (*Vibrio* phage VH2_2019). The ability of *Vibrio* phage to infect across species has often been reported (Chen et al., 2020; Misol et al., 2020), *Vibrio* phages have great potential to treat mixed *Vibrio* contamination.

Core Gene Identification of Phage BUCT549

BUCT549 and another eight vibrio phages closest to BUCT549 were selected for core gene identification. Homology analysis and clustering were carried out with all annotated proteins, and a total of 159 clusters were divided into nine phages. The

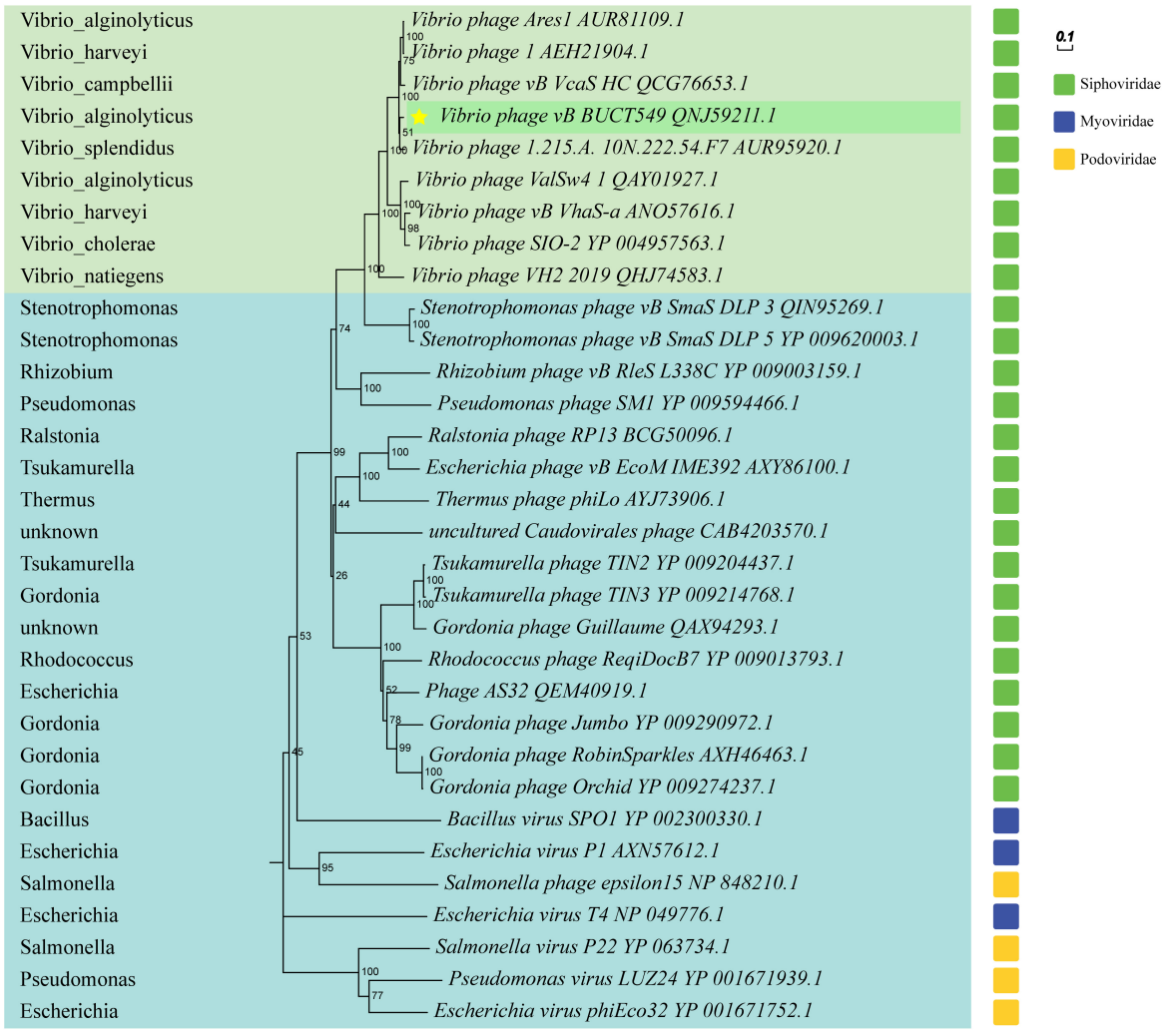

FIGURE 7 | Phylogenetic trees based on terminase large subunit, and partial phages of the *Myoviridae* and *Podoviridae* are selected as outgroups. *Vibrio* phages are marked in light green, and other host phages are marked in light blue. Hosts for all phages are shown on the left of the phylogenetic trees.

number of genes shared by different phages is independent of the species of the host. BUCT549 shares 112 genes with *V. alginolyticus* phage Ares1 but shares 64 genes with another *V. alginolyticus* phage ValSw4_1. The number of genes that BUCT549 shares with two *V. harveyi* phages or two *Vibrio campbllii* phages is also different. BUCT549 shares 105 genes with *V. harveyi* phage 1 and 72 genes with *V. harveyi* phage vB_VhaS-a, and it shares 98 genes with *V. campbllii* phage vB_VcaS_HC and 72 genes with *V. campbllii* phage SIO-2 (**Figure 9A**). The 23 annotated genes are linked to other phages using different colored lines (**Figure 9B**). Nineteen genes, including DNA polymerase (ORF6), portal protein (ORF7), major capsid protein (ORF77), tail proteins (ORF81 and ORF85) and terminase large subunit (ORF114) present in all *Vibrio* phages, demonstrate the feasibility of using such conserved proteins coded by core genes to determine evolutionary relationships. The amount of TMhelix containing protein in *Vibrio* phages is different, two TMhelix containing proteins are shared in nine phages and two

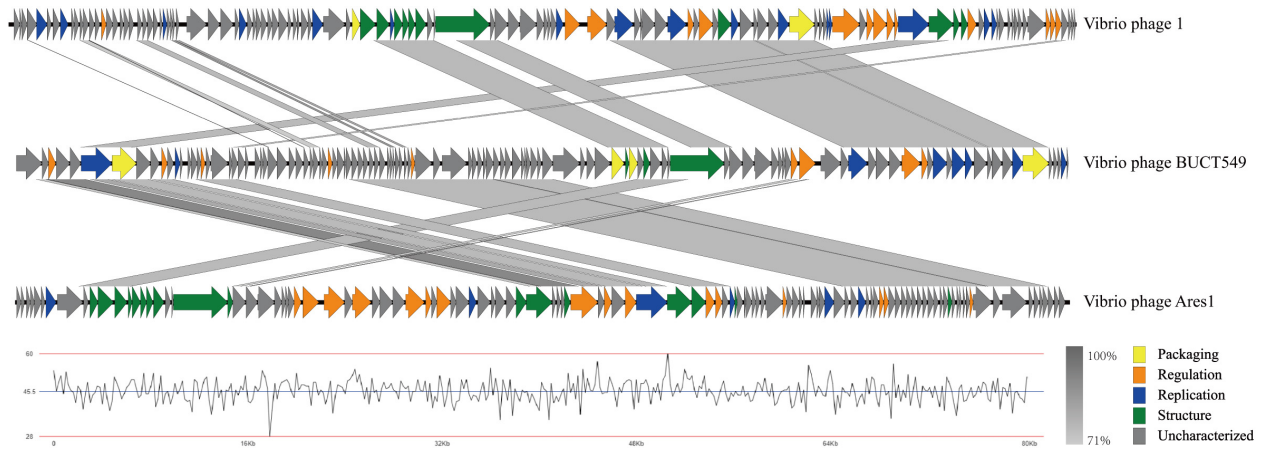

FIGURE 8 | Multiple-sequence alignment of phage genomes. The whole genomes of *Vibrio* phage BUCT549, *Vibrio* phage 1, and *Vibrio* phage Ares 1, compared using Easyfig. The gray shading indicates sequence similarities between the genomes. The lower half of the graph indicates the GC content of phage BUCT549.

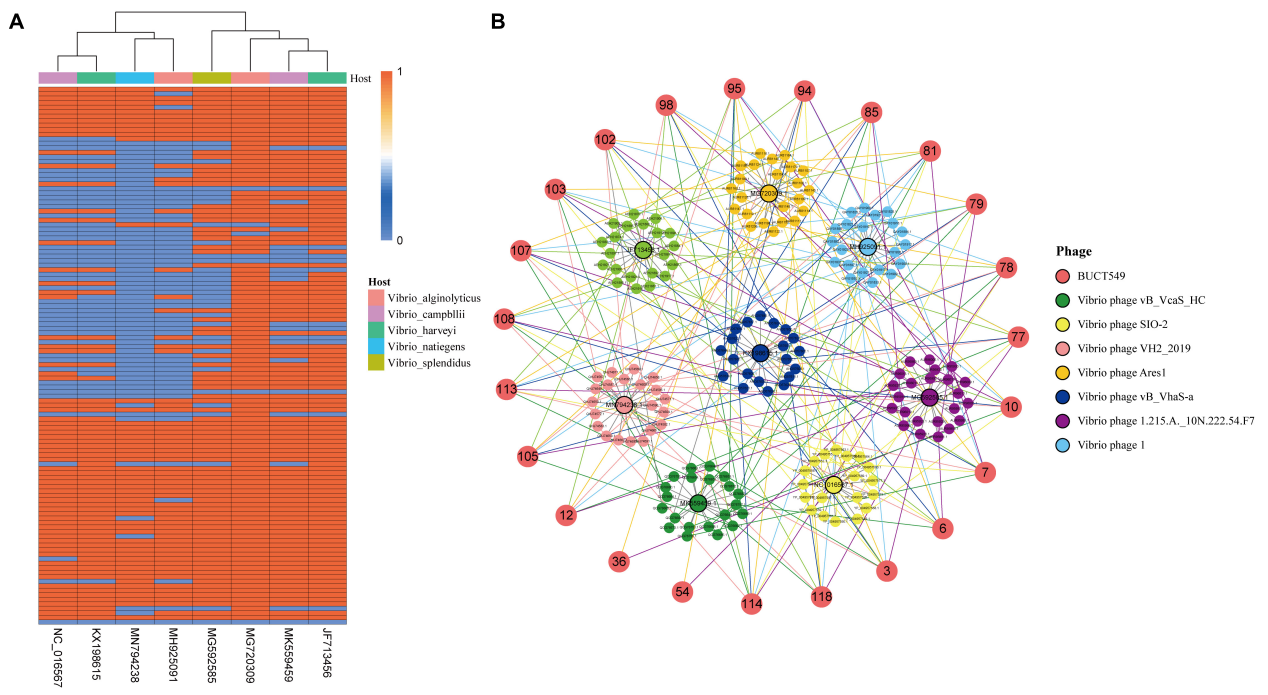

FIGURE 9 | Analysis of genes shared by BUCT549 with other *Vibrio* phages. **(A)** The heat map shows the different *Vibrio* phage genes compare to BUCT549 with red representing phage sharing the gene with BUCT549 and blue representing not sharing the gene. Phage host species are colored above the heat map. **(B)** Relationship between the annotated genes of BUCT549 and other phage genes, the connecting lines represent the gene shared by phages.

TMhelix containing proteins are only present in three phages. The interaction between TMhelix protein plays a key role in the structure and function of membrane proteins (Zhang and Lazaridis, 2009), and the TMhelix proteins in the phage may be involved in the regulation of host bacterial membrane proteins.

CONCLUSION

In the present study, we identified a novel phage strain in the family *Siphoviridae*, which uses the *V. alginolyticus* as a host. There is no virulence and pathogenicity genes in its genome, and it has the ability to be used as a potential antimicrobial agent. Simultaneously, BUCT549 grew over a wide pH (3.0–11.0) and temperature (up to 60°C) range, which showed it can be used as a potential antibacterial agent in aquatic products or the medical industry. Biological characteristics of phage BUCT549 and the analysis of genomic data find that the phage could infect the host with MSHA-related proteins in the host flagellum as the receptor and complete the life process. Flagella are widespread in *Vibrio*, and deeper mining of this kind of receptors could help broaden the range of hosts for phage application. We also observed that bacteria are able to evolve by shedding flagella to escape phage recognition. Meanwhile, BUCT549 was able to infect a strain of *V. parahaemolyticus*, showing the broad spectrum of *Vibrio* bacteriophages. The number of genes shared by BUCT549 with other *Vibrio* phages is independent of the host species. The core genes, such as DNA polymerase, terminase large subunit, and major capsid protein, are widespread in phages, but the number of regulation proteins are different in phages, suggesting that phages differ in their ability to interact with their hosts. In conclusion, *Vibrio* phages have great potential in production and medical fields, and a detailed elucidation of phage life processes will help the rapid application of phages.

DATA AVAILABILITY STATEMENT

The sequence of the phage BUCT549 used for the study is available in Genebank under the accession number MT735629.1.

AUTHOR CONTRIBUTIONS

YT and TS conceived and designed the study. JL, FT, and YH performed the experiments, analyzed the data, and prepared the initial draft of the manuscript. WL and YL contributed in sequencing work. FZ, HR, and QP provided the bacteria and phage samples. All authors checked and reviewed the manuscript.

FUNDING

This research was funded by the Key Project of Beijing University of Chemical Technology (No. XK1803-06), the National Key Research and Development Program of China (Nos. 2018YFA0903000, 2020YFC2005405, 2020YFA0712100, and 2020YFC0840805), Funds for First-Class Discipline Construction (No. XK1805), the Inner Mongolia Key Research and Development Program (No. 2019ZD006), the National Natural Science Foundation of China (Nos. 81672001 and 81621005), NSFC-MFST project (China-Mongolia) (No. 31961143024), and the Fundamental Research Funds for Central Universities (Nos. BUCTRC201917 and BUCTZY2022).

SUPPLEMENTARY MATERIAL

The Supplementary Material for this article can be found online at: https://www.frontiersin.org/articles/10.3389/fmicb.2021.668319/full#supplementary-material

REFERENCES

Adriaenssens, E., and Brister, J. R. (2017). How to Name and Classify Your Phage: an Informal Guide. *Viruses* 9:70. doi: 10.3390/v9040070

Altekruse, S. F., Bishop, R. D., Baldy, L. M., Thompson, S. G., Wilson, S. A., Ray, B. J., et al. (2000). Vibrio gastroenteritis in the US Gulf of Mexico region: the role of raw oysters. *Epidemiol. Infect.* 124, 489–495. doi: 10.1017/s0950268899003714

Bolger, A. M., Lohse, M., and Usadel, B. (2014). Trimmomatic: a flexible trimmer for Illumina sequence data. *Bioinformatics* 30, 2114–2120. doi: 10.1093/bioinformatics/btu170

Bortolaia, V., Kaas, R. S., Ruppe, E., Roberts, M. C., Schwarz, S., Cattoir, V., et al. (2020). ResFinder 4.0 for predictions of phenotypes from genotypes. *J. Antimicrob. Chemother.* 75, 3491–3500. doi: 10.1093/jac/dkaa345

Brettin, T., Davis, J. J., Disz, T., Edwards, R. A., Gerdes, S., Olsen, G. J., et al. (2015). RASTtk: a modular and extensible implementation of the RAST algorithm for building custom annotation pipelines and annotating batches of genomes. *Sci. Rep.* 5:8365. doi: 10.1038/srep08365

Campos, J., Martínez, E., Izquierdo, Y., and Fando, R. (2010). VEJ{phi}, a novel filamentous phage of *Vibrio cholerae* able to transduce the cholera toxin genes. *Microbiology* 156, 108–115. doi: 10.1099/mic.0.032235-0

Chen, F., Mackey, A. J., Stoeckert, C. J. Jr., and Roos, D. S. (2006). OrthoMCL-DB: querying a comprehensive multi-species collection of ortholog groups. *Nucleic Acids Res.* 34, D363–D368. doi: 10.1093/nar/gkj123

Chen, L., Liu, Q., Fan, J., Yan, T., Zhang, H., Yang, J., et al. (2020). Characterization and Genomic Analysis of ValSw3-3, a New *Siphoviridae Bacteriophage* Infecting Vibrio alginolyticus. *J. Virol.* 94, e00066–20. doi: 10.1128/jvi.00066-20

Chen, Y., Sun, E., Song, J., Yang, L., and Wu, B. (2018). Complete Genome Sequence of a Novel T7-Like Bacteriophage from a *Pasteurella multocida* Capsular Type A Isolate. *Curr. Microbiol.* 75, 574–579. doi: 10.1007/s00284-017-1419-3

Clausen, P., Aarestrup, F. M., and Lund, O. (2018). Rapid and precise alignment of raw reads against redundant databases with KMA. *BMC Bioinformatics* 19:307. doi: 10.1186/s12859-018-2336-6

Cosentino, S., Voldby Larsen, M., Møller Aarestrup, F., and Lund, O. (2013). PathogenFinder–distinguishing friend from foe using bacterial whole genome sequence data. *PLoS One* 8:e77302. doi: 10.1371/journal.pone.0077302

Gautheret, D., and Lambert, A. (2001). Direct RNA motif definition and identification from multiple sequence alignments using secondary structure profiles. *J. Mol. Biol.* 313, 1003–1011. doi: 10.1006/jmbi.2001.5102

Horseman, M. A., and Surani, S. (2011). A comprehensive review of Vibrio vulnificus: an important cause of severe sepsis and skin and soft-tissue infection. *Int. J. Infect. Dis.* 15, e157–66. doi: 10.1016/j.ijid.2010.11.003

Jacobs Slifka, K. M., Newton, A. E., and Mahon, B. E. (2017). Vibrio alginolyticus infections in the USA, 1988-2012. *Epidemiol. Infect.* 145, 1491–1499. doi: 10.1017/s0950268817000140

Jonson, G., Lebens, M., and Holmgren, J. (1994). Cloning and sequencing of *Vibrio cholerae* mannose-sensitive haemagglutinin pilin gene: localization of

mshA within a cluster of type 4 pilin genes. *Mol. Microbiol.* 13, 109–118. doi: 10.1111/j.1365-2958.1994.tb00406.x

Jouravleva, E. A., McDonald, G. A., Marsh, J. W., Taylor, R. K., Boesman-Finkelstein, M., and Finkelstein, R. A. (1998). The *Vibrio cholerae* mannose-sensitive hemagglutinin is the receptor for a filamentous bacteriophage from V. cholerae O139. *Infect. Immun.* 66, 2535–2539. doi: 10.1128/iai.66.6.2535-2539.1998

Khemayan, K., Prachumwat, A., Sonthayanon, B., Intaraprasong, A., Sriurairatana, S., and Flegel, T. W. (2012). Complete genome sequence of virulence-enhancing Siphophage VHS1 from Vibrio harveyi. *Appl. Environ. Microbiol.* 78, 2790–2796. doi: 10.1128/aem.05929-11

Li, P., Lin, H., Mi, Z., Xing, S., Tong, Y., and Wang, J. (2019). Screening of Polyvalent Phage-Resistant *Escherichia coli* Strains Based on Phage Receptor Analysis. *Front. Microbiol.* 10:850. doi: 10.3389/fmicb.2019.00850

Lowe, T. M., and Chan, P. P. (2016). tRNAscan-SE On-line: integrating search and context for analysis of transfer RNA genes. *Nucleic Acids Res.* 44, W54–W57. doi: 10.1093/nar/gkw413

Lowe, T. M., and Eddy, S. R. (1997). tRNAscan-SE: a program for improved detection of transfer RNA genes in genomic sequence. *Nucleic Acids Res.* 25, 955–964. doi: 10.1093/nar/25.5.955

Misol, G. N. Jr., Kokkari, C., and Katharios, P. (2020). Biological and Genomic Characterization of a Novel Jumbo Bacteriophage, vB_VhaM_pir03 with Broad Host Lytic Activity against Vibrio harveyi. *Pathogens* 9:1051. doi: 10.3390/pathogens9121051

Mohamad, N., Mohd Roseli, F. A., Azmai, M. N. A., Saad, M. Z., Md Yasin, I. S., Zulkiply, N. A., et al. (2019). Natural Concurrent Infection of Vibrio harveyi and V. alginolyticus in Cultured Hybrid Groupers in Malaysia. *J. Aquat. Anim. Health* 31, 88–96. doi: 10.1002/aah.10055

Moraru, C., Varsani, A., and Kropinski, A. M. (2020). VIRIDIC-A Novel Tool to Calculate the Intergenomic Similarities of Prokaryote-Infecting Viruses. *Viruses* 12:1268. doi: 10.3390/v12111268

Newton, A., Kendall, M., Vugia, D. J., Henao, O. L., and Mahon, B. E. (2012). Increasing rates of vibriosis in the United States, 1996-2010: review of surveillance data from 2 systems. *Clin. Infect. Dis.* 54, S391–S395. doi: 10.1093/cid/cis243

Osunla, C. A., and Okoh, A. I. (2017). Vibrio Pathogens: a Public Health Concern in Rural Water Resources in Sub-Saharan Africa. *Int. J. Environ. Res. Public Health* 14:1188. doi: 10.3390/ijerph14101188

Robert, X., and Gouet, P. (2014). Deciphering key features in protein structures with the new ENDscript server. *Nucleic Acids Res.* 42, W320–W324. doi: 10.1093/nar/gku316

Subramanian, B., Gao, S., Lercher, M. J., Hu, S., and Chen, W. H. (2019). Evolview v3: a webserver for visualization, annotation, and management of phylogenetic trees. *Nucleic Acids Res.* 47, W270–W275. doi: 10.1093/nar/gkz357

Sullivan, M. J., Petty, N. K., and Beatson, S. A. (2011). Easyfig: a genome comparison visualizer. *Bioinformatics* 27, 1009–1010. doi: 10.1093/bioinformatics/btr039

Suttle, C. A. (2007). Marine viruses–major players in the global ecosystem. *Nat. Rev. Microbiol.* 5, 801–812. doi: 10.1038/nrmicro1750

Utada, A. S., Bennett, R. R., Fong, J. C. N., Gibiansky, M. L., Yildiz, F. H., Golestanian, R., et al. (2014). *Vibrio cholerae* use pili and flagella synergistically to effect motility switching and conditional surface attachment. *Nat. Commun.* 5:4913. doi: 10.1038/ncomms5913

Xi, H., Dai, J., Tong, Y., Cheng, M., Zhao, F., Fan, H., et al. (2019). The Characteristics and Genome Analysis of vB_AviM_AVP, the First Phage Infecting Aerococcus viridans. *Viruses* 11:104. doi: 10.3390/v11020104

Zhang, J., and Lazaridis, T. (2009). Transmembrane helix association affinity can be modulated by flanking and noninterfacial residues. *Biophys J.* 96, 4418–4427. doi: 10.1016/j.bpj.2009.03.008

Conflict of Interest: FZ, HR, and QP are from Qingdao Phagepharm Bio-tech Co., Ltd.

The remaining authors declare that the research was conducted in the absence of any commercial or financial relationships that could be construed as a potential conflict of interest.

frontiers in Microbiology

ORIGINAL RESEARCH
published: 17 June 2021
doi: 10.3389/fmicb.2021.658374

Evolution of Bacterial Cross-Resistance to Lytic Phages and Albicidin Antibiotic

*Kaitlyn E. Kortright[1], Simon Doss-Gollin[2], Benjamin K. Chan[2] and Paul E. Turner[1,2]**

[1] Program in Microbiology, Yale School of Medicine, New Haven, CT, United States, [2] Department of Ecology and Evolutionary Biology, Yale University, New Haven, CT, United States

Due to concerns over the global increase of antibiotic-resistant bacteria, alternative antibacterial strategies, such as phage therapy, are increasingly being considered. However, evolution of bacterial resistance to new therapeutics is almost a certainty; indeed, it is possible that resistance to alternative treatments might result in an evolved trade-up such as enhanced antibiotic resistance. Here, we hypothesize that selection for *Escherichia coli* bacteria to resist phage T6, phage U115, or albicidin, a DNA gyrase inhibitor, should often result in a pleiotropic trade-up in the form of cross-resistance, because all three antibacterial agents interact with the Tsx porin. Selection imposed by any one of the antibacterials resulted in cross-resistance to all three of them, in each of the 29 spontaneous bacterial mutants examined in this study. Furthermore, cross-resistance did not cause measurable fitness (growth) deficiencies for any of the bacterial mutants, when competed against wild-type *E. coli* in both low-resource and high-resource environments. A combination of whole-genome and targeted sequencing confirmed that mutants differed from wild-type *E. coli via* change(s) in the *tsx* gene. Our results indicate that evolution of cross-resistance occurs frequently in *E. coli* subjected to independent selection by phage T6, phage U115 or albicidin. This study cautions that deployment of new antibacterial therapies such as phage therapy, should be preceded by a thorough investigation of evolutionary consequences of the treatment, to avoid the potential for evolved trade-ups.

Keywords: phage, antibiotic, resistance, evolution, trade-up

OPEN ACCESS

Edited by:
Robert Czajkowski, University of Gdańsk, Poland

Reviewed by:
Malgorzata Barbara Lobocka, Institute of Biochemistry and Biophysics, Polish Academy of Sciences, Poland
Erhard Bremer, University of Marburg, Germany

***Correspondence:**
Paul E. Turner
paul.turner@yale.edu

Specialty section:
This article was submitted to Antimicrobials, Resistance and Chemotherapy, a section of the journal Frontiers in Microbiology

Received: *25 January 2021*
Accepted: *10 May 2021*
Published: *17 June 2021*

Citation:
Kortright KE, Doss-Gollin S, Chan BK and Turner PE (2021) Evolution of Bacterial Cross-Resistance to Lytic Phages and Albicidin Antibiotic. Front. Microbiol. 12:658374. doi: 10.3389/fmicb.2021.658374

INTRODUCTION

As global concerns grow over the widespread emergence of antibiotic-resistant bacteria, attention has increasingly turned to antibiotic alternatives such as phage therapy: the use of bacteria-specific viruses, bacteriophages (phages), to treat bacterial infections. Although phage therapy is frequently seen as a novel medical technology, the approach originated in the early 20th century soon after phages were discovered (d'Herelle, 1917, 1930). However, roughly a decade after the discovery of phages, penicillin was discovered and focus shifted instead to research and deployment of antibiotics (Fleming, 1929). Recently, Western medicine's interest in phage therapy has resurged as a tool for treating antibiotic resistant infections (Kortright et al., 2019); however, just as antibiotics select for the evolution of antibiotic resistance, phages select for the evolution of phage resistance (Luria and Delbruck, 1943; Azam and Tanji, 2019). To avoid the historical mistakes that resulted in

multi- and even pan-drug resistant strains, the evolutionary consequences of phage therapy need to be considered and investigated prior to its widespread use (Cohan et al., 2020).

While the evolution of phage resistance in bacteria is perhaps inevitable, phage therapy strategies can be devised to leverage the evolution of phage resistance as an asset, rather than a limitation (Kortright et al., 2019). In particular, by using lytic phages that interact with bacterial virulence factors and molecules that confer antibiotic resistance, these phages should kill bacteria while selecting for phage resistance that may compromise—or pleiotropically "trade-off" with—virulence or antibiotic-resistance traits (Kortright et al., 2019). Theory, *in vitro* experiments and emergency patient treatment provide evidence that certain phages can direct favorable "trade-off" outcomes, where the therapy kills the target pathogen while selecting for reduced virulence or increased antibiotic sensitivity in the remaining bacterial population (Chan et al., 2018; Gurney et al., 2020; Rodriguez-Gonzalez et al., 2020). This approach exemplifies one goal of evolutionary medicine: applying "evolution thinking" to improve the effectiveness of therapy (Stearns, 2012; Turner, 2016).

However, not all bacterial mutations for phage resistance may constitute a genetic change that alters fitness to create a costly trade-off (Burmeister and Turner, 2020). Instead, the opposite may happen whereby evolution of phage resistance results in an additional fitness gain, also known as a "trade-up." Indeed, it is possible that the fitness effects of evolved phage resistance might pleiotropically trade-up with virulence or antibiotic resistance (Moulton-Brown and Friman, 2018; Burmeister et al., 2020). To examine this possibility, here we studied the interactions of *Escherichia coli* with two lytic phages and an antibiotic that all require the Tsx porin to enter the cell. Tsx is a substrate-specific outer-membrane porin, which uptakes nucleosides and deoxynucleotides into the periplasmic space (Maier et al., 1988). Phages T6 and U115 are shown to use the Tsx porin as a receptor for binding to *E. coli* (Kortright et al., 2020). Additionally, the Tsx porin uptakes the antibiotic albicidin, a phytotoxic DNA-gyrase inhibitor with clinical potential produced by *Xanthomonas albilineans*, an agriculturally important pathogen that causes leaf scald in sugar cane grasses (Birch and Patil, 1987; Birch et al., 1990; Rott et al., 1996; Hashimi et al., 2007; Kretz et al., 2015; von Eckardstein et al., 2017; Rostock et al., 2018; Hashimi, 2019). Earlier studies examined whether phage T6 or albicidin selected for cross resistance of *E. coli* to the other antibacterials, and found mixed evidence for this idea (Fsihi et al., 1993; Schneider et al., 1993); but these studies looked at small numbers of resistant mutants in a *tsx* knockout background with exogenous expression of Tsx from a plasmid, making it difficult to discern whether or not evolution of cross-resistance would be a general outcome. Here, we isolated larger collections of spontaneous mutants to test the hypothesis that selection for *E. coli* resistance to phage T6, phage U115, or albicidin should tend to produce cross-resistance to the other antibacterial agents, due to converging selection at the *tsx* locus.

Our results confirmed that the predicted pleiotropic trade-ups evolved frequently; selection exerted by any one of the antibacterials led to perfect (100%) cross-resistance of *E. coli* mutants to all three antibacterials. Moreover, we observed that cross-resistance was generally "cost-free" in the absence of phage and antibiotic selection, evidenced by equivalent growth of bacterial mutants relative to their wild-type ancestor in both high- and low-resource laboratory environments. In addition, we used sequence analysis to show that a wide variety of mutations at the *tsx* locus of *E. coli* may govern cross-resistance. Our study suggests that prior characterization of evolutionary consequences of antibacterial treatments, particularly the mechanistic interactions of lytic phages and antibiotics with target bacteria, can be used to inform treatment strategies that potentially avoid the evolution of undesired trade-ups.

RESULTS

Phages T6 and U115 Each Select for Cross-Resistance to the Other Phage and to Albicidin

Because phages T6 and U115 both rely on the Tsx porin for cell-binding, we predicted that evolution of resistance to one phage should often lead to cross-resistance against the other phage. To test this idea, we used a classic fluctuation analysis (see "Materials and Methods") to obtain a collection of spontaneous mutants of *E. coli* that were resistant to each phage individually. We used a paired approach, where each of 10 independently-grown bacterial cultures were used to isolate one T6-resistant and one U115-resistant strain (20 mutants total). Results for efficiency of plaquing (EOP) assays (see "Materials and Methods") confirmed that growth of phage T6 on each of the 10 T6-resistant mutants (T6R1 through T6R10) was below the limit of detection, compared to normal infectivity of the phage on wild-type bacteria (**Supplementary Table 1**). Similarly, EOP experiments showed that phage U115 was unable to grow on each of the 10 U115-resistant mutants (U115R1 through U115R10), relative to expected infectivity on the wild-type (**Supplementary Table 1**). Furthermore, we found positive support for our hypothesis; in all 20 cases, evolved bacterial resistance to phage T6 provided cross-resistance to phage U115 using EOP assays, and *vice versa* (**Supplementary Table 1**). We concluded that independent selection for *E. coli* resistance to one phage provided cross-resistance to the other phage.

We then used antibiotic-resistance assays (see "Materials and Methods") to test the prediction that evolution of phage resistance should often lead to cross-resistance to the antibiotic albicidin. We first used *E. coli* strains BW25113 and BW25113Δ*icdC* as two positive controls, to confirm that these albicidin-sensitive bacteria fail to form confluent lawns (i.e., they show zones of inhibited growth) when exposed to albicidin-producing *X. albilineans* strain XA23, but grow normally on *X. albilineans* strain LS126 which does not produce albicidin. Results (**Figure 1**) showed that the controls behaved as expected, with zones of growth inhibition around XA23 indicating sensitivity of both bacterial strains to albicidin. We estimated that wild-type BW25113 had a mean clearing ratio

(a ratio of the zone of clearing divided by the area of the *X. albilineans* spot) of 4.88 ± 0.47 s.d. in the presence of XA23 albicidin-producing bacteria, and that BW25113Δ*icdC* bacteria showed a mean clearing ratio of 5.094 ± 0.524 s.d. (**Supplementary Figure 1A**). As a negative control, the Tsx knockout, BW25113Δ*tsx*, had no zone of inhibited growth on either XA23 or LS126 (**Figure 1**); in both cases the mean clearing ratio of BW25113Δ*tsx* was 1.0 ± 0.0 s.d. (**Supplementary Figure 1A**). A test of the hypothesis confirmed our prediction was correct; all 20 phage-resistant mutants showed no zones of growth inhibition around XA23 or LS126 (**Figure 1** and **Supplementary Figure 1B**) and presented mean clearing ratios of 1.0 ± 0.0 s.d. on XA23 and LS126 (**Supplementary Figure 1A**), indicating that all the phage-resistant mutants were completely resistant to albicidin as well.

Selection for Albicidin Resistance Confers Cross-Resistance to Phages T6 and U115

We used albicidin selection (see "Materials and Methods") to isolate nine independent spontaneous mutants of *E. coli* (albR1 through albR9). Using the above-described growth challenges on *X. albilineans* strains XA23 and LS126, our results confirmed that each mutant was albicidin resistant (**Figure 1** and **Supplementary Figures 1A,B**). We then tested whether the albicidin-resistant mutants were cross-resistant to infection with phage T6 and phage U115. Results showed that in all 9 strains tested, acquisition of albicidin resistance conferred cross-resistance to both phages T6 and U115 (**Supplementary Table 1**). We concluded that the evolution of cross-resistance was absolute in this study system, such that evolution of resistance to one of the three antibacterials provided perfect cross-resistance to all of the selective agents.

Cross-Resistance to Albicidin and Phages T6 and U115 Is Cost-Free for *Escherichia coli*

To further examine the evolution of antibacterial cross-resistance, bacterial growth assays (see "Materials and Methods") were performed with replication ($n = 3$) in LB medium. Controls confirmed that wild-type *E. coli* strain BW25113 showed no discernable growth in the presence of either phage T6 or U115 (**Figure 2A**), and that growth of the *tsx*-knockout strain, BW25113Δ*tsx*, was similar in the presence and absence of each phage (**Figure 2B**). In contrast, all 10 of the T6-resistant mutants grew normally in the presence and absence of phage T6 (representative data shown in **Figures 2C,D**; see **Supplementary Figures 2B–I** for all results). Similarly, growth of all 10 U115-resistant mutants was unaffected by presence or absence of phage U115 (representative data in **Figures 2E,F**; see **Supplementary Figures 2J–Q** for all results). Lastly, the 9 albicidin-resistant mutants were capable of approximately equivalent growth in the presence and absence of either phage T6 or U115 (representative data in **Figures 2G,H**; see **Supplementary Figures 2R–X** for all results).

A visual comparison of the growth-curve results suggested that all the resistant mutants grew similarly to wild-type strain BW25113 in the absence of each phage (**Figure 2** and **Supplementary Figure 2**). To examine this outcome more closely, we analyzed the growth data with GrowthCurver (Sprouffske and Wagner, 2016) to estimate intrinsic growth rate (r) as a proxy for bacterial fitness (**Figure 2I**). None of the resistant mutants had an r that differed significantly from that of BW25113. These results suggested that there are no appreciable growth costs associated with bacterial evolution of resistance to phage T6, phage U115 and albicidin. While resistance to any of the antibacterials did not affect bacterial fitness under the tested conditions, we could not eliminate the possibility that our growth assays failed to detect minor fitness differences.

Thus, we conducted additional experiments, in an attempt to measure more subtle fitness differences among bacterial strains. To do so, we performed replicated ($n = 3$) competition assays (see "Materials and Methods") for each test strain to gauge its fitness relative to a genetically-marked wild-type strain (BW25113Δ*icdC*) in the absence of phage and antibiotic selection. Competitive indexes (CIs) were calculated as the ratio of resistant-mutant colony forming units (CFU) to CFU of the common competitor strain, BW25113Δ*icdC,* to the ratio of BW25113Δ*icdC* CFU to wild-type, BW25113, CFU. Each ratio was normalized by the starting ratio of each competing strain. Results showed no significant differences in CIs of the resistant mutants as compared to the common competitor when competed in a resource-rich complex LB medium for 72 h (**Figure 3**). Furthermore, when competed in a resource-poor (minimal glucose) defined M9 medium for 24 h (**Figure 3**), all of the resistant mutants have CIs higher than the CI of BW25113Δ*icdC* with albR4 having the only statistically significant CI. Therefore, it appeared that all T6-resistant, U115-resistant and albicidin-resistant mutants suffered no growth deficits, compared to wild-type bacteria, in the absence of phage and antibiotic selection.

All Phage-Resistant and Albicidin-Resistant Mutants Have Mutations in *tsx*

Owing to the importance of the Tsx porin in the interactions of all three antibacterials with cells, evolution of *E. coli* cross-resistance suggested that genetic changes in the *tsx* gene were likely involved. To examine this idea, we conducted whole genome sequencing (WGS) of all 29 strains. While some strains showed some single nucleotide variants (SNVs) and short insertions or deletions (indels) in *tsx*, many strains had no observable mutations in any genes using multiple variant calling pipelines including GATK (Van der Auwera et al., 2013) and breseq (Deatherage and Barrick, 2014). While WGS and variant calling pipelines are amenable for detecting SNVs and short indels, structural variants (SVs), including movement of transposable elements, are not easily detected (Ewing, 2015). Therefore, we conducted targeted Sanger sequencing of *tsx* in all 29 resistant mutants. As expected, results for the wild-type showed no mutations in *tsx*; however, mutations in *tsx* were identified in all 29 resistant mutants. For the 10 T6-resistant strains we observed

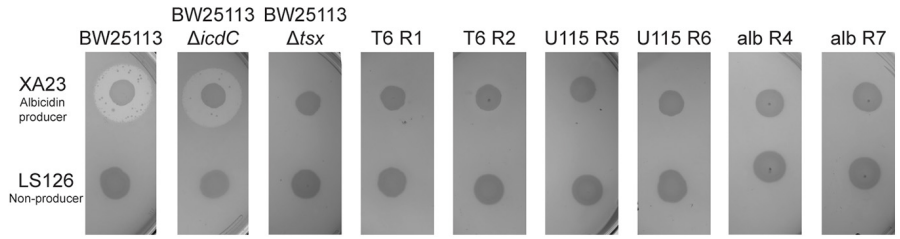

FIGURE 1 | Tests of albicidin resistance for representative spontaneous mutants of *E. coli*, selected for resistance to phage T6, phage U115, or albicidin. Wild-type BW25113 and the positive-control BW25113Δ*icdC* showed inhibited growth on agar plates with albicidin-producing *X. albilineans* (XA23), and normal growth on the non-producer, LS126. In contrast, mutants (T6R1, T6R2, U115R5, U115R6, albR4, and albR7) and negative-control BW25113Δ*tsx* grew equally well in the presence/absence of albicidin-producing bacteria.

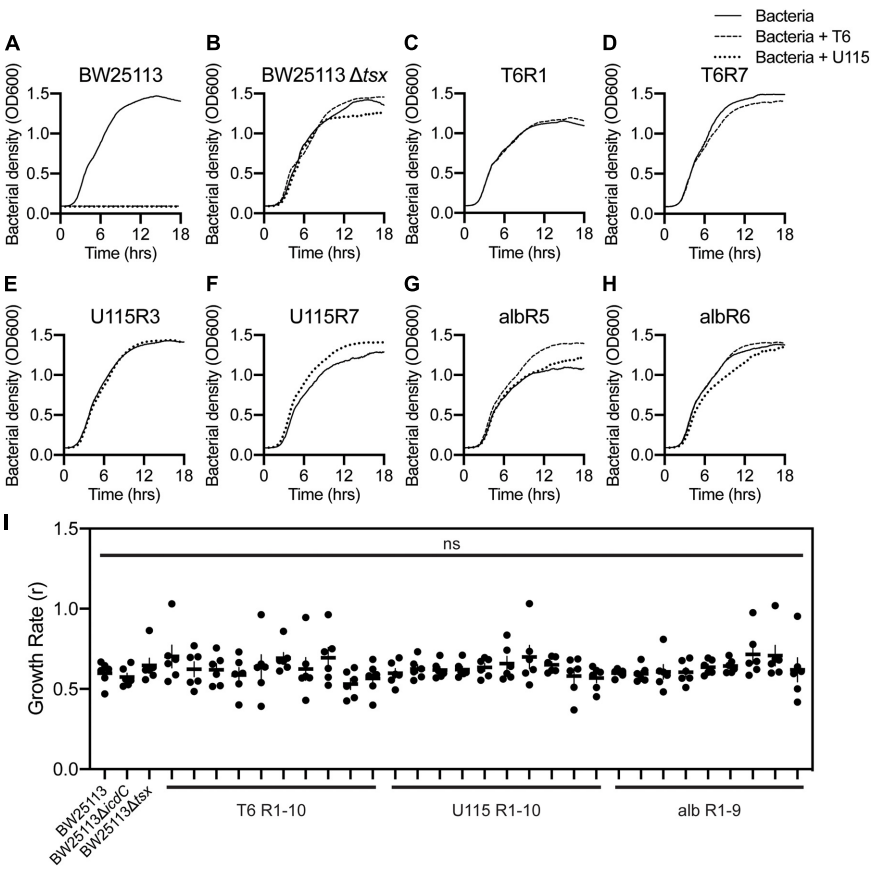

FIGURE 2 | Growth dynamics of representative *E. coli* mutants selected for resistance to phage T6, phage U115, or albicidin, in environments with and without each phage. **(A,B)** Wild-type BW25113 bacteria grew only in phage absence (solid line), whereas Tsx knockout strain BW25113Δ*tsx* grew similarly in phage-free as well as T6 (dashed line) and U115 (dotted line) environments. **(C–H)** Each of the representative resistant mutants grew similarly in the presence/absence of phages T6 and U115, regardless of their prior selection for phage or albicidin resistance. **(I)** Intrinsic growth rate (*r*; proxy for fitness) estimates from growth-curve data [**(A–H)** and **Supplementary Figure 2**] showed that each strain did not differ statistically from BW25113 ($P > 0.05$; unpaired *t*-tests).

the following mutations in the *tsx* gene: three insertion sequence (IS) elements, three deletions, three nonsense mutations and one missense mutation (**Figure 4A** and **Table 1**). For the 10 U115-resistant strains, we documented the following in *tsx*: four IS elements, two deletions, one insertion, two missense mutations, and two nonsense mutations (**Figure 4A** and **Table 1**). Interestingly, of the 10 pairs of phage-resistant mutants isolated from the same parent culture, only three pairs (T6R4/U115R4; T6R8/U115R8; T6R10/U115R10) showed identical mutations in *tsx* (**Figure 4B** and **Table 1**). For the nine albicidin-resistant mutants we observed six IS elements, two deletions, and one missense mutation in *tsx* (**Figure 4A**). Of the 29 mutations observed, three were in the promoter (*tsxp2*) region and four were in the signal sequence peptide of Tsx (**Figure 4B** and

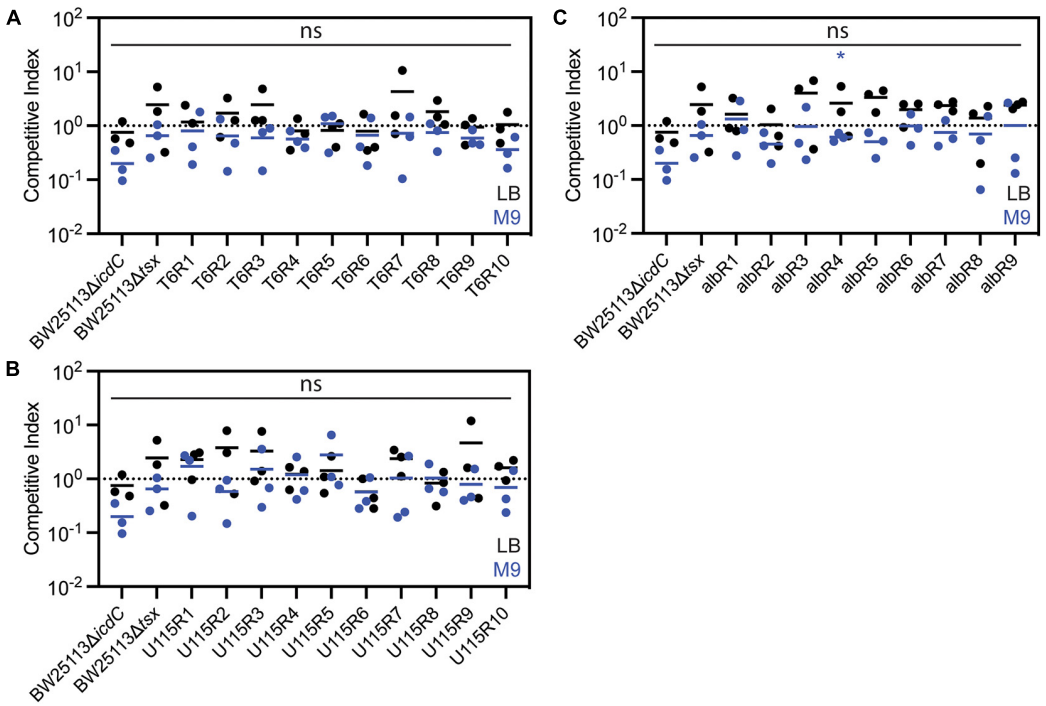

FIGURE 3 | Competition assays in LB media (black) and M9 media (blue) showed that *E. coli* mutants resistant to phage T6 **(A)**, phage U115 **(B)**, or albicidin **(C)** did not measurably differ in fitness, relative to a non-resistant wild-type strain. Each point represents results from independent competition assays ($n = 3$), and statistical significance was determined using a *t*-test comparing competitive index of the resistant mutant relative to the competitive index of BW25113Δ*icdC*. None of the competitive indexes of the resistant mutants were statistically significant in LB media. Competitive indexes of resistant mutants that were statistically significant in M9 media are indicated with * ($P < 0.05$, unpaired *t*-test).

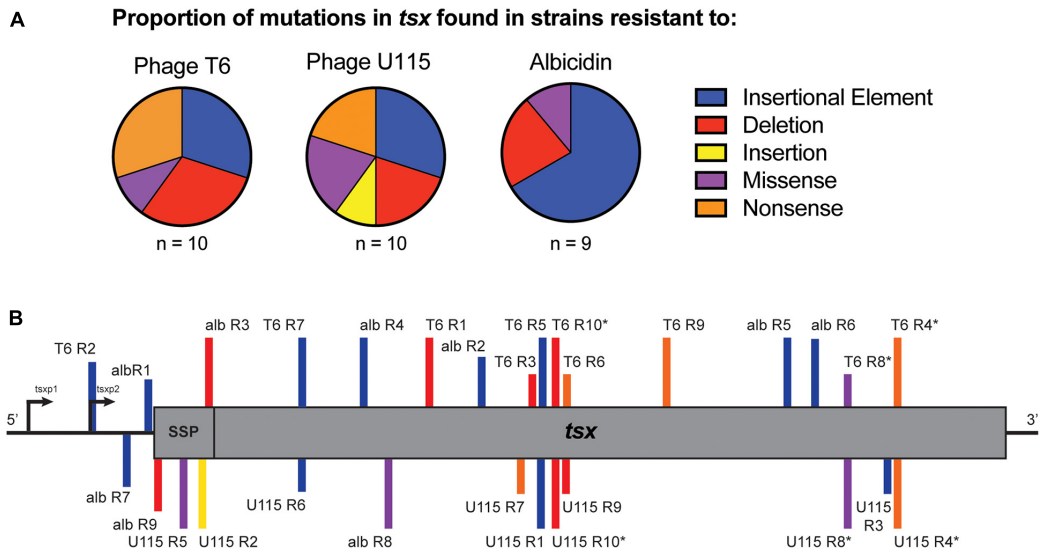

FIGURE 4 | (A) Proportions of *tsx* mutations observed in sets of *E. coli* strains, selected for spontaneous resistance to either phage T6, phage U115 or albicidin. Mutations were due to insertion sequence elements (blue), deletions (red), insertions (yellow), missense mutations (purple) and nonsense mutations (orange). **(B)** Locations of *tsx* mutations for each resistant mutant (SSP, signal sequence peptide; *, indicates paired mutants).

Table 1). In addition, our data showed that eight of the 29 mutations in *tsx* clustered within the region spanning base pairs 375–435 (**Figure 4B**).

The different missense mutations observed in this experiment were mapped (**Figure 5**) onto the crystal structure of Tsx (Ye and van den Berg, 2004) along with previously observed

TABLE 1 | Putative resistance mutations in the *tsx* gene, for each *E. coli* mutant selected for spontaneous resistance to either phage T6, phage U115, or albicidin.

Strains	Mutation type	Alteration in *tsx*	Alteration in Tsx
T6 R1	Deletion	deletion of 291-321	E79Stop
T6 R2	Insertional Element	IS2 at -75	promoter region
T6 R3	Deletion	deletion of 402-733	
T6 R4	Nonsense	G773A *	W236Stop
T6 R5	Insertional Element	IS2 at 403	
T6 R6	Nonsense	G435A	W124Stop
T6 R7	Insertional Element	IS2 at 165	IS2
T6 R8	Missense	T725G *	L220R
T6 R9	Nonsense	G535T	E157Stop
T6 R10	Deletion	deletion of 410-420 *	R146Stop
U115 R1	Insertional Element	IS3 at 400	
U115 R2	Insertion	insertion (1bp) at 53	signal peptide; E24Stop
U115 R3	Insertional Element	IS1 at 774	
U115 R4	Nonsense	G773A *	W236Stop
U115 R5	Missense	T31A	signal peptide; V11E
U115 R6	Insertional Element	IS2 at 161	
U115 R7	Nonsense	C375G	Y103Stop
U115 R8	Missense	T725G *	L220R
U115 R9	Deletion	deletion of 429-435	L135Stop
U115 R10	Deletion	deletion of 410-420 *	R146Stop
alb R1	Insertional Element	IS 1 at -3	promoter region
alb R2	Insertional Element	IS1 at 344	
alb R3	Deletion	deletion of 64	signal peptide; L89Stop
alb R4	Insertional Element	IS5 at 116	
alb R5	Insertional Element	IS2 at 665	
alb R6	Insertional Element	IS1 at 692	
alb R7	Insertional Element	IS1 at -16	promoter region
alb R8	Missense	G161C	R32P
alb R9	Deletion	deletion of 4	signal peptide; L89Stop

** Indicates paired phage resistant mutants with the same mutation.*

missense mutations (**Figure 5** and **Supplementary Table 2**) that conferred resistance to either phage T6 or albicidin (Fsihi et al., 1993; Schneider et al., 1993). Mutant albR8 had a missense mutation R32P in the same surface exposed loop as three missense mutations (F27L, G28R, and G28E) observed by Fsihi et al. (1993) in mutants that were selected for albicidin resistance (**Figure 5**). Paired mutants T6R8 and U115R8 had the same missense mutation, L220R, in a beta strand that was in the region of a missense mutation (S217R) observed by Fsihi et al. (1993) in another mutant selected for resistance to albicidin (**Figure 5**). The third missense mutation observed in this study (V11E) in U115R5 is in the N-terminal signal peptide (**Table 1**).

While it is likely that these mutations are conferring resistance to phage T6, phage U115 and albicidin, this was not experimentally confirmed *via* recombinant genetics because the work fell outside the scope of the current study.

DISCUSSION

The phage life cycle relies on surface-exposed molecules to initiate infection, and on bacterial metabolism to replicate inside cells. Since phages T6 and U115 both require Tsx as a primary receptor, it is not surprising that spontaneous mutants to one phage confer resistance to the other phage (Kortright et al., 2020). However, it is interesting that all 20 phage resistant mutants are also cross-resistant to albicidin and that all nine albicidin resistant mutants are cross-resistant to both phages. It was previously observed that T6-resistant mutants maintained their sensitivity to colicin-K, another antibiotic that enters *via* the Tsx porin (Schneider et al., 1993). While all three antibacterials used in the current study require Tsx as a receptor, it is unclear whether replication of phages T6 and U115 and the mechanism of action of albicidin also converge on the same gene to confer resistance. Albicidin is a DNA gyrase inhibitor that blocks topoisomerase II, an enzyme which cleaves both strands of DNA to modulate supercoiling during DNA replication, gene regulation, and transcription (Hashimi et al., 2007). Phages require the DNA replication machinery of the host bacterial cell to make viral progeny within the cell; however, many phages, including T6, encode their own topoisomerases (Huang et al., 1985). Furthermore, the minimum inhibitory concentrations (MICs) of ciprofloxacin (another DNA gyrase inhibitor) and ampicillin for wild-type BW25113 bacteria and for each of the 29 resistant mutants did not differ statistically (**Supplementary Table 3**). These observations of unchanged phenotypes imply that selection by phage T6, phage U115, and albicidin seems to evolutionarily converge on the *tsx* locus, rather than involving changes at other loci. Indeed, the results of the targeted sequencing indicated this possibility, because each mutant was observed to undergo a change in the *tsx* gene (i.e., as opposed to no mutation at this locus, suggesting resistance occurred *via* a different mechanism). While the identified mutations were not validated as the causative mutations of resistance, it seems likely that the 29 different mutations found in *tsx* were conferring resistance to phage T6, phage U115, and albicidin. The combination of *tsx* mutations observed in all 29 resistant mutants and the lack of detectable fitness defects in these strains indicate that Tsx may be superfluous for *E. coli* in the laboratory environment regardless of media type (high resource, complex versus low resource, defined).

The 29 observed mutations in *tsx* fall within the promoter region, as well as various other locations along the gene. However, there seems to be a cluster of "hotspots" for mutational changes in the region spanning 332 to 435 base pairs. These residues make up a surface exposed alpha helix and a beta strand that spans the outer membrane of the bacteria (Ye and van den Berg, 2004). All of the mutations in this region were observed in resistant strains resulting from phage selection but not albicidin selection, indicating that perhaps amino acid residues 88 through 123 are likely important for phage binding.

Moreover, of the 10 "paired" phage-resistant mutants, only three of the pairs (T6R4/U115R4; T6R8/U115R8;

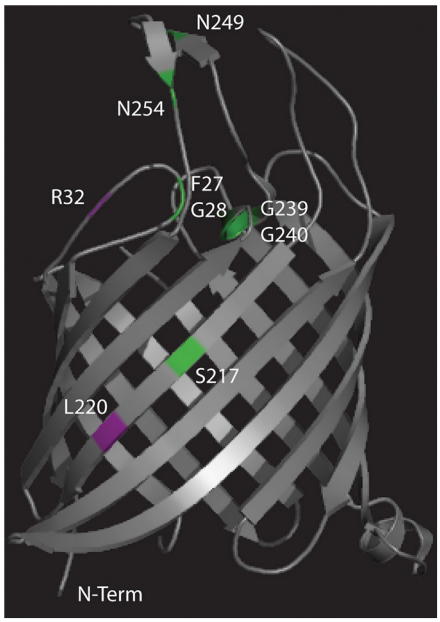

FIGURE 5 | Crystal structure of Tsx (Ye and van den Berg, 2004) with the locations of the missense mutations observed in this study mapped in purple and the locations of missense mutations observed in previous studies (Fsihi et al., 1993; Schneider et al., 1993) mapped in green.

T6R10/U115R10) showed the same *tsx* mutation. This means that even in a clonal population of *E. coli*, there are often multiple spontaneous mutants with different changes in *tsx*. This finding indicates that the number of resistant mutants observed to arise during fluctuation assays cannot be used to compute a rate of spontaneous mutation; instead, these data should only be used to calculate a rate of spontaneous phenotypic resistance.

Expression and proper localization of Tsx at the outer membrane occurs *via* two promoters and a signal sequence peptide, respectively (Bremer et al., 1990). Minor promoter, *tsxp1*, is repressed by transcription factor DeoR while major promoter, *tsxp2*, is controlled by the cAMP-CRP complex. Of the three mutations that were observed in the promoter region, all three were in the region of tsxp2, the promoter which results in a higher number of *tsx* transcripts. Likely these mutants (T6R2, albR7, and albR1) are not producing Tsx. Similarly, the four mutants with mutations in the signal sequence peptide region (albR9, U115R5, U115R2, and albR3) likely do not properly express Tsx at the outer membrane.

Indeed, it is probable that many of the resistant mutants do not stably express Tsx in the outer membrane. Mutants with an insertional element disrupting *tsx* (T6R2, T6R5, T6R7, U115R1, U115R3, U115R6, albR1, albR2, albR4, albR5, albR6, and albR7) or indels and nonsense mutaitons at the beginning of *tsx* (T6R1, T6R3, T6R6, T6R9, T6R10, U115R7, U115R9, and U115R10) likely do not express Tsx. Furthermore, Tsx is probably not stably expressed at the outer membrane in resistant mutants with nonsense mutations toward the end of the gene (T6R4 and U115R4). However, it is more likely that Tsx is expressed in resistant mutants with missense mutations (T6R8, U115R5, U115R8, and albR8). Interestingly, of the three different missense mutations observed (T6R8 and U115R8 were paired resistant mutants that share the same mutation), two out of three of them were located in regions where previous missense mutations conferring resistance to albicidin—but not to phage T6—had been observed (Fsihi et al., 1993). It is possible that the L220R mutation (T6R8 and U115R8) in one of the membrane-spanning beta strands is sufficient to disrupt the proper folding and insertion of Tsx in the outer membrane. The V11E mutation (U115R5) in the signal sequence likely disrupts the proper localization of Tsx. The third missense mutation, R32P (albR8), is in a surface exposed loop. Since this mutant was resistant to albicidin, phage T6 and phage U115, it is likely that this particular surface exposed loop is essential for binding of these three antimicrobials; future experiments would be needed to confirm this idea.

It is also interesting that the profile of *tsx* mutations was different for the phage-selected resistant mutants, compared with the antibiotic-selected resistant mutants. There were six albicidin-resistant mutants with an IS element inserted in *tsx*, while three of each of the phage-resistant mutants showed IS-element changes in *tsx*. This observation could be due either to a difference in selection pressures of phages versus antibiotics, or to a difference in the method of selection to amass these mutants. Underlying these possibilities are two opposing ideas. It has been previously assumed that insertion and excision of IS elements are stochastic events. However, recent evidence suggests that IS movement may actually be a form of directed mutagenesis in which IS elements target specific chromosomal loci to reduce stress under certain environmental conditions (Humayun et al., 2017). The isolation of phage-resistant mutants in this study relied on spontaneous mutations accumulated in an overnight culture, while the isolation of antibiotic-resistant mutants allowed for both selection of spontaneous resistant mutants as well as evolution in the presence of albicidin. This difference suggests that the larger proportion of IS element insertions in *tsx* found in the set of albicidin-resistant mutants might be caused by direct targeting of *tsx* by IS elements under stressful conditions. Without further experiments that use the same method to select for spontaneous phage and albicidin resistant mutants, we cannot rule out that a difference in selection pressures between phages and the antibiotic resulted in the skew of IS-element-insertion changes in *tsx* found in the albicidin-resistant mutants.

Finally, it is worth noting that all 29 resistant mutants have gained fitness relative to wild-type in the presence of albicidin or phage, with no discernable growth cost when bacteria are grown without phage and antibiotic selection. Bacteria can utilize nucleosides as a carbon source in environments where carbon is limiting (Tozzi et al., 2006; Mulcahy et al., 2010) and nucleoside-uptake mutations are shown to impair bacterial fitness in a low-carbon environment (Gumpenberger et al., 2016). In this study, we used competition assays to show that

phage/antibiotic resistant mutants maintained robust growth in both carbon-rich (LB medium) and carbon-limited (M9 medium) environments. However, it is possible that a cost of antibacterial resistance might occur in different lab-media or other environments not examined here. Antibiotic cross-resistance has extreme clinical relevance as selected resistance to a single antibiotic can also result in evolution of multi-drug resistance. Here, we showed that phage resistance can result in antibiotic resistance, and *vice versa*, at no fitness cost. This highlights a potential pitfall of the future therapeutic use of any antimicrobial whether it be phage or antibiotics. Without a clear understanding of the evolutionary implications of treatment, antimicrobial selection can result in both resistance and cross-resistance at no fitness cost to the bacteria.

MATERIALS AND METHODS

Strains and Culture Conditions

Strains in this study are listed in **Supplementary Table 4**. *E. coli* strains were cultured for 24 h with shaking incubation at 37°C in lysogeny broth (Luria and Delbruck, 1943). M9 minimal medium (6 g Na_2HPO_4, 3 g KH_2PO_4, 0.5 g NaCl, 1 g NH_4Cl, 1 mM $MgSO_4$, 0.1 mM $CaCl_2$, 0.1% (w/v) glucose per liter) was used for competition assays (see below). The Tsx knockout, BW25113Δ*tsx*, was used as a negative control in many experiments. A pseudogene knockout, BW25113Δ*icdC*, was used as a control for the Kan^R cassette and as a marked competitor in the competition assays. Where appropriate, LB was supplemented with kanamycin at 30 μg/mL (LB Kan30). *X. albilineans* strains (provided by D. Gabriel, U Florida) were cultured for 48 h with shaking at 30°C in Modified Wilbrinks (MW) medium (Rott et al., 1994). Lysates of phages T6 and U115 were obtained by mixing each phage with *E. coli* strain BW25113 in LB medium and culturing for 24 h at 37°C, followed by filtration (0.22 μm) to remove bacteria.

Isolation of Phage-Resistant Bacterial Mutants

Ten cultures of *E. coli* strain BW25113 were grown independently as described above, and diluted samples were spread on LB agar (1.5%) plates, pre-saturated with either phage T6 or phage U115. After overnight incubation at 37°C, one colony was chosen randomly from each plate and colony-purified three times. For each of the 20 isolated mutants, phage resistance was confirmed *via* efficiency of plaquing (EOP) assays, which compared plaquing ability of phage T6 or U115 on the test mutant relative to growth on wild-type strain BW25113.

Isolation of Antibiotic-Resistant Bacterial Mutants

X. albilineans strain XA23 was cultured as described above, and a 10 μL sample was spotted onto each of ten Sucrose Peptone agar (SPA) plates that were incubated for 5 days at 30°C (Birch and Patil, 1985). A sample from each of ten independently-grown cultures of BW25113 was then overlaid on one of the SPA plates, and incubated overnight at 37°C. Colonies that appeared in the zone of growth inhibition around the XA23 spot represented spontaneous *E. coli* mutants that were resistant to albicidin. One plate was lost due to contamination; from each of the remaining nine plates, one colony was randomly chosen and colony-purified three times. Albicidin resistance of each mutant was verified by plating a sample of a grown-up culture of the isolate on an XA23 spot, as described above.

Antibiotic-Resistance Assays

Xanthomonas albilineans strains XA23 and LS126 were each cultured for 48 h at 30°C, and their optical densities at wavelength $\lambda = 600$ nm (OD_{600}) were estimated *via* spectrophotometry. Each culture was then diluted in MW medium, to obtain $OD_{600} = 0.25$. Then, a 10-μL sample of each diluted culture was spotted on a SPA plate, allowed to dry completely and then incubated for 5 days at 30°C. SPA plates were overlaid with 4 mL of LB top agar (0.75%) with 1 mL of a test *E. coli* strain at $OD_{600} = 0.25$, and incubated overnight at 37°C. The next day, plates were imaged. Images were quantified using ImageJ, by thresholding until either the *X. albilineans* spots or *E. coli* clearings were outlined and the area within the outline was quantified. The ratio of the area of the zone of clearing to the area of the *X. albilineans* spot was used to define albicidin sensitivity: a ratio of greater than 1.0 indicates albicidin sensitivity, while a ratio of 1.0 indicates albicidin resistance.

Minimum inhibitory concentrations (MICs) of ampicillin and ciprofloxacin were determined using the twofold dilution method (MacLowry et al., 1970).

Bacterial Growth Curves

E. coli bacteria were cultured overnight as described above. Dilutions of a test strain in LB medium were placed in wells of a flat-bottomed 96-well plate, in the absence of phage or mixed with phage at a multiplicity-of-infection (MOI; ratio of phage particles to host cells) of ∼10. Plates were incubated with shaking for 18 h in an automated spectrophotometer at 37°C, and OD_{600} measurements were obtained every 10 min. Growth curve data were fit to a logarithmic curve using GrowthCurver and growth parameters were extracted (Sprouffske and Wagner, 2016). All growth curve data are deposited on Dryad.

Bacterial Competition Assays

Replicated ($n = 3$) competition assays were conducted in both LB and M9 media by mixing two bacterial strains at a 1:1 initial ratio. Competition assays in LB were serially passaged (1:100 dilution) every 24 h for 72 h total. Competition assays in M9 were measured after 24 h. At the end of each experiment, a diluted sample of each competition was plated on LB agar to measure viable bacterial density (colony-forming units; CFU), and on LB Kan30 agar to estimate the CFU of a Kan^R competitor; the density of the Kan^S competitor was estimated by subtraction. Competitive indexes were calculated as the ratio of resistant-mutant CFU to the CFU of BW25113Δ*icdC* divided by the ratio of BW25113Δ*icdC* CFU to BW25113 CFU. Each ratio was normalized by the starting ratio of each competing strain.

Sequencing

Sequencing libraries were prepared using Illumina's Nextera prep kit. Whole genome sequencing was done using paired-end 150 bp reads on the Illumina NextSeq platform or paired-end 300bp reads on the Illumina HiSeq platform. For targeted sequencing, primers (5′-CTGTGAAACGAAACATATTTTTG-3′ and 5′-CGTGCTTTTGTTGGC-3′) were designed ∼100 base pairs upstream and downstream of *E. coli* gene *tsx*, and used to amplify *tsx* of each resistant mutant and the ancestral BW25113 strain. Amplicons were Sanger sequenced at the Yale DNA Analysis Facility on Science Hill. Mutations were identified by comparing sequencing reads to *tsx* loci of the reference strain GenBank CP009273.1.

DATA AVAILABILITY STATEMENT

Sequence data are available at NCBI SRA accession #PRJNA693868. All other data are available on Dryad (https://doi.org/10.5061/dryad.ghx3ffbmn).

AUTHOR CONTRIBUTIONS

KK and BC designed study. KK and SD-G conducted the experiments. KK, SD-G, BC, and PT wrote and edited the manuscript. All authors contributed to the article and approved the submitted version.

ACKNOWLEDGMENTS

We thank Andrew Goodman, Barbara Kazmierczak, Daniel Weinberger, and James Bull for helpful feedback on this study. We thank Dean Gabriel (U Florida) for kindly providing *X. albilineans* strains used in this study.

SUPPLEMENTARY MATERIAL

The Supplementary Material for this article can be found online at: https://www.frontiersin.org/articles/10.3389/fmicb.2021.658374/full#supplementary-material

REFERENCES

Azam, A. H., and Tanji, Y. (2019). Bacteriophage-host arm race: an update on the mechanism of phage resistance in bacteria and revenge of the phage with the perspective for phage therapy. *Appl. Microbiol. Biotechnol.* 103, 2121–2131. doi: 10.1007/s00253-019-09629-x

Birch, R. G., and Patil, S. S. (1985). Preliminary characterization of an antibiotic produced by *Xanthomonas albilineans* which inhibits DNA synthesis in *Escherichia coli*. *Microbiology* 131, 1069–1075. doi: 10.1099/00221287-131-5-1069

Birch, R. G., and Patil, S. S. (1987). Evidence that an albicidin-like phytotoxin induces chlorosis in sugarcane leaf scald disease by blocking plastid DNA replication. *Physiol. Mol. Plant Pathol.* 30, 207–214. doi: 10.1016/0885-5765(87)90034-8

Birch, R. G., Pemberton, J. M., and Basnayake, W. V. (1990). Stable albicidin resistance in *Escherichia coli* involves an altered outer-membrane nucleoside uptake system. *J. Gen. Microbiol.* 136, 51–58. doi: 10.1099/00221287-136-1-51

Bremer, E., Middendorf, A., Martinussen, J., and Valentinhansen, P. (1990). Analysis of the *tsx* gene, which encodes a nucleoside-specific channel-forming protein (Tsx) in the outer membrane of *Escherichia coli*. *Gene* 96, 59–65. doi: 10.1016/0378-1119(90)90341-n

Burmeister, A. R., and Turner, P. E. (2020). Trading-off and trading-up in the world of bacteria-phage evolution. *Curr. Biol.* 30, R1120–R1124. doi: 10.1016/j.cub.2020.07.036

Burmeister, A. R., Fortier, A., Roush, C., Lessing, A. J., Bender, R. G., Barahman, R., et al. (2020). Pleiotropy complicates a trade-off between phage resistance and antibiotic resistance. *Proc. Natl. Acad. Sci. U S A.* 117, 11207–11216. doi: 10.1073/pnas.1919888117

Chan, B. K., Turner, P. E., Kim, S., Mojibian, H. R., Elefteriades, J. A., and Narayan, D. (2018). Phage treatment of an aortic graft infected with *Pseudomonas aeruginosa*. *Evol. Med. Public Health* 2018, 60–66. doi: 10.1093/emph/eoy005

Cohan, F. M., Zandi, M., and Turner, P. E. (2020). Broadscale phage therapy is unlikely to select for widespread evolution of bacterial resistance to virus infection. *Virus Evol.* 6:veaa060. doi: 10.1093/ve/veaa060

d'Herelle, F. (1930). Studies upon Asiatic cholera. *Yale J. Biol. Med.* 1:195.

Deatherage, D. E., and Barrick, J. E. (2014). Identification of mutations in laboratory-evolved microbes from next-generation sequencing data using breseq. *Methods Mol. Biol.* 1151, 165–188. doi: 10.1007/978-1-4939-0554-6_12

d'Herelle, F. (1917). Sur un microbe invisible antagoniste des bacilles dysentériques. *Comptes Rendus Acad. Sci.* 165:373.

Ewing, A. D. (2015). Transposable element detection from whole genome sequence data. *Mob DNA* 6:24. doi: 10.1186/s13100-015-0055-3

Fleming, A. (1929). On the antibacterial action of cultures of a Penicillium, with special reference to their use in the isolation of *B. influenzae*. *Br. J. Exp. Pathol.* 10, 226–236.

Fsihi, H., Kottwitz, B., and Bremer, E. (1993). Single amino-acid substitutions affecting the substrate specificity of the *Escherichia Coli* K-12 nucleoside-specific Tsx channel. *J. Biol. Chem.* 268, 17495–17503. doi: 10.1016/s0021-9258(19)85361-9

Gumpenberger, T., Vorkapic, D., Zingl, F. G., Pressler, K., Lackner, S., Seper, A., et al. (2016). Nucleoside uptake in *Vibrio cholerae* and its role in the transition fitness from host to environment. *Mol. Microbiol.* 99, 470–483. doi: 10.1111/mmi.13143

Gurney, J., Brown, S. P., Kaltz, O., and Hochberg, M. E. (2020). Steering phages to combat bacterial pathogens. *Trends Microbiol.* 28, 85–94. doi: 10.1016/j.tim.2019.10.007

Hashimi, S. M. (2019). Albicidin, a potent DNA gyrase inhibitor with clinical potential. *J. Antibiot.* 72, 785–792. doi: 10.1038/s41429-019-0228-2

Hashimi, S. M., Wall, M. K., Smith, A. B., Maxwell, A., and Birch, R. G. (2007). The phytotoxin albicidin is a novel inhibitor of DNA gyrase. *Antimicrob. Agents Chemother.* 51, 181–187. doi: 10.1128/aac.00918-06

Huang, W. M., Wei, L. S., and Casjens, S. (1985). Relationship between bacteriophage T4 and T6 DNA topoisomerases. T6 39-protein subunit is equivalent to the combined T4 39-and 60-protein subunits. *J. Biol. Chem.* 260, 8973–8977. doi: 10.1016/s0021-9258(17)39444-9

Humayun, M. Z., Zhang, Z., Butcher, A. M., Moshayedi, A., and Saier, M. H. Jr. (2017). Hopping into a hot seat: Role of DNA structural features on IS 5-mediated gene activation and inactivation under stress. *PLoS One* 12:e0180156. doi: 10.1371/journal.pone.0180156

Kortright, K. E., Chan, B. K., and Turner, P. E. (2020). High-throughput discovery of phage receptors using transposon insertion sequencing of bacteria. *Proc. Natl. Acad. Sci. U S A.* 117, 18670–18679. doi: 10.1073/pnas.2001888117

Kortright, K. E., Chan, B. K., Koff, J. L., and Turner, P. E. (2019). Phage therapy: a renewed approach to combat antibiotic-resistant bacteria. *Cell Host Microbe* 25, 219–232. doi: 10.1016/j.chom.2019.01.014

Kretz, J., Kerwat, D., Schubert, V., Gratz, S., Pesic, A., Semsary, S., et al. (2015). Total synthesis of albicidin: a lead structure from *Xanthomonas albilineans* for potent antibacterial gyrase inhibitors. *Angewandte Chemie Int. Edition* 54, 1969–1973. doi: 10.1002/anie.201409584

Luria, S. E., and Delbruck, M. (1943). Mutations of bacteria from virus sensitivity to virus resistance. *Genetics* 28, 491–511. doi: 10.1093/genetics/28.6.491

MacLowry, J. D., Jaqua, M. J., and Selepak, S. T. (1970). Detailed methodology and implementation of a semiautomated serial dilution microtechnique for antimicrobial susceptibility testing. *Appl. Microbiol.* 20, 46–53. doi: 10.1128/am.20.1.46-53.1970

Maier, C., Bremer, E., Schmid, A., and Benz, R. (1988). Pore-forming activity of the Tsx protein from the outer membrane of *Escherichia coli*. Demonstration of a nucleoside-specific binding site. *J. Biol. Chem.* 263, 2493–2499. doi: 10.1016/s0021-9258(18)69233-6

Moulton-Brown, C. E., and Friman, V. P. (2018). Rapid evolution of generalized resistance mechanisms can constrain the efficacy of phage-antibiotic treatments. *Evolut. Applicat.* 11, 1630–1641. doi: 10.1111/eva.12653

Mulcahy, H., Charron-Mazenod, L., and Lewenza, S. (2010). *Pseudomonas aeruginosa* produces an extracellular deoxyribonuclease that is required for utilization of DNA as a nutrient source. *Environ. Microbiol.* 12, 1621–1629. doi: 10.1111/j.1462-2920.2010.02208.x

Rodriguez-Gonzalez, R. A., Leung, C. Y., Chan, B. K., Turner, P. E., and Weitz, J. S. (2020). Quantitative models of phage-antibiotic combination therapy. *mSystems* 5, 756–719. doi: 10.1128/mSystems.00756-19

Rostock, L., Driller, R., Gratz, S., Kerwat, D., von Eckardstein, L., Petras, D., et al. (2018). Molecular insights into antibiotic resistance - how a binding protein traps albicidin. *Nat. Commun.* 9:3095.

Rott, P. C., Costet, L., Davis, M. J., Frutos, R., and Gabriel, D. W. (1996). At least two separate gene clusters are involved in albicidin production by *Xanthomonas albilineans*. *J. Bacteriol.* 178, 4590–4596. doi: 10.1128/jb.178.15.4590-4596.1996

Rott, P., Abel, M., Soupa, D., Feldmann, P., and Letourmy, P. (1994). Population dynamics of *Xanthomonas albilineans* in sugarcane plants as determined with an antibiotic-resistant mutant. *Plant Dis.* 78, 241–247. doi: 10.1094/pd-78-0241

Schneider, H., Fsihi, H., Kottwitz, B., Mygind, B., and Bremer, E. (1993). Identification of a segment of the *Escherichia coli* Tsx protein that functions as a bacteriophage receptor area. *J. Bacteriol.* 175, 2809–2817. doi: 10.1128/Jb.175.10.2809-2817.1993

Sprouffske, K., and Wagner, A. (2016). Growthcurver: an R package for obtaining interpretable metrics from microbial growth curves. *BMC Bioinformat.* 17:172. doi: 10.1186/s12859-016-1016-7

Stearns, S. C. (2012). Evolutionary medicine: its scope, interest and potential. *Proce. R. Soc. B Biol. Sci.* 279, 4305–4321. doi: 10.1098/rspb.2012.1326

Tozzi, M. G., Camici, M., Mascia, L., Sgarrella, F., and Ipata, P. L. (2006). Pentose phosphates in nucleoside interconversion and catabolism. *FEBS J.* 273, 1089–1101. doi: 10.1111/j.1742-4658.2006.05155.x

Turner, P. E. (2016). "Evolutionary medicine," in *How Evolution Shapes Our Lives: Essays on Biology and Society*, Chap. 7, eds J. B. Losos and R. E. Lenski (Princeton,NJ: Princeton University Press).

Van der Auwera, G. A., Carneiro, M. O., Hartl, C., Poplin, R., Del Angel, G., Levy-Moonshine, A., et al. (2013). From FastQ data to high confidence variant calls: the Genome Analysis Toolkit best practices pipeline. *Curr. Protoc. Bioinform.* 43:bi1110s43. doi: 10.1002/0471250953.bi1110s43

von Eckardstein, L., Petras, D., Dang, T., Cociancich, S., Sabri, S., Gratz, S., et al. (2017). Total synthesis and biological assessment of novel albicidins discovered by mass spectrometric networking. *Chem. Eur. J.* 23, 15316–15321. doi: 10.1002/chem.201704074

Ye, J., and van den Berg, B. (2004). Crystal structure of the bacterial nucleoside transporter Tsx. *EMBO J.* 23, 3187–3195. doi: 10.1038/sj.emboj.7600330

Conflict of Interest: PT is a co-founder of Felix Biotechnology Inc., and declares a financial interest in this company that seeks to commercially develop phages for use as therapeutics. PT discloses two provisional patent applications involving phage therapy.

The remaining authors declare that the research was conducted in the absence of any commercial or financial relationships that could be construed as a potential conflict of interest.

frontiers in Microbiology

ORIGINAL RESEARCH
published: 28 June 2021
doi: 10.3389/fmicb.2021.657524

Differential Bacteriophage Efficacy in Controlling *Salmonella* in Cattle Hide and Soil Models

*Yicheng Xie[1,2], Tyler Thompson[1], Chandler O'Leary[2,3], Stephen Crosby[3], Quang X. Nguyen[3], Mei Liu[2] and Jason J. Gill[1,2]**

[1] Department of Animal Science, Texas A&M University, College Station, TX, United States, [2] Center for Phage Technology, Texas A&M University, College Station, TX, United States, [3] Department of Biochemistry and Biophysics, Texas A&M University, College Station, TX, United States

Asymptomatic *Salmonella* carriage in beef cattle is a food safety concern and the beef feedlot environment and cattle hides are reservoirs of this pathogen. Bacteriophages present an attractive non-antibiotic strategy for control of *Salmonella* in beef. In this study, four diverse and genetically unrelated *Salmonella* phages, Sergei, Season12, Sw2, and Munch, were characterized and tested alone and in combination for their ability to control *Salmonella* in cattle hide and soil systems, which are relevant models for *Salmonella* control in beef production. Phage Sergei is a member of the genus *Sashavirus,* phage Season12 was identified as a member of the *Chivirus* genus, Sw2 was identified as a member of the T5-like *Epseptimavirus* genus, and Munch was found to be a novel "jumbo" myovirus. Observed pathogen reductions in the model systems ranged from 0.50 to 1.75 $\log_{10}$ CFU/cm^2 in hides and from 0.53 to 1.38 $\log_{10}$ CFU/g in soil, with phages Sergei and Sw2 producing greater reductions (~1 $\log_{10}$ CFU/cm^2 or CFU/g) than Season12 and Munch. These findings are in accordance with previous observations of phage virulence, suggesting the simple ability of a phage to form plaques on a bacterial strain is not a strong indicator of antimicrobial activity, but performance in liquid culture assays provides a better predictor. The antimicrobial efficacies of phage treatments were found to be phage-specific across model systems, implying that a phage capable of achieving bacterial reduction in one model is more likely to perform well in another. Phage combinations did not produce significantly greater efficacy than single phages even after 24 h in the soil model, and phage-insensitive colonies were not isolated from treated samples, suggesting that the emergence of phage resistance was not a major factor limiting efficacy in this system.

Keywords: bacteriophage, *Salmonella*, food safety, antimicrobials, beef cattle

OPEN ACCESS

Edited by:
Krishna Mohan Poluri, Indian Institute of Technology Roorkee, India

Reviewed by:
Andrea Isabel Moreno Switt, Pontificia Universidad Católica de Chile, Chile
Hany Anany, Agriculture and Agri-Food Canada (AAFC), Canada

***Correspondence:**
Jason J. Gill
jason.gill@tamu.edu

Specialty section:
This article was submitted to Antimicrobials, Resistance and Chemotherapy, a section of the journal Frontiers in Microbiology

Received: *23 January 2021*
Accepted: *04 June 2021*
Published: *28 June 2021*

Citation:
Xie Y, Thompson T, O'Leary C, Crosby S, Nguyen QX, Liu M and Gill JJ (2021) Differential Bacteriophage Efficacy in Controlling Salmonella in Cattle Hide and Soil Models. Front. Microbiol. 12:657524. doi: 10.3389/fmicb.2021.657524

INTRODUCTION

In the United States, foodborne illnesses caused by *Salmonella* are estimated to number more than 1.2 million each year, with more than 23,000 hospitalizations and 450 deaths (Scallan et al., 2011); culture-confirmed *Salmonella* incidence has ranged from 10.9 to 14.8 cases per 100,000 population from the years 2001–2016 (Centers for Disease Control, 2016). *Salmonella*

is associated with a wide range of food commodities and about 4% of commercial ground beef in the United States is contaminated with *Salmonella* (Bosilevac et al., 2009), and ground beef contributed to almost a quarter of beef-related *Salmonella* outbreaks from 1973 to 2011 (Laufer et al., 2015). Lymph nodes, which are commonly present in lean trimmings destined for ground beef production, can harbor *Salmonella* without the animal displaying symptoms of illness (Gragg et al., 2013), indicating asymptomatic carriage of *Salmonella* in the lymph nodes of cattle contributes to contamination of ground beef (Bosilevac et al., 2009). *Salmonella* serovars Anatum, Montevideo, and Muenchen are among those most consistently recovered from the lymph nodes of cattle (Gragg et al., 2013; Belk et al., 2018; Nickelson et al., 2019). The lymph nodes of cattle may be colonized by *Salmonella* via oral intake of contaminated water or feeds, or via insect bites or skin abrasions (Pullinger et al., 2007; Edrington et al., 2013; Brown et al., 2015; Olafson et al., 2016). Previous work has shown that the feedlot environment is a reservoir of *Salmonella* that could subsequently contribute to the colonization of lymph nodes of cattle (Gragg et al., 2013; Xie et al., 2016; Belk et al., 2018).

Bacteriophages (phage) are viruses that infect bacteria, and are the most abundant biological entities on earth, estimated to number some 10^{31} to 10^{32} virions (Brussow, 2005; Barr et al., 2013). Phages are ubiquitous in natural environment as well as in plants and animals as a part of their normal flora. Feeding environments of both beef and dairy cattle were previously identified as reservoirs of *Salmonella* phages (Switt et al., 2013; Xie et al., 2016; Duenas et al., 2017). The increasing spread of bacterial resistance to antibiotics has become a worldwide threat, resulting in a renewal of interest in exploring bacteriophage as a potential alternative to control pathogenic bacteria in Western countries (Sulakvelidze, 2011).

The U.S. Department of Agriculture (USDA), Food and Drug Administration (FDA) and Environmental Protection Agency (EPA) have approved phage-based commercial products that are now available as antimicrobial interventions in pre-harvest and post-harvest food production (Goodridge and Bisha, 2011). Previous studies have shown that *Salmonella* phages are able to reduce bacterial loads in poultry (Atterbury et al., 2007; Hungaro et al., 2013; Grant et al., 2017), swine (Harris, 2000), seafood (Galarce et al., 2014), beef (Bigwood et al., 2008), produce (Bai et al., 2019), and multiple other foods (Islam et al., 2020) which suggests a role for phages as an antimicrobial intervention against *Salmonella* from "farm to fork" in food production (García et al., 2010; Sillankorva et al., 2012).

The generic term "phages" refers to an extremely diverse set of organisms; it is not unusual for different phages infecting a single strain of bacteria to have no recognizable sequence similarity. When large and diverse collections of phages are available, a question arises as to which phages should be selected for use as antibacterials. Multiple *in vitro* assays exist for evaluating phage host range and potential efficacy, including assays measuring plaque formation (Khan Mirzaei and Nilsson, 2015), clearance of liquid cultures (Xie et al., 2018), or genome copy number (Gayder et al., 2019). In this study we are interested in determining the relationship between performance in liquid culture, plaque formation, and actual efficacy, using cattle hides and feedlot soil as models of "real world" application systems. Four characterized and genomically unrelated phages capable of infecting the same *S.* Anatum host were selected for use.

Phages are capable of targeting bacterial hosts with high specificity by recognizing unique bacterial surface structures. This specificity reduces collateral damage to other resident microbiota but also allows the target bacteria to become phage resistant by mutational loss of the receptor, which prevents bacterial adsorption (Gill and Hyman, 2010). Phages of *Salmonella* are able to utilize lipopolysaccharides (LPS), outer membrane proteins (OMPs) and flagella as receptors (Lindberg, 1973). It has been suggested that using a cocktail composed of two or more phages targeting different receptors can delay or inhibit the emergence phage resistance (Gill and Hyman, 2010; Bull et al., 2014) and this has been demonstrated in some systems (Yoichi et al., 2005; Bai et al., 2019). Therefore, cross-resistance characterization of individual phages is a key step in rationally developing phage cocktails that are capable of overcoming bacterial insensitivity (Gill and Hyman, 2010).

In this study, we characterize four genetically unrelated lytic *Salmonella* phages and examine their patterns of cross-resistance to formulate phage cocktails capable of overcoming phage resistance. We then study their efficacy *in vitro* and in two model systems with relevance for the potential control of *Salmonella* transmission in the beef cattle feedlot, with the intention of improving the microbiological safety of ground beef.

MATERIALS AND METHODS

Bacterial Strains and Culture Conditions

S. Anatum strain FC1033C3 was isolated previously in fecal samples from a cattle feedlot located in south Texas (Xie et al., 2016). *S.* Montevideo strain USDA3 and *S.* Newport USDA2 used for phage propagation were obtained from T. Edrington (USDA, College Station, TX, United States). Bacteria were cultured on trypticase soy broth (TSB, Becton-Dickinson) or trypticase soy agar [TSA, TSB plus 1.5% w/v Bacto agar (Becton-Dickinson)] aerobically at 37°C. A nalidixic acid-resistant derivative of *S.* Anatum FC1033C3 was obtained by plating an overnight bacterial culture on TSA supplemented with 25 mg/L nalidixic acid and selecting for surviving colonies. Bacterial inocula used in the hide and soil models was prepared in peptone water (0.1% peptone (w/v), Becton, Dickinson and Co., Franklin Lakes, NJ, United States). Xylose lysine deoxycholate agar (XLD, Becton-Dickinson) supplemented with 25 mg/L nalidixic acid and 0.1% (w/v) cycloheximide was used to recover *Salmonella* in the hide and soil models.

Bacteriophage Strains and Culture Conditions

The initial isolation of phage Sergei, Season12, Munch and Sw2 was described in a previous study (Xie et al., 2016). Sergei and Sw2 were isolated on *S.* Anatum FC1033C3, Season12 was isolated on *S.* Newport USDA2 and Munch was isolated on *S.* Montevideo USDA3. Phage stocks were enumerated by the soft

agar overlay method as described previously (Xie et al., 2018). High-titer phage stocks were prepared by propagating phage on their respective host strains (Xie et al., 2018) by the confluent plate lysate method (Adams, 1959). For use in the hide and soil models, phage lysates were centrifuged at 8,000 × *g*, 4°C, for 16–18 h and phage pellets gently were resuspended in phage buffer (100 mM NaCl, 25 mM Tris–HCl pH 7.4, 8 mM $MgSO_4$, 0.01% w/v gelatin) and stored at 4°C. Phage stocks were adjusted in phage buffer to achieve concentrations of 10^8 and 10^9 PFU/mL before use in the hide and soil models.

Transmission Electron Microscopy Imaging

Transmission electron microscopy of phages was performed by staining virions with 2% uranyl acetate and imaging in a JEOL 1200 EX transmission microscope operating at an acceleration voltage of 100 kV as previously described (Valentine et al., 1968; Gill et al., 2011). Head dimensions and tail length were measured using ImageJ (Schneider et al., 2012; Piya et al., 2017) and standardized against images of a carbon grating replica of known dimensions (Ted Pella, cat# 607). Virion head height was measured from vertex to vertex from the top of the tail to the top of the head, and head width was measured face to face perpendicular to the axis of the tail.

Genomic DNA Extraction, Sequencing and Bioinformatic Analysis

Phage genomic DNA was prepared by using a modified Wizard® DNA Clean-Up System (Promega, Madison, WI, United States) (Carmody et al., 2010; Gill et al., 2011) and stored at 4°C. Phage genomic DNA was sequenced as paired-end 250 bp reads using the Illumina MiSeq platform. Read quality control, read trimming, and read assembly was achieved by FastQC (bioinformatics.babraham.ac.uk), FastX Toolkit (hannonlab.cshl.edu), and SPAdes 3.5.0 (Bankevich et al., 2012) respectively. PCR and Sanger sequencing of the products was used for genome closure. Glimmer3 (Delcher et al., 1999) and MetaGeneAnnotator (Noguchi et al., 2008) were used to predict protein coding genes with manual correction, and tRNA genes were predicted via ARAGORN (Laslett and Canback, 2004). Putative protein functions were assigned based on sequence homology detected by BLASTp (Camacho et al., 2009) and conserved domains detected by InterProScan 5 (Jones et al., 2014) and HHpred (Zimmermann et al., 2018). Bioinformatic analyses were performed via CPT Galaxy (Cock et al., 2013) and WebApollo (Lee et al., 2013) interfaces (cpt.tamu.edu).

Characterization of Cross Resistance of Phages

Phage-resistant mutants of *S.* Anatum FC1033C3 were selected by co-culturing the bacterium with a large excess (∼10^8 PFU, MOI ∼10) of each of the four phages in soft agar overlays as described above and isolating surviving bacterial colonies. Phage-insensitive mutants were subcultured three times. Phage insensitivity was determined by measuring phage efficiency of plating (EOP) on each phage-resistant strain and the phage-sensitive parental strain to determine if resistance to one of the test phages conferred resistance to other phages in the collection (Xie et al., 2018). Phage activity against the parental strain FC1033C3 was measured alone and in combination in a microplate-format assay. A mid-log culture (OD_{550nm} ∼0.5) was diluted 1,000-fold in TSB and aliquoted to a sterile 96-well microtiter plate at 180 μL per well. Wells were then inoculated with 20 μL of single phages or phage mixtures to final concentrations of 10^8 and 10^6 PFU/mL. The plates were incubated at 37°C with double orbital shaking in a Tecan Spark 10M plate reader (Tecan Group Ltd., Männedorf, Switzerland) and growth was monitored by measuring OD_{550nm} at 30-min intervals for 12 h. Growth curves were achieved by plotting OD after baseline adjustment against time. Three biological replicates were performed for each condition.

Cattle Hide Model

An overnight culture of the nalidixic acid-resistant *S.* Anatum strain FC1033C3 was centrifuged, washed three times with peptone water and inoculated into a sterile gelatin-based slurry at a final concentration of ∼ 6.8 $\log_{10}$ CFU/mL to mimic the adherent properties of soil and fecal contamination (Villarreal-Silva et al., 2016). Cattle hide pieces were obtained from Texas A&M Rosenthal Meat Science and Technology Center during harvest with a circular punch to achieve hide swatches with an average surface size of 70 cm^2. Five mL of slurry was applied to the freshly collected cattle hide swatches and allowed 30 min of contact time at 37°C, followed by removal of excess material with a plastic cell spreader. Inoculated hide pieces were sprayed with 5 mL of individual phages or phage combinations at concentrations of 10^8 or 10^9 PFU/mL and held at 37°C for 1 h in a humidified environment. Phages Sergei, Season12, Munch and SW2, representing four distinct phage types, were used; two phage combinations, Sergei + Munch and Sergei + Sw2, were also evaluated, based on the lack of cross-resistance shown by these phages (see below and **Table 2**). Sham treatments were performed as controls by spraying 5 mL of phage buffer onto inoculated hide pieces. Treated hide pieces were placed in filtered stomacher bags with 100 mL of peptone water and homogenized in a stomacher for 60 s, and 5 mL of homogenized mixtures were centrifuged at 8,000 × *g* for 10 min and pellets were resuspended in 5 mL peptone water, serially diluted and spread on XLD supplemented with 25 mg/L nalidixic acid and 0.1% cycloheximide. Plates were incubated at 37°C for 18 h and colonies enumerated. Each experiment was performed in three biological replicates.

Soil Model

The bacterial inoculum was prepared and washed in peptone water as described above. Soil was collected from a cattle feedlot located in College Station, TX and soil compositional analysis was performed at the Soil, Water and Forage Testing Laboratory at Texas A&M University. Soil was determined to be composed of 55% sand, 28% silt, and 17% clay. Silica sand was obtained from a commercial supplier (Standard Sand, Millipore-Sigma). Soil and sand were sterilized by autoclaving three times at 121°C for 30 min, and 10 g aliquots of sterilized materials were placed into plastic 90 mm Petri plates. Soil or sand was inoculated by

spraying 3 mL of inoculum, and allowing 30 min of contact time at 37°C. Inoculated samples were sprayed with 3 mL of individual phages or phage combinations as appropriate at concentrations of 10^8 or 10^9 PFU/mL and held at 37°C for 1 or 24 h treatment periods in a humidified environment. Sham treatments were performed as controls by spraying 3 mL of phage buffer onto inoculated sand and soil samples in Petri plates. Treated samples were placed in filtered stomacher bags with 100 ml of peptone water and homogenized by hand massage for 60 s, and 5 mL of homogenized mixtures were centrifuged at 8,000 × *g* for 10 min and pellets were resuspended in 5 mL peptone water, serially diluted and spread on XLD agar supplemented with 25 mg/l nalidixic acid and 0.1% cycloheximide. Plates were incubated at 37°C for 18 h and colonies enumerated. Each experiment was performed in three biological replicates.

Statistical Analysis

Bacterial survival from different phage treatments in the hide or soil models were analyzed for differences between treatments by one-way analysis of variance (ANOVA) at $\alpha = 0.05$ via JMP v12.1.0 (JMP® Statistical Discovery™ From SAS, Cary, NC, United States). Significantly different bacterial concentrations between treatments were determined by pairwise Student's *t*-tests ($P < 0.05$).

Accession Numbers

Phage genomes are deposited in NCBI GenBank under the following accession numbers: KY002061 (Sergei); MK286578 (Season12); MK268344 (Munch); MH631454 (Sw2).

RESULTS

Bacteriophage Characterization

The four phages used in this study were previously isolated as described (Xie et al., 2016, 2018). Results of transmission electron microscopy are shown in **Figure 1**, with phages Sergei, Season12, and Sw2 exhibiting typical siphophage morphology with long, non-contractile tails and phage Munch exhibiting myophage morphology with a long, contractile tail and a slightly prolate head. The phage Munch virion is exceptionally large, with a head width of 99 nm. All phage genomes were sequenced to completion on the Illumina platform, and closure was confirmed by PCR. Genome maps of Season12, Munch and Sw2 are shown in **Supplementary Figures 1–3**, respectively. A genome map of Sergei is shown in Zeng et al. (2019). Phage dimensions and general genome characteristics are summarized in **Table 1**.

Phage Sergei belongs to a group of closely related phages similar to the *Salmonella* phage 9NA (KJ802832) that was proposed as a new virus genus (Casjens et al., 2014; Zeng et al., 2019); DNA-level similarity to other related phages places Sergei as likely its own species within the *Sashavirus* genus, with 93.5% similarity to *Salmonella* phage Sasha (NC_047786) as determined by progressiveMauve (Darling et al., 2010). Phage Sergei has a genome of 56,051 bp with a GC content of 43.5%. The genome of phage Sergei is presumably terminally redundant and circularly permuted based on its close relationship to phage 9NA; the annotation of this genome and its relatives is described in detail elsewhere (Zeng et al., 2019).

Phage Season12 was found to be 91% identical to *Salmonella* phage Chi (KM458633) at the DNA level determined by progressiveMauve, placing it in the *Chivirus* genus. The genome of Season12 is 59,059 bp in length with a GC content of 56.5%. The genome assembled into a single linear contig at 34.8-fold coverage starting with a 12-bp predicted 5′-overhang cohesive (*cos*) end (5′-GGTGCGCAGAGC-3′) that is conserved in phage Chi and other Chi-like phages (Hendrix et al., 2015; Leavitt et al., 2017). There are 76 protein coding genes predicted in the genome of Season12, in which 50 are of unknown function. Genes associated with DNA replication and transcription, such as DNA primase, DNA polymerase and DNA helicase, and structural proteins such as the portal, major capsid protein and major tail protein share high degree of identity (∼80 – 99%) with Chi. The predicted Season12 tail fiber protein is >99% identical to that found in Chi, with only two amino acid variations. No tRNA genes were detected in Season12. Three tandem repeats (protein identity ranging from 24 to 37%) of a gene encoding a hypothetical protein were identified downstream of the Season12 tail fiber protein. This tandem gene repeat is also found in the genomes of closely related phages such as Chi, iEPS5 (KC677662) and SPN19 (JN871591).

Phage Munch is a so-called "jumbo" phage with a large genome of 350,103 bp and a relatively low GC content of 35.6%. The genome was sequenced to 12.4-fold coverage and was predicted to be terminally redundant and non-permuted by PhageTerm (Garneau et al., 2017); the genome was reopened at the boundary of a predicted 21,296 bp direct terminal repeat identified by this tool. The "jumbo" phage classification is an informal grouping that includes a diverse set of phages with genomes greater than ∼200 kb (Yuan and Gao, 2017). The phage Munch genome has 532 predicted protein coding genes and 22 tRNAs. Of these predicted protein coding sequences, only 118 could be assigned a putative function. Like many jumbo phages, Munch is not closely related to any other known phage; the low DNA sequence identity to other phage genomes (<30% as determined by progressiveMauve) indicates Munch is likely the founding member of an as-yet unclassified myoviral genus. At the protein level, the most closely related phage to Munch is phage 121Q (KM507819), which shares 270 proteins with Munch based on a BLASTp analysis with an *E* value cutoff of 0.001. Other related phages include vB_Eco_slurp01 (LT603033, 268 shared proteins), vB_CsaM_GAP32 (JN882285.1, 265 shared proteins) and PBECO 4 (KC295538.1, 264 shared proteins).

Three regions containing repeated DNA sequence were identified in the Munch genome by Dotmatcher (**Supplementary Figure 4**; Cock et al., 2013). Protein sequences within these regions were further compared using BLASTp. Genes from the repeat region located in the first 20 kb of the genome did not display detectable similarity in protein sequence, suggesting that if these proteins are the result of gene duplication, this event would have occurred in the distant past. The second repeat region was located completely within the tail fiber protein gene (position 140,830–145,512) (**Supplementary Figure 2**), however,

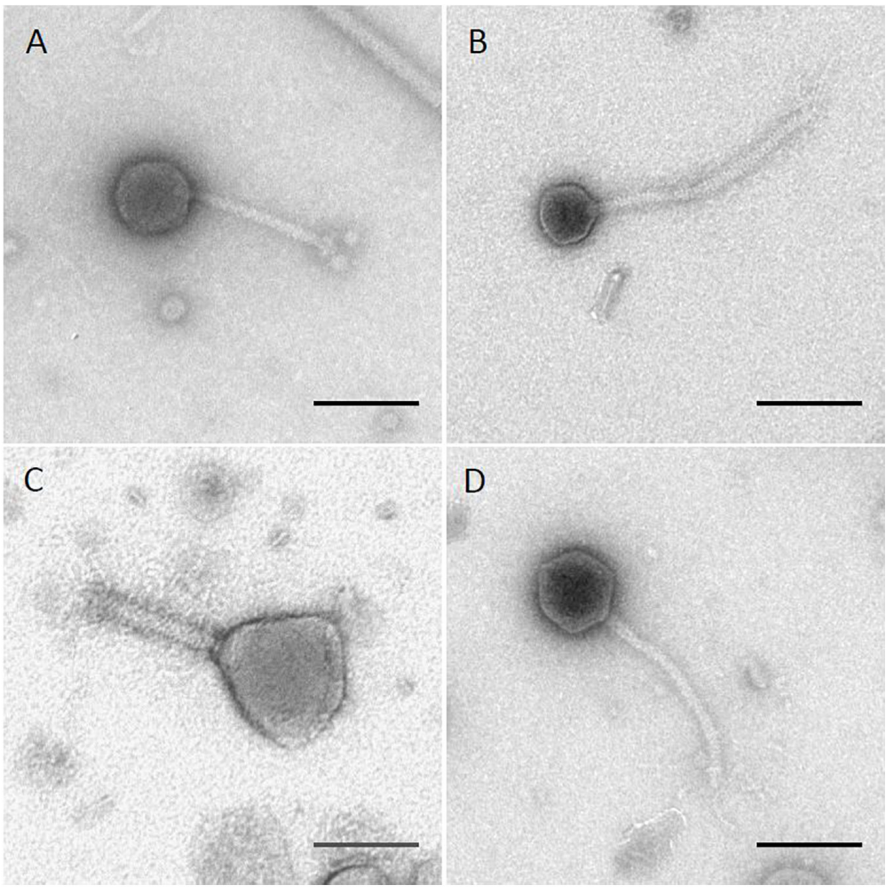

FIGURE 1 | TEM images of four *Salmonella* phages. **(A)** phage Sergei; **(B)** phage Season12; **(C)** phage Munch; **(D)** phage Sw2. Black lines indicate 100 nm for scale.

TABLE 1 | Phage virion dimension and general genome characteristics.

Bacteriophage	Morphology			Genome		
	Head (nm)	Tail (nm)	Morphotype	Length (bp)	Genus	GC Content (%)
Sergei	69 × 63	156 × 11	Sipho	56,051	*Sashavirus*	43.4
Season12	57 × 54	231 × 12	Sipho	57,039	*Chivirus*	56.5
Munch	119 × 99	125 × 23	Myo	350,103	Unclassified	35.6
Sw2	77 × 72	185 × 8	Sipho	114,274	*Epseptimavirus*	40.2

Virion head dimensions are displayed as head height × head width. Virion tail dimensions are displayed as tail length × tail width.

no obvious repeated protein motif was identified in this gene product. The final repeat region which spans the right-most ∼20 kb of the genome contains 13 tandem repeats of a gene encoding a predicted DNA condensation protein (IPR009091).

The 114,274 bp genome of phage Sw2 was sequenced to 73.5-fold coverage. Sw2 has a GC content of 40.2% and the genome was reopened to a predicted 8,123 bp non-permuted terminal repeat as determined by PhageTerm (Garneau et al., 2017). Phage Sw2 shares 59% DNA sequence identity with the well-studied *Siphoviridae* phage T5 (NC_005859.1), and contains 197 predicted protein coding genes, of which 82 could be assigned a function. There are 29 tRNA sequences annotated in the genome of Sw2. The current ICTV taxonomy of phages has classified Sw2 as its own species in the genus *Epseptimavirus*.

Characterization of Phage-Resistant Mutants

Mutants of *S.* Anatum FC1033C3 insensitive to phages Sergei, Season12, Munch, and Sw2 were obtained by culturing the bacterium with an excess of each phage. The efficiency of plating (EOP) of each phage was determined on each insensitive mutant standardized to the phage titer obtained by plating on the parental strain FC1033C3 (**Table 2**). Phage Sergei and Season12 were able to infect each other's phage-insensitive

TABLE 2 | Phage efficiencies of plating (EOP) on the parental strain *S.*Anatum FC1033C3 and its four phage-insensitive derivatives.

Bacteriophage	Bacterial Strain				
	***S.* Anatum FC1033C3**	**Sergei^R**	**Season12^R**	**Munch^R**	**Sw2^R**
Sergei	1.00	$<10^{-7}$	0.98	0.75	0.70
Season12	1.00	1.10	$<10^{-7}$	$<10^{-7}$	1.15
Munch	1.00	0.02	0.02	$<10^{-7}$	0.02
Sw2	1.00	1.17	1.42	1.42	$<10^{-7}$

EOP's are normalized to the titer of each phage on the parental strain. Mutant strains are insensitive to the phages used to select them and have varying sensitivities to the other three phages tested.

mutants with EOP's close to 1, showing that Sergei and Season12 are genetically independent for phage resistance. In contrast, phage Munch was able infect the Season12-insensitive mutant at a roughly 100-fold reduced EOP but Season12 was completely unable infect the Munch-insensitive mutant, showing a partially dependent phenotype for phage insensitivity. Phage Munch exhibited this 100-fold reduction in EOP on Sergei, Season12 and Sw2-insensitive mutants, suggesting that Munch infection is easily perturbed by the development of insensitivity to multiple other phages.

Efficacy Testing on Single and Mixed Phages Against *S.* Anatum FC1033C3 in a Microtiter Plate Liquid Assay

Because phages select for phage-insensitive mutants at relatively high frequencies, it was hypothesized that using a combination of phages that are genetically independent for phage insensitivity can improve antimicrobial efficacy (Gill and Hyman, 2010). Based on the results shown in **Table 3**, a pair of two-phage cocktails were formulated that contained phages that were either genetically independent for insensitivity (Sergei and Munch) or partially dependent (Munch and Season12). The performance of these phage cocktails was evaluated in a microtiter plate assay and compared to the performance of the individual phages.

Results obtained from this experiment are shown in **Figure 2**. When testing phages Sergei, Munch or Season12 alone against the wild type *Salmonella* strain, regrowth of bacterial culture was observed starting at 7, 6, and 5 h, respectively. This observation of bacterial regrowth is consistent with the rise of phage-insensitive mutants in the culture. By using a combination of two phages with genetically independent resistance (Sergei and Munch), no regrowth was observed during the 12-h experiment, demonstrating a significant improvement of antimicrobial efficacy against the test *Salmonella* strain. In contrast, by using a combination of two phages with partially dependent resistance (Season12 and Munch), no improvement of antimicrobial efficacy over the individual phage was observed.

Ability of Phages to Reduce *Salmonella* Populations in Model Systems

Treatments with single phages and mixtures of phages with genetically independent resistance were tested against *S.* Anatum FC1033C3 in model systems of *Salmonella*-contaminated cattle hides and soil, two common reservoirs for *Salmonella* in the beef cattle feedlot (Gragg et al., 2013; Xie et al., 2016). In the hide model, all phage treatments except phage Season12 were able to significantly reduce *Salmonella* populations on cattle hides compared to the positive control (**Figure 3**) at 5.74 $\log_{10}$ CFU/cm^2. A reduction of 1.75 $\log_{10}$ CFU/cm^2 was obtained by phage Sw2 alone at 10^9 PFU/mL, which was the highest bacterial reduction among all treatments performed. Limited dosage effects were observed across phage treatments, with statistically significant differences only observed between the two phage treatment concentrations in phages Sergei and Sw2. No significant differences were observed between the phage mixtures (Sergei + Munch, Sergei + Sw2) and phage Sergei alone, indicating the phage mixtures provided no added efficacy over using a single phage.

In the sterile soil model sampled 1 hr post-treatment, statistically significant reductions were observed only with phage

TABLE 3 | Comparison of two methods for measuring phage virulence and the observed phage efficacy in reducing *S.* Anatum loads in two model systems.

Phage isolate	Phage virulence scores		Reductions in model systems with phage concentration at 10^9 PFU/ml		
	Spot assay (EOP)[1]	**Microtiter assay (10^8 PFU/ml)[2]**	**Cattle hide ($\log_{10}$ CFU/cm^2)**	**Soil ($\log_{10}$ CFU/g)**	
				1 h	**24 h**
Sergei	0.5–1	55	1.60*	1.38*	0.45*
Season12	0.5–1	10	0.50	0.22	0.33
Munch	0.5–1	27	0.83*	0.53*	0.33
Sw2	0.05–0.5	86	1.75*	0.77*	0.88*

Asterisks by $\log_{10}$ reductions in model systems indicate statistically significant reductions compared to the control ($P < 0.05$). Host range scores from Spot Assays and Microtiter Assays are taken from Xie et al. (2018). Note that estimation of phage virulence based on plaque formation (Spot Assay) is a poor predictor of phage efficacy in the hide and soil model systems; phages with higher virulence in liquid culture (Microtiter Assay) tend to perform better in the model systems.

[1]An EOP of ~0.5 – 1 corresponds to a score of 4, and an EOP of ~0.05 – 0.5 corresponds to a score of 3, as described in Xie et al. (2018).

[2]The microtiter plate assay was conducted by monitoring bacterial growth by optical density in the presence of phage in a 96-well microtiter plate. The score is equal to the area between bacterial growth observed in the positive (no phage) control and the phage-treated culture. A score of zero would indicate complete insensitivity to the phage and a score of 100 would indicate complete elimination of bacterial growth. Method and results are described in Xie et al. (2018).

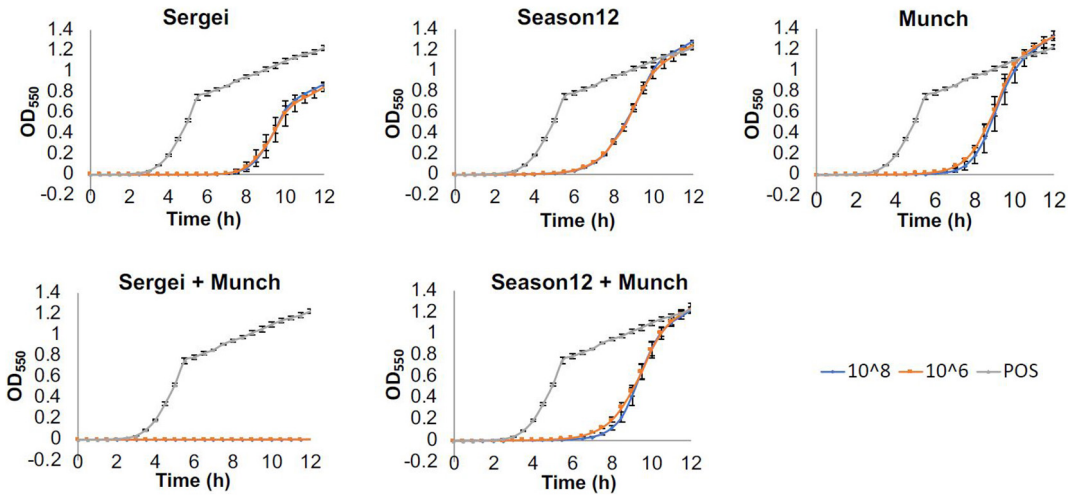

FIGURE 2 | Efficacies of phages alone and in combination against *S.* Anatum FC1033C3 in a microtiter-plate based assay. Wells of 96-well microtiter plates were inoculated with bacterial culture (~10^5 CFU/mL) and challenged with single phages or phage mixtures at concentrations of 10^8 or 10^6 PFU/mL, and growth was monitored by measuring OD_{550nm} at 30-min intervals for 12 h. Growth curves were achieved by plotting OD after baseline adjustment against time. Three biological replicates were performed for each assay. Blue, orange and gray curves represent growth profiles of phage treatments at 10^8 PFU/mL, phage treatments at 10^9 PFU/mL and positive (no phage) control.

concentrations at 10^9 CFU/mL for phages Munch, Sergei and Sw2 alone, and with phage mixtures Sergei + Sw2 and Sergei + Munch (**Figure 4A**). Phage Sergei was able to reduce the bacterial load from 6.33 $\log_{10}$ CFU/g (control) to 4.95 CFU/g, and Sergei alone and its combination with Munch showed a statistically significant dosage effect ($P < 0.05$). At the 24 h sampling time, the bacterial load in the soil had grown to 8.95 $\log_{10}$ CFU/g in the control treatment, and phage Sw2 and its combination with Sergei was able to significantly reduce the bacterial population in soil compared to the control treatment at either treatment concentration. Sergei alone significantly reduced bacterial load only when applied at 10^9 PFU/mL. Phage treatment with Sw2 at a concentration of 10^9 PFU/mL resulted in the greatest reduction in this model of $\log_{10}$ 0.82 CFU/g. To examine the role of phage resistance in this model, 60 *S.* Anatum colonies were recovered from soils following treatment with phage Sergei and Sergei + Munch in one of the experimental replicates. Of the 10 colonies recovered from each phage treatment after 1 h, and the 20 colonies recovered from each treatment after 24 h, none were resistant to either phage Sergei or Munch, indicating that the arisal of phage-resistant bacterial mutants was not a significant issue in this system (**Supplementary Table 1**).

Comparing the bacterial survival between these two models, treatments with phages appeared to demonstrate better efficacies in the hide model than the soil model. Phages are known to interact with charged particles in soils which may interfere with their ability to efficiently diffuse and locate their hosts (Bitton, 1975). To further examine this system, phage Sw2 was applied to a sterile quartz sand model inoculated under the same conditions as the soil model. The sand model was intended to mimic the physical structure of soil while providing a more uniform substrate (Redman et al., 1999). Results from the sand

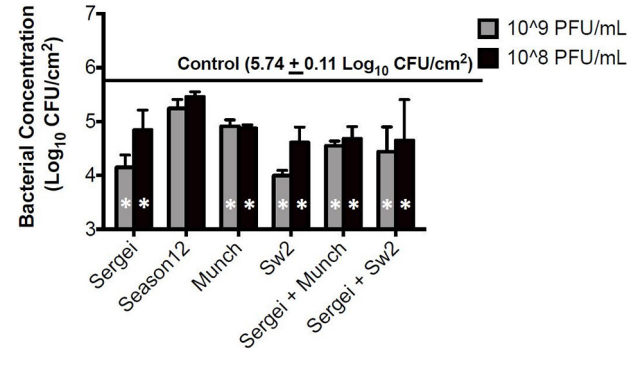

FIGURE 3 | Bacterial survival after phage treatments in the cattle hide model. Bars indicate bacterial survival after 1 h phage treatment. Bar shading indicates two phage treatment concentrations at 10^8 and 10^9 PFU/mL, and the solid line parallel to the *X*-axis indicates the bacterial load in the positive (no phage) control. Error bars indicate standard deviation across three biological replicates. White stars in the bars represent significant difference in the treatment from the positive control. The detection limit of this assay is 1.15 $\log_{10}$ CFU/cm^2.

model are displayed in **Figure 5**. Sw2 was able to significantly reduce the *Salmonella* population by 0.8 $\log_{10}$ CFU/g at the 1 hr sample time and continued to suppress bacterial growth by 0.64 $\log_{10}$ CFU/g at 24 h; both of these reductions are statistically significant compared to the control treatments. The sand model supported reduced bacterial growth compared to the soil model, reaching only 7.0 $\log_{10}$ CFU/g after 24 h compared to the 8.95 $\log_{10}$ CFU/g reached in the soil model. However, the $\log_{10}$ reductions in bacterial loads produced by phage in the sand model were not markedly better than those observed in the soil model (**Figure 5**).

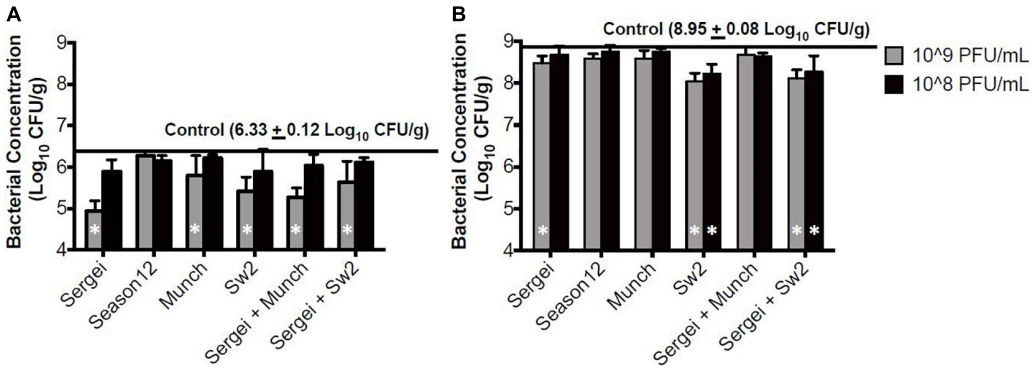

FIGURE 4 | Bacterial survival after phage treatments in the sterile soil model. **(A,B)** indicate bacterial survival following phage treatments of 1 and 24 h, respectively. Bar shading indicates two phage treatment concentrations at 10^8 and 10^9 PFU/mL, and the solid line parallel to the *X*-axis indicates the bacterial load in the positive (no phage) control. Error bars indicate standard deviation across three biological replicates. White stars in the bars represent significant difference in the treatment from the positive control. The detection limit of this assay is 2 $\log_{10}$ CFU/g.

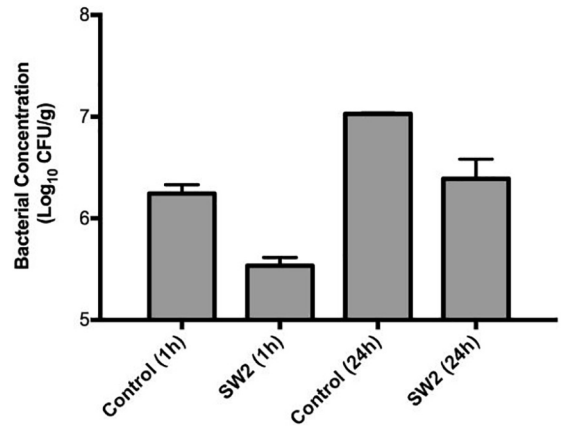

FIGURE 5 | Bacterial survival in a sterile sand model after treatment with sterile buffer (control) or phage Sw2 at 10^9 PFU/mL. Bacterial loads were measured 1 and 24 h after treatment. The detection limit of this assay is 2 $\log_{10}$ CFU/g.

DISCUSSION

Characterization of Phages

With the exception of phage Munch, phage genomes showed high levels of similarity to other well-known phage types. Conserved structural proteins found in phages Sergei, Season12, and Sw2 provided useful information to understand the dynamics of phage infection. In particular, the characterization of phage tail fiber proteins is useful for prediction of phage receptors and interpretation of phage cross-resistance patterns.

Sergei is related to phage 9NA, and is a member of the *Sashavirus* genus. The structural proteins of Sergei, including the portal protein, major capsid proteins and major tail proteins share high (∼90%) identity within this phage group. Phage Sergei encodes two predicted receptor-binding proteins, a tail tip protein (gp60, APU92897) with a lambda J-like conserved domain and a tailspike protein (gp61, APU92898). The tail tip protein is conserved in 9NA-like phages including Sasha, Sergei and 9NA (Zeng et al., 2019). The tailspike protein is related to the 9NA tailspike (gp55, YP_009101225) but its sequence is conserved only at the N-terminus, with an unrelated C-terminal domain. The Sergei gp61 C-terminal domain contains a pectate lyase fold domain (IPR011050) and is related to predicted tail fiber proteins found in other *S.* Anatum prophages, suggesting Sergei also uses the bacterial LPS as its receptor (Zeng et al., 2019).

Phage Season12 is a member of the *Chivirus* genus, with strong DNA sequence similarity to phage Chi itself. Bacteriophage Chi was first isolated in 1936 and is known for its use of bacterial flagella to infect *Salmonella* spp. (Meynell, 1961). The adsorption mechanism of Chi-like phages has been studied in related phages iEPS5 (Choi et al., 2013) and YSD1 (Dunstan et al., 2019). Choi et al. (2013) indicated that phage iEPS5 were only able to infect the bacterial host when the flagellum is rotating counterclockwise, suggesting the physical movement of flagellum generates power that drives phages toward to the bacterial surface. The overall similarity of phage Season12 to Chi and their nearly identical (96% identity) major tail fiber proteins (gp31 in both phages) strongly suggests the use of the flagellum as the major receptor of Season12.

Phage Munch has an unusually large genome of >350 kb, and a head diameter of ∼100 nm, making it the largest *Salmonella* phage isolated to date. The term "jumbo phage" is generally given to phages with genome sizes larger than 200 kb (Yuan and Gao, 2017), and like many such phages, a large proportion of its genes (78%) could not be annotated with a known function. The majority of jumbo phages have been isolated against GC-rich Gram-negative hosts, but these phages tend to display an AT-rich genome (Mesyanzhinov et al., 2002; Yuan and Gao, 2017); phage Munch is no exception, with an overall GC content of 35.6%. Structural proteins annotated in Munch, such as major capsid proteins, portal proteins and baseplate proteins, are predominantly related to structural proteins found in coliphage T4. Other genes associated with nucleotide metabolism and

replication were also annotated, however, no virus-encoded RNA polymerase (RNAP) was identified. Based on protein sequence similarity, phage Munch is most closely related to other jumbo phages such as 121Q (KM507819.1), GAP32 (JN882285.1), and PBECO 4 (KC295538.1). These phages were noted to reside in a single cluster in a recent comparison of 52 jumbo phage genomes (Yuan and Gao, 2017), and these phages appear to be only distantly related to other more well-studied jumbo phages such as phiKZ or KVP40. Phage Munch also has almost no detectable relationship with the 240 kb *Salmonella* jumbo phage SPN3US (JN641803), with only a single SPN3US protein (gp224) having detectable similarity to a Munch protein by BLASTp. A region of tandemly repeated genes was identified in the rightmost ∼20 kb of the Munch genome, in which 13 repeats of a putative DNA condensation protein, separated by three unrelated hypothetical proteins, were identified. This repeat region was not found in any related jumbo phages such as phages 121Q, vB_Eco_slurp01 (LT603033.1), GAP32, PBECO 4, and vB_KleM-RaK2 (JQ513383.1). Tandem gene duplications have been observed in other jumbo phages such as 121Q and G (Hua et al., 2017). Hua et al. (2017) suggested that jumbo phages may expand their genomes though tandem duplications after head size expansion due to a sudden lack of selective pressure to constrain their genome size. The two putative tail fiber proteins in phage Munch (gp252 and gp287) show low levels of homology to those found in other jumbo phages, and the bacterial receptors recognized by these phages are not known.

Sw2 is a member of the T5-like *Epseptimavirus* genus. The Sw2 genome encodes 29 tRNAs, compared to the 16 identified in T5 (Wang et al., 2005). Like other T5-like phages, the genome of Sw2 can be divided into pre-early genes, early and late genes (Wang et al., 2005). Proteins encoded in pre-early genes are associated with host shutdown, including 5′-deoxyribonucleotidase, A1, and A2 (Wang et al., 2005). The early gene cluster functions related to DNA metabolism, replication, regulation, and lysis, followed by late gene region consists of virion structure (Wang et al., 2005). Sw2 encodes an L-shaped tail fiber (gp180), a second putative tail fiber (gp179) and a receptor-binding protein (gp200). In T5, the L-shaped tail fiber (Ltf) recognizes the host O-antigen (Heller and Braun, 1982) and the receptor-binding protein (Oad, also called Pb5) recognizes the outer membrane protein FhuA (Braun et al., 1994). The gp179-gp180 dual tail fiber module in Sw2 is similar to that observed in the T5-like phages DT57C and DT571/2, suggesting this phage may also possess a complex, possibly branched tail fiber structure as reported in these phages (Golomidova et al., 2016). This may explain the relatively broad host range of this phage, which is capable of infecting diverse *Salmonella* serotypes including Anatum, Dublin, and Heidelberg (Xie et al., 2018). The Sw2 receptor-binding protein gp200 is related to its T5 counterpart ($E = 10^{-29}$) at the N and C termini, but there is significant divergence between the two sequences (∼27% overall identity). Sw2 gp200 is more closely related to the receptor-binding protein of the T5-like phage BF23 (Hrs, AAZ03642), with 73% overall identity. Phage BF23 utilizes the *E. coli* outer membrane protein BtuB as its receptor (Mondigler et al., 2006), which suggests that phage Sw2 gp200 also recognizes this receptor in its *S.* Anatum host. The presence of these tail proteins in Sw2 suggests that this phage uses a two-stage strategy of reversible followed by irreversible binding similar to that used by phage T5.

Phage binding to the host receptor is the initial step of infection, and bacteria spontaneously develop resistance to phage mainly via loss of receptors (Labrie et al., 2010). Therefore, in phage therapeutic applications, it has been proposed that phage cocktails should be used that recognize independent receptors, to prevent the emergence of phage resistance and improve efficacy (Gill and Hyman, 2010). Based on the phage cross-resistance patterns observed in **Table 2**, phages Sergei, Season12 and Sw2 recognize genetically independent receptors as they were still able to infect the mutants resistant to the other phages, and phage mixtures that recognize independent receptors showed greater efficacy in liquid culture (**Figure 2**). The cross-resistance patterns of these phages are generally consistent with phage receptor usage as predicted by genomic analysis, as the recognition of LPS by phage Sergei, for example, is not expected to be affected by loss of the flagella (used by Season12) or BtuB (used by Sw2). An exception to this pattern is seen in the case of phage Munch; this phage shows a ∼100-fold reduced EOP on all phage-resistant mutants, and phage Season12 is also not able to infect the Munch-resistant mutant host (**Table 3**). This latter effect may reflect a significant cell wall defect associated with resistance to phage Munch that interferes with flagella function, or perhaps loss of a secondary receptor at the cell surface required by Season12 for infection.

Antimicrobial Activity of Phages in Model Systems

The ability of a phage to rapidly negatively impact a bacterial population, often referred to as "virulence," is an integrated result of its ability to adsorb to new hosts and release progeny phage (Payne and Jansen, 2001; Gallet et al., 2009; Lindberg et al., 2014). The host ranges and *in vitro* virulence of phages Sergei, Season12, Munch and Sw2 were determined in a previous study using spot assays on soft agar overlays and a microtiter plate-based assay of phage virulence (Xie et al., 2018). While these four phages displayed similar abilities to produce plaques in spot titer assays on soft agar overlays, phages Sergei and Sw2 displayed greater virulence against *S.* Anatum FC1033C3 in liquid culture (Xie et al., 2018). To better demonstrate the correlation between *in vitro* phage virulence and antimicrobial efficacy in model systems, the results obtained for these phages in previous and current studies are summarized in **Table 3**. Phages Sergei and Sw2 were most effective in controlling bacterial growth in liquid culture, and also achieved the highest bacterial reductions in both the hide and soil model systems, implying that measurement of phage virulence in liquid culture can be a predictor of phage efficacies in other, more complex systems. Phages Season12 and Munch were capable of efficiently making plaques on agar overlays but did not exhibit strong antibacterial activity in either the microtiter plate virulence assay or the two model systems of *S.* Anatum colonization (**Table 3**). The tendency of spot assays to overestimate phage virulence was also observed by Henry et al. (2013) in a mouse model of

Pseudomonas aeruginosa infection. A similar trend was also noted by Lindberg et al. (2014), where phage growth rate in liquid culture was a strong predictor of phage *in vivo* efficacy in a *P. aeruginosa* insect infection model. This contrasts with observations by Bull et al. (2012), where two phages with similar *in vitro* virulence displayed markedly different efficacies in a rodent model. This phenomenon was attributed to the ability of one of the phages to produce an additional therapeutic protein, a capsular depolymerase, which attenuates bacterial virulence *in vivo* (Mushtaq et al., 2004; Lin et al., 2017). Taken together, these findings suggest that, barring the presence of emergent effects that are only observable in the model system, the virulence or efficacy of a phage is largely phage-dependent and model-independent. Phages such as Sergei or Sw2 are better at controlling bacterial populations in simple liquid culture systems (Xie et al., 2018) and this ability extended to other more physically complex systems such as animal hides or soil in this study.

While individual phage efficacy was conserved across systems, the overall magnitude of the effect on bacterial populations varied slightly between systems. The phage treatments displayed overall reduced antimicrobial efficiency in the soil model compared to the hide model (**Figures 3**, **4** and **Table 3**). Input MOI's of phage in the soil and hide systems were ∼10 (10^8 PFU/ml treatments) or ∼100 (10^9 PFU/ml treatments), providing enough phage to infect >99.99% of the bacterial cells in these systems, yet only ∼1.5-fold to ∼50-fold reductions in *Salmonella* loads were observed (**Table 3**), suggesting that phages were inhibited in their ability to successfully encounter their bacterial targets in these systems, and this effect was more pronounced in the soil system than the hide system. This lack of phage-host encounters is supported by the complete absence of phage resistance in 40 bacterial colonies recovered from soil 24 h after treatment with phage Sergei or Sergei + Munch, indicating the persistence of *Salmonella* in the phage-treated soil was not due to the emergence of phage resistance (**Supplementary Table 1**). Phage can adsorb to charged particles found in natural soils (Bitton, 1975; Burge and Enkiri, 1978), which may affect their ability to freely diffuse and encounter new hosts. The ability of phage Sw2 to reduce bacterial loads was also evaluated in a model system of pure quartz sand, which provided a more uniform matrix than natural soil. As shown in **Figures 4A**, **5**, phage Sw2 showed a similar ability to control *Salmonella* in both the sand and soil models at 1 h post-treatment, indicating that phage efficacy in soil is not highly dependent on the composition of a particular soil matrix and suggesting that it is the high surface area and reduced diffusion that play major roles in determining phage activity. This phenomenon would also explain why treatments with phage combinations did not exhibit synergistic effects compared to single phage treatments, in contrast to Bai et al. (2019), who observed significantly greater reductions of *Salmonella* using combinations of receptor-independent phages in produce models which present a relatively smooth surface and less inhibition of phage diffusion.

In addition to information on phage lifestyle and receptor usage, bioinformatic analysis may also provide additional predictive information of phage efficacy. The Chi-like nature of Season12 suggests that it requires an active bacterial flagellum for infection (Schade and Adler, 1967; Hendrix et al., 2015). Conditions in the models tested in this study are sub-optimal for *Salmonella* growth and survival, potentially resulting in a stress response (Shen and Fang, 2012) which can lead to downregulation of genes responsible for flagellar synthesis and decreased motility (Fan et al., 2016). Flagellar loss or lack of flagellar rotation can negatively impact the infection process of Chi-like phages, which may further reduce the efficacy of this type of phage in model systems. In addition, the presentation of *Salmonella* flagella is subject to phase variation (Bonifield and Hughes, 2003), and it is possible that Season12 cannot use these flagellar antigens as receptors with equal efficiency. These observations are consistent with the poor efficacy observed for phage Season12 in both model systems (**Figures 3**, **4**), and may indicate against using flagellar-adsorbing Chi-like phages in applications where flagellar activity may be impaired.

Phages have re-emerged as an attractive alternative to combat pathogenic bacteria that have become resistant to antibiotics, or that colonize sites where the use of chemical antimicrobials is not appropriate. The capacity of phages to efficiently infect and lyse their targets is essential for successful phage therapy (Gill and Hyman, 2010; Nilsson, 2014; Roach and Debarbrieux, 2017), but the ability to predict which phages provide greatest efficacy is still an evolving field. In this study, genomic and microbiological approaches were leveraged to characterize and apply four phages that infect the same *S.* Anatum strain. Genomic analysis showed the phages were unrelated, and predictions of the phage receptors were consistent with observed patterns of phage cross-resistance. Phages that displayed greater virulence in *in vitro* assays achieved best reductions of *Salmonella* loads (up to 1.75 $\log_{10}$) in cattle hide and soil models, supporting the concept that phage efficacy tends to be phage-specific rather than model-specific. Reductions in bacterial loads on the order of 10-fold to 50-fold could provide a significant food safety benefit by reducing cattle hide and lymph node carriage and subsequent downstream contamination of beef products.

DATA AVAILABILITY STATEMENT

The datasets presented in this study can be found in online repositories. The names of the repository/repositories and accession number(s) can be found below: https://www.ncbi.nlm.nih.gov/nucleotide/KY002061; https://www.ncbi.nlm.nih.gov/nucleotide/MK286578; https://www.ncbi.nlm.nih.gov/nucleotide/MK268344 and https://www.ncbi.nlm.nih.gov/nucleotide/MH631454.

AUTHOR CONTRIBUTIONS

YX and JG conceived of the study. YX conducted phage isolation and *in vitro* experiments with the assistance of TT, CO'L, and ML. YX and ML sequenced the phage genomes. SC, QN, ML, and JG annotated the genomes and conducted bioinformatic analyses. YX, ML, and JG assembled the manuscript. All authors contributed to the article and approved the submitted version.

FUNDING

This project was supported by funding from the National Science Foundation (DBI1565146), Beef Checkoff, National Cattlemen's Beef Association, Texas Beef Cattle, and the North American Meat Institute.

ACKNOWLEDGMENTS

We would like to thank Tamra Tolen, Abby Korn, Jacob Chamblee, and Shayna Smith for technical assistance with this project, T. Matthew Taylor for provision of strains and technical advice, and Adriana Hernandez and Gabby Kuty-Everett for assistance with genome sequencing and assembly. We would also like to thank Ray Riley for access to cattle hides and Jackson McReynolds of Passport Food Safety Systems for provision of equipment.

SUPPLEMENTARY MATERIAL

The Supplementary Material for this article can be found online at: https://www.frontiersin.org/articles/10.3389/fmicb.2021.657524/full#supplementary-material

REFERENCES

Adams, M. H. (1959). *Bacteriophages*. New York, NY: Interscience Publishers.

Atterbury, R. J., Van Bergen, M. A., Ortiz, F., Lovell, M. A., Harris, J. A., De Boer, A., et al. (2007). Bacteriophage therapy to reduce *Salmonella* colonization of broiler chickens. *Appl. Environ. Microbiol.* 73, 4543–4549. doi: 10.1128/aem.00049-07

Bai, J., Jeon, B., and Ryu, S. (2019). Effective inhibition of *Salmonella typhimurium* in fresh produce by a phage cocktail targeting multiple host receptors. *Food Microbiol.* 77, 52–60. doi: 10.1016/j.fm.2018.08.011

Bankevich, A., Nurk, S., Antipov, D., Gurevich, A. A., Dvorkin, M., Kulikov, A. S., et al. (2012). SPAdes: a new genome assembly algorithm and its applications to single-cell sequencing. *J. Comput. Biol.* 19, 455–477. doi: 10.1089/cmb.2012.0021

Barr, J. J., Auro, R., Furlan, M., Whiteson, K. L., Erb, M. L., Pogliano, J., et al. (2013). Bacteriophage adhering to mucus provide a non-host-derived immunity. *Proc. Natl. Acad. Sci. U S A.* 110, 10771–10776. doi: 10.1073/pnas.1305923110

Belk, A. D., Arnold, A. N., Sawyer, J. E., Griffin, D. B., Taylor, T. M., Savell, J. W., et al. (2018). Comparison of *Salmonella* prevalence rates in bovine lymph nodes across feeding stages. *J. Food Prot.* 81, 549–553. doi: 10.4315/0362-028X.JFP-17-254

Bigwood, T., Hudson, J. A., Billington, C., Carey-Smith, G. V., and Heinemann, J. A. (2008). Phage inactivation of foodborne pathogens on cooked and raw meat. *Food Microbiol.* 25, 400–406. doi: 10.1016/j.fm.2007.11.003

Bitton, G. (1975). Adsorption of viruses onto surfaces in soil and water. *Water Res.* 9, 473–484. doi: 10.1016/0043-1354(75)90071-90078

Bonifield, H. R., and Hughes, K. T. (2003). Flagellar phase variation in *Salmonella enterica* is mediated by a posttranscriptional control mechanism. *J. Bacteriol.* 185, 3567–3574. doi: 10.1128/JB.185.12.3567-3574.2003

Bosilevac, J. M., Guerini, M. N., Kalchayanand, N., and Koohmaraie, M. (2009). Prevalence and characterization of *Salmonellae* in commercial ground beef in the United States. *Appl. Environ. Microbiol.* 75, 1892–1900. doi: 10.1128/AEM.02530-2538

Braun, V., Killmann, H., and Herrmann, C. (1994). Inactivation of FhuA at the cell surface of *Escherichia coli* K-12 by a phage T5 lipoprotein at the periplasmic face of the outer membrane. *J. Bacteriol.* 176, 4710–4717. doi: 10.1128/jb.176.15.4710-4717.1994

Brown, T. R., Edrington, T. S., Genovese, K. J., Loneragan, G. H., Hanson, D. L., and Nisbet, D. J. (2015). Oral *Salmonella* challenge and subsequent uptake by the peripheral lymph nodes in calves. *J. Food Prot.* 78, 573–578. doi: 10.4315/0362-028X.JFP-14-416

Brussow, H. (2005). Phage therapy: the *Escherichia coli* experience. *Microbiology* 151(Pt 7), 2133–2140. doi: 10.1099/mic.0.27849-0

Bull, J. J., Otto, G., and Molineux, I. J. (2012). In vivo growth rates are poorly correlated with phage therapy success in a mouse infection model. *Antimicrob Agents Chemother* 56, 949–954. doi: 10.1128/AAC.05842-11

Bull, J. J., Vegge, C. S., Schmerer, M., Chaudhry, W. N., and Levin, B. R. (2014). Phenotypic resistance and the dynamics of bacterial escape from phage control. *PLoS One* 9:e94690. doi: 10.1371/journal.pone.0094690

Burge, W. D., and Enkiri, N. K. (1978). Virus adsorption by five soils. *J. Env. Qual.* 7, 73–76. doi: 10.2134/jeq1978.00472425000700010015x

Camacho, C., Coulouris, G., Avagyan, V., Ma, N., Papadopoulos, J., Bealer, K., et al. (2009). BLAST+: architecture and applications. *BMC Bioinformatics* 10:421. doi: 10.1186/1471-2105-10-421

Carmody, L. A., Gill, J. J., Summer, E. J., Sajjan, U. S., Gonzalez, C. F., Young, R. F., et al. (2010). Efficacy of bacteriophage therapy in a model of *Burkholderia cenocepacia* pulmonary infection. *J. Infect. Dis.* 201, 264–271. doi: 10.1086/649227

Casjens, S. R., Leavitt, J. C., Hatfull, G. F., and Hendrix, R. W. (2014). Genome Sequence of *Salmonella* Phage 9NA. *Genome Announc* 2:e00531-14. doi: 10.1128/genomeA.00531-514

Centers for Disease Control (2016). *National Enteric Disease Surveillance: Salmonella Annual Report, 2016*. Available online at: https://www.cdc.gov/nationalsurveillance/pdfs/2016-Salmonella-report-508.pdf (accessed April 20, 2021).

Choi, Y., Shin, H., Lee, J. H., and Ryu, S. (2013). Identification and characterization of a novel flagellum-dependent *Salmonella*-infecting bacteriophage, iEPS5. *Appl. Environ. Microbiol.* 79, 4829–4837. doi: 10.1128/AEM.00706-713

Cock, P. J., Gruning, B. A., Paszkiewicz, K., and Pritchard, L. (2013). Galaxy tools and workflows for sequence analysis with applications in molecular plant pathology. *PeerJ* 1:e167. doi: 10.7717/peerj.167

Darling, A. E., Mau, B., and Perna, N. T. (2010). progressiveMauve: multiple genome alignment with gene gain, loss and rearrangement. *PLoS One* 5:e11147. doi: 10.1371/journal.pone.0011147

Delcher, A. L., Harmon, D., Kasif, S., White, O., and Salzberg, S. L. (1999). Improved microbial gene identification with GLIMMER. *Nucleic Acids Res.* 27, 4636–4641. doi: 10.1093/nar/27.23.4636

Duenas, F., Rivera, D., Toledo, V., Tardone, R., Herve-Claude, L. P., Hamilton-West, C., et al. (2017). Short communication: characterization of *Salmonella* phages from dairy calves on farms with history of diarrhea. *J. Dairy Sci.* 100, 2196–2200. doi: 10.3168/jds.2016-11569

Dunstan, R. A., Pickard, D., Dougan, S., Goulding, D., Cormie, C., Hardy, J., et al. (2019). The flagellotropic bacteriophage YSD1 targets *Salmonella* typhi with a Chi-like protein tail fibre. *Mol. Microbiol.* 112, 1831–1846. doi: 10.1111/mmi.14396

Edrington, T. S., Loneragan, G. H., Hill, J., Genovese, K. J., Brichta-Harhay, D. M., Farrow, R. L., et al. (2013). Development of challenge models to evaluate the efficacy of a vaccine to reduce carriage of *Salmonella* in peripheral lymph nodes of cattle. *J. Food Prot.* 76, 1259–1263. doi: 10.4315/0362-028X.JFP-12-319

Fan, Y. Q., Evans, C. R., and Ling, J. Q. (2016). Reduced protein synthesis fidelity inhibits flagellar biosynthesis and motility. *Sci. Rep.* 6:30960. doi: 10.1038/srep30960

Galarce, N. E., Bravo, J. L., Robeson, J. P., and Borie, C. F. (2014). Bacteriophage cocktail reduces *Salmonella enterica* serovar enteritidis counts in raw and smoked salmon tissues. *Rev. Argent Microbiol.* 46, 333–337. doi: 10.1016/S0325-7541(14)70092-70096

Gallet, R., Shao, Y., and Wang, I. N. (2009). High adsorption rate is detrimental to bacteriophage fitness in a biofilm-like environment. *BMC Evol. Biol.* 9:241. doi: 10.1186/1471-2148-9-241

García, P., Rodríguez, L., Rodríguez, A., and Martínez, B. (2010). Food biopreservation: promising strategies using bacteriocins, bacteriophages and

endolysins. *Trends Food Sci. Technol.* 21, 373–382. doi: 10.1016/j.tifs.2010.04.010

Garneau, J. R., Depardieu, F., Fortier, L. C., Bikard, D., and Monot, M. (2017). PhageTerm: a tool for fast and accurate determination of phage termini and packaging mechanism using next-generation sequencing data. *Sci. Rep.* 7:8292. doi: 10.1038/s41598-017-07910-7915

Gayder, S., Parcey, M., Castle, A. J., and Svircev, A. M. (2019). Host range of bacteriophages against a world-wide collection of erwinia amylovora determined using a quantitative PCR assay. *Viruses* 11:910. doi: 10.3390/v11100910

Gill, J. J., and Hyman, P. (2010). Phage choice, isolation, and preparation for phage therapy. *Curr. Pharm. Biotechnol.* 11, 2–14. doi: 10.2174/138920110790725311

Gill, J. J., Summer, E. J., Russell, W. K., Cologna, S. M., Carlile, T. M., Fuller, A. C., et al. (2011). Genomes and characterization of phages Bcep22 and BcepIL02, founders of a novel phage type in *Burkholderia cenocepacia*. *J. Bacteriol.* 193, 5300–5313. doi: 10.1128/JB.05287-5211

Golomidova, A. K., Kulikov, E. E., Prokhorov, N. S., Guerrero-Ferreira Rcapital, Es, C., Knirel, Y. A., et al. (2016). Branched lateral tail fiber organization in T5-Like bacteriophages DT57C and DT571/2 is revealed by genetic and functional analysis. *Viruses* 8:26. doi: 10.3390/v8010026

Goodridge, L. D., and Bisha, B. (2011). Phage-based biocontrol strategies to reduce foodborne pathogens in foods. *Bacteriophage* 1, 130–137. doi: 10.4161/bact.1.3.17629

Gragg, S. E., Loneragan, G. H., Brashears, M. M., Arthur, T. M., Bosilevac, J. M., Kalchayanand, N., et al. (2013). Cross-sectional study examining *Salmonella enterica* carriage in subiliac lymph nodes of cull and feedlot cattle at harvest. *Foodborne Pathog Dis.* 10, 368–374. doi: 10.1089/fpd.2012.1275

Grant, A., Parveen, S., Schwarz, J., Hashem, F., and Vimini, B. (2017). Reduction of *Salmonella* in ground chicken using a bacteriophage. *Poult. Sci.* 96, 2845–2852. doi: 10.3382/ps/pex062

Harris, D. L. (2000). *Reduction of Salmonella by bacteriophage Treatment – NPB # 99-230 The Effect of Bacteriophage Treatment as an Intervention Strategy to Reduce the Rapid Dissemination of Salmonella typhimurium in Experimentally Infected Pigs*. Ames, IA: Iowa State University.

Heller, K., and Braun, V. (1982). Polymannose O-antigens of *Escherichia coli*, the binding sites for the reversible adsorption of bacteriophage T5+ via the L-shaped tail fibers. *J. Virol.* 41, 222–227. doi: 10.1128/jvi.41.1.222-227.1982

Hendrix, R. W., Ko, C. C., Jacobs-Sera, D., Hatfull, G. F., Erhardt, M., Hughes, K. T., et al. (2015). Genome sequence of *Salmonella* phage chi. *Genome Announc.* 3:e01229-14. doi: 10.1128/genomeA.01229-1214

Henry, M., Lavigne, R., and Debarbieux, L. (2013). Predicting in vivo efficacy to guide the choice of therapeutic bacteriophages to treat pulmonary infections. *Antimicrob Agents Chemother.* 57, 5961–5968. doi: 10.1128/AAC.01596-1513

Hua, J., Huet, A., Lopez, C. A., Toropova, K., Pope, W. H., Duda, R. L., et al. (2017). Capsids and genomes of jumbo-sized bacteriophages reveal the evolutionary reach of the HK97 Fold. *mBio* 8:e01579-17. doi: 10.1128/mBio.01579-1517

Hungaro, H. M., Mendonça, R. C. S., Gouvêa, D. M., Vanetti, M. C. D., and Pinto, C. L. D. O. (2013). Use of bacteriophages to reduce *Salmonella* in chicken skin in comparison with chemical agents. *Food Res. Int.* 52, 75–81. doi: 10.1016/j.foodres.2013.02.032

Islam, M. S., Zhou, Y., Liang, L., Nime, I., Yan, T., Willias, S. P., et al. (2020). Application of a broad range lytic phage LPST94 for biological control of *Salmonella* in Foods. *Microorganisms* 8:247. doi: 10.3390/microorganisms8020247

Jones, P., Binns, D., Chang, H. Y., Fraser, M., Li, W., McAnulla, C., et al. (2014). InterProScan 5: genome-scale protein function classification. *Bioinformatics* 30, 1236–1240. doi: 10.1093/bioinformatics/btu031

Khan Mirzaei, M., and Nilsson, A. S. (2015). Isolation of phages for phage therapy: a comparison of spot tests and efficiency of plating analyses for determination of host range and efficacy. *PLoS One* 10:e0118557. doi: 10.1371/journal.pone.0118557

Labrie, S. J., Samson, J. E., and Moineau, S. (2010). Bacteriophage resistance mechanisms. *Nat. Rev. Microbiol.* 8, 317–327. doi: 10.1038/nrmicro2315

Laslett, D., and Canback, B. (2004). ARAGORN, a program to detect tRNA genes and tmRNA genes in nucleotide sequences. *Nucleic Acids Res.* 32, 11–16. doi: 10.1093/nar/gkh152

Laufer, A. S., Grass, J., Holt, K., Whichard, J. M., Griffin, P. M., and Gould, L. H. (2015). Outbreaks of *Salmonella* infections attributed to beef – United States, 1973-2011. *Epidemiol. Infect.* 143, 2003–2013. doi: 10.1017/S0950268814003112

Leavitt, J. C., Heitkamp, A. J., Bhattacharjee, A. S., Gilcrease, E. B., and Casjens, S. R. (2017). Genome sequence of *Escherichia coli* tailed phage utah. *Genome Announc.* 5:e01494-16. doi: 10.1128/genomeA.01494-1416

Lee, E., Helt, G. A., Reese, J. T., Munoz-Torres, M. C., Childers, C. P., Buels, R. M., et al. (2013). Web Apollo: a web-based genomic annotation editing platform. *Genome Biol.* 14:R93. doi: 10.1186/gb-2013-14-8-r93

Lin, H., Paff, M. L., Molineux, I. J., and Bull, J. J. (2017). Therapeutic application of phage capsule depolymerases against K1, K5, and K30 capsulated *E. coli* in mice. *Front. Microbiol.* 8:2257. doi: 10.3389/fmicb.2017.02257

Lindberg, A. A. (1973). Bacteriophage receptors. *Annu. Rev. Microbiol.* 27, 205–241. doi: 10.1146/annurev.mi.27.100173.001225

Lindberg, H. M., McKean, K. A., and Wang, I.-N. (2014). Phage fitness may help predict phage therapy efficacy. *Bacteriophage* 4:e964081. doi: 10.4161/21597073.2014.964081

Mesyanzhinov, V. V., Robben, J., Grymonprez, B., Kostyuchenko, V. A., Bourkaltseva, M. V., Sykilinda, N. N., et al. (2002). The genome of bacteriophage phiKZ of *Pseudomonas aeruginosa*. *J. Mol. Biol.* 317, 1–19.

Meynell, E. W. (1961). A phage, phi chi, which attacks motile bacteria. *J. Gen. Microbiol.* 25, 253–290. doi: 10.1099/00221287-25-2-253

Mondigler, M., Ayoub, A. T., and Heller, K. J. (2006). The DNA region of phage BF23 encoding receptor binding protein and receptor blocking lipoprotein lacks homology to the corresponding region of closely related phage T5. *J. Basic Microbiol.* 46, 116–125. doi: 10.1002/jobm.200510047

Mushtaq, N., Redpath, M. B., Luzio, J. P., and Taylor, P. W. (2004). Prevention and cure of systemic *Escherichia coli* K1 infection by modification of the bacterial phenotype. *Antimicrob. Agents Chemother.* 48, 1503–1508. doi: 10.1128/aac.48.5.1503-1508.2004

Nickelson, K. J., Taylor, T. M., Griffin, D. B., Savell, J. W., Gehring, K. B., and Arnold, A. N. (2019). Assessment of *Salmonella* prevalence in lymph nodes of U.S. and mexican cattle presented for slaughter in Texas. *J. Food Prot.* 82, 310–315. doi: 10.4315/0362-028X.JFP-18-288

Nilsson, A. S. (2014). Phage therapy-constraints and possibilities. *Upsala J. Med. Sci.* 119, 192–198. doi: 10.3109/03009734.2014.902878

Noguchi, H., Taniguchi, T., and Itoh, T. (2008). MetaGeneAnnotator: detecting species-specific patterns of ribosomal binding site for precise gene prediction in anonymous prokaryotic and phage genomes. *DNA Res.* 15, 387–396. doi: 10.1093/dnares/dsn027

Olafson, P. U., Brown, T. R., Lohmeyer, K. H., Harvey, R. B., Nisbet, D. J., Loneragan, G. H., et al. (2016). Assessing transmission of *Salmonella* to bovine peripheral lymph nodes upon horn fly feeding. *J. Food Prot.* 79, 1135–1142. doi: 10.4315/0362-028x.Jfp-15-414

Payne, R. J., and Jansen, V. A. (2001). Understanding bacteriophage therapy as a density-dependent kinetic process. *J. Theor. Biol.* 208, 37–48. doi: 10.1006/jtbi.2000.2198

Piya, D., Vara, L., Russell, W. K., Young, R., and Gill, J. J. (2017). The multicomponent antirestriction system of phage P1 is linked to capsid morphogenesis. *Mol. Microbiol.* 105, 399–412. doi: 10.1111/mmi.13705

Pullinger, G. D., Paulin, S. M., Charleston, B., Watson, P. R., Bowen, A. J., Dziva, F., et al. (2007). Systemic translocation of *Salmonella enterica* serovar Dublin in cattle occurs predominantly via efferent lymphatics in a cell-free niche and requires type III secretion system 1 (T3SS-1) but not T3SS-2. *Infect. Immun.* 75, 5191–5199. doi: 10.1128/IAI.00784-787

Redman, J. A., Grant, S. B., Olson, T. M., Adkins, J. M., Jackson, J. L., Castillo, M. S., et al. (1999). Physicochemical mechanisms responsible for the filtration and mobilization of a filamentous bacteriophage in quartz sand. *Water Res.* 33, 43–52. doi: 10.1016/S0043-1354(98)00194-198

Roach, D. R., and Debarbrieux, L. (2017). Phage therapy: awakening a sleeping giant. *Emerg. Top. Life Sci.* 1, 93–103. doi: 10.1042/ETLS20170002

Scallan, E., Hoekstra, R. M., Angulo, F. J., Tauxe, R. V., Widdowson, M. A., Roy, S. L., et al. (2011). Foodborne illness acquired in the united states-major pathogens. *Emerg. Infect. Dis.* 17, 7–15. doi: 10.3201/Eid1701.P11101

Schade, S., and Adler, J. (1967). Purification and chemistry of bacteriophage chi. *J. Virol.* 1, 591–598. doi: 10.1128/jvi.1.3.591-598.1967

Schneider, C. A., Rasband, W. S., and Eliceiri, K. W. (2012). NIH Image to ImageJ: 25 years of image analysis. *Nat. Methods* 9, 671–675. doi: 10.1038/nmeth.2089

Shen, S., and Fang, F. C. (2012). Integrated stress responses in *Salmonella*. *Int. J. Food Microbiol.* 152, 75–81. doi: 10.1016/j.ijfoodmicro.2011.04.017

Sillankorva, S. M., Oliveira, H., and Azeredo, J. (2012). Bacteriophages and their role in food safety. *Int. J. Microbiol.* 2012:863945. doi: 10.1155/2012/863945

Sulakvelidze, A. (2011). Safety by nature: potential bacteriophage applications. *Microb Magazine* 6, 122–126. doi: 10.1128/microbe.6.122.1

Switt, A. I., den Bakker, H. C., Vongkamjan, K., Hoelzer, K., Warnick, L. D., Cummings, K. J., et al. (2013). *Salmonella* bacteriophage diversity reflects host diversity on dairy farms. *Food Microbiol.* 36, 275–285. doi: 10.1016/j.fm.2013.06.014

Valentine, R. C., Shapiro, B. M., and Stadtman, E. R. (1968). Regulation of glutamine synthetase. XII. electron microscopy of the enzyme from *Escherichia coli*. *Biochemistry* 7, 2143–2152. doi: 10.1021/bi00846a017

Villarreal-Silva, M., Genho, D. P., Ilhak, I., Lucia, L. M., Dickson, J. S., Gehring, K. B., et al. (2016). Tracing surrogates for enteric pathogens inoculated on hide through the beef harvesting process. *J. Food Prot.* 79, 1860–1867. doi: 10.4315/0362-028X.JFP-15-481

Wang, J., Jiang, Y., Vincent, M., Sun, Y., Yu, H., Wang, J., et al. (2005). Complete genome sequence of bacteriophage T5. *Virology* 332, 45–65. doi: 10.1016/j.virol.2004.10.049

Xie, Y., Savell, J. W., Arnold, A. N., Gehring, K. B., Gill, J. J., and Taylor, T. M. (2016). Prevalence and characterization of *Salmonella enterica* and *Salmonella* bacteriophages recovered from beef cattle feedlots in South Texas. *J. Food Prot.* 79, 1332–1340. doi: 10.4315/0362-028X.JFP-15-526

Xie, Y., Wahab, L., and Gill, J. J. (2018). Development and validation of a microtiter plate-based assay for determination of bacteriophage host range and virulence. *Viruses* 10:189. doi: 10.3390/v10040189

Yoichi, M., Abe, M., Miyanaga, K., Unno, H., and Tanji, Y. (2005). Alteration of tail fiber protein gp38 enables T2 phage to infect *Escherichia coli* O157:H7. *J. Biotechnol.* 115, 101–107. doi: 10.1016/j.jbiotec.2004.08.003

Yuan, Y., and Gao, M. (2017). Jumbo bacteriophages: an overview. *Front. Microbiol.* 8:403. doi: 10.3389/fmicb.2017.00403

Zeng, C., Gilcrease, E. B., Hendrix, R. W., Xie, Y., Jalfon, M. J., Gill, J. J., et al. (2019). DNA packaging and genomics of the *Salmonella* 9NA-Like phages. *J. Virol.* 93:e00848-19. doi: 10.1128/JVI.00848-819

Zimmermann, L., Stephens, A., Nam, S. Z., Rau, D., Kubler, J., Lozajic, M., et al. (2018). A completely reimplemented MPI bioinformatics toolkit with a new HHpred server at its core. *J. Mol. Biol.* 430, 2237–2243. doi: 10.1016/j.jmb.2017.12.007

Conflict of Interest: JG consultant, Merck & Co. (June 2019); Member, Scientific Advisory Board, Deerland Enzymes Inc. YX currently employed at Bio-Rad, Hercules, CA.

The remaining authors declare that the research was conducted in the absence of any commercial or financial relationships that could be construed as a potential conflict of interest.

frontiers in Microbiology

ORIGINAL RESEARCH
published: 30 June 2021
doi: 10.3389/fmicb.2021.653501

First Molecular Characterization of *Siphoviridae*-Like Bacteriophages Infecting *Staphylococcus hyicus* in a Case of Exudative Epidermitis

Julia Tetens[1†], *Sabrina Sprotte*[2†], *Georg Thimm*[1], *Natalia Wagner*[2], *Erik Brinks*[2], *Horst Neve*[2], *Christina Susanne Hölzel*[1*‡] and *Charles M. A. P. Franz*[2‡]

[1] *Institute of Animal Breeding and Husbandry, Kiel University, Kiel, Germany,* [2] *Department of Microbiology and Biotechnology, Max Rubner-Institut, Federal Research Institute of Nutrition and Food, Kiel, Germany*

OPEN ACCESS

Edited by:
Krishna Mohan Poluri, Indian Institute of Technology Roorkee, India

Reviewed by:
Sandra Patricia Morales, Independent Researcher, Sydney, NSW, Australia
Jason Gill, Texas A&M University, United States

***Correspondence:**
Christina Susanne Hölzel
choelzel@tierzucht.uni-kiel.de

†*These authors share first authorship*

‡*These authors share last authorship*

Specialty section:
This article was submitted to Virology, a section of the journal Frontiers in Microbiology

Received: *14 January 2021*
Accepted: *19 May 2021*
Published: *30 June 2021*

Citation:
Tetens J, Sprotte S, Thimm G, Wagner N, Brinks E, Neve H, Hölzel CS and Franz CMAP (2021) First Molecular Characterization of Siphoviridae-Like Bacteriophages Infecting Staphylococcus hyicus in a Case of Exudative Epidermitis. Front. Microbiol. 12:653501. doi: 10.3389/fmicb.2021.653501

Exudative epidermitis (EE), also known as greasy pig disease, is one of the most frequent skin diseases affecting piglets. Zoonotic infections in human occur. EE is primarily caused by virulent strains of *Staphylococcus* (*S.*) *hyicus*. Generally, antibiotic treatment of this pathogen is prone to decreasing success, due to the incremental development of multiple resistances of bacteria against antibiotics. Once approved, bacteriophages might offer interesting alternatives for environmental sanitation or individualized treatment, subject to the absence of virulence and antimicrobial resistance genes. However, genetic characterization of bacteriophages for *S. hyicus* has, so far, been missing. Therefore, we investigated a piglet raising farm with a stock problem due to EE. We isolated eleven phages from the environment and wash water of piglets diagnosed with the causative agent of EE, i.e., *S. hyicus*. The phages were morphologically characterized by electron microscopy, where they appeared *Siphoviridae*-like. The genomes of two phages were sequenced on a MiSeq instrument (Illumina), resulting in the identification of a new virulent phage, PITT-1 (PMBT8), and a temperate phage, PITT-5 (PMBT9). Sequencing of three host bacteria (*S. hyicus*) from one single farm revealed the presence of two different strains with genes coding for two different exfoliative toxin genes, i.e., *exh*A (2 strains) and *exh*C (1 strain). The *exh*C-positive *S. hyicus* strain was only weakly lysed by most lytic phages. The occurrence of different virulent *S. hyicus* strains in the same outbreak limits the prospects for successful phage treatment and argues for the simultaneous use of multiple and different phages attacking the same host.

Keywords: bacteriophages, *Staphylococcus hyicus*, *Siphoviridae*-like, exudative epidermitis, pig

INTRODUCTION

Greasy pig disease, also known as exudative epidermitis, is a common skin disease in young piglets and weaners causing significant morbidity and mortality in naïve herds. The main cause of this disease are pathogenic strains of *Staphylococcus* (*S.*) *hyicus* that produce exfoliative toxins (Foster, 2012). *S. hyicus* is part of the commensal skin microbiome of healthy pigs (Nagase et al., 2002). Virulence is closely associated with the production of exfoliative toxins

that target the cells of the *Stratum spinosum* in the epidermis (Nishifuji et al., 2008). Originally, six exfoliative toxins (ExhA, ExhB, ExhC, ExhD, SHETA, and SHETB) were described (Sato et al., 2000; Ahrens and Andresen, 2004) and recently a new exfoliative toxin (ExhE) has additionally been characterized (Imanishi et al., 2019). Although *S. hyicus* can directly penetrate the skin, skin lesions—resulting for example from biting—are primarily the starting point of greasy pig disease (Frana and Hau, 2019). Diseased piglets show skin lesions at first on the head and on hairless skin of the medial aspect of legs (Andrews, 1979). Lesions can progress to cover the whole body with a greasy brown exudate that may lead to dehydration and animal death (Foster, 2012). Antibiotics are regularly used for treatment, but the presence of *S. hyicus* isolates that exhibit broad-spectrum resistance to antimicrobials have been increasingly reported (Aarestrup and Jensen, 2002; Futagawa-Saito et al., 2009; Park et al., 2013b). This is alarming not only from a veterinary, but also from a One Health perspective and requires alternative strategies for therapy as well as prevention. To protect piglets from this disease, vaccination of gestating sows using attenuated strains isolated from the affected herd is a common practice. Nevertheless, this autogenous vaccination is apparently not able to protect all piglets against greasy pig disease. Furthermore, scientific evidence for the efficacy of autogenous vaccines against *S. hyicus*, as described at least once by Arsenakis et al. (2018), is scarce.

Bacteriophages (phages), defined as viruses that infect and kill bacteria, might offer an alternative opportunity for prevention and therapy of diseases (Gigante and Atterbury, 2019). Virulent or lytic phages bind to specific receptors on the bacterial cell surface, inject their genetic material and then hijack the bacterial replication machinery to produce the next generation of phage progeny and subsequently lyse the host cell (Howard-Varona et al., 2017). Temperate phages, on the other hand, do not primarily produce phage progeny and lysis of host cells, as they integrate their genetic material into the bacterial genome and reproduce their genome passively (vertically) from mother to daughter bacterial cells (Salmond and Fineran, 2015). Compared with antibiotics, the risk to develop phage resistance is much lower, as phages may overcome mutations in bacteria that lead to resistance mechanisms (Labrie et al., 2010). In general, phages reveal high specificity. Thus, phages only kill target bacterial species or even strains (Rakhuba et al., 2010) but do not destroy the host's commensal microbiota. In reverse conclusion, this implies a need to extensively screen for an effective phage for every pathogen considered (Rohde et al., 2018).

In this study, we investigated a piglet raising farm with greasy pig disease as a stock problem in order to isolate, identify and characterize bacteriophages for *S. hyicus*. To our knowledge, this is the first attempt to characterize bacteriophages for *S. hyicus* using molecular biological methods.

METHODS, TECHNIQUES

Sample Collection

Isolation and Selection of *Staphylococcus hyicus*

Samples were scraped from the skins of 25 weaners (42–63 days of age and 19–26 kg of body weight) which showed typical clinical signs of greasy pig disease using sterile cotton swabs. All swabs were directly streaked out on Columbia blood agar (7% sheep blood; Oxoid, Wesel, Germany) and incubated at 37°C for 24 h.

Phage Isolation

Five different environmental samples were collected on the farm in parallel with sampling for *S. hyicus*. Two of these samples were liquid pig manure originating from two different pig houses on the corresponding farm. Another sample originated from washing water of a heavily infected piglet and a further sample originated from wastewater of a slatted floor. The last sample was a combination of washing water of an infected piglet and wastewater of a slatted floor. Two hundred and fifty milliliter of all five environmental samples were first centrifuged (14,300 × *g*, 15 min, 4°C) and then filtered through a 0.45 μm membrane filter (Filtropur S, Sarstedt, Nürnbrecht, Germany). A 5 ml aliquot filtrate of each of the five environmental samples was mixed with 100 μl $CaCl_2$ (1 M) and 100 μl of a fresh overnight culture of the host bacterium *S. hyicus* (described in Isolation and Selection of *Staphylococcus hyicus* & Bacteriological Investigations). The mixture was incubated overnight at 37°C, then centrifuged at 18,000 × *g* for 15 min to remove residual bacterial cells. The supernatant was filtered again using a 0.45 μm membrane filter.

Bacteriological Investigations

Identification of *S. hyicus*

Colonies were picked from Columbia blood agar and incubated on Baird-Parker and Chocolate agar (Oxoid) at 37°C for 24 h. Isolates suspected as *S. hyicus* on the basis of hemolytic reaction on Chocolate agar and typical growth on Baird-Parker-agar (i.e., black, shiny, convex colonies, lack of clear zones, no precipitation), were chosen for Gram-staining and basic biochemical standard tests (i.e., catalase-test, oxidase-test, clumping-factor test). Five strains presenting Gram-positive, catalase-positive, oxidase-negative, clumping-factor- and coagulase-negative cocci were chosen for species confirmation PCR.

Antibiotic Susceptibility Tests

All five *S. hyicus* strains were tested for cefoxitin-resistance using disk diffusion in order to indicate a methicillin-resistant phenotype. Disk diffusion tests were performed according to EUCAST instructions (http://www.eucast.org). Strains were suspended in 0.9% NaCl solution at a density equivalent to a 0.5 McFarland standard and spread in dense lines in two rectangular and one diagonal layer on Mueller-Hinton agar plates using sterile cotton swabs (Oxoid, Wesel, Germany). Antibiotic disks containing cefoxitin (30 μg) were loaded onto the plates. After incubation for 18 h, the inhibition zone diameters were measured upon inspection against a dark background illuminated with reflected light. Zone diameters were interpreted based on EUCAST breakpoints for *Staphylococcus* spp.

Phage Isolation and Characterization

Spot Testing

To determine the presence of phages, spot tests were performed with all five filtrates and five PCR-confirmed *S. hyicus* strains using the double-layer agar method. In detail, 300 μl of a fresh

overnight culture of each *S. hyicus* strain were mixed with 100 µl of 40 mM $CaCl_2$ and 3 ml of Caso-soft agar [Caso broth with 0.7% (w/w) agar] held at 50°C and immediately poured onto plate count agar. After the solidification of the soft agar, 100 µl of each filtrate, respectively, was spotted in the middle of the plate on the bacterial lawn and all 25 plates were incubated at 37°C for 24 h. After incubation, plates were observed for the presence of lysis zones. When lysis zones appeared, they were carefully scraped off and resuspended in 4 mL of SM-buffer [0.58% NaCl, 0.25% $MgSO_4 \times 7H_2O$, 0.24% Tris-HCl (pH 7.4)] for 24 h. Afterwards, the suspension was vortexed and again sterile filtered and stored at 4°C.

Plaque Testing

For isolation and purification of bacteriophages, a plaque assay (i.e., double-layer agar method) was performed. For this, 10-fold serial dilutions of the phage filtrates were produced. Subsequently, 100 µl of each of the phage dilutions 10^{-2}, 10^{-4}, 10^{-6}, and 10^{-8} were mixed with 300 µl of a fresh overnight culture of the corresponding host bacterium, 100 µl 40 mM $CaCl_2$ and 3 ml of Caso-soft agar held at 50°C and immediately poured onto a plate-count agar plate. After solidification, the soft agar plates were incubated at 37°C for 24 h. Plaques showing different morphologies were picked and pure phage isolates were obtained through three successive single plaque isolation steps.

Transmission Electron Microscopy

Phage lysates were first dialyzed for 20 min against modified SM-buffer [20 mM Tris-HCl (pH 7.2), 10 mM NaCl, 20 mM $MgSO_4$]. Dialysed phages were adsorbed for 20 min to ultrathin carbon films. After a 20-min fixation with 1% glutaraldehyde and subsequent negative staining with 2% (wt/vol) uranyl acetate, transmission electron microscopy was performed at an accelerating voltage of 80 kV (Tecnai 10; FEI Thermo Fisher Scientific, Eindhoven, The Netherlands). Micrographs were captured with a MegaView G2 CCD camera (Emsis, Muenster, Germany).

Host Range

The host range and EOP values of phages PITT 1–PITT 11 were determined for various *S. hyicus* and *S. aureus* isolates from this study, using the plaque assay as described above. In addition, *S. hyicus*, *S. epidermidis*, and *S. aureus* strains from our own bacterial culture collections and the German Collection of Microorganisms and Cell Cultures (DSMZ, Braunschweig, Germany) were included (DSM 17421, DSM 20459, L2-82, L2-92, L2-93, and L2-152 = DSM 1798; L2-246, L2-248 = DSM 105272, respectively). Strains from our own bacterial culture collections were identified either by MALDI-TOF-MS or 16S-amplicon-sequencing (*S. epidermidis*, primer pair *27F*: AGRGTTYGAT YMTGGCTCAG and *1492R*: RGYTACCTTGTTACGACTT). The plaque assay was used to determine the number of plaques produced on the lawns of susceptible *Staphylococcus* strains. The EOP value represents the ratio of plaques obtained with the susceptible test strain when compared to plaques obtained with the isolation strain. All experiments were done in duplicate.

MOLECULAR BIOLOGICAL METHODS

DNA-Extraction Methods

DNA Extraction for Species-Specific PCR

For species-specific PCR, bacterial DNA was extracted by means of a simple lysostaphin-proteinase K-boiling-protocol: from a pure culture of *S. hyicus*, three colonies were picked, suspended in 0.5 ml TE-buffer plus 0.25 ml of lysostaphin and incubated for 1 h at 37°C. After adding 10 µl proteinase K, the suspension was incubated again for 2 h at 56°C. Finally, the suspension was boiled (100°C) for 10 min and was put immediately on ice for 2 min. The suspension was centrifuged at 13,000 × *g* for 3 min and 1 µl of the supernatant was used in the PCR reaction.

DNA Extraction for Genome Sequencing of Bacteria

Bacterial DNA for genome sequencing was extracted from early log-phase cultures after 3 h of incubation at 37°C as follows: suspensions were centrifuged 1 min at 16,000 × *g*, the pellet was resuspended in 200 µl Caso broth, transferred to a ZR BashingBead™ Lysis Tube (Zymo Research, Freiburg, Germany) and homogenized in a Precellys 24 device (Bertin Technologies). DNA was then extracted using the Quick-DNA™ Fungal/Bacterial Miniprep Kit (Zymo Research) according to the manufacturer's protocol.

DNA Extraction From Bacteriophages

For DNA extraction, the Quick-DNA™ Fungal/Bacterial Miniprep Kit was used with some modifications: Several agar plates with phage-derived, confluent lysis were prepared and treated as follows: Plates were floated with 5 ml of SM-buffer and incubated for 3 h at room temperature on an orbital shaker (100 rpm). Next, the buffer-phage suspension was pipetted into two 2-ml tubes, which were centrifuged for 3 min at 8,000 × *g*. After filtration (0.45 µm), the supernatant was centrifuged again for 2.5 h at 14,000 × *g* at 4°C. Pellets were resuspended in 200 µl of SM buffer. RNase and DNase (20 µg ml^{-1} each), respectively, were added for over-night incubation at 37°C. Inactivation of the enzymes was performed for 5 min at 75°C. One milliliter lysis solution from the DNA isolation kit was added and mixed thoroughly for 10 s. Proteinase K was then added at a final concentration of 80 µg ml^{-1} and the sample was incubated first for 30 min at 55°C, then at 65°C for 15 min while inverting the sample 2–3 times. Following this, the sample was mixed with 640 µl isopropanol and loaded onto a DNA-binding column from the kit. For all subsequent steps, the protocol of the manufacturer was followed. Finally, DNA amounts were quantified using a Qubit 3 fluorometer (Invitrogen, Darmstadt, Germany).

Species-Specific PCR (*S. hyicus*)

Presumptive strains were confirmed as *S. hyicus* by PCR as described by Voytenko et al. (2006), using primers for the *sod*A gene and two primers for the spacer region between the genes that code for 16S rRNA and 23S rRNA (one specific for *S. hyicus*, one specific for the genus *Staphylococcus*).

RAPD-PCR

RAPD-PCR was performed as described elsewhere (Gutiérrez et al., 2011) using random OPL5-primer (5′-ACGCAGGCAC-3′)

and phage DNA concentrations of 10 ng per PCR-reaction. PCR-conditions were 4 cycles at 94/20/72°C (45/120/60 s), followed by 26 cycles at 94/36/72°C [5/30 plus (n_{cycle} minus 1), 30 s] and a final elongation at 75°C for 7 min. PCR products were transferred to a 0.8% agarose-gel and separated at 100 V for 55 min.

Genome Sequencing and Analysis

Phage DNA was sequenced to characterize the phages with respect to their lytic or temperate life cycle. Genomes of host bacterial strains were sequenced in order to assess their clonal identity and to determine which exfoliative toxin genes were present. Phage DNA was extracted and DNA-concentration was confirmed to be at least 50 ng μl^{-1} using a Qubit 3 fluorometer (Invitrogen, Darmstadt, Germany). The genome was sheared into 450 bp fragments using a Covaris M220 Focused-Ultrasonicator (Covaris, INC, Massachusetts, USA) and the phage DNA library was prepared using a TruSeq Nano DNA LT Library Prep Kit. The MiSeq Reagent Nano Kit v2 (500 cycles) (Illumina, Munich, Germany) was used for sequencing on a MiSeq high throughput sequencer (Illumina). The same library preparation procedure was used for sequencing the bacterial genomes, however, for sequencing these on a MiSeq high throughput sequencer, the MiSeq Reagent Kit v3 (600 cycles) (Illumina) was used. Both sequencing runs produced 2 × 250 bp paired-end reads, which were *de novo* assembled with PATRIC Version 3.5.41 (Wattam et al., 2017). Open reading frames (ORFs) were automatically predicted by PATRIC and afterwards manually analyzed for their putative functions with BLASTP (Altschul et al., 1990) and SMART (Letunic and Bork, 2018). Phage genomes were screened for tRNA-encoding genes with tRNAscan-SE v. 2.0 (Lowe and Chan, 2016) and for acquired virulence and antibiotic resistance genes using ResFinder 4.0 (Bortolaia et al., 2020). Genomes were visualized using Geneious Version 9.1.8 (Kearse et al., 2012). SNP analysis of the bacterial genomes was conducted using CSI Phylogeny 1.4 (Kaas et al., 2014). *S. hyicus* strain ATCC 11249, the closest relative according to BLAST, was used as reference genome. Furthermore the bacterial genomes were analyzed for the presence of exfoliative toxin genes *exh*A, *exh*B, *exh*C and *exh*D using Geneious and primer sequences reported in Ahrens and Andresen (2004). The toxin gene amplicons were compared to the complete gene sequences deposited with the following GenBank accession numbers: ExhA (AF515453); ExhB (AF515454); ExhC (AF515455); and ExhD (AF515456) (Ahrens and Andresen, 2004).

RESULTS

Isolation of Bacteria

Samples from 23 of the 25 weaners yielded presumptive *S. hyicus* isolates with typical reactions and characteristic morphology on chocolate agar. Further investigations were performed with five strains from five pigs kept in two different houses and four different compartments. These isolates (07/2 4A, 07/12 1A, 07/12 2A, 83/7 1B, 83/11 1A) were confirmed as *S. hyicus* by species specific PCR. The disk diffusion assay indicated susceptibility for cefoxitin and thus the absence of a methicillin-resistant phenotype.

Phage Isolation and Morphology

Liquid pig manure samples failed to result in positive spot tests with phage-derived lysis zones. By contrast, all three samples of rinsing water, which were collected from the slatted floor and/or diseased animals, yielded positive spot test results, visible as phage lysis zones.

From seven plates with clear lysis spots, all lysate dilutions (1:100) up to 10^{-6} yielded clear plaques. Two weakly positive reactions (sample C with 07/12 1A and sample C with 07/12 2A) could not be confirmed by plaque assays. Most plaques revealed similar morphology, but finally 11 different plaques with different morphologies could be selected for further investigation (**Table 1**).

Based on EOP-analysis, phages showed different lytic activities (**Table 2**). Phages PITT-4 and PITT-5 lysed only their primary host, while PITT-7 had the broadest host range, efficiently lysing 6 out of 7 strains. PITT-6, PITT-10, and PITT-11 lysed 5 out of 7 strains. Only PITT-6 and PITT-7 were able to lyse *S. hyicus* DSM 17421, while only PITT-7, PITT-10, PITT-11 were able to lyse *S. hyicus* DSM 20459. However, it should be noted that the EOP values were significantly reduced when the titers of these phages were determined on non-host strains (**Table 2**). Phage isolates had neither activity against *S. aureus* DSM 105272 nor against *S. aureus* field strains from bovine udders.

The case isolates of *S. hyicus* differed in their host properties: isolate 07/2-4A, 07/12-2A, and 83/11-1A were very efficiently lysed by most phages except PITT-4 and PITT-5. By contrast, 83/7-1B was not lysed by PITT-2, PITT-3, and PITT-9 and weakly lysed by all other phages except PITT-4 and PITT-5, which were isolated with 83/7-1B as the primary host. One of the isolates, 07/12-1A was resistant against all tested phages (**Table 2**). Host range was independent from the place of isolation: Phages isolated in one house showed good lytic activity against bacterial strains from the other house. The multispecies phage Twort (DSM 17442) had weak lytic activity for its *S. hyicus* host strain DSM 17421 (offered by the DSMZ for propagation), but no lytic activity in the DSM type strain or any of the field strains from this study (data not shown).

Transmission Electron Microscopy

By transmission electron microscopy, two different morphological groups of *Siphoviridae* phages could be distinguished (**Figure 1**). Nine phages (PITT-1-3 & 6-11) exhibit large isometric heads (diameter: 69–74 nm) and long, flexible tails (length: 323–346 nm). A notably thin tail fiber (length: 76–86 nm) is also visible under the distal end of the tail of phages PITT-1, 2, and PITT-7-11 (see arrows in **Figures 1a–c,f,g**). A unique morphological characteristic of phage PITT-6 is the presence of a distinct collar (i.e., neck passage structure) beneath the capsid (see asterisk in **Figure 1f**).

The second morphotype is represented by phages PITT-4 and PITT-5 (**Figures 1d,e**). These two *Siphoviridae* phages have smaller isometric heads (diameter: 59 nm) and shorter (147–160 nm) tails terminating with remarkably large and complex baseplate structures which are composed of a smaller upper

TABLE 1 | Origin of the *S. hyicus* phages and host strains used for isolation.

Combination		Rinsing water from		
		House 1		House 2
		A (slatted floor)	B (diseased pig)	C (slatted floor + diseased pig)
Bacterial isolate used for primary enrichment	**07/2-4A**	–#	**PITT-1 (PMBT8)**	–
	07/12-1A	–	–	No plaque*
	07/12-2A	–	PITT-2, PITT-3	No plaque*
	83/7-1B	–	PITT-4	**PITT-5 (PMBT9)**
	83/11-1A	PITT-10, PITT-11	PITT-8, PITT-9	PITT-6, PITT-7

 # "–" Means negative in spot test, plaque test not done.
**Weak lysis zone when spot-tested, not confirmed when plaque-tested.*
*Strains and phages highlighted in **bold** were selected for DNA sequence analysis.*

TABLE 2 | Phage titers (plaque-forming units, pfu/ml) and efficiency of plating (EOP).

		PITT-1	PITT-2	PITT-3	PITT-4	PITT-5	PITT-6	PITT-7	PITT-8	PITT-9	PITT-10	PITT-11
S. hyicus												
DSM 17421	Titer	– (a)	– (a)	– (a)	– (a)	– (a)	1.6×10^6	2.8×10^6	– (a)	– (a)	– (a)	– (a)
	EOP						2.1×10^{-2}	2.8×10^{-2}				
DSM 20459	Titer	– (a)	– (a)	– (a)	– (a)	– (a)	– (a)	2.3×10^6	– (a)	– (a)	1.0×10^5	1.0×10^5
	EOP							2.3×10^{-2}			4.0×10^{-3}	2.4×10^{-3}
07/2-4A	Titer	**1.3×10^7**	2.2×10^4	8.3×10^5	– (a)	– (a)	2.4×10^7	9.4×10^7	6.9×10^7	2.9×10^7	1.5×10^7	5.1×10^7
	EOP	**1**	1.7×10^0	4.9×10^0			3.2×10^{-1}	9.4×10^{-1}	3.8×10^{-1}	4.8×10^{-1}	6.0×10^{-1}	1.2×10^0
07/12-1A	Titer	– (a)	– (a)	– (a)	– (a)	– (a)	– (a)	– (a)	– (a)	– (a)	– (a)	– (a)
	EOP											
07/12-2A	Titer	8.2×10^6	**1.3×10^4**	**1.7×10^5**	– (a)	– (a)	4.8×10^7	9.6×10^7	1.0×10^8	2.9×10^7	3.1×10^6	6.2×10^6
	EOP	6.3×10^{-1}	**1**	**1**			6.3×10^{-1}	9.6×10^{-1}	5.6×10^{-1}	4.8×10^{-1}	1.2×10^{-1}	1.5×10^{-1}
83/7-1B	Titer	1.9×10^3	– (a)	– (a)	**5.5×10^6**	**8.4×10^6**	1.5×10^4	5.9×10^4	1.2×10^3	– (a)	2.8×10^2	1.6×10^3
	EOP	1.5×10^{-4}			**1**	**1**	2.0×10^{-4}	5.9×10^{-4}	6.7×10^{-6}		1.1×10^{-5}	3.8×10^{-5}
83/11-1A	Titer	6.8×10^6	3.8×10^4	7.2×10^5	– (a)	– (a)	**7.6×10^7**	**1.0×10^8**	**1.8×10^8**	**6.1×10^7**	**2.5×10^7**	**4.2×10^7**
	EOP	5.2×10^{-1}	2.9×10^0	4.2×10^0			**1**	**1**	**1**	**1**	**1**	**1**

In bold: Host strain used for phage propagation.
– (a): Limit of detection: <10 pfu/ml.
No plaques were obtained on the following strains: S. epidermidis DSM 1798, S. epidermidis field strain L2– (a)82 (origin: plume), S. aureus DSM 105272, 5 S. aureus field strains (origin: bovine udder).

baseplate disc (open triangles in **Figures 1d,e**) and a larger lower baseplate structure (filled triangles in **Figures 1d,e**). A bundle of short fiber-like appendages is attached below these baseplate discs. For phage PITT-4, phage particles with empty capsids could only be captured (**Figure 1d**).

sharing three other bands. Notably, pattern II phages were only detected in house 1.

Due to differences in morphology and host range we expected the most pronounced differences between phages of pattern III and all other isolates, irrespective of their amplicon pattern. Thus, PITT-1 and PITT-5 were selected for sequencing.

Genetic Diversity of Isolated Phages

RAPD-PCR

RAPD-PCR (**Figure 2**) revealed five different amplicon patterns: I (PITT-1), IIa (PITT-2,3), IIb (PITT-8,9,10,11), III (PITT-4,5), and IV (PITT-6,7). Pattern I was unique for a single phage isolate from house 1. Pattern IIa/b was the most common pattern representing phages from different primary bacterial hosts and samples (A, B). RAPD-patterns IIa (host 07/12-2A) and IIb (host 83/11-1A) differed in presence or absence of one band, while

Sequencing and Comparative Genomic Analysis

The sequence of PITT-1 (PMBT8) resulted in a genome size of 88,129 bp with a mol% GC content of 31.6 and was deposited in the NCBI Genbank under acc. no. MK893987. PITT-5 (PMBT9) had a genome size of 41,624 bp and a mol% GC content of 36.2. Both phage genomes harbored no tRNA-encoding genes (**Figures 3A,B**). Using ResFinder, no acquired antibiotic resistance and virulence genes were identified in phage genomes.

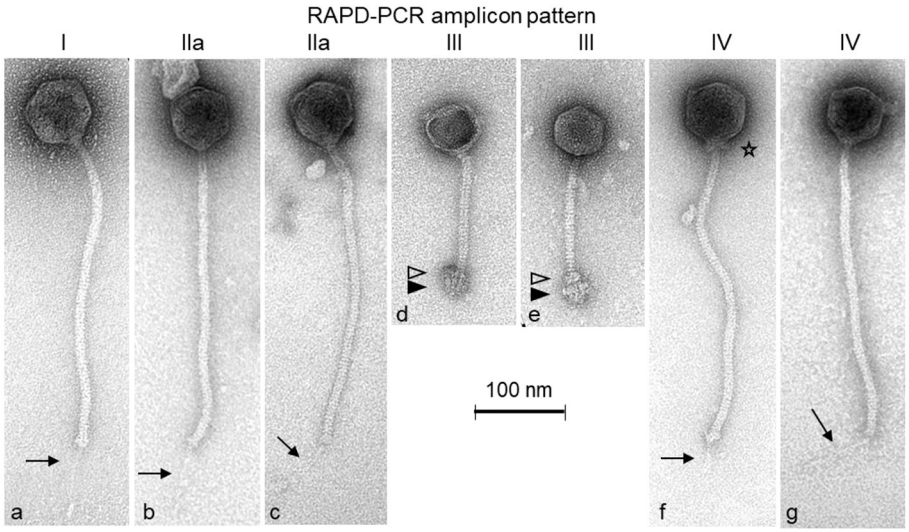

FIGURE 1 | Transmission electron micrographs of the *S. hyicus* phages PITT-1 **(a)**, PITT-2 **(b)**, PITT-3 **(c)**, PITT-4 **(d)**, PITT-5 **(e)**, PITT-6 **(f)**, and PITT-7 **(g)** negatively stained with 2% (w/v) uranyl acetate. Structural details are indicated by arrows (faint distal central tail fibers), by open triangles (upper disc of complex baseplate structure), by filled triangles (lower disc of complex baseplate structure), and by an asterisk (collar/neck passage structure). All micrographs are shown with the same magnification (see 100-nm size reference bar). The RAPD-PCR patterns I, IIa, III-IV (see also **Figure 2**) are indicated on top of the micrographs.

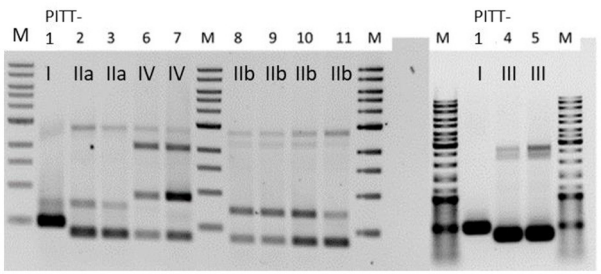

FIGURE 2 | RAPD-patterns of *S. hyicus* phages PITT-1-11. Pattern I and II a/II b were exclusively found in samples from house 1. Pattern III was identified for 2 phages from both houses. The two phages with pattern IV were both detected in samples from house 2. PITT-1 is shown twice.

The 88,129-bp genome of the virulent phage PITT-1 (PMBT8) comprises 122 putative open reading frames (ORFs) with 36 showing an assigned function and 86 hypothetical proteins (**Figure 3A**). An analysis of the PITT-1 genome with NCBI megablast resulted in only low similarities (coverage 8 and 6%; identity 78.99 and 78.92%) to the *S. epidermidis* phages vB_SepS_SEP9 (Melo et al., 2014) and 6ec (Aswani et al., 2014), respectively, which are members of the genus *Sextaecvirus* within the family *Siphoviridae*. Even when using less stringent searching conditions with discontiguous megablast, the coverage increased only to 29 and 32%, respectively, while identity decreased to 71%. With 32 and 71%, similar coverage and identity values were determined when comparing with the *S. aureus* phage VB-SauS-SA genome sequence. The multispecies *Staphylococcus* phage Twort, which can be propagated in *S. hyicus*, had only low similarity, with only 2% query coverage in the discontiguous megablast algorithm.

Protein blast (BLASTP) for assigned structural genes revealed a higher similarity between phage PITT-1 and *S. epidermidis* phages vB_SepS_SEP9 and 6ec, than comparisons based on overall nucleotide analysis. Similarities ranged from low similarities for the tape measure protein, i.e., 99% coverage and 42% identity for phage 6ec, 99% coverage and 41% identity for phage vB_SepS_SEP9, to higher similarities for the head maturation protein, i.e., 98% coverage and 74% identity (phage vB_SepS_SEP9) and 98% coverage and 67% identity (phage 6ec). However, using BLASTP, other proteins showed low similarities with a concurrent lower coverage, i.e., the holin protein which showed an identical coverage of 65% and identity of 45% for both *S. epidermidis* phages (vB_SepS_SEP9 and 6ec). Using BLASTP, no significant similarity was found between the assigned genes of PITT-1 and those of the multispecies *Staphylococcus* phage Twort.

The 41,624-bp genome of phage PITT-5 (PMBT9, deposited in GenBank under acc. MW221967; **Figure 3B**) revealed a moderate similarity to other phages in the databases: 37% coverage and 83.26% identity with the *S. aureus* phage EW, acc. AY954959 (Kwan et al., 2005), which belongs to the genus *Phietavirus* of the *Siphoviridae* phages.

Analysis of the protein sequences of the assigned structural proteins revealed high similarities to protein sequences deduced from the genomes of potential *Staphylococcus* prophages obtained from the databases. Moreover, some structural gene products also showed high similarities to proteins of isolated phages, like the head-tail protein (99% coverage, 90% identity to *Staphylococcus aureus* phage EW) or the capsid and scaffold protein (99% coverage, 95% identity to *Staphylococcus* phage SAP3). However, other structural proteins e.g., the tape-measure protein showed lower similarities (99% coverage, 64% identity to *Staphylococcus* phage IME1365_01, acc. no. KY653129). It

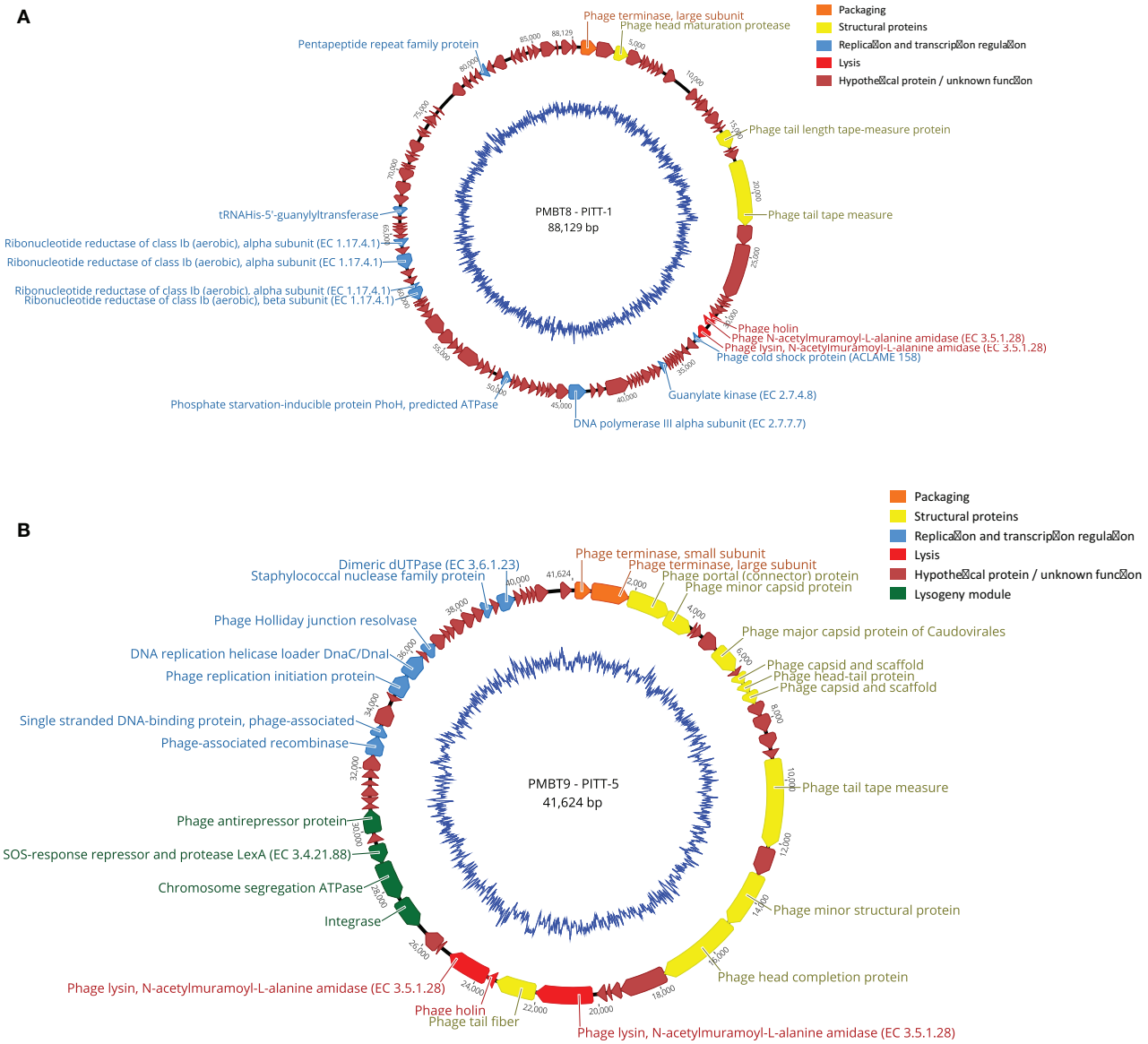

FIGURE 3 | (A,B) Genome map of phages PITT-1 (PMBT8, 88,129 bp, **A**) and PITT-5 (PMBT-9, 41,624 bp, **B**) with structural and functional annotations. An automated annotation was obtained from PATRIC and all ORFs were subsequently manually annotated with BLASTP and SMART. Arrows indicate the predicted ORFs, which are labeled and color-coded based on their predicted function. The genomes are shown starting upstream of ORF1 that specifies the phage terminase large subunit. The ORFs involved in DNA packaging are marked in orange, the ORFs for structural proteins are marked in yellow and the ORF involved in lysis is marked in red. Blue arrows represent ORFs for phage DNA transcription and replication. Hypothetical ORFs and ORFs with no phage-related function are shown in dark red. The genome maps were generated using Geneious version 9.1.8.

is remarkable that this phage genome comprises an obviously intact lysogeny module with genes for an integrase, a SOS-response/LexA-like repressor and an antirepressor, indicating this phage still has the potential to integrate its genome into host strains.

Genetic Diversity of Host Bacteria

We also sequenced the genomes of three representative host bacteria, i.e., *S. hyicus* strains 07/2-4A, 83/7-1B, and 83/11-1A, respectively. These bacteria were the primary hosts used for enrichment of PITT-1, PITT-4 & 5, and PITT-6-11, respectively. SNP analysis revealed little diversity in the genomes of *S. hyicus* strains 07/2-4A and 83/11-1A suggesting they might be clonal strains, while *S. hyicus* strain 83/7-1B showed clear differences to those strains (**Table 3**). Additionally, sequencing resulted in the identification of two different *exh* virulence genes for these isolates, namely *exh*A in 07/2-4A and 83/11-1A, and *exh*C in 83/7-1B.

TABLE 3 | SNP matrix of *S. hyicus strains*.

SNP* distance	07/2-4A	83/11-1A	83/7-1B
07/2-4A	0	15	5,226
83/11-1A	15	0	5,227
83/7-1B	5,226	5,227	0

**Single nucleotide polymorphism.*

DISCUSSION

Since EE is not under systematic control regulated by European law or by the OIE, there is a lack of monitoring data and the prevalence is unknown. However, the Iowa State University states that EE occurs "in most major swine raising countries (…), one case occasionally seen by most swine practitioners." (https://vetmed.iastate.edu/vdpam/FSVD/swine/index-diseases/greasy-pig). Farm outbreaks can affect a vast number of animals: in a German case of farm shutdown required by local authorities, 258 pig pens were simultaneously affected by EE according to media reports based on interviews with official authorities [(https://www.swr.de/-/id=14731830/property=download/nid=233454/16d4gu4/droht-ferkelzuechter-straathof-das-aus.pdf), last access 2020.11.27]. It is important to note that the causative agent of EE, coagulase-variable *S. hyicus*, episodically also causes zoonotic disease in humans (Casanova et al., 2011). There is no approved vaccination against greasy pig disease; farm-specific vaccines are applied to control local outbreaks [StIKo-Vet, FLI Germany, (https://stiko-vet.fli.de/de/aktuelles/)] and antibiotics are used to treat acute disease. Often, penicillin G is the drug of choice, although susceptibility results contradict this empiric tradition (Park et al., 2013a). Bacteriophages might offer interesting alternatives for individual topical treatment, as well as for sanitation of the environment. Despite current restrictive approval of bacteriophages in the EU, Fernández et al. (2018) are convinced that it is "only a matter of time that (…) drawbacks can be overcome." Thus, the detection and proper characterization of new bacteriophages is of common interest. We isolated a set of 11 *S. hyicus* phages (belonging to 2 morphologically different groups of *Siphoviridae*) from the same piglet farm suffering from EE. Host *S. hyicus* bacteria and bacteriophages were spread between two different pig houses. Bacteriophages were most frequently detected when samples were taken by rinsing diseased pigs with tap water.

In our study, at least two different *S. hyicus* strains were isolated from clinically affected animals on the same farm. Both strains carried different virulence genes of the *exh*-type (*exh*A / *exh*C). In a Danish study on 314 isolates from 60 cases of EE, *exh*A (20%) and *exh*C (18%) were also prevalent among virulent strains, although *exh*B (33%) was the most common virulence gene (Andresen and Ahrens, 2004). However, distribution of different *exh*-genes differs by geography (González-Martín et al., 2020), with *exh*A being the most prevalent *exh*-gene in Japan in 2007 (Futagawa-Saito et al., 2007). In our study, *S. hyicus* strains with different *exh*-genes differed in their susceptibility to phages: while the *exh*A-positive strains 07/2-4A and 83/11-1A were efficiently lysed by all but two phages, the *exh*C-positive strain 83/7-1B was only weakly lysed by most phages, except PITT-4 and PITT-5. The occurrence of at least two different, but virulent *S. hyicus* strains on the same farm thus would have implications for herd-specific phage application, but also for farm-specific vaccination.

Sequencing of two phages as representatives of the two different morphotypes revealed that the lytic phage PITT-1 (PMBT8, acc. No. MK893987) had very little resemblance with multispecies *Staphylococcus* phage Twort, the only *S. hyicus*-effective phage with a sequence entry in the NCBI Genbank). The sequence identity was higher to *S. epidermidis Siphoviridae* phages (vB_SepS_SEP9 and 6ec; Aswani et al., 2014; Melo et al., 2014), but with a query coverage still as low as 29–32%. Despite their genetic diversity, these three phages showed a very similar morphology—icosahedral heads and elongated flexible tails. This may be associated with the higher similarity observed for blastp analysis of specific structural proteins when compared to the overall phage nucleic acid sequence analysis. PITT-1 revealed the largest head [74 nm compared to 64 nm (SEP9) and 69 nm (6ec)] but the shortest tail [346 nm compared to 375 nm (SEP9) and 362 nm (6ec)]. A second phage, PITT-5, was sequenced, which differed from phage PITT-1 with respect to morphology, narrow host range and DNA-sequence. The phage PITT-5 may not be well-adapted to lytic propagation, as it reveals only low (or no) lytic activity against all of the investigated host strains, except for its primary host.

Notably, only few bacteriophages specific for strains of coagulase-negative or -variable *Staphylococcus* species have been characterized in detail, and the number of recorded phages for coagulase-negative staphylococci was reported to be below 10 in 2014 (Melo et al., 2014). Historically, phages for *S. hyicus* had been repeatedly described for the purpose of phage typing (Hájek and Horák, 1981; Kawano et al., 1983; Kibenge et al., 1983; Shimizu et al., 1987a,b; Wegener, 1993a,b). However, no further characteristics (e.g., morphologies or sequence data) of these phages are publicly available. In contrast to our host range assessment, the host range of some of these phages comprised also strains of *S. epidermidis* (Kawano et al., 1983), as well as strains of *S. intermedius* (which were not tested in our study).

The phage PITT-5 appears to be a temperate phage and is therefore probably not suitable for therapeutic or sanitation applications. Thus, the strictly lytic nature of PITT-1 makes this phage a promising candidate for further studies, which should include *in vivo* trials. The lack of antibiotic resistance genes and virulence genes encourages further investigations on phage PITT-1. However, the diversity of virulent *S. hyicus* strains isolated in the same farm environment, might require the application of blends of phages with different host ranges.

DATA AVAILABILITY STATEMENT

The datasets presented in this study can be found in online repositories. The names of the repository/repositories and accession number(s) can be found in the article.

ETHICS STATEMENT

Ethical review and approval was not required for the animal study because samples were taken for the purpose of routine veterinary diagnostics, which does not need any ethical approval according to national and European law. Written informed consent was obtained from the owners for the participation of their animals in this study.

AUTHOR CONTRIBUTIONS

JT conceived and described the isolation of bacteriophages and bacteria. JT and SS conceived and described the cultural experiments. SS described the molecular characterization of the bacteriophages. GT performed and described the isolation of bacteriophages, bacteria, and the cultural experiments. EB performed the genomic characterization. EB and SS created and described the sequencing data and the genome maps. NW and HN conceived, performed, and described the electron microscopy analysis. CH conceived the isolation of bacteriophages, bacteria, the cultural experiments, and wrote the discussion. CF conceived the genomic characterization. CH and CF conceived the structure of the manuscript. All authors commented on the first drafts of the manuscript and contributed to the final version.

ACKNOWLEDGMENTS

We kindly thank Angela Back, Gesa Gehrke, and Evelyn Lass for technical assistance and Franziska Witte together with Inka Lammertz and Evelyn Lass for contributing additional host range experiments.

REFERENCES

Aarestrup, F. M., and Jensen, L. B. (2002). Trends in antimicrobial susceptibility in relation to antimicrobial usage and presence of resistance genes in *Staphylococcus hyicus* isolated from exudative epidermitis in pigs. *Vet. Microbiol.* 89, 83–94. doi: 10.1016/S0378-1135(02)00177-3

Ahrens, P., and Andresen, L. O. (2004). Cloning and sequence analysis of genes encoding *Staphylococcus hyicus* exfoliative toxin types A, B, C, and D. *J. Bacteriol.* 186, 1833–1837. doi: 10.1128/JB.186.6.1833-1837.2004

Altschul, S. F., Gish, W., Miller, W., Myers, E. W., and Lipman, D. J. (1990). Basic local alignment search tool. *J. Mol. Biol.* 215, 403–410. doi: 10.1016/S0022-2836(05)80360-2

Andresen, L. O., and Ahrens, P. (2004). A multiplex PCR for detection of genes encoding exfoliative toxins from *Staphylococcus hyicus*. *J. Appl. Microbiol.* 96, 1265–1270. doi: 10.1111/j.1365-2672.2004.02258.x

Andrews, J. J. (1979). Ulcerative glossitis and stomatitis associated with exudative epidermitis in suckling swine. *Vet. Pathol.* 16, 432–437. doi: 10.1177/030098587901600406

Arsenakis, I., Boyen, F., Haesebrouck, F., and Maes, D. G. D. (2018). Autogenous vaccination reduces antimicrobial usage and mortality rates in a herd facing severe exudative epidermitis outbreaks in weaned pigs. *Vet. Rec.* 182:744. doi: 10.1136/vr.104720

Aswani, V. H., Tremblay, D. M., Moineau, S., and Shukla, S. K. (2014). Complete genome Sequence of a *Staphylococcus epidermidis* bacteriophage isolated from the anterior nares of humans. *Genome Announc.* 2, e00549–e00514. doi: 10.1128/genomeA.00549-14

Bortolaia, V., Kaas, R. S., Ruppe, E., Roberts, M. C., Schwarz, S., Cattoir, V., et al. (2020). ResFinder 4.0 for predictions of phenotypes from genotypes. *J. Antimicrob. Chemother.* 75, 3491–3500. doi: 10.1093/jac/dkaa345

Casanova, C., Iselin, L., Steiger, N., von, Droz, S., and Sendi, P. (2011). *Staphylococcus hyicus* bacteremia in a farmer. *J. Clin. Microbiol.* 49, 4377–4378. doi: 10.1128/JCM.05645-11

Fernández, L., Gutiérrez, D., Rodríguez, A., and García, P. (2018). Application of bacteriophages in the agro-food sector: a long way toward approval. *Front. Cell. Infect. Microbiol.* 8:296. doi: 10.3389/fcimb.2018.00296

Foster, A. P. (2012). Staphylococcal skin disease in livestock. *Vet. Dermatol.* 23, 342–351.e63. doi: 10.1111/j.1365-3164.2012.01093.x

Frana, T. S., and Hau, S. J. (2019). "Staphylococcosis," in *Diseases of Swine, 11th Edn.,* eds J. J. Zimmermann, L. A. Karriker, A. Ramirez, K. J. Schwartz, G. W. Stevenson, and J. Zhang (Wiley). doi: 10.1002/9781119350927.ch60

Futagawa-Saito, K., Ba-Thein, W., and Fukuyasu, T. (2009). Antimicrobial susceptibilities of exfoliative toxigenic and non-toxigenic *Staphylococcus hyicus* strains in Japan. *J. Vet. Med. Sci.* 71, 681–684. doi: 10.1292/jvms.71.681

Futagawa-Saito, K., Ba-Thein, W., Higuchi, T., Sakurai, N., and Fukuyasu, T. (2007). Nationwide molecular surveillance of exfoliative toxigenic *Staphylococcus hyicus* on pig farms across Japan. *Vet. Microbiol.* 124, 370–374. doi: 10.1016/j.vetmic.2007.04.036

Gigante, A., and Atterbury, R. J. (2019). Veterinary use of bacteriophage therapy in intensively-reared livestock. *Virol. J.* 16:155. doi: 10.1186/s12985-019-1260-3

González-Martín, M., Corbera, J. A., Suárez-Bonnet, A., and Tejedor-Junco, M. T. (2020). Virulence factors in coagulase-positive staphylococci of veterinary interest other than *Staphylococcus aureus*. *Vet. Quart.* 40, 118–131. doi: 10.1080/01652176.2020.1748253

Gutiérrez, D., Martín-Platero, A. M., Rodríguez, A., Martínez-Bueno, M., García, P., and Martínez, B. (2011). Typing of bacteriophages by randomly amplified polymorphic DNA (RAPD)-PCR to assess genetic diversity. *FEMS Microbiol. Lett.* 322, 90–97. doi: 10.1111/j.1574-6968.2011.02342.x

Hájek V., and Horák V. (1981). Typing of Staphylococci with phages derived from Staphylococcus hyicus. *Zentralbl. Bakteriol. Mikrobiol. Hyg. A Suppl.* 10, 93–98.

Howard-Varona, C., Hargreaves, K. R., Abedon, S. T., and Sullivan, M. B. (2017). Lysogeny in nature: mechanisms, impact and ecology of temperate phages. *ISME J.* 11, 1511–1520. doi: 10.1038/ismej.2017.16

Imanishi, I., Nicolas, A., Caetano, A.-C. B., Castro, T. L., d., P., Tartaglia, N. R., et al. (2019). Exfoliative toxin E, a new *Staphylococcus aureus* virulence factor with host-specific activity. *Sci. Rep.* 9:16336. doi: 10.1038/s41598-019-52777-3

Kaas, R. S., Leekitcharoenphon, P., Aarestrup, F. M., and Lund, O. (2014). Solving the problem of comparing whole bacterial genomes across different sequencing platforms. *PLoS ONE* 9:e104984. doi: 10.1371/journal.pone.0104984

Kawano, J., Shimizu, A., and Kimura, S. (1983). Bacteriophage typing of Staphylococcus hyicus subsp. *hyicus isolated from pigs. Am. J. Vet. Res.* 44, 1476–1479.

Kearse, M., Moir, R., Wilson, A., Stones-Havas, S., Cheung, M., Sturrock, S., et al. (2012). Geneious basic: an integrated and extendable desktop software platform for the organization and analysis of sequence data. *Bioinformatics* 28, 1647–1649. doi: 10.1093/bioinformatics/bts199

Kibenge, F. S. B., Rood, J. I., and Wilcox, G. E. (1983). Lysogeny and other characteristics of Staphylococcus hyicus isolated from chickens. *Vet. Microbiol.* 8, 411–415. doi: 10.1016/0378-1135(83)90054-8

Kwan, T., Liu, J., DuBow, M., Gros, P., and Pelletier, J. (2005). The complete genomes and proteomes of 27 *Staphylococcus aureus* bacteriophages. *Proc. Nat. Acad. Sci. U.S.A.* 102, 5174–5179. doi: 10.1073/pnas.0501140102

Labrie, S. J., Samson, J. E., and Moineau, S. (2010). Bacteriophage resistance mechanisms. *Nat. Rev. Microbiol.* 8, 317–327. doi: 10.1038/nrmicro2315

Letunic, I., and Bork, P. (2018). 20 years of the SMART protein domain annotation resource. *Nucleic Acid Res.* 46, D493–D496. doi: 10.1093/nar/gkx922

Lowe, T. M., and Chan, P. P. (2016). tRNAscan-SE On-line: integrating search and context for analysis of transfer RNA genes. *Nucleic Acids Res.* 44, W54–W57. doi: 10.1093/nar/gkw413

Melo, L. D. R., Sillankorva, S., Ackermann, H.-W., Kropinski, A. M., Azeredo, J., and Cerca, N. (2014). Characterization of *Staphylococcus epidermidis* phage vB_SepS_SEP9 - a unique member of the Siphoviridae family. *Res. Microbiol.* 165, 679–685. doi: 10.1016/j.resmic.2014.09.012

Nagase, N., Sasaki, A., Yamashita, K., Shimizu, A., Wakita, Y., Kitai, S., et al. (2002). Isolation and species distribution of staphylococci from animal and human skin. *J. Vet. Med. Sci.* 64, 245–250. doi: 10.1292/jvms.64.245

Nishifuji, K., Sugai, M., and Amagai, M. (2008). Staphylococcal exfoliative toxins: "molecular scissors" of bacteria that attack the cutaneous defense barrier in mammals. *J. Dermatol. Sci.* 49, 21–31. doi: 10.1016/j.jdermsci.2007.05.007

Park, J., Friendship, R. M., Poljak, Z., Weese, J. S., and Dewey, C. E. (2013a). An investigation of exudative epidermitis (greasy pig disease) and antimicrobial resistance patterns of *Staphylococcus hyicus* and *Staphylococcus aureus* isolated from clinical cases. *Can. Vet. J.* 54, 139–144.

Park, J., Friendship, R. M., Weese, J. S., Poljak, Z., and Dewey, C. E. (2013b). An investigation of resistance to β-lactam antimicrobials among staphylococci isolated from pigs with exudative epidermitis. *BMC Vet. Res.* 9:211. doi: 10.1186/1746-6148-9-211

Rakhuba, D. V., Kolomiets, E. I., Dey, E. S., and Novik, G. I. (2010). Bacteriophage receptors, mechanisms of phage adsorption and penetration into host cell. *Pol. J. Microbiol.* 59, 145–155. doi: 10.33073/pjm-2010-023

Rohde, C., Wittmann, J., and Kutter, E. (2018). Bacteriophages: a therapy concept against multi-drug-resistant bacteria. *Surg. Infect.* 19, 737–744. doi: 10.1089/sur.2018.184

Salmond, G. P. C., and Fineran, P. C. (2015). A century of the phage: past, present and future. *Nat. Rev. Microbiol.* 13, 777–786. doi: 10.1038/nrmicro3564

Sato, H., Watanabe, T., Higuchi, K., Teruya, K., Ohtake, A., Murata, Y., et al. (2000). Chromosomal and extrachromosomal synthesis of exfoliative toxin from *Staphylococcus hyicus*. *J. Bacteriol.* 182, 4096–4100. doi: 10.1128/JB.182.14.4096-4100.2000

Shimizu, A., Kawano, J., Teranishi, H., Hazue, S., Fujinami, T., Kimura, S., and Sugihara, K. (1987a). Isolation of Staphylococcus species from the tonsils of healthy pigs and phage patterns of isolates. *Jap. J. Vet. Sci.* 49, 703–709.

Shimizu, A., Teranishi, H., Kawano, J., and Kimura, S. (1987b). Phage patterns of Staphylococcus hyicus subsp. *hyicus isolated from chickens, cattle and pigs Zentralbl. Bakteriol. Mikrobiol. Hyg. A* 265, 57–61. doi: 10.1016/s0176-6724(87)80152-9

Voytenko, A. V., Kanbar, T., Alber, J., Lämmler, C., Weiss, R., Prenger-Berninghoff, E., et al. (2006). Identification of *Staphylococcus hyicus* by polymerase chain reaction mediated amplification of species specific sequences of superoxide dismutase A encoding gene sodA. *Vet. Microbiol.* 116, 211–216. doi: 10.1016/j.vetmic.2006.03.009

Wattam, A. R., Davis, J. J., Assaf, R., Boisvert, S., Brettin, T., Bun, C., et al. (2017). Improvements to PATRIC, the all-bacterial bioinformatics database and analysis resource center. *Nucleic Acid Res.* 45, D535–D542. doi: 10.1093/nar/gkw1017

Wegener, H. C. (1993a): Diagnostic value of phage typing, antibiogram typing, and plasmid profiling of Staphylococcus hyicus from piglets with exudative epidermitis. *Zentralbl. Veterinarmed. B.* 40, 13–20. doi: 10.1111/j.1439-0450.1993.tb00103.x

Wegener, H. C. (1993b): Development of a phage typing system for Staphylococcus hyicus. *Res. Microbiol.* 144, 237–244. doi: 10.1016/0923-2508(93)90049-8

Conflict of Interest: The authors declare that the research was conducted in the absence of any commercial or financial relationships that could be construed as a potential conflict of interest.

frontiers in Microbiology

ORIGINAL RESEARCH
published: 05 July 2021
doi: 10.3389/fmicb.2021.682255

The Efficacy of Phage Therapy in a Murine Model of *Pseudomonas aeruginosa* Pneumonia and Sepsis

*Xu Yang[1], Anwarul Haque[1,2], Shigenobu Matsuzaki[3], Tetsuya Matsumoto[1,2] and Shigeki Nakamura[1]**

[1] Department of Microbiology, Tokyo Medical University, Tokyo, Japan, [2] Department of Infectious Diseases, School of Medicine, International University of Health and Welfare, Narita, Japan, [3] Department of Medical Laboratory Science, Kochi Gakuen University, Kochi, Japan

The emergence of multi-drug resistant *Pseudomonas aeruginosa* necessitates the search for treatment options other than antibiotic use. The use of bacteriophages is currently being considered as an alternative to antibiotics for the treatment of bacterial infections. A number of bacteriophages were introduced to treat pneumonia in past reports. However, there are still lack of knowledge regarding the dosages, application time, mechanism and safety of phage therapy against *P. aeruginosa* pneumonia. We used the bacteriophage KPP10 against *P. aeruginosa* strain D4-induced pneumonia mouse models and observed their outcomes in comparison to control models. We found that the nasal inhalation of highly concentrated KPP10 (MOI = 80) significantly improved survival rate in pneumonia models ($P < 0.01$). The number of viable bacteria in both lungs and in serum were significantly decreased ($P < 0.01$) in phage-treated mice in comparison to the control mice. Pathological examination showed that phage-treated group had significantly reduced bleeding, inflammatory cell infiltration, and mucus secretion in lung interstitium. We also measured inflammatory cytokine levels in the serum and lung homogenates of mice. In phage-treated models, serum TNFα, IL-1β, and IFN-γ levels were significantly lower ($P < 0.05$, $P < 0.01$, and $P < 0.05$, respectively) than those in the control models. In the lung homogenate, the mean IL-1β level in phage-treated models was significantly lower ($P < 0.05$) than that of the control group. We confirmed the presence of phage in blood and lungs, and evaluated the safety of bacteriophage use in living models since bacteriophage mediated bacterial lysis arise concern of endotoxic shock. The study results suggest that phage therapy can potentially be used in treating lung infections caused by *Pseudomonas aeruginosa*.

Keywords: ***Pseudomonas aeruginosa*, pneumonia, sepsis, bacteriophage, phage therapy**

OPEN ACCESS

Edited by:
Krishna Mohan Poluri,
Indian Institute of Technology Roorkee, India

Reviewed by:
Oana Ciofu,
University of Copenhagen, Denmark
Mariana Carmen Chifiriuc,
University of Bucharest, Romania

***Correspondence:**
Shigeki Nakamura
shigenak@tokyo-med.ac.jp

Specialty section:
This article was submitted to Antimicrobials, Resistance and Chemotherapy, a section of the journal Frontiers in Microbiology

Received: *18 March 2021*
Accepted: *31 May 2021*
Published: *05 July 2021*

Citation:
Yang X, Haque A, Matsuzaki S, Matsumoto T and Nakamura S (2021) The Efficacy of Phage Therapy in a Murine Model of Pseudomonas aeruginosa Pneumonia and Sepsis. Front. Microbiol. 12:682255. doi: 10.3389/fmicb.2021.682255

INTRODUCTION

Pseudomonas aeruginosa is a gram-negative opportunistic pathogen and is one of the main pathogens that cause nosocomial infections. It is a common etiology for infections in immunocompromised patients (Parker et al., 2008; Gellatly and Hancock, 2013) and in respiratory-associated pneumonia in ICU settings. Antimicrobial therapy is the choice of treatment

in *Pseudomonas* infections; however, due to the emergence of multi-drug resistant *P. aeruginosa*, there have been cases wherein antibiotics have failed (Nathwani et al., 2014; Jernigan et al., 2020). Phage therapy is considered as a treatment option against bacterial infections because of its ability to lyse bacterial cells. Compared to antimicrobial therapy, phage therapy has advantages such as high specificity, sterilization, self-propagation, and protection of mutation-mediated antibiotic-resistance development (Matsuzaki et al., 2005). In recent years, due to the emergence of multi-drug resistant bacteria, phage therapy has attracted widespread attention due to its possession of a completely different mechanism of action compared to antibiotic therapy (Viertel et al., 2014).

Although phage therapy has a long history, the safety of phage therapy has not yet been fully studied (Caflisch et al., 2019; Kwiatek et al., 2020) especially in the context of infections caused by gram-negative bacteria that pose a risk of endotoxemia (Buttenschoen et al., 2010; Dickson and Lehmann, 2019). Endotoxins are present in the cell walls of most gram-negative bacteria, and even very low doses can strongly trigger human inflammatory reactions, and in severe cases can cause endotoxin shock and death (Lepper et al., 2002; Surbatovic et al., 2013). Like bactericidal antibiotics, bacteriophage causes release of endotoxins when they lyse gram-negative bacteria (Dufour et al., 2017). Past reports showed that phage therapy was used in children to treat persistent lung infections with cystic fibrosis caused by *P. aeruginosa* (Krylov et al., 2016; Parkins et al., 2018); however, there are several reports of pneumonia with *P. aeruginosa* in patients with non-cystic fibrosis (Patey et al., 2019). Therefore, we aimed to evaluate the therapeutic effect of phage therapy on pulmonary *P. aeruginosa* infection using animal models.

MATERIALS AND METHODS

Bacteria Strain

The *P. aeruginosa* standard strain D4 was isolated from the blood of neutropenic mice which had bacteremia (Matsumoto et al., 1997a,b, 1998a,b,c; Watanabe et al., 2007); this was stored in LB medium containing 50% glycerol at −80°C.

Animal Care and Use

Six weeks old Male, pathogen-free, ICR mice that were purchased (Sankyo Labo Service Co., Ltd.) and were housed under specific-pathogen-free conditions and were supplemented with standard laboratory food and water *ad libitum*. The facility was maintained at a constant temperature (27°C), humidity (65%), and 12/12 h light/dark cycle.

Anesthesia Protocol

The anesthesia mixture used was prepared by combining the following: 2 mL midazolam (5 mg/mL; FUJIFILM Wako Co., Ltd.), Vetorphale 2.5 mL (5 mg/mL; Meiji Seika Pharma Co., Ltd.), medetomidine hydrochloride 0.75 mL (1 mg/ml; Kyoritsu Seiyaku), normal saline 19.75 mL (Otsuka Pharmaceutical Co., Ltd.). The mice were anesthetized by subcutaneously injecting the anesthesia mixer at a dose of 0.1 mL/10 g. The animal study was reviewed and approved by Tokyo Medical University Animal Care and Use Committee.

Phage

Using *P. aeruginosa* strain (P20) as the host, bacteriophage strain KPP10 was isolated from a water sample collected from a river in Kochi Prefecture, Japan. Strain P20 was derived from clinical specimens of Kochi Medical University Hospital in Kochi Prefecture, Japan. The KPP10 bacteriophage belongs to the Myoviridae family, morphological type A1, and has strong lytic activity against *P. aeruginosa* D4 (Watanabe et al., 2007; Uchiyama et al., 2012). Previous reports indicate that bacteriophage KPP10 is a lytic bacteriophage, which has no pathogenicity or pathogenicity-related genes, so it is expected to be very suitable for use as a therapeutic bacteriophage (Uchiyama et al., 2012).

Bacteriophage Culture

LB medium was inoculated with 1% v/v of overnight bacterial culture at the exponential growth phase and was incubated at 37°C for 2 h to reach an approximate OD_{600} of 0.2–0.4. Then, the phage was added at MOI = 10 and was incubated at 37°C for 5 h with gentle stirring (100 rpm) to facilitate cell lysis. Cell debris was removed by centrifugation (20 min, 1,750 × *g*, 4°C). The supernatant was filtered using a 0.22 μm disposable filter (CORNING 430521) and the phage were stored at 4°C for downstream use.

Phage Count

The phages were counted using the plaque assay method according to standard protocols (Parker et al., 2008). Phage dilutions were prepared using physiological saline. Using 2% agar as the bottom layer, 20 mL of LB agar medium (Sigma) containing 100 μL of phage dilution and 100 μL of exponentially growing bacterial solution were plated on agar plates at 45°C. The plate was then incubated at 37°C overnight, afterward, the plaques were counted.

PEG Precipitation

The bacteriophage was mixed with polyethylene glycol (PEG) 6000 [10% total (wt/vol); FUJIFILM Wako] and NaCl (0.5 M; FUJIFILM Wako), and were kept in rotation overnight at 4°C. Then, these were centrifuged for 15 min at a speed of 11,000 × *g* in 4°C (TOMY RX200) to collect the precipitate, and pellet was suspended in phage buffer to dilute the phage concentration 200 times. We noticed that the use of ultracentrifugation to concentrate the phage solution led to ammonium acetate and cesium chloride release, which proved to be toxic. As such, we used high-speed centrifugation in the presence of PEG precipitation. In the method described by Bourdin et al. (2014) chloroform was used to remove bacterial proteins in the concentrate after centrifugation; however, KPP10 is not chloroform-resistant (data not shown), so this step was omitted.

Pseudomonas aeruginosa Pneumonia Model

Pseudomonas aeruginosa D4 cultured on LB agar plates overnight at 37°C was adjusted to 2.5 × 10^9 colony forming unit (CFU)/mL using sterile physiological saline. To produce the *P. aeruginosa* pneumonia model, 20 μl of bacterial suspension was inoculated through intranasal route in anesthetized mice. These mice were randomly divided in two groups and 10 μL of KPP10 bacteriophage (4 × 10^{11}/mL plaque forming unit, PFU) (MOI = 80) was administered in these mice intranasally after 2 h (group 1) and 8 h (group 2) of bacterial inoculation. Past study suggested that higher dose (MOI) of bacteriophage can promptly kill bacteria and help to minimize the chance of resistant development to phage (Taha et al., 2018). In addition, another study using in-vitro models showed that KPP10 became resistant to *P. aeruginosa* D4 strains at 210 min. of administration (Watanabe et al., 2007). Considering number and short therapeutic window of phage from these studies, we administered the bacteriophage in mice at a highest concentration (MOI) that we could harvest in our laboratory (MOI = 80). The mice in negative control (NC) group were inhaled 10 μL of phage buffer after 2 h of inoculation. We used imipenem/cilastatin sodium to prepare a positive control (PC) group. After 2 h post inoculation of *P. aeruginosa*, 25 mg/kg of imipenem/cilastatin sodium (MSD Co., Ltd.) was injected subcutaneously to a group of randomly selected mice at every 12 h for 3 days (Coopersmith et al., 2003). All groups were monitored daily for 6 days to calculate their survival rate.

Analysis of survival data showed that there was no significant difference in survival rates between the mice those inhaled KPP10 at 2 h and 8 h p.i. Therefore, in the bacteriology and histopathology experiments we only included the Pa pneumonia mice inhaled either phage KPP10 or phage buffer at 2 h p.i.

Pathological Examination of Lung Tissue

After 2 h of inhalation of 20 μL *P. aeruginosa* D4 (1.25 × 10^9/mL CFU), the treatment group inhaled 10 μL phage KPP10 (2 × 10^{11}/mL PFU), and the control group inhaled 10 μL of sterile phage buffer. After 24 h, mice were euthanized by isoflurane inhalation. The lungs and trachea were removed under sterile conditions, and the specimens were fixed with 10% formalin (FUJIFILM Wako). The specimen was embedded and sliced, and then stained with H&E stain.

Determination of Viable Bacteria and Phage in the Lung and Serum

Pseudomonas aeruginosa pneumonia mice were randomly divided in treatment and control groups. After 2 h post infection, the treatment group inhaled 10 μL (MOI = 80) of phage KPP10 (2 × 10^{11} PFU/mL), and the control group inhaled 10 μL of phage buffer. After 24 h, live mice were euthanized by isoflurane inhalation to collect their blood from cardiac ventricles and the whole lung under sterile conditions. A tissue homogenizer (Nakayama Co., Ltd., 16–80) was used to homogenize the lung tissues in physiological saline, after which EDTA (final concentration 0.05 M) was added, and the tissue debris were removed by centrifugation at 8,000 × *g* for 2 min at 4°C. Collected lungs were kept on ice during all steps. Blood samples were coagulated in a vacuum blood collection tube (Nipro Corporation Limited), and the serum was separated from blood cells by centrifugation at 10,000 × *g* for 5 min. The serum and lung tissue homogenate samples were diluted with sterile physiological saline and inoculated on NAC agar plates (Eiken Chemical Co., Ltd.), and incubated at 37°C for 24 h.

Serum and lung tissue homogenate samples were prepared using physiological saline. Using 2% agar as the bottom layer, 20 mL of LB agar medium (Sigma) containing 100 μL of samples and 100 μL of exponentially growing bacterial solution were plated on agar plates at 45°C. The plate was then incubated at 37°C overnight, afterward the plaques were counted. Serum and lung tissue homogenate samples were stored at −30°C for downstream analyses.

Measurement of Cytokine and High Mobility Group Box 1 (HMGB1) Level

TNF-α, IL-1β, and IFN-γ concentrations in serum and lung tissue samples and serum HMGB1 concentration were assayed using mouse uncoated ELISA Kit (Thermo Fisher Scientific, MA, United States) and mouse/rat HMGB1 ELISA Kit (Arigo Biolaboratories Co., Ltd., Hsinchu City, Taiwan) according to the manufacturer's protocols, respectively.

Determination of Endotoxin Levels in Serum

We used a commercial limulus amebocyte lysate (LAL) endotoxin detection kit (FUJIFILM Wako) to measure the endotoxin levels of the collected mouse serum samples. Mouse serum samples were diluted 10-fold using physiological saline (Otsuka Pharmaceutical). Then, 100 μL of the diluted serum sample was added to the endotoxin sample pretreatment solution (FUJIFILM Wako), mixed, and incubated at 70°C for 10 min, after which ice water was immediately added to the mixture and to cool for 2 min. Afterward, 200 μL of the treated sample was then added to the LAL reagent, thoroughly mixed, and measurement was done using Toxinometer MT-6500 (FUJIFILM Wako).

Statistical Analysis

Survival analysis was performed using the chi-square test, and the survival rate by the Kaplan–Meier method. All other assay data are presented as the mean ± standard deviation (SD). Differences between groups were examined using the Mann–Whitney *U* test (P values < 0.05 were considered to indicate a statistically significant difference).

RESULTS

Survival Rate of *Pseudomonas aeruginosa* Pneumonia Model

In order to evaluate whether KPP10 has a protective effect against pneumonia caused by *P. aeruginosa* D4, we compared survival

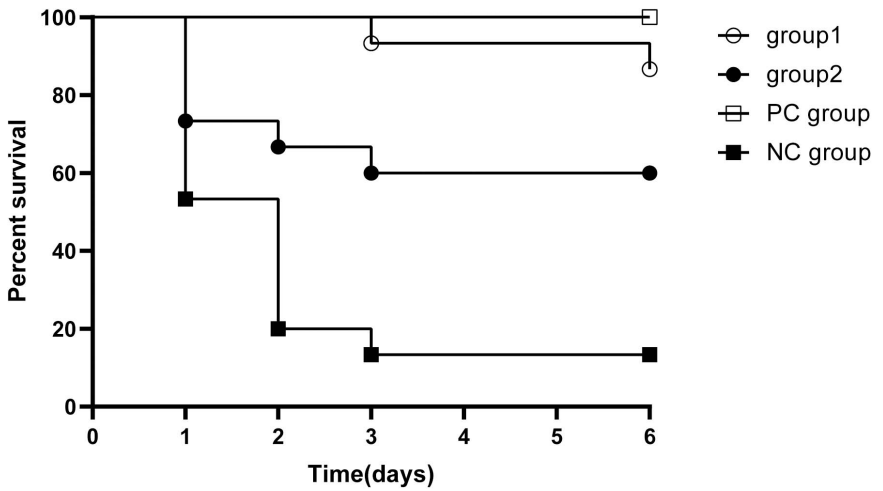

FIGURE 1 | Survival rate in pneumonia mice. All mice inhaled 20 μL *P. aeruginosa* D4 (2.5×10^9 CFU/ml). Group 1 ($n = 15$) inhaled 10 μl phage KPP10 (10 μl 4×10^{11} PFU/ml) at 2 h post bacterial inoculation. Group 2 ($n = 15$) inhaled 10 μl phage KPP10 (10 μl 4×10^{11} PFU/ml) at 8 h post bacterial inoculation. Negative control (NC) group inhaled 10 μL of phage buffer at 2 h post bacterial inoculation and the positive control (PC) group received subcutaneous injection imipenem/cilastatin sodium (25 mg/kg) at 2 h post infection and at every 12 h interval for 3 days. Survival rate in group 1, group 2 and PC mice were significantly higher ($p < 0.01$) when individually compared with the survival rate of NC mice. CFU denotes colony forming unit. PFU denotes plaque forming unit.

rates between four groups (**Figure 1**). The survival rate of mice in the group 1, group 2 and the PC group were significantly higher when individually compared with that of the NC mice (87% vs. 13%; $p < 0.01$, 60% vs. 13%; $p < 0.01$, 100% vs. 13%; $p < 0.01$). The survival rate between group 1 and group 2 and between group 1 mice and PC group had no significant differences (87% vs. 60%; $p = 0.99$, 87 vs. 100%; $p = 0.143$). This indicates that KPP10 has a protective effect against pneumonia caused by *P. aeruginosa* D4. Moreover, even with an administration of phage at a delayed time point of post infections, survival rate in pneumonic mice improved.

Pathological Examination

In order to confirm the effect of KPP10 on pneumonia caused by *P. aeruginosa* D4, we observed pathological changes in the lung tissues of phage-treated and control mice; results are shown in **Figure 2**. We observed that 24 h after *P. aeruginosa* inhalation, a large number of bacteria were present in the lungs of the control mice (**Figure 2B**). The alveoli were filled with red blood cells and mucus, and there was a tendency for severe pulmonary bleeding. Inflammatory cell infiltration in the lung interstitium was also observed. In contrast, in the lungs of treated mice, *P. aeruginosa* D4 was observed to be cleared, the observed bleeding tendency was mild, and only a small amount of RBCs were left in the pulmonary interstitium (**Figure 2D**). This indicates that KPP10 effectively eliminated *P. aeruginosa* D4 in the lungs.

Number of Viable Bacteria and Phage in Lung and Serum

To confirm the effect of KPP10 on *P. aeruginosa* D4 in the lungs, we counted the viable bacteria and phage in the mouse lungs and serum. As shown in **Figure 3**, the number of viable bacteria in the lungs of the phage treatment group was significantly lower than that of the control group (treatment group 3,165 CFU/lung vs. control group 227,250 CFU/lung; $p < 0.01$) (**Figure 3A**), and the number of viable bacteria in the serum of the phage treatment group was also significantly lower than that of the control group (treatment group 64 CFU/mL vs. control group 202,111 CFU/mL; $p < 0.01$) (**Figure 3B**). This indicates that the *P. aeruginosa* D4 was significantly cleared from lungs and blood of the mice at 24 h post inhalation of KPP10. On the contrary, a large number of viable phages were persisting in the lungs in phage treatment group (2,217,833,333 PFU/lung), and the viable phages were also detected in serum (170 PFU/mL) (**Figure 3C**).

A question could be raised that bacteriophage came in contact with bacteria during harvesting and platting procedures and it could be worth if bacteria is separated from phage or phage activity is blocked by any means before culturing the bacteria in lungs and serum. A number of past studies (Watanabe et al., 2007; Mai et al., 2015; Hua et al., 2018) showed phage efficacy, in particularly phage KPP10 efficacy, in infection models describing the correlation between survival and bacterial numbers in circulation and in different organs in infected and control models. In our study, we followed the same method to demonstrate the efficacy of KPP10 in Pa infection models. In addition, we kept the collected samples on ice during all steps from the harvesting to culturing, which should reduce the activities of bacteria and phage to a minimum level without affecting their viability.

Cytokine Levels in Serum and Lung Tissue Homogenate Samples

We measured the levels of inflammatory cytokines TNFα, IL-1β, IFN-γ, and HMGB1 in the mice serum and lung homogenates. In the serum samples, levels of TNFα, IL-1β and IFN-γ in the phage-treated mice were significantly lower than those in the control mice (TNFα in treatment group: 185.82 pg/mL vs.

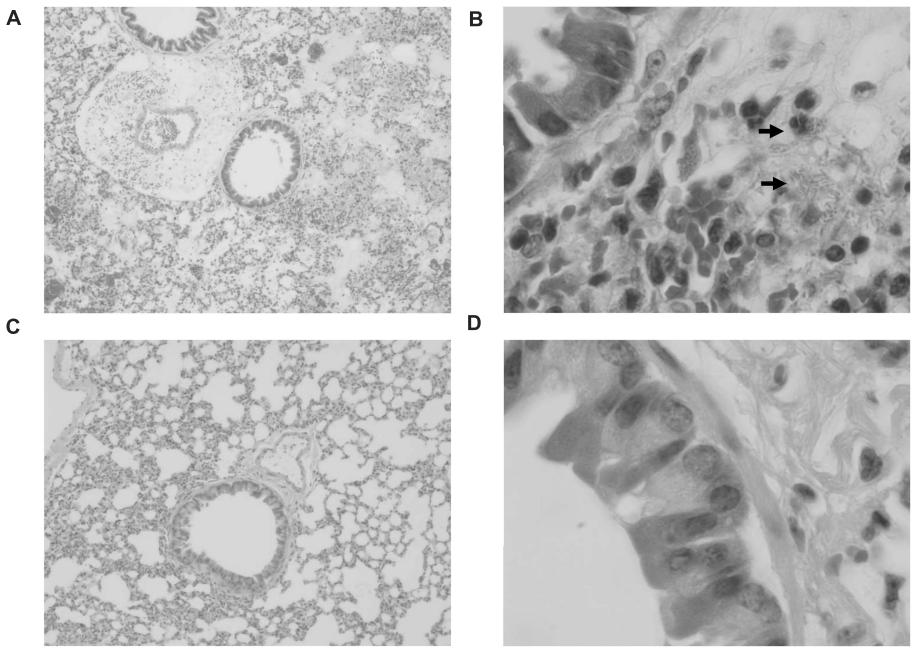

FIGURE 2 | Pathological micrograph of mouse lungs. In the control group (n = 6), 50× magnification **(A)** showed that the alveoli were filled with red blood cells and mucus, and a tendency of severe pulmonary bleeding was observed. At 1,000 × magnification **(B)**, there are a large number of bacteria in the lungs, and inflammatory cell infiltrations in the lung interstitium can be seen. In the treatment group (n = 6), a small amount of red blood cells in the alveoli can be seen at 50 × magnification **(C)**. At 1,000 × magnification **(D)**, the infiltration of inflammatory cells can be seen whereas no bacteria can be found.

control group: 3,026.24 pg/mL; $p < 0.05$; IL-1β in treatment group: 130.60 pg/mL vs. control group: 3,910.77 pg/m; $p < 0.01$; IFN-γ in treatment group: 307.02 pg/mL vs. control group: 2,192.05 pg/mL; $p < 0.05$) (**Figure 4B**). There was no significant difference observed in HMGB1. In the lung samples after tissue homogenization, the IL-1β level of the phage-treated group was significantly lower than that of the control group (treatment group: 2,179.33 pg/lung vs. control group 6,099.86 pg/lung; $p < 0.05$), TNFα level showed a decreasing tendency, whereas IFN-γ and HMGB1 showed an increasing tendency (**Figure 4A**).

Endotoxin Levels of Serum Samples

To assess whether *P. aeruginosa* D4-induced pneumonia treated with KPP10 may introduce a risk of endotoxic shock, we measured the endotoxin levels in the serum of mice. As shown in **Figure 5**, endotoxin levels in the serum of the phage treatment group were significantly lower than those of the control group (treatment group: 38.51 pg/mL vs. control group: 2,337.03 pg/mL; $p < 0.01$). The decreased endotoxin (LPS) level in phage treated mice reflects the lower number of bacteria in mice circulation, which also correlate with the data of bacterial burden in phage-treated and non-treated mice in this study.

DISCUSSION

Pseudomonas aeruginosa is an important opportunistic pathogen, and its strong adaptability enables it to survive in various environments including surfaces of medical devices (Gellatly and Hancock, 2013). This makes *P. aeruginosa* one of the common pathogens causing pneumonia in patients relying on mechanical ventilation (Parker et al., 2008). *P. aeruginosa* has strong natural resistance to antibiotics, and its acquired antibiotic resistance is also gradually increasing (Berube et al., 2016). In terms of the need for new antibiotics due to increase in antibiotic resistance, the World Health Organization has classified *P. aeruginosa* under Priority 1 (Critical), which means that the establishment of phage therapy as a treatment modality that can replace antibiotic therapy is urgent [Viertel et al., 2014; World Health Organization (WHO), 2013]. Here, we showed that phage therapy is comparable with antimicrobial therapy for treating *P. aeruginosa* pneumonia.

Decrement of bacterial load in infected host due to bactericidal effect of phage is a known phenomenon (Rodriguez-Gonzalez et al., 2020). In this study, quantification of live bacteria and phage in the lungs and serum and, pathological changes in lung fields in experimental models are corresponding to the phenomenon. Moreover, we observed that the pneumonic mice those didn't receive phage therapy mostly died within 24 h post infection. This finding supports the notion that phage replication rate in suitable bacteria is very high and it causes lysis of the infected bacteria within several hours (Payne and Jansen, 2001). Our study evident that the early administration of phage (at 2 h post infection) saved more infected mice than that of later administration at 8 h post infection. It is noticeable that the phage level in the lungs of the phage-treated mice was very high at 24 h p.i. It can be explained by the well-known characteristics of phage, that it releases progeny bacteriophages during lysis of

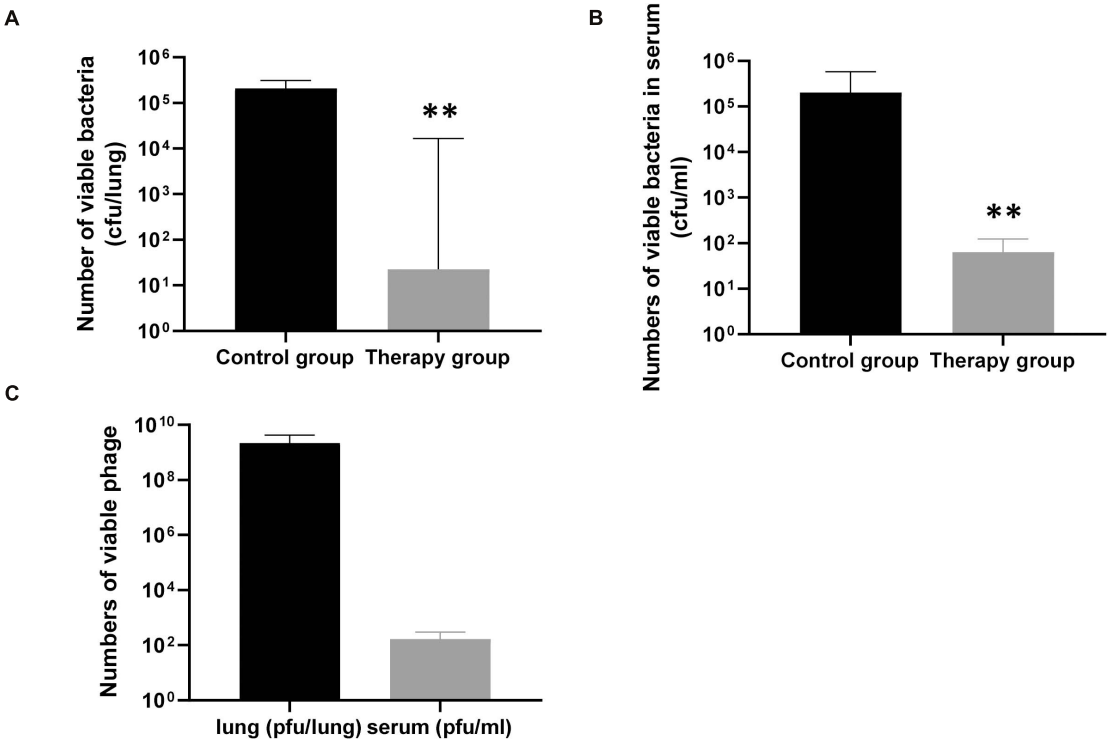

FIGURE 3 | The number of viable bacteria and phage in the lungs and serum of mice 24 h after infection. The number of viable bacteria in the lungs **(A)**, the phage treatment group (n = 6) was significantly lower than that of the control group (n = 6). The number of viable bacteria in the serum **(B)**, the phage treatment group (n = 6) was also significantly lower than that of the control group (n = 6). Data are presented as mean ± SEM of two experiments. The number of viable phages in the lungs and serum **(C)** of phage-treated mice 24 h after infection. Data are presented as mean ± SEM of two experiments (** < 0.01 vs. untreated control). CFU denotes colony forming unit. PFU denotes plaque forming unit.

bacteria. We have to admit that nasal inhalation of bacteria and bacteriophages cannot guarantee their even distribution in the lungs and multiple bacteriophages may infect the same bacteria due to the very high MOI. The number of bacteriophages in the area with low MOI will increase while the number of phages in the area with a higher MOI will decrease. This is the cause why phage level in the lungs of the mice in the treatment group remained high or basically unchanged at 24 h p.i.

Although previous many studies made pneumonia models in their experimental animals using inhalation of bacteria, but didn't consider or describe the development of pulmonary septicemia in their models (Debarbieux et al., 2010; Forti et al., 2018). Here in our study, we explored the presence of bacteria and bacteriophage in blood, indicating that phage inhalation is not only beneficial to protect pulmonary infections but also to manage the septicemia triggered by pulmonary infections.

There is evidence that when a local acute bacterial infection occurs, T cells become activated and infiltrate the infected site (Sadikot et al., 2005). Infiltrating T cells produce IFN-γ to enhance phagocytic cells, especially polymorphonuclear neutrophils (PMN), to combat bacterial infection (Wagner et al., 2008). This may explain why phage-treated mice had high levels of IFN-γ in the lungs and very low levels of IFN-γ in the serum. We believe that this is beneficial in combating *P. aeruginosa*-mediated lung infections.

HMGB1 is considered to be the lethal endogenous mediator of endotoxins in mice. HMGB1 can be produced under the stimulation of endotoxins, TNFα, and IL-1β (Martinotti et al., 2015); moreover, recent studies have shown that cell damage also leads to HMGB1 expression (Kang et al., 2014). The levels of endotoxin, TNFα, and IL-1β in the phage treatment group were significantly lower than those in the control group, but the level of HMGB1 were higher than that of the control group. This suggests that treatment with KPP10 may induce cell damage. Here, we did not include experiments that would exclude the effects of cell damage, which is a limitation of our study.

Since 1900, phage therapy has been widely studied as treatment against bacterial infections. Phage therapy has many advantages: it has bactericidal properties, is self-generating, has little effect on normal microflora, is also effective against antibiotic-resistant bacteria, and seems to be able to destroy bacterial biofilms (Harper et al., 2014); however, controversy still exists regarding safety of phage therapy. While phages do not infect human cells, the endotoxin released by the phage associated Gram negative bacteria during bactericidal process of phage may trigger endotoxic shock in patients (Dickson and Lehmann, 2019). Phage therapy is currently used to treat skin infections and persistent lung infections in patients with cystic fibrosis (Krylov et al., 2016; Chang et al., 2020). The safety of phage therapy for treatment of acute lung infections caused

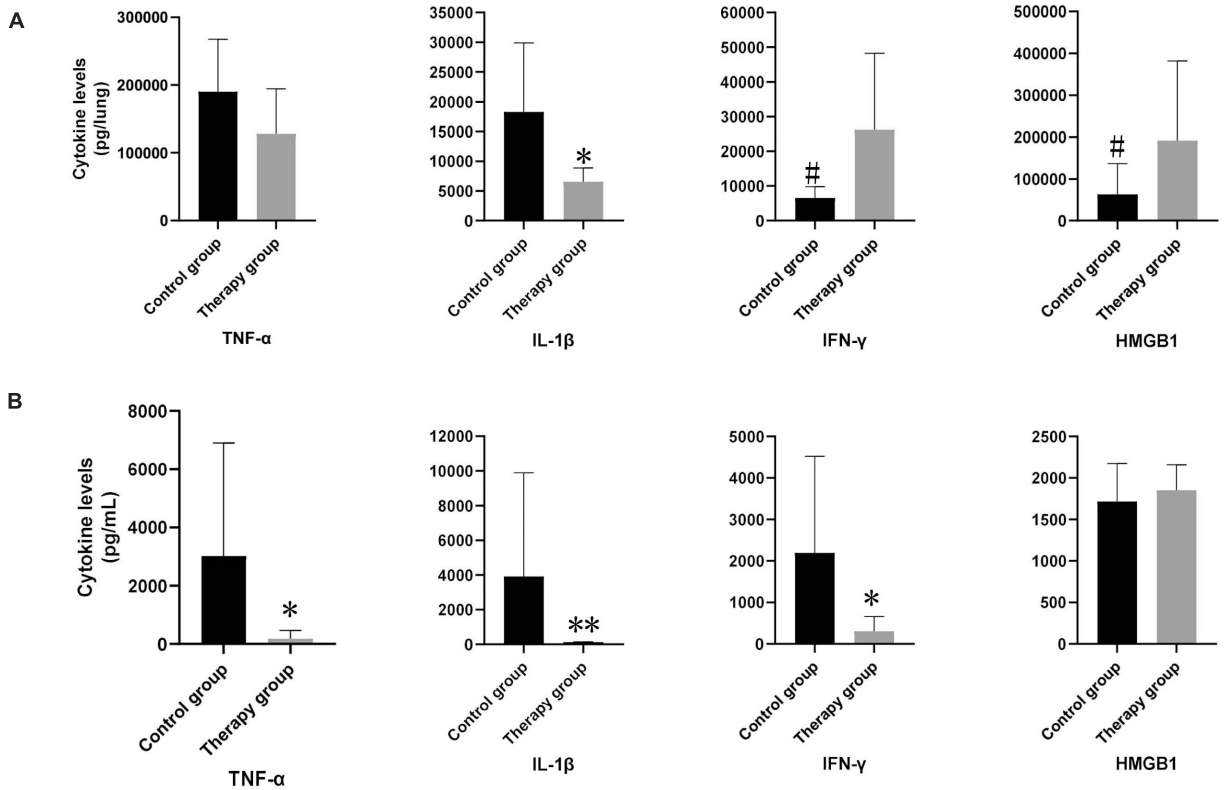

FIGURE 4 | The levels of inflammatory cytokines in mouse lungs and serum. In lung samples **(A)**, the levels of IL-1β in phage-treated mice (n = 6) were significantly lower than those in control mice (n = 6). In serum samples **(B)**, the levels of TNF-α, IL-1β and IFN-γ in phage-treated group were significantly lower than that of the control group, however, HMGB1 had no significant difference. Data are presented as mean ± SEM of two experiments (* < 0.05, ** < 0.01 vs. untreated control).

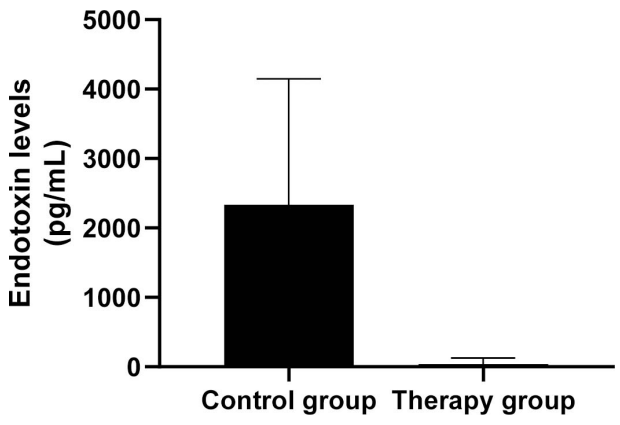

FIGURE 5 | Endotoxin levels in mouse serum. The level of endotoxin in the serum of phage-treated mice (n = 6) was significantly lower than that of the control mice (n = 6). Data are presented as mean ± SEM of two experiments (** < 0.01 vs. untreated control).

by gram-negative bacteria needs further study, though previous studies have shown that treatment with bacteriophage strain KPP10 can protect mice from intestinal septicemia caused by *P. aeruginosa* D4 (Matsumoto et al., 1997a,b, 1998a,b,c; Watanabe et al., 2007). We find that inhaled KPP10 also exerts a significant protective effect against pneumonia caused by *P. aeruginosa* D4.

The additional advantages of KPP10 bacteriophage and *P. aeruginosa* D4 strain are that the detail genomic data of these elements are readily available. No study investigated KPP10 against *P. aeruginosa* pneumonia before ours, although many phages have been studied in the past. We noticed that in some studies those used the same animal models as ours, the survival rate of the phage treatment group did not reach 100%, which can often be achieved by antibiotic therapy (Hua et al., 2018; Jeon and Yong, 2019). However, bacteriological data showed that the level of bacteria in the lung was significantly reduced. Therefore, we are concerned that phage therapy has the risk of causing endotoxic shock. Considering effectiveness and safety of phage KPP10 revealed by this study, phage therapy may be useful in treating lung *P. aeruginosa* infections. Further research should be conducted to elucidate the safety of phage therapy and the possibility of it being used as an alternative treatment in clinical settings.

DATA AVAILABILITY STATEMENT

The raw data supporting the conclusions of this article will be made available by the authors, without undue reservation.

ETHICS STATEMENT

The animal study was reviewed and approved by Tokyo Medical University Animal Care and Use Committee.

AUTHOR CONTRIBUTIONS

SN and TM: conception and design of the study, interpretation of data, and review the article. XY and AH: analysis and interpretation of data, collection and assembly of data, and drafting of the article. SM: phage preparation. All authors contributed to the article and approved the submitted version.

ACKNOWLEDGMENTS

We would like to thank T. Sugawara (Tokyo Medical University Hospital Central Clinical Laboratory) for his technical assistance.

REFERENCES

Berube, B. J., Rangel, S. M., and Hauser, A. R. (2016). *Pseudomonas aeruginosa*: breaking down barriers. *Curr. Genet.* 62, 109–113. doi: 10.1007/s00294-015-0522-x

Bourdin, G., Schmitt, B., Guy, L. M., Germond, J. E., Zuber, S., Michot, L., et al. (2014). Amplification and purification of T4-Like *Escherichia coli* phages for phage therapy: From laboratory to pilot scale. *Appl. Environ. Microbiol.* 80, 1469–1476. doi: 10.1128/AEM.03357-13

Buttenschoen, K., Radermacher, P., and Bracht, H. (2010). Endotoxin elimination in sepsis: Physiology and therapeutic application. *Langenbeck's Arch. Surg.* 395, 597–605. doi: 10.1007/s00423-010-0658-6

Caflisch, K. M., Suh, G. A., and Patel, R. (2019). Biological challenges of phage therapy and proposed solutions: a literature review. *Expert Rev. Anti. Infect. Ther.* 17, 1011–1041. doi: 10.1080/14787210.2019.1694905

Chang, R. Y. K., Morales, S., Okamoto, Y., and Chan, H. K. (2020). Topical application of bacteriophages for treatment of wound infections. *Transl. Res.* 220, 153–166. doi: 10.1016/j.trsl.2020.03.010

Coopersmith, C. M., Amiot, D. M., Stromberg, P. E., Dunne, W. M., Davis, C. G., Osborne, D. F., et al. (2003). Antibiotics improve survival and alter the inflammatory profile in a murine model of sepsis from *Pseudomonas aeruginosa* pneumonia. *Shock* 19, 408–14. doi: 10.1097/01.shk.0000054370.24363.ee

Debarbieux, L., Leduc, D., Maura, D., Morello, E., Criscuolo, A., Grossi, O., et al. (2010). Bacteriophages can treat and prevent *pseudomonas aeruginosa* lung infections. *J. Infect. Dis.* 201, 1096–104. doi: 10.1086/651135

Dickson, K., and Lehmann, C. (2019). Inflammatory response to different toxins in experimental sepsis models. *Int. J. Mol. Sci.* 20:341. doi: 10.3390/ijms20184341

Dufour, N., Delattre, R., Ricard, J. D., and Debarbieux, L. (2017). The lysis of pathogenic *Escherichia coli* by bacteriophages releases less endotoxin than by β-lactams. *Clin. Infect. Dis.* 64, 1582–1588. doi: 10.1093/cid/cix184

Forti, F., Roach, D. R., Cafora, M., Pasini, M. E., Horner, D. S., Fiscarelli, E. V., et al. (2018). Design of a broad-range bacteriophage cocktail that reduces *pseudomonas aeruginosa* biofilms and treats acute infections in two animal models. *Antimicrob. Agents Chemother.* 62, 2573–17. doi: 10.1128/AAC.02573-17

Gellatly, S. L., and Hancock, R. E. W. (2013). *Pseudomonas aeruginosa*: New insights into pathogenesis and host defenses. *Pathog. Dis.* 67, 159–173. doi: 10.1111/2049-632X.12033

Harper, D. R., Parracho, H. M. R. T., Walker, J., Sharp, R., Hughes, G., Werthén, M., et al. (2014). Bacteriophages and biofilms. *Antibiotics* 3, 270–284. doi: 10.3390/antibiotics3030270

Hua, Y., Luo, T., Yang, Y., Dong, D., Wang, R., Wang, Y., et al. (2018). Phage therapy as a promising new treatment for lung infection caused by carbapenem-resistant *Acinetobacter baumannii* in mice. *Front. Microbiol.* 2017:659. doi: 10.3389/fmicb.2017.02659

Jeon, J., and Yong, D. (2019). Two novel bacteriophages improve survival in Galleria mellonella infection and mouse acute pneumonia models infected with extensively drug-resistant *Pseudomonas aeruginosa*. *Appl. Environ. Microbiol.* 128, 2900–18. doi: 10.1128/AEM.02900-18

Jernigan, J. A., Hatfield, K. M., Wolford, H., Nelson, R. E., Olubajo, B., Reddy, S. C., et al. (2020). Multidrug-resistant bacterial infections in U.S. hospitalized patients, 2012-2017. *N. Engl. J. Med.* 382, 1309–1319. doi: 10.1056/NEJMoa1914433

Kang, R., Chen, R., Zhang, Q., Hou, W., Wu, S., Cao, L., et al. (2014). HMGB1 in health and disease. *Mol. Aspects Med.* 40, 1–116.

Krylov, V., Shaburova, O., Pleteneva, E., Bourkaltseva, M., Krylov, S., Kaplan, A., et al. (2016). Modular approach to select bacteriophages targeting *Pseudomonas aeruginosa* for their application to children suffering with cystic fibrosis. *Front. Microbiol.* 7:631. doi: 10.3389/fmicb.2016.01631

Kwiatek, M., Parasion, S., and Nakonieczna, A. (2020). Therapeutic bacteriophages as a rescue treatment for drug-resistant infections – an in vivo studies overview. *J. Appl. Microbiol.* 128, 985–1002. doi: 10.1111/jam.14535

Lepper, P., Held, T., Schneider, E., Bölke, E., Gerlach, H., and Trautmann, M. (2002). Clinical implications of antibiotic-induced endotoxin release in septic shock. *Intensive Care Med.* 28, 824–833. doi: 10.1007/s00134-002-1330-6

Mai, V., Ukhanova, M., Reinhard, M. K., Li, M., and Sulakvelidze, A. (2015). Bacteriophage administration significantly reduces *shigella* colonization and shedding by *shigella*-challenged mice without deleterious side effects and distortions in the gut microbiota. *Bacteriophage* 2015:124. doi: 10.1080/21597081.2015.1088124

Martinotti, S., Patrone, M., and Ranzato, E. (2015). Emerging roles for HMGB1 protein in immunity, inflammation, and cancer. *Immuno Targets Ther.* 4, 101–109.

Matsumoto, T., Tateda, K., Furuya, N., Miyazaki, S., Ohno, A., Ishii, Y., et al. (1998a). Efficacies of alkaline protease, elastase and exotoxin A toxoid vaccines against gut-derived *Pseudomonas aeruginosa* sepsis in mice. *J. Med. Microbiol.* 47, 303–308. doi: 10.1099/00222615-47-4-303

Matsumoto, T., Tateda, K., Miyazaki, S., Furuya, N., Ohno, A., Ishii, Y., et al. (1998b). Effect of immunisation with *Pseudomonas aeruginosa* on gut-derived sepsis in mice. *J. Med. Microbiol.* 47, 295–301. doi: 10.1099/00222615-47-4-295

Matsumoto, T., Tateda, K., Miyazaki, S., Furuya, N., Ohno, A., Ishii, Y., et al. (1998c). Effect of interleukin-10 on gut-derived sepsis caused by *Pseudomonas aeruginosa* in mice. *Antimicrob. Agents Chemother.* 42, 2853–2857. doi: 10.1128/aac.42.11.2853

Matsumoto, T., Tateda, K., Miyazaki, S., Furuya, N., Ohno, A., Ishii, Y., et al. (1997a). Immunomodulating effect of fosfomycin on gut-derived sepsis caused by *Pseudomonas aeruginosa* in mice. *Antimicrob. Agents Chemother.* 41, 308–313. doi: 10.1128/aac.41.2.308

Matsumoto, T., Tateda, K., Miyazaki, S., Furuya, N., Ohno, A., Ishii, Y., et al. (1997b). Adverse effects of tumour necrosis factor in cyclophosphamide-treated mice subjected to gut-derived *Pseudomonas aeruginosa* sepsis. *Cytokine* 9, 763–769. doi: 10.1006/cyto.1997.0222

Matsuzaki, S., Rashel, M., Uchiyama, J., Sakurai, S., Ujihara, T., Kuroda, M., et al. (2005). Bacteriophage therapy: A revitalized therapy against bacterial infectious diseases. *J. Infect. Chemother.* 11, 211–219. doi: 10.1007/s10156-005-0408-9

Nathwani, D., Raman, G., Sulham, K., Gavaghan, M., and Menon, V. (2014). Clinical and economic consequences of hospital-acquired resistant and multidrug-resistant *Pseudomonas aeruginosa* infections: A systematic review and meta-analysis. *Antimicrob. Resist. Infect.* 3:32. doi: 10.1186/2047-2994-3-32

Parker, C. M., Kutsogiannis, J., Muscedere, J., Cook, D., Dodek, P., Day, A. G., et al. (2008). Ventilator-associated pneumonia caused by multidrug-resistant organisms or *Pseudomonas aeruginosa*: Prevalence, incidence, risk factors, and outcomes. *J. Crit. Care* 23, 18–26. doi: 10.1016/j.jcrc.2008.02.001

Parkins, M. D., Somayaji, R., and Waters, V. J. (2018). Epidemiology, Biology, and Impact of Clonal *Pseudomonas aeruginosa* Infections in Cystic Fibrosis. *Clin. Microbiol. Rev.* 31:19. doi: 10.1128/CMR.00019-18

Patey, O., McCallin, S., Mazure, H., Liddle, M., Smithyman, A., and Dublanchet, A. (2019). Clinical indications and compassionate use of phage therapy: Personal experience and literature review with a focus on osteoarticular infections. *Viruses* 11:18. doi: 10.3390/v11010018

Payne, R. J. H., and Jansen, V. A. A. (2001). Understanding bacteriophage therapy as a density-dependent kinetic process. *J. Theor. Biol.* 208, 37–48. doi: 10.1006/jtbi.2000.2198

Rodriguez-Gonzalez, R. A., Leung, C. Y., Chan, B. K., Turner, P. E., and Weitz, J. S. (2020). Quantitative models of phage-antibiotic combination therapy. *mSystems* 5:784. doi: 10.1101/633784

Sadikot, R. T., Blackwell, T. S., Christman, J. W., and Prince, A. S. (2005). Pathogen-host interactions in *pseudomonas aeruginosa* pneumonia. *Am. J. Respir. Crit. Care Med.* 171, 1209–1223. doi: 10.1164/rccm.200408-1044SO

Surbatovic, M., Jevdjic, J., Veljovic, M., Popovic, N., Djordjevic, D., and Radakovic, S. (2013). Immune response in severe infection: Could life-saving drugs be potentially harmful? *Sci. World J.* 2013:852. doi: 10.1155/2013/961852

Taha, O. A., Connerton, P. L., Connerton, I. F., and El-Shibiny, A. (2018). Bacteriophage ZCKP1: A potential treatment for *Klebsiella pneumoniae* isolated from diabetic foot patients. *Front. Microbiol.* 2018:127. doi: 10.3389/fmicb.2018.02127

Uchiyama, J., Rashel, M., Takemura, I., Kato, S., Ujihara, T., Muraoka, A., et al. (2012). Genetic characterization of *Pseudomonas aeruginosa* bacteriophage KPP10. *Arch. Virol.* 157, 733–738. doi: 10.1007/s00705-011-1210-x

Viertel, T. M., Ritter, K., and Horz, H. P. (2014). Viruses versus bacteria-novel approaches to phage therapy as a tool against multidrug-resistant pathogens. *J. Antimicrob. Chemother.* 69, 2326–2336. doi: 10.1093/jac/dku173

Wagner, C., Kotsougiani, D., Pioch, M., Prior, B., Wentzensen, A., and Hänsch, G. M. (2008). T lymphocytes in acute bacterial infection: Increased prevalence of CD11b+ cells in the peripheral blood and recruitment to the infected site. *Immunology* 125, 503–509. doi: 10.1111/j.1365-2567.2008.02863.x

Watanabe, R., Matsumoto, T., Sano, G., Ishii, Y., Tateda, K., Sumiyama, Y., et al. (2007). Efficacy of bacteriophage therapy against gut-derived sepsis caused by *Pseudomonas aeruginosa* in mice. *Antimicrob. Agents Chemother.* 51, 446–452. doi: 10.1128/AAC.00635-06

World Health Organization (2013). *Global Priority List of Antibiotic-Resistant Bacteria to Guide Research, Discovery, and Development of New Antibiotics*. Geneva: WHO.

Conflict of Interest: The authors declare that the research was conducted in the absence of any commercial or financial relationships that could be construed as a potential conflict of interest.

frontiers in Microbiology

ORIGINAL RESEARCH
published: 14 July 2021
doi: 10.3389/fmicb.2021.649673

A Novel Polyvalent Bacteriophage vB_EcoM_swi3 Infects Pathogenic *Escherichia coli* and *Salmonella enteritidis*

*Bingrui Sui, Lili Han, Huiying Ren, Wenhua Liu and Can Zhang**

College of Veterinary Medicine, Qingdao Agricultural University, Qingdao, China

A novel virulent bacteriophage vB_EcoM_swi3 (swi3), isolated from swine feces, lyzed 9% (6/65) of *Escherichia coli* and isolates 54% (39/72) of *Salmonella enteritidis* isolates, which were all clinically pathogenic multidrug-resistant strains. Morphological observation showed that phage swi3 belonged to the *Myoviridae* family with an icosahedral head (80 nm in diameter) and a contractile sheathed tail (120 nm in length). At the optimal multiplicity of infection of 1, the one-step growth analysis of swi3 showed a 25-min latent period with a burst size of 25-plaque-forming units (PFU)/infected cell. Phage swi3 remained stable both at pH 6.0–8.0 and at less than 50°C for at least 1 h. Genomic sequencing and bioinformatics analysis based on genomic sequences and the terminase large subunit showed that phage swi3 was a novel member that was most closely related to *Salmonella* phages and belonged to the *Rosemountvirus* genus. Phage swi3 harbored a 52-kb double-stranded DNA genome with 46.02% GC content. Seventy-two potential open reading frames were identified and annotated, only 15 of which had been assigned to functional genes. No gene associated with pathogenicity and virulence was identified. The effects of phage swi3 in treating pathologic *E. coli* infections *in vivo* were evaluated using a mouse model. The administration of a single intraperitoneal injection of swi3 (10^6 PFU) at 2 h after challenge with the *E. coli* strain (serotype K88) (10^8 colony-forming units) sufficiently protected all mice without toxic side effects. This finding highlighted that phage swi3 might be used as an effective antibacterial agent to prevent *E. coli* and *S. enteritidis* infection.

Keywords: bacteriophage vB_EcoM_swi3, *Escherichia coli*, *Salmonella enteritidis*, biological characteristics, genomic analysis, phage therapy

OPEN ACCESS

Edited by:
Krishna Mohan Poluri, Indian Institute of Technology Roorkee, India

Reviewed by:
Ahmed Askora, Zagazig University, Egypt
Heejoon Myung, Hankuk University of Foreign Studies, South Korea

***Correspondence:**
Can Zhang
cleverflame@163.com

Specialty section:
This article was submitted to Antimicrobials, Resistance and Chemotherapy, a section of the journal Frontiers in Microbiology

Received: *13 January 2021*
Accepted: *17 May 2021*
Published: *14 July 2021*

Citation:
Sui B, Han L, Ren H, Liu W and Zhang C (2021) A Novel Polyvalent Bacteriophage vB_EcoM_swi3 Infects Pathogenic Escherichia coli and Salmonella enteritidis. Front. Microbiol. 12:649673. doi: 10.3389/fmicb.2021.649673

INTRODUCTION

Pathogenic *Escherichia coli* and *Salmonella enteritidis* are the major opportunistic pathogens in animals and humans and are frequently reported worldwide (Majowicz et al., 2010; Yang et al., 2017; Jajere, 2019). Rearing animals on a large scale can increase pathogen infections. Particularly in young animals in high-density farming models, outbreaks caused by *E. coli* and *S. enteritidis* are usually associated with gastroenteritis and diarrhea and lead to serious infections and high mortality rates. To control enteric infections, antibiotics are widely used in breeding farms to treat infections. However, the widespread use of antibiotics had led to a series of problems, such as drug

resistance, environmental pollution, and antibiotic residues in animal products (Paitan, 2018; Poirel et al., 2018; Jajere, 2019; Thames and Theradiyil Sukumaran, 2020). The prevention and control of bacterial infection urgently require the development of alternative antibiotic products.

Bacteriophages (phages) are viruses that exclusively infect bacteria and are widely distributed in the environment (Parikka et al., 2017). In the past decade, phages have demonstrated a promising alternative antibiotic role in the control of pathogenic bacteria in animals and humans (Chang et al., 2018; Rehman et al., 2019). Additionally, phages are a resource for many biotechnological applications, such as antimicrobial enzymes, bacteria typing, and phage display libraries (Salmond and Fineran, 2015). However, the host range of reported phages is commonly limited to a single species, and few phages can infect more than one species. Therefore, phage cocktails were developed to control polymicrobial infections in phage therapy. In our opinion, a broader-spectrum phage would presumably lead to fewer failures due to a mismatched host and phage combination. *Myoviridae* phages usually exhibit a broader host range than *Siphoviridae* and *Podoviridae* (Chibani-Chennoufi et al., 2004). Moreover, it is necessary to acquire a clear understanding of biology and genetic information to ensure effectiveness and safety before the use of phages. A suitable phage candidate for effective biocontrol should be a lytic phage with a broad host range against a variety of bacterial strains and should not carry virulence and pathogenicity genes in the genome. To date, the reported phages in the database have only been the tip of the iceberg, and most of them belong to the *Myoviridae* or the *Siphoviridae* families of tailed phages (Yu et al., 2006).

In this study, a novel polyvalent bacteriophage vB_EcoM_swi3 was isolated and characterized. Phage swi3 showed a wide host range; it could lyze 9% (6/65) of *E. coli* strain and 54% (39/72) of *S. enteritidis* strain, and it showed a good protective effect in a mouse model challenged with pathogenic *E. coli*. These data provide valuable information to assess the potential of phage swi3 as a biocontrol agent against pathogenic bacteria.

MATERIALS AND METHODS

Bacterial Strains and Animals

Sixty-five pathogenic *E. coli* and 72 pathogenic *S. enteritidis* clinical isolates were used in this study (these strains were identified as different strains from different batches of diseased animals in Hebei, Shandong, and Jilin from 2010 to 2020, and drug sensitivity tests revealed different drug resistances). The bacterial strains were cultured in Luria–Bertani culture (LB) at 37°C and stored in 30% glycerol at −80°C.

Female BALB/c mice, 5 weeks of age (20–25 g in weight), were purchased from the Experimental Animal Center of Shandong, China.

All animal procedures were performed in strict accordance with the Regulations for the Administration of Affairs Concerning Experimental Animals, approved through the State Council of the People's Republic of China (1988.11.1), and with the approval of the Animal Welfare and Research Ethics Committee at Qingdao Agricultural University.

Propagation and Morphology of Phage Swi3

A pathogenic clinical strain of *E. coli* (serotype K88), hereafter named *E. coli* K88, was used in this study for phage isolation. Feces and seawater samples were collected from a pig farm in Shandong, China. Phage isolation was performed using the standard enrichment method as described before but with slight modifications (Lu et al., 2017). In brief, an overnight culture of 50 ml of *E. coli* K88 was cocultured with collected samples at 37°C for 24 h and then centrifuged at 12,000 rpm for 30 min. The supernatant was filtered with a sterile disposable membrane filter (0.22 μm). Then, 100 μl of the filtered supernatant was added to 100 μl of log-phase *E. coli* K88 and mixed with 3 ml of prewarmed NA top agar (0.7% agar), spread on an NA plate, and cultured for 4 h at 37°C. A single plaque was selected and picked from the plate. Then, the plaque was leached overnight with 0.9% normal saline. This procedure was repeated three times to obtain purified phages. Electron micrographs of purified phage particles were obtained according to a standard method (Kreienbaum et al., 2020). A 10-μl phage sample was dropped onto carbon-coated grids, negatively stained with 2% (w/v) aqueous uranyl acetate (pH 4.0) for 5 min, and air-dried. The samples were observed with a transmission electron microscope (HT7700, Hitachi, Japan) at 80-kV accelerating voltage.

Host Range Determination of Phage Swi3

Sixty-five *E. coli* and 72 *S. enteritidis* clinical isolates were used to test the host range of phage swi3 by the spot method. Briefly, 10 μl of diluted phage suspension (1×10^5 PFU/ml) was spotted on each bacterial lawn on agar plates and incubated at 37°C for 4 h. The presence of plaques was examined. Additionally, the efficiency of plating was tested as described before (Ding et al., 2020).

Optimal Multiplicity of Infection of Phage Swi3

To determine the optimal multiplicity of infection (MOI) of phage swi3, *E. coli* K88 was cultured in LB broth at 37°C with shaking at 250 rpm until the early exponential phase (5×10^7 CFU/ml). Phage swi3 was cocultured with *E. coli* K88 in 10 ml of LB broth at different MOIs (0.0001, 0.001, 0.01, 0.1, 1, and 10) (Abedon, 2016). A culture of bacteria without phage swi3 (0 MOI) was used as a control. After 2.5 h of incubation, the culture was centrifuged at 10,000 rpm for 10 min, and then the supernatant was used to determine the phage titers of phage swi3 by the double-layered agar method. The MOI resulting in the highest phage titer was considered an optimal MOI and used in subsequent large-scale phage production.

One-Step Growth of Phage Swi3

The burst size and the latent period of phage swi3 were determined by one-step growth analysis as previously described

(Sun et al., 2012). In brief, 200 μl of phage suspension (10^6 PFU) was mixed with 200 ml of bacterial culture (5×10^6 CFU/ml), incubated at 37°C for 5 min, and then centrifuged, and the cell pellet was resuspended in 500 μl of LB broth. Aliquots were taken, and the phage titers were immediately determined by the double-layered agar method. This assay was performed in triplicate.

Thermal/pH Stability of Phage Swi3

The stability of phage swi3 was tested as previously described (Akhwale et al., 2019). Briefly, thermal stability was assessed by incubating the phage swi3 (4×10^8 PFU/ml) at 40, 50, 60, 70, and 80°C, and aliquots (100 μl) were taken at 20, 40, and 60 min. To evaluate the stability of phage swi3 at various pH values (2, 3, 4, 5, 6, 7, 8, 9, 10, 11, 12, and 13), phage suspensions were incubated in LB broth with different pH values at 37°C for 1, 2, and 3 h and then assayed by the double-layered agar method. All assays were performed in triplicate.

Sequencing and Genome Analysis of Phage Swi3

Phage genomic DNA was extracted using a Virus Genome Extract DNA/RNA Kit (Tiangen, Inc., Beijing, China) according to the manufacturer's instructions. Then, the extracted genomic DNA was sent to Biozeron Company (Shanghai, China) for high-throughput sequencing on an Illumina HiSeq platform and assembled with ABySS, v2.0.2[1]. Contigs were assembled using the *de novo* assembly algorithm Newbler, version 3.0, with default parameters (Bao et al., 2014). Potential open reading frames were predicted and annotated using RAST[2] and GeneMark[3] (Besemer and Borodovsky, 2005; Aziz et al., 2008). Additionally, the genome sequence, the terminase large subunit, and the tail-associated protein amino acid sequence of phage swi3 were compared separately in the GenBank database of NCBI, and all homologous phages were selected to construct the phylogenetic tree of phage swi3 using the neighbor-joining method with default parameters in MEGAX software. The genomes of phage swi3, *Salmonella phage BP63* (KM366099.1), *Salmonella phage LSE7621* (MK568062.1), *Salmonella phage UPF_BP2* (NC_048649.1), and *Salmonella phage vB_SenM_PA13076* (MF740800.1) were compared and performed using Mauve software with a default parameter (Darling et al., 2004).

Antibacterial Activity of Phage Swi3 in a Mouse Model Challenged With *E. coli* K88

To test the antibacterial activity of phage swi3, the 50% lethal dose (LD50) of *E. coli* K88 was first determined. In brief, 28 5-week-old female BALB/c mice were randomly divided into four groups. Each group was treated orally with different doses of *E. coli* K88 (10^6, 10^7, 10^8, and 10^9 CFU). The LD50 was determined based on the mortality of mice and used in subsequent challenge tests. To test the protective effect of phage swi3 on mice, 42 5-week-old female BALB/c mice were randomly divided into six groups (a–f). Groups a–d were inoculated orally with 10^8 CFU of *E. coli* K88. Then, groups a–c were inoculated intraperitoneally with a single dose (10^5, 10^6, and 10^7 PFU, respectively) of phage swi3 at 2 h after the bacterial challenge. Control group d was inoculated with an equivalent volume of LB instead of phage swi3, control group e was treated with 10^7 PFU of phage swi3 without *E. coli* K88 challenge, and control group f only took an equal volume of LB orally. Then, the mice were observed daily for 5 days to record the clinical signs and cumulative mortality. At the same time, blood and feces were collected every 2 h on the first day and every 24 h after the first day to detect the metabolic dynamics of bacteria and phage swi3 in the mice.

Nucleotide Sequence Accession Number

The sequence data of swi3 were deposited at GenBank under accession number MT768059.

RESULTS

Morphology of Phage Swi3

A novel virulent phage was isolated from *E. coli* K88 and observed by transmission electron microscopy. Phage swi3 has a regular icosahedral head (80 nm in diameter) and a contractile sheathed tail 120 nm in length (**Figure 1**). Thus, phage swi3 belonged to the family *Myoviridae*, order *Caudovirales*, following the current guidelines of the International Committee on Taxonomy of Viruses (ICTV). According to the novel universal system of bacteriophage naming, the suggested full name of phage swi3 will be vB_EcoM_swi3 (Lavigne et al., 2009).

Host Range of Phage Swi3

The swi3 host range was determined using 65 *E. coli* strains and 72 *S. enteritidis* strains (**Supplementary Table 1**). Interestingly, phage swi3 showed characteristics of a wide range across species, not only having a certain lytic ability for six of the 65 *E. coli* strains but also having a lytic ability for 39 of the 72 *S. enteritidis* strains.

The Growth of Phage Swi3

The biological characteristics of phage swi3 were measured by the double-layer plate method (Zhang et al., 2013). When the MOI was 1, phage swi3 had the highest titer of 6.4×10^8 PFU/ml after proliferation. The one-step growth analysis showed that the incubation period of swi3 was approximately 25 min, after which there was a rapid increase in the number of released viral particles. It took about 75 min for swi3 to reach the growth plateau phase with a burst size of approximately 25 PFU/infected cells (**Figure 2A**). In addition, phage swi3 remained stable in the pH range of 6–8 (**Figure 2B**) and at a temperature less than 50°C for at least 1 h (**Figure 2C**).

Genome Analysis of Phage Swi3

The genome of phage swi3 was sequenced and analyzed. The general characteristics of the genome include a total of 52,782 bp

[1]http://www.bcgsc.ca/platform/bioinfo/software/abyss

[2]http://rast.nmpdr.org

[3]http://opal.biology.gatech.edu/GeneMark/

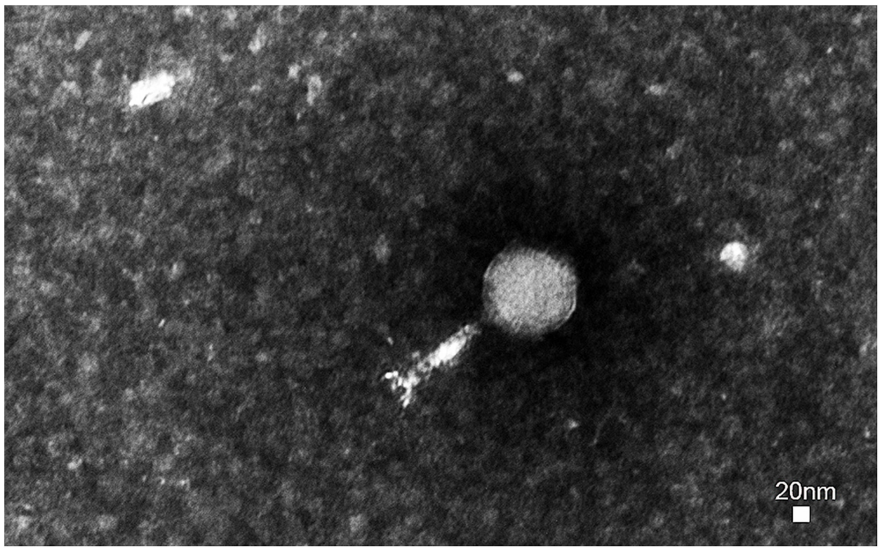

FIGURE 1 | Morphology of phage swi3. Phage swi3 was negatively stained with 2% uranyl acetate and observed by transmission electron microscopy at an accelerating voltage of 80 kV. The scale bars represent 20 nm.

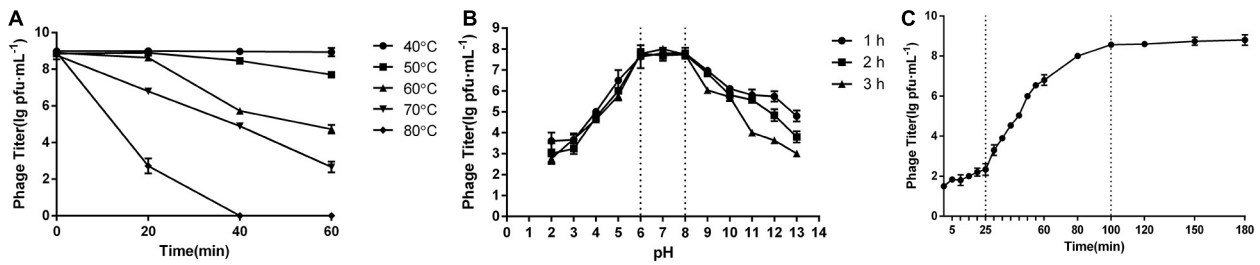

FIGURE 2 | Biological characteristics of phage swi3. **(A)** One-step growth curve, **(B)** pH stability, and **(C)** thermal stability. Data are expressed as means. At the optimal multiplicity of infection of 1, the one-step growth analysis of swi3 showed a 25-min latent period with a burst size of 25-plaque-forming units (PFU)/infected cell. Phage swi3 remained stable both at pH 6.0–8.0 and less than 50°C for at least 1 h.

with an overall GC content of 46.02%. Seventy-two *orf*s were predicted, 39 of which were positive-stranded, while the others were negative-stranded. Only 15 of 72 *orf*s were annotated as functional genes, including six structural-related genes (*orf* 19, *orf* 20, *orf* 21, *orf* 22, *orf* 27, and *orf* 33), seven genes associated with transcription and replication (*orf* 14, *orf* 18, *orf* 52, *orf* 53, *orf* 57, *orf* 59, and *orf* 72), and two lysis-related genes (*orf* 44 and *orf* 45). A detailed phage swi3 genome annotation showed that the *orf*s related to transcription and replication were mainly concentrated in the downstream part of the whole genome, while the structurally related *orfs* were mainly concentrated in the upstream part of the whole genome sequence (**Figure 3**).

Phylogenetic Analysis of Phage Swi3

The phylogenetic tree of phage swi3 was constructed based on the genomic sequence, the terminase large subunit (encoded by *orf* 19) sequence, the tail-associated protein (encoded by *orf* 27), and the tail tape measure protein (encoded by *orf* 33), using the neighbor-joining method with the default parameters in MEGAX software.

Based on the terminase large subunit, most comparable phages had less than 60% homology, a total of 10 phages in NCBI showed high similarities (>94%), and all of them belonged to *Salmonella* phages. Only *Salmonella virus BP63* (KM366099.1) was included in ICTV, with 98% coverage rate and 97.73% identity. The phylogenetic tree showed that 11 phages belonged to two groups, phage swi3 and eight more phages belonged to the *Rosemountvirus* genus, and the other two phages belonged to the *Loughboroughvirus* genus (**Supplementary Figure 1**). Based on the whole-genome sequence, the phylogenetic tree was highly consistent with that of the terminase large subunit; all homologous phages were divided into two groups, and phage swi3 belonged to the *Rosemountvirus* genus. Additionally, all the homologous phages were *Salmonella* phages (**Supplementary Figure 2**). The genomic comparison results showed that no rearrangement or inversion occurred in the phage swi3 genome (**Supplementary Figure 3**).

Only two tail-related proteins were annotated among the known *orfs*: the tail-associated protein (encoded by *orf* 27) and the tail tape measure protein (encoded by *orf* 33). Their

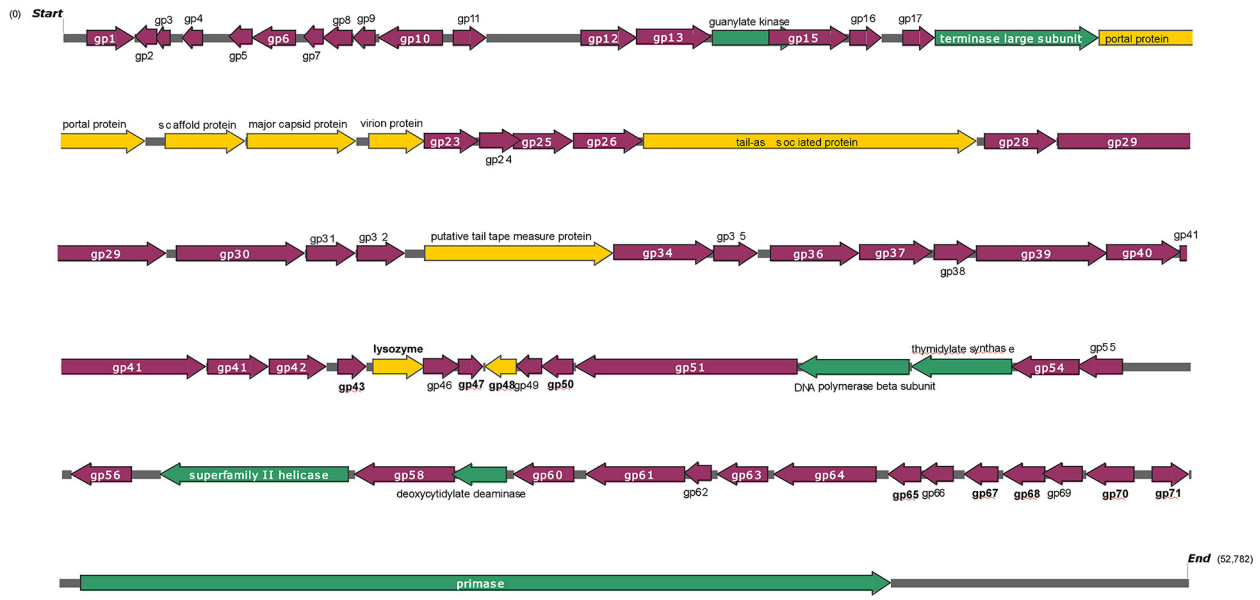

FIGURE 3 | Genome structure of phage swi3. The arrow represents the direction of transcription. Different colors represent open reading frames with different predictive functions. The structural proteins are represented in yellow, blue indicates cleavage-related proteins, the proteins associated with transcriptional transcription are expressed in green, and hypothetical proteins are represented in purple.

phylogenetic trees were constructed. Based on the tail-associated protein, only four comparable phages were found in the NCBI database with a high homology (>82.7%), and all of them were *Salmonella* phages. Other phages in the database showed less than 45% homology (**Supplementary Figure 4**). Based on the tail tape measurement protein, all homologous phages also belonged to *Salmonella* phages with more than 70% similarity (**Supplementary Figure 5**).

Protective Effects of Phage Swi3 in a Mouse Model Challenged With *E. coli* K88

The LD50 of *E. coli* K88 on mice was determined as 10^8 CFU, and the protective effects of phage swi3 were tested in a mouse model challenged with *E. coli* K88. There were obvious protective effects of phage swi3 in the bacteria-challenged mouse model ($p < 0.05$). After the challenge with *E. coli* K88, all mice in control group d died within 1 day; their lungs, liver, spleen, and kidneys showed varying degrees of bleeding and swelling, and *E. coli* K88 was isolated from these diseased organs. All mice in control groups f and e had good health until the end of the experiment, and no organ lesions were found (**Supplementary Figure 6**). In groups a–c, different doses of phage swi3 showed a good protective effect on *E. coli* K88-challenged mice. Compared with control group d, except for one mouse in group a that died on the second day, all mice survived, and no organ lesions were found (**Figure 4A**). The results indicated that a single intraperitoneal injection of swi3 (10^6 PFU) at 2 h after oral challenge with *E. coli* K88 could sufficiently protect all mice without toxic side effects.

In addition, the dynamics of bacteria and phages in the blood and feces were measured. *E. coli* K88 entered the blood and reached its peak (10^8 CFU/ml) 1.5 h after inoculation. Phage swi3 was intraperitoneally injected into the mice, detected in the blood in a short time, and then cleared *E. coli* K88 within 8.5–51 h in the blood; no bacteria or phage could be detected after 51 h (**Figures 4B,C**). Meanwhile, the dynamics of phage swi3 in feces were also measured. With the increase in phage inoculation dose, the phage detection time in feces was prolonged, ranging from 23 to 99 h (**Figure 4D**).

DISCUSSION

Escherichia coli and *Salmonella enteritidis* are becoming increasingly important opportunistic pathogens worldwide that endanger animal breeding industries. The difficulties in treating multidrug-resistant strains and the specificity of phage therapy prompted researchers to focus on phage therapy. In this study, we isolated a novel lytic phage swi3 from swine feces, which showed a broad host range against multidrug-resistant *E. coli* and *S. enteritidis*.

Generally, bacteriophages show strong host specificity and usually display a species-limited host range. To our knowledge, few phages infecting more than one species of bacteria have been reported (Park et al., 2012; Amarillas et al., 2016; Pham-Khanh et al., 2019). In this study, phage swi3 was isolated from *E. coli* k88, but the phylogenetic tree analysis results based on the whole-genome sequence and the terminase large subunit showed that all phages with homology in the database were *S. enteritidis* phages, and the tail-associated protein and the tail tape measure protein were also *S. enteritidis* phages, which attracted our attention. In general, the host range of phages is

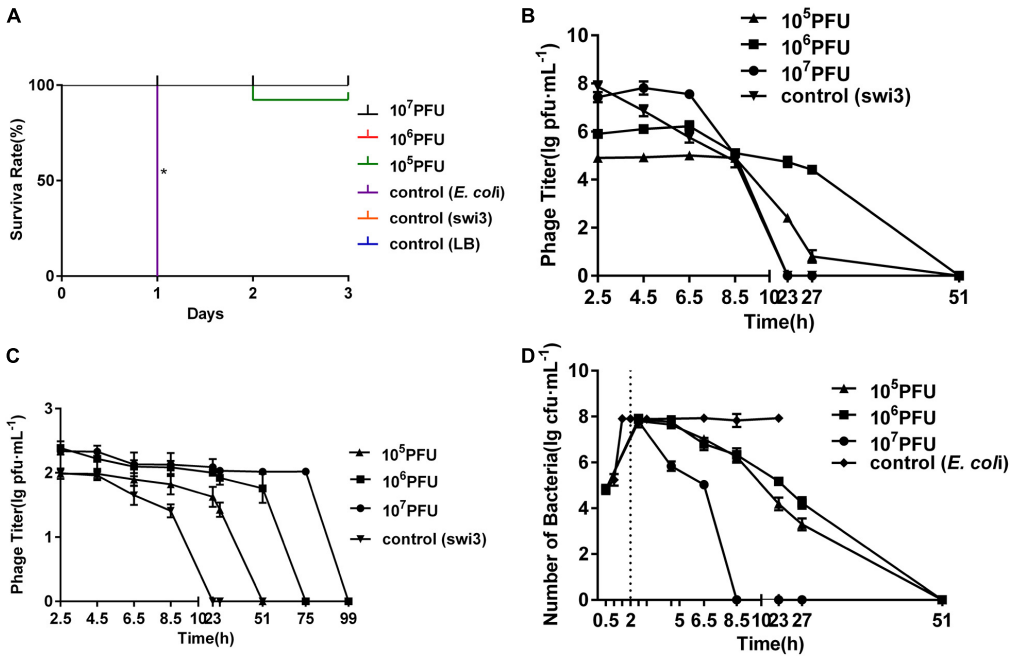

FIGURE 4 | Phage swi3 rescued mice from *Escherichia coli* K88 infection. **(A)** Survival rates. The mice were inoculated orally with 10^8 colony-forming units of the *E. coli* K88 strain. The data were expressed as means ± SD and statistically analyzed using the one-way ANOVA method at a level of significance $^*p < 0.05$ (GraphPad Software, Inc., San Diego, CA, United States). At 2 h later, different phage doses were introduced intraperitoneally to treat the challenged mice. **(B)** Dynamic changes of bacteria in blood in different groups. **(C)** Dynamic changes of phage in blood in different groups. **(D)** Dynamic changes of phage in feces in different groups.

related to their genomes. Therefore, two tail-related proteins were selected for BLAST analysis with the sequences in the database. The phylogenetic tree based on the tail-associated protein and the tail tape measure protein also showed a homology with the *S. enteritidis* phages. Thus, we hypothesized that phage swi3 might be able to lyze *S. enteritidis* phages. To test our hypothesis, *S. enteritidis* strains were selected to detect the host range of phage swi3, and 39 of 72 strains could be lyzed. Therefore, the phage swi3 could lyze not only *E. coli* but also *S. enteritidis*. The verification test showed that the host bacterial species of the phage could be preliminarily inferred through homology analysis, which was helpful to determine the phage host spectrum. It was speculated that the interspecific recognition mechanism of phage swi3 might be related to its infection process. The phage swi3 belonged to *Myoviridae*, which first bound to the corresponding receptor on the surface of the host bacteria through the receptor binging protein (RBP) on the tail fiber so that the phage adsorbed to the surface of the host bacteria and then initiated the process of phage infection (Bertozzi Silva et al., 2016). The phage swi3 could lyze *Salmonella* and *E. coli*, so its RBP needed to recognize receptors not only on the surface of *E. coli* but also on the surface of *S. enteritidis*. In addition, it was possible that the unknown *orf*-encoded proteins of phage swi3 were involved in the host adsorption process, which requires further analysis and verification. Phage swi3 could infect *E. coli* and *S. enteritidis* efficiently and showed a wide host range, which made it suitable for use as a biological control agent.

In the past 10 years, the application of phages in the prevention and control of bacterial diseases in animal reproduction has been widely reported. The results of animal experiments *in vivo* are different, but they all showed that phage preparations have no toxicity or side effects on the animal body, and due to the characteristics of phage proliferation with the host bacteria, a low-dose phage preparation can have a good bactericidal effect (Schneider et al., 2018; Balasubramanian et al., 2019; Kaabi and Musafer, 2019). In this study, a mouse model challenged with *E. coli* K88 was used to test the protective effect of phage swi3. The results showed that a low dose of 10^6 PFU of phage swi3 could protect mice from *E. coli* attack without any obvious side effects, and the phage was cleared within a short period of time because of the animal immune clearance response, which was consistent with previous reports (Li et al., 2015).

In conclusion, phage swi3 had a broad host spectrum including *E. coli* and *S. enteritidis*; it can clear bacteria in animals within a short time without side effects and has a potential value in the treatment of bacterial diseases.

DATA AVAILABILITY STATEMENT

The datasets presented in this study can be found in online repositories. The names of the repository/repositories and accession number(s) can be found below: https://www.ncbi.nlm.nih.gov/genbank/, MT768059.

ETHICS STATEMENT

The animal study was reviewed and approved by the Animal Welfare and Research Ethics Committee at Qingdao Agriculture University.

AUTHOR CONTRIBUTIONS

BS performed the experiments, analyzed the data, and wrote this manuscript. LH, HR, and WL performed the experiments. CZ designed the experiments and revised the manuscript. All authors contributed to the article and approved the submitted version.

FUNDING

This work was supported by the National Key R&D Program of China (2018YFD0501403) and the Shandong Key Research and Development Program (2019GNC106108).

SUPPLEMENTARY MATERIAL

The Supplementary Material for this article can be found online at: https://www.frontiersin.org/articles/10.3389/fmicb.2021.649673/full#supplementary-material

REFERENCES

Abedon, S. T. (2016). Phage therapy dosing: the problem(s) with multiplicity of infection (MOI). *Bacteriophage* 6:e1220348. doi: 10.1080/21597081.2016.1220348

Akhwale, J. K., Rohde, M., Rohde, C., Bunk, B., Sproer, C., Boga, H. I., et al. (2019). Isolation, characterization and analysis of bacteriophages from the haloalkaline lake Elmenteita, Kenya. *PLoS One* 14:e0215734. doi: 10.1371/journal.pone.0215734

Amarillas, L., Chaidez, C., Gonzalez-Robles, A., and Leon-Felix, J. (2016). Complete genome sequence of new bacteriophage phiE142, which causes simultaneously lysis of multidrug-resistant *Escherichia coli* O157:H7 and *Salmonella enterica*. *Stand. Genomic Sci.* 11:89. doi: 10.1186/s40793-016-0211-5

Aziz, R. K., Bartels, D., Best, A. A., DeJongh, M., Disz, T., Edwards, R. A., et al. (2008). The RAST Server: rapid Annotations using Subsystems Technology. *BMC Genomics* 9:75. doi: 10.1186/1471-2164-9-75

Balasubramanian, S., Osburne, M. S., BrinJones, H., Tai, A. K., and Leong, J. M. (2019). Prophage induction, but not production of phage particles, is required for lethal disease in a microbiome-replete murine model of enterohemorrhagic E. coli infection. *PLoS Pathog.* 15:e1007494. doi: 10.1371/journal.ppat.1007494

Bao, E., Jiang, T., and Girke, T. (2014). AlignGraph: algorithm for secondary de novo genome assembly guided by closely related references. *Bioinformatics* 30, i319–i328. doi: 10.1093/bioinformatics/btu291

Bertozzi Silva, J., Storms, Z., and Sauvageau, D. (2016). Host receptors for bacteriophage adsorption. *FEMS Microbiol. Lett.* 363:fnw002. doi: 10.1093/femsle/fnw002

Besemer, J., and Borodovsky, M. (2005). GeneMark: web software for gene finding in prokaryotes, eukaryotes and viruses. *Nucleic Acids Res.* 33, W451–W454.

Chang, R. Y. K., Wallin, M., Lin, Y., Leung, S. S. Y., Wang, H., Morales, S., et al. (2018). Phage therapy for respiratory infections. *Adv. Drug Deliv. Rev.* 133, 76–86. doi: 10.1016/j.addr.2018.08.001

Chibani-Chennoufi, S., Bruttin, A., Dillmann, M. L., and Brussow, H. (2004). Phage-host interaction: an ecological perspective. *J. Bacteriol.* 186, 3677–3686. doi: 10.1128/JB.186.12.3677-3686.2004

Darling, A. C., Mau, B., Blattner, F. R., and Perna, N. T. (2004). Mauve: multiple alignment of conserved genomic sequence with rearrangements. *Genome Res.* 14, 1394–1403. doi: 10.1101/gr.2289704

Ding, T., Sun, H., Pan, Q., Zhao, F., Zhang, Z., and Ren, H. (2020). Isolation and characterization of Vibrio parahaemolyticus bacteriophage vB_VpaS_PG07. *Virus Res.* 286:198080. doi: 10.1016/j.virusres.2020.198080

Jajere, S. M. (2019). A review of *Salmonella enterica* with particular focus on the pathogenicity and virulence factors, host specificity and antimicrobial resistance including multidrug resistance. *Vet. World* 12, 504–521. doi: 10.14202/vetworld.2019.504-521

Kaabi, S. A. G., and Musafer, H. K. (2019). An experimental mouse model for phage therapy of bacterial pathogens causing bacteremia. *Microb. Pathog.* 137:103770. doi: 10.1016/j.micpath.2019.103770

Kreienbaum, M., Dorrich, A. K., Brandt, D., Schmid, N. E., Leonhard, T., Hager, F., et al. (2020). Isolation and Characterization of Shewanella Phage Thanatos Infecting and Lysing Shewanella oneidensis and Promoting Nascent Biofilm Formation. *Front. Microbiol.* 11:573260. doi: 10.3389/fmicb.2020.573260

Lavigne, R., Darius, P., Summer, E. J., Seto, D., Mahadevan, P., Nilsson, A. S., et al. (2009). Classification of Myoviridae bacteriophages using protein sequence similarity. *BMC Microbiol.* 9:224. doi: 10.1186/1471-2180-9-224

Li, Z., Venegas, V., Nagaoka, Y., Morino, E., Raghavan, P., Audhya, A., et al. (2015). Necrotic Cells Actively Attract Phagocytes through the Collaborative Action of Two Distinct PS-Exposure Mechanisms. *PLoS Genet.* 11:e1005285. doi: 10.1371/journal.pgen.1005285

Lu, L., Cai, L., Jiao, N., and Zhang, R. (2017). Isolation and characterization of the first phage infecting ecologically important marine bacteria Erythrobacter. *Virol. J.* 14:104. doi: 10.1186/s12985-017-0773-x

Majowicz, S. E., Musto, J., Scallan, E., Angulo, F. J., Kirk, M., O'Brien, S. J., et al. (2010). The Global Burden of Nontyphoidal*Salmonella*Gastroenteritis. *Clin. Infect. Dis.* 50, 882–889. doi: 10.1086/650733

Paitan, Y. (2018). Current Trends in Antimicrobial Resistance of *Escherichia coli*. *Curr. Top. Microbiol. Immunol.* 416, 181–211. doi: 10.1007/82_2018_110

Parikka, K. J., Le Romancer, M., Wauters, N., and Jacquet, S. (2017). Deciphering the virus-to-prokaryote ratio (VPR): insights into virus-host relationships in a variety of ecosystems. *Biol. Rev. Camb. Philos. Soc.* 92, 1081–1100. doi: 10.1111/brv.12271

Park, M., Lee, J. H., Shin, H., Kim, M., Choi, J., Kang, D. H., et al. (2012). Characterization and comparative genomic analysis of a novel bacteriophage, SFP10, simultaneously inhibiting both *Salmonella enterica* and *Escherichia coli* O157:H7. *Appl. Environ. Microbiol.* 78, 58–69. doi: 10.1128/AEM.06231-11

Pham-Khanh, N. H., Sunahara, H., Yamadeya, H., Sakai, M., Nakayama, T., Yamamoto, H., et al. (2019). Isolation, Characterisation and Complete Genome Sequence of a Tequatrovirus Phage, *Escherichia* phage KIT03, Which Simultaneously Infects *Escherichia coli* O157:H7 and *Salmonella enterica*. *Curr. Microbiol.* 76, 1130–1137. doi: 10.1007/s00284-019-01738-0

Poirel, L., Madec, J.-Y., Lupo, A., Schink, A.-K., Kieffer, N., Nordmann, P., et al. (2018). Antimicrobial Resistance in *Escherichia coli*. *Microbiol. Spectr.* 6, 289–316. doi: 10.1128/microbiolspec.ARBA-0026-2017

Rehman, S., Ali, Z., Khan, M., Bostan, N., and Naseem, S. (2019). The dawn of phage therapy. *Rev. Med. Virol.* 29:e2041. doi: 10.1002/rmv.2041

Salmond, G. P. C., and Fineran, P. C. (2015). A century of the phage: past, present and future. *Nat. Rev. Microbiol.* 13, 777–786. doi: 10.1038/nrmicro3564

Schneider, G., Szentes, N., Horváth, M., Dorn, Á, Cox, A., Nagy, G., et al. (2018). Kinetics of Targeted Phage Rescue in a Mouse Model of Systemic *Escherichia coli* K1. *BioMed Res. Int.* 2018:7569645. doi: 10.1155/2018/7569645

Sun, W. J., Liu, C., Yu, L., Cui, F. J., Qiang, Z., Yu, S. L., et al. (2012). A novel bacteriophage KSL-1 of 2-Keto-gluconic acid producer *Pseudomonas* fluorescens K1005: isolation, characterization and its remedial action. *BMC Microbiol.* 12:127. doi: 10.1186/1471-2180-12-127

Thames, H. T., and Theradiyil Sukumaran, A. (2020). A Review of *Salmonella* and Campylobacter in Broiler Meat: emerging Challenges and Food Safety Measures. *Foods* 9:776. doi: 10.3390/foods9060776

Yang, S. C., Lin, C. H., Aljuffali, I. A., and Fang, J. Y. (2017). Current pathogenic *Escherichia coli* foodborne outbreak cases and therapy development. *Arch. Microbiol.* 199, 811–825. doi: 10.1007/s00203-017-1393-y

Yu, M. X., Slater, M. R., and Ackermann, H. W. (2006). Isolation and characterization of Thermus bacteriophages. *Arch. Virol.* 151, 663–679. doi: 10.1007/s00705-005-0667-x

Zhang, C., Li, W., Liu, W., Zou, L., Yan, C., Lu, K., et al. (2013). T4-like phage Bp7, a potential antimicrobial agent for controlling drug-resistant *Escherichia coli* in chickens. *Appl. Environ. Microbiol.* 79, 5559–5565. doi: 10.1128/AEM.01505-13

Conflict of Interest: The authors declare that the research was conducted in the absence of any commercial or financial relationships that could be construed as a potential conflict of interest.

frontiers in Microbiology

ORIGINAL RESEARCH
published: 09 August 2021
doi: 10.3389/fmicb.2021.669618

Novel *Klebsiella pneumoniae* K23-Specific Bacteriophages From Different Families: Similarity of Depolymerases and Their Therapeutic Potential

Roman B. Gorodnichev[1]†, Nikolay V. Volozhantsev[2†], Valentina M. Krasilnikova[2], Ivan N. Bodoev[1], Maria A. Kornienko[1], Nikita S. Kuptsov[1], Anastasia V. Popova[2], Galina I. Makarenko[1], Alexander I. Manolov[1], Pavel V. Slukin[2], Dmitry A. Bespiatykh[1], Vladimir V. Verevkin[2], Egor A. Denisenko[2], Eugene E. Kulikov[3], Vladimir A. Veselovsky[1], Maja V. Malakhova[1], Ivan A. Dyatlov[2], Elena N. Ilina[1] and Egor A. Shitikov[1]*

[1]Department of Molecular Biology and Genetics, Federal Research and Clinical Center of Physical-Chemical Medicine, Moscow, Russia, [2]Department of Molecular Microbiology, State Research Center for Applied Microbiology and Biotechnology, Moscow, Russia, [3]Research Center of Biotechnology of the Russian Academy of Sciences, Winogradsky Institute of Microbiology, Moscow, Russia

Antibiotic resistance is a major public health concern in many countries worldwide. The rapid spread of multidrug-resistant (MDR) bacteria is the main driving force for the development of novel non-antibiotic antimicrobials as a therapeutic alternative. Here, we isolated and characterized three virulent bacteriophages that specifically infect and lyse MDR *Klebsiella pneumoniae* with K23 capsule type. The phages belonged to the *Autographiviridae* (vB_KpnP_Dlv622) and *Myoviridae* (vB_KpnM_Seu621, KpS8) families and contained highly similar receptor-binding proteins (RBPs) with polysaccharide depolymerase enzymatic activity. Based on phylogenetic analysis, a similar pattern was also noted for five other groups of depolymerases, specific against capsule types K1, K30/K69, K57, K63, and KN2. The resulting recombinant depolymerases Dep622 (phage vB_KpnP_Dlv622) and DepS8 (phage KpS8) demonstrated narrow specificity against *K. pneumoniae* with capsule type K23 and were able to protect *Galleria mellonella* larvae in a model infection with a *K. pneumoniae* multidrug-resistant strain. These findings expand our knowledge of the diversity of phage depolymerases and provide further evidence that bacteriophages and phage polysaccharide depolymerases represent a promising tool for antimicrobial therapy.

Keywords: ***Klebsiella pneumoniae*, multidrug-resistance, capsular type, capsule depolymerase, bacteriophage, *Galleria mellonella***

OPEN ACCESS

Edited by:
Robert Czajkowski, University of Gdansk, Poland

Reviewed by:
Flavia Squeglia, Institute of Biostructure and Bioimaging, National Research Council (CNR), Italy
Marco Maria D'Andrea, University of Rome Tor Vergata, Italy
Hugo Oliveira, University of Minho, Portugal

***Correspondence:**
Roman B. Gorodnichev
gorodnichev.r.b@gmail.com

†These authors have contributed equally to this work

Specialty section:
This article was submitted to Virology, a section of the journal Frontiers in Microbiology

Received: *19 February 2021*
Accepted: *14 July 2021*
Published: *09 August 2021*

Citation:
Gorodnichev RB, Volozhantsev NV, Krasilnikova VM, Bodoev IN, Kornienko MA, Kuptsov NS, Popova AV, Makarenko GI, Manolov AI, Slukin PV, Bespiatykh DA, Verevkin VV, Denisenko EA, Kulikov EE, Veselovsky VA, Malakhova MV, Dyatlov IA, Ilina EN and Shitikov EA (2021) Novel Klebsiella pneumoniae K23-Specific Bacteriophages From Different Families: Similarity of Depolymerases and Their Therapeutic Potential. Front. Microbiol. 12:669618. doi: 10.3389/fmicb.2021.669618

INTRODUCTION

Klebsiella pneumoniae is a widespread Gram-negative, non-motile, facultative anaerobic bacterium naturally occurring in soil, sewage, or plants. These bacteria are traditionally considered as commensals and can be found on human skin and in the gastrointestinal and respiratory tracts (Paczosa and Mecsas, 2016). Despite this, *K. pneumoniae* is the world's second most common nosocomial

pathogen, capable of causing a wide range of infections such as septicemia, pneumonia, urinary tract infections, and surgical- and catheter-related infections (Podschun and Ullmann, 1998).

The extensive use of antibiotics to treat *Klebsiella*-associated infections has led to the emergence and spread of drug resistance. According to data from the European Centre for Disease Prevention and Control, nearly 40% of the *K. pneumoniae* isolates in Europe are resistant to at least one class of antibiotic – fluoroquinolones, third-generation cephalosporins, aminoglycosides, or carbapenems (European Centre for Disease Prevention and Control, 2019). Of these, the isolates carrying extended-spectrum beta-lactamases or carbapenemases encoding genes are considered especially difficult to treat. As previously reported, these isolates cause infections with high morbidity and mortality rates (Cantón et al., 2012; Tzouvelekis et al., 2012; Munoz-Price et al., 2013; Girmenia et al., 2015; Tängdén and Giske, 2015; Lee et al., 2016).

In light of the antibiotic resistance crisis, the development of new approaches to antimicrobial therapy is especially relevant. One promising alternative to the use of antibiotics is therapy with virulent bacteriophages (phages; Górski et al., 2020). Phages are natural killers that can rapidly and selectively infect and lyse pathogenic bacteria, including *K. pneumoniae* clones associated with antibiotic resistance. Bacteriophage therapy has been clinically used since the beginning of the 20th century, and no known significant side effects have been identified throughout the entire history of use (Payne and Jansen, 2000). Nowadays, the efficiency and safety of bacteriophage therapy have been confirmed in mammal and *Galleria mellonella* models and in humans (Chhibber et al., 2008; Hung et al., 2011; D'Andrea et al., 2017; Manohar et al., 2019). The natural limitation of the approach is the usually narrow host range of individual bacteriophages, so the phage cocktails have to be employed to combat an unknown pathogen (Clark and March, 2006).

The host range of *K. pneumoniae* phages shows a good correlation with the type of capsular polysaccharide (CPS; Pires et al., 2016). To date, at least 130 types of CPS have been described, which is the key virulence factor protecting the bacteria from the immune system and the action of some antibiotics (Stewart, 1996; Yu et al., 2015; Wyres et al., 2016). Isolates characterized by the overexpression of capsular polysaccharides often possess an enhanced virulence and have been categorized as a separate group called hypervirulent *K. pneumoniae* (hvKp). In addition to hyperexpression of the capsule, frequently regulated by the rmpA/rmpA2 gene, hvKp may also carry other virulence factors, such as yersiniabactin, colibactin, aerobactin, and salmochelin. HvKp has been described as a cause of primary purulent liver abscesses in the Asia-Pacific region (Liu et al., 1986; Fang et al., 2005; Turton et al., 2007; Shon et al., 2013).

The main factor that allows phages to infect the *K. pneumoniae* cell is the presence of a specific receptor-binding protein (RBP) – a processive enzyme with depolymerase activity (Pires et al., 2016). Depolymerases are enzymes that can cleave capsular polysaccharides, clearing the way for phage adsorption to the surface of a bacterial cell, followed by injection of phage DNA. Phage-borne depolymerases are usually presented as a structural component of the phage adsorption apparatus (tail fibers, tail spikes, or base plates; Pires et al., 2016; Knecht et al., 2020). Most of the phage genomes encode only one depolymerase, but some phages have two or more depolymerases that allow them to infect multiple capsular types (Pan et al., 2017; Latka et al., 2019). Characterizing the diversity of phage depolymerases is of particular interest, as this could lead to the development of a new class of antivirulence agents. It has been shown that phage depolymerases could increase the rate of bacterial killing by serum *in vitro* and significantly increase survival in mice and *G. mellonella* larvae models (Majkowska-Skrobek et al., 2018; Solovieva et al., 2018; Volozhantsev et al., 2020). Additionally, phage-borne depolymerases can be used for the rapid determination of microbial capsule types or disruption of bacterial biofilms (Scorpio et al., 2008).

Currently, over 30 specific polysaccharide-depolymerases have been characterized (Lin et al., 2014; Majkowska-Skrobek et al., 2016, 2018; Hsieh et al., 2017; Pan et al., 2017, 2019; Latka et al., 2019; Domingo-Calap et al., 2020a,b; Liu et al., 2020; Volozhantsev et al., 2020). However, phages and depolymerases specific for *K. pneumoniae* K23 capsular type have not been characterized yet. In this study, we described the biological characteristics and performed a genomic analysis of one new podovirus vB_KpnP_Dlv622 and two new myoviruses (vB_KpnM_Seu621 and KpS8) infecting specifically the strains of *K. pneumoniae* with capsule type K23. In addition, we compared their depolymerases and assayed their protective activity in *G. mellonella* larvae during infection with a clinical multidrug-resistant (MDR) *K. pneumoniae* strain.

MATERIALS AND METHODS

Bacterial Strains and Their Characterization

A collection comprising 32 clinical *K. pneumoniae* isolates from the Clinical Hospital №123 (Odintsovo, Russia) and 51 strains from the State Collection of Pathogenic Microorganisms and Cell Cultures, SCPM-Obolensk (State Research Center for Applied Microbiology and Biotechnology, Obolensk, Russia) were included in this study (**Supplementary Table 3**). All bacteria were grown in the Nutrient Medium No. 1 (SRCAMB, Obolensk, Russia), or in the lysogeny broth (LB) medium (Himedia, India) at 37°C. Bacterial identification was performed by MALDI-TOF mass spectrometry as described previously (Kornienko et al., 2016). The antibiotic susceptibility was tested using the disc diffusion method according to Clinical and Laboratory Standards Institute guidelines 28th edition (Clinical and Laboratory Standards Institute, 2018). Multilocus sequence typing (MLST) of *K. pneumoniae* strains was performed by determining the nucleotide sequences of seven housekeeping genes as described previously (Diancourt et al., 2005). The capsular type was determined by *wzi* gene sequencing (Brisse et al., 2013).

Bacteriophage Isolation and Purification

Two *K. pneumoniae* K23 strains (Kp-9068 and KPi4275) were used as hosts for bacteriophage isolation. Phages vB_KpnM_Seu621 and vB_KpnP_Dlv622 were isolated from the Chermyanka

river water samples and phage KpS8 was isolated from sewage by a previously described method (Van Twest and Kropinski, 2009), with slight modifications. In brief, 15 ml of sewage or river water samples were centrifuged at 10,000 *g* for 15 min, and the supernatant was filtered using a 0.22-μm sterile membrane syringe filter (Millipore, United States). Filtered supernatant and 0.2 ml of early log-phase host cultures (OD_{600nm} = 0.3) were added to 15 ml of double-concentrated LB broth and incubated overnight with agitation (200 rpm) at 37°C to amplify the phages. Further, the culture was centrifuged at 10,000 *g* for 15 min and subsequently filtered through 0.22-μm filters. Obtained lysates were serially diluted in LB and spotted on double-layer agar plates of host-strains for phage detection and isolation. Three rounds of single plaque purification and re-infection of exponentially growing host strains yielded pure bacteriophage suspensions. Bacteriophage titers were determined using a double-agar overlay plaque assay (Mazzocco et al., 2009).

Electron Microscopy of Phage Particles

Purified phage preparations were analyzed by transmission electron microscopy using a JOEL JSM 100 CXII electron microscope (JOEL, Japan) at an acceleration voltage of 100 kV with a Gatan Erlangshem CCD camera (Gatan, Inc.). Carbon-coated grids with collodion supporting film were negatively stained with 1% uranyl acetate in methanol.

Host Range Determination

The host range of phages was determined by the spot test using 83 *K. pneumoniae* strains. Briefly, 100 μl of log-phase (OD_{600nm} = 0.3) culture of each strain was added to 5 ml of top agar, which was subsequently poured onto a bottom agar plate. Around 5 μl of phage lysate at a titer of 10^6 PFU/ml were spotted onto freshly seeded lawns of the strains and left to dry before overnight incubation at 37°C. Additionally, the efficiency of plating (EOP) assay was also performed for phage-sensitive strains as previously described (Solovieva et al., 2018). The average EOP value for a phage-bacterium ratio was classified according to Mirzaei and Nilsson (2015): highly productive (EOP $\geq$ 0.5), medium productive (0.1 $\leq$ EOP $<$ 0.5), low productive (0.001 $<$ EOP $<$ 0.1), or inefficient (EOP $\leq$ 0.001; Horváth et al., 2020).

Thermal Tolerance of Phages

The stability of phages at different temperatures was determined by incubating 1 ml of phage lysate (10^9 PFU/ml) at different temperatures (4, 37, 45, 55, 65, and 75°C) for 1 h, and then the phage titer was determined using the double-layer agar method (Mazzocco et al., 2009). The assay was performed in triplicate.

Adsorption Assay and One-Step Growth Curve

The adsorption rate was estimated as described earlier with a slight modification (Kropinski, 2009). Host strains were grown to exponential phase (OD_{600nm} = 0.3) and mixed with bacteriophage at a multiplicity of infection (MOI) of 0.01. Every 2 min from 2 to 17 min, aliquots were taken and treated with 2% chloroform, shaken briefly and set aside for 10 min at RT. The titers of free phage were quantified by plaque assay. Determining the number of PFU of the unbound phage in the supernatant and subtracting it from the total number of inputs PFU gave phage adsorption percentage.

The dynamic changes in the number of phage particles during a replicative cycle were performed as described earlier (Ciacci et al., 2018). Aliquots of phage lysates were added to an exponential phase host strains (OD_{600nm} = 0.3) in MOI of 0.01 and allowed to adsorb for 10 min at 37°C. The mixture was then centrifuged at 10,000 *g* for 5 min and the pellet was resuspended in 10 ml of LB broth to remove free phage particles. Aliquots were taken at 15, 20, 40, 50, 60, 70, and 80 min post-infection and treated with 2% chloroform, shaken briefly, set aside for 10 min at RT, and centrifuged. Finally, the titers of the lysates were quantified by plaque assay. The burst size was calculated as the ratio of the final count of released phage particles to the initial count of infected bacterial cells during the latent period. Independent experiments were repeated three times.

DNA Sequencing and Analysis

A standard phenol-chloroform extraction protocol was used for phage DNA isolation as described previously (Green et al., 2012). The whole-genome sequencing of bacteriophages was performed with a high-throughput Illumina HiSeq system. The assembly was performed using SPAdes (v.3.14.0; Bankevich et al., 2012). Terminal repeats were predicted with the PhageTerm tool (Garneau et al., 2017). Open reading frames (ORFs) were predicted using GeneMarkS (version 4.32; Besemer et al., 2001), Phast (Zhou et al., 2011), and VGAS (Zhang et al., 2019). tRNAScan-SE (Chan and Lowe, 2019) and ARAGORN (Laslett and Canback, 2004) were used to predict tRNA. The putative functions of the proteins encoded by each ORF were retrieved manually using BLASTp, HHPred, Phast, and InterPro. ORFs were also compared against Virulence Factors of Pathogenic Bacteria (VFDB; Liu et al., 2019) and Antibiotic Resistance Genes Databases (ARDB; Liu and Pop, 2009) to verify the safety of the phages. The annotated genome sequences of bacteriophages vB_KpnM_Seu621, vB_KpnP_Dlv622, and KpS8 were deposited in the NCBI GenBank database under accession numbers MT939253, MT939252, and MT178275, respectively. Phylogenetic analysis was performed using the amino acid sequences of RNA polymerase for *Autographiviridae* family phages and major capsid protein for *Myoviridae* family phages as recommended by the International Committee on Taxonomy of Viruses (ICTV) classification. The phylogenetic tree was constructed with the Genome-BLAST Distance Phylogeny method implemented by the VICTOR webserver (Meier-Kolthoff and Göker, 2017). Depolymerase domain multiple sequences alignment was performed using MAFFT (v.7.475; Katoh and Standley, 2013). ProtTest (v.3.4.2) was used to define the best suitable amino acid substitution model (Darriba et al., 2011). Maximum likelihood trees were inferred with RAxML-NG (v.1.0.2) with Blosum62+G+F substitution model suggested by ProtTest (Kozlov et al., 2019). Trees were visualized with the ggtree package for R (Yu et al., 2017).

Preparation of Recombinant CPS Depolymerases and Determination of Their Activity

To obtain recombinant CPS depolymerases, coding sequences for the genes kps8_053 and dlv622_00059 containing the putative depolymerase domains were amplified by PCR using specific oligonucleotide primer pairs: DepS8F_NcoI 5'-ACGCCATG GACTGGGTCACTCTTGAAAT-3' and DepS8R_XhoI 5'-ATACT CGAGCCCGTTCACCCTTGAAA-3'; Dep622F_NcoI 5'-TACCA TGGCTTTGACAAAGTTAGTAC-3' and Dep622R_XhoI 5'-TA CTCGAGCACCCCCGTCAACCGC-3'. Amplified fragments were cloned into a pET22b expression vector (Novagen, United States) *via* the *NcoI* and *XhoI* restriction sites and then transformed into *Escherichia coli* BL21 (DE3). Resulting constructs were quality-checked *via* Sanger sequencing. Protein expression was performed in LB medium supplemented with ampicillin at 100 mg/L. Transformed cells were grown at 37°C until the optical density reached the value of 0.4 at 600 nm. The medium was cooled to the temperature of 16°C followed by expression induction with 1 mM isopropyl-1-thio-β-D-galactopyranoside (IPTG). After further incubation at 16°C overnight, the cells were harvested by centrifugation at 3,700 *g* for 20 min, 4°C. The cell pellets were resuspended in 1/50 of the original cell volume in buffer A (20 mM Tris pH 8.0, 0.5 M NaCl, 20 mM imidazole) and then lysed by sonication. The cell debris was removed by centrifugation at 16,000 *g* for 30 min, at 4°C. The supernatants were loaded onto nickel Ni^{2+}-charged 5 ml GE HisTrap columns (GE Healthcare Life Sciences) equilibrated with buffer A, and eluted with a 20–500 mM imidazole linear gradient in buffer A. The fractions containing the target proteins were pooled together and then dialyzed against 20 mM Tris pH 8.0, 200 mM NaCl, 0.5 mM DTT buffer at 4°C. The protein samples were concentrated with Sartorius ultrafiltration devices (molecular weight cutoff of 10,000) and stored at 4°C. The CPS-degrading activity of the recombinant proteins was assayed in a spot test using *K. pneumoniae* strains of different capsular types.

Phage KpS8 and vB_KpnP_Dlv622 Adsorption Inhibition Assay

Bacterial cell suspension (~2×10^8 CFU/ml) in SM-buffer (8 mM $MgCl_2$, 100 mM NaCl, 50 mM Tris-HCl pH 7.5) with added recombinant depolymerase (400 μg/ml) and a phage sample (~10^7 PFU/ml) were first brought to 37°C. Then equal volumes of the phage and cell suspension were mixed. After 5 min incubation at 37°C, bacterial cells with adsorbed phages were precipitated by centrifugation at 14,000 *g* for 1 min and the titer of non-adsorbed phages was determined in the supernatant.

Galleria mellonella Larvae Infection Model

Greater Wax moth larvae (*G. mellonella*) were obtained from a laboratory culture maintained at State Research Center for Applied Microbiology and Biotechnology, Obolensk. The larvae were reared on an artificial nutrient medium (maize flour – nine parts, wheat flour – four parts, dry brewer's yeasts, dry milk, beeswax, bee honey, and glycerol – five parts each) at 27°C for 25–27 days and were subsequently selected for the experiments. The larvae were inoculated with a bacterial suspension or bacteria simultaneously with the depolymerase enzyme into the hemocoel using an insulin syringe. Bacterial suspensions of an overnight agar *K. pneumoniae* Kp-9068 culture in phosphate-buffered saline (PBS) buffer with cell concentration of 3×10^8 CFU per injection, 3×10^7 CFU, 3×10^6 CFU, 3×10^5 CFU, and 3×10^4 CFU were used to infect the larvae. Three larvae groups were used in the experiments: (1) larvae infected with bacteria only; (2) larvae infected with bacteria and DepS8 enzyme; and (3) larvae infected with bacteria and Dep622 enzyme. Each test was performed in triplicate, with 50 larvae per trial (10 larvae for each bacterial dose). The final dose of the enzymes was 2 μg per larvae for all trials. In addition, three control groups were used: larvae injected with PBS and larvae injected with depolymerase DepS8 or Dep622. Infected larvae were incubated at 37°C for 5 days and mortality was recorded daily. The GraphPad Prism software (GraphPad Software, Inc., La Jolla, United States) was used for statistical analysis and graphical presentation of the results. Statistical analysis was performed for pairwise comparisons between larvae infected with bacteria only and larvae infected with bacteria simultaneously with depolymerase DepS8 or Dep622 using log-rank (Mantel-Cox) test. Values of $p < 0.05$ were considered as statistically significant.

A dose of bacteria that is sufficient to kill 50% of a larvae population (LD_{50}) was calculated from the cumulative mortality observed 5 days after dosing by the Ashmarin-Vorobiev modification of Karber's method (Ashmarin and Vorobyev, 1962).

RESULTS

Isolation and Phenotypic Characterization of Three Novel *Klebsiella pneumoniae* Phages

Phages vB_KpnM_Seu621 and vB_KpnP_Dlv622 were isolated in 2018 from the freshwater of the Chermyanka river (Moscow, Russia). Phage KpS8 was isolated in 2016 from sewage samples in the Moscow region, Russia. *Klebsiella pneumoniae* strain Kp-9068 was used as a host for isolation vB_KpnM_Seu621 and vB_KpnP_Dlv622 phages. The KpS8 phage was isolated using the KPi4275 strain as a host. Both strains had a multidrug-resistant phenotype (resistance to three or more classes of antibiotics), belonged to sequence type 11 (ST11), and had a K23 capsular type (**Supplementary Table 3**).

Phage vB_KpnP_Dlv622 had morphological features typical of the *Podoviridae* family: symmetrical polyhedral head (51 nm in diameter) and a short, noncontractile tail (12 nm long; **Figure 1A**). Both vB_KpnM_Seu621 and KpS8 phages, had an isometric head of 75–78 nm in diameter and a contractile tail of 104–113 nm in length, with the overgrowths on a terminal side (**Figures 1B,C**), suggesting that the phages belong to the *Myoviridae* family.

Different plaque morphology was exhibited by the phages. The vB_KpnP_Dlv622 phage formed clear circular plaques with a diameter of about 2–3 mm with halos (**Figure 1D**). Phages vB_KpnM_Seu621 and KpS8 were able to form similar circular

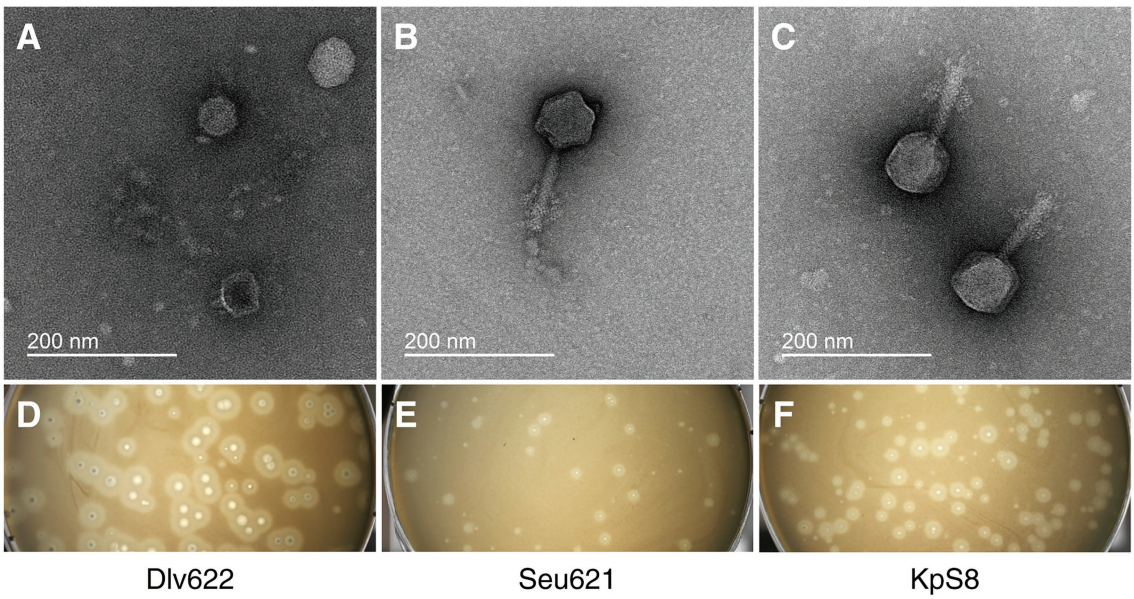

FIGURE 1 | Initial characterization of *Klebsiella* phages vB_KpnP_Dlv622, vB_KpnM_Seu621, and KpS8. Transmission electron microscopy of phages Dlv622 **(A)**, Seu621 **(B)**, and KpS8 **(C)**. Plaque morphology of phages Dlv622 **(D)**, Seu621 **(E)**, and KpS8 **(F)**.

plaques with a diameter of about 0.5–1 mm, surrounded by hazy halos (**Figures 1E,F**). Previous studies have suggested that the translucent halos were related to a putative phage-derived polysaccharide depolymerase (Wang et al., 2019).

Studies on phage adsorption have shown that all phages were able to adsorb to the Kp9068 strain by 6–7 min of incubation (**Supplementary Figure 1A**). The results of a one-step growth assay revealed similar latency and burst periods for all three phages of approximately 30 min (**Supplementary Figure 1B**). The burst sizes were approximately 66 PFU/cell for the vB_KpnP_Dlv622 phage and 85 and 96 PFU/cell for the vB_KpnM_Seu621 and KpS8, respectively.

The stability test of vB_KpnP_Dlv622, vB_KpnM_Seu621, and KpS8 phages showed that the phages were relatively stable in a range of temperature between 4 and 55°C (**Supplementary Figure 2**). vB_KpnM_Seu621 and KpS8 phages retained high plaque-forming activity even after incubation at 65°C, indicating good thermal stability. Incubation at a temperature of 75°C demonstrated a significant decrease in titer of all bacteriophages from 10^9 PFU/ml to 10^2–10^5 PFU/ml.

Genome Sequencing and Comparative Genomics

The complete genome of the vB_KpnP_Dlv622 phage was 44,687 bp long, with a G + C content of 54% and two 278 bp long direct repeats located at both ends. Bioinformatic analysis revealed 59 ORFs with a total length of 41,477 bp (coding percentage, 92.8%). BLAST analysis showed that this phage belongs to the *Autographiviridae* family. To verify this, amino acid sequences of RNA polymerase were used to estimate phylogenetic relationships between vB_KpnP_Dlv622 phage and 46 phages recommended by ICTV and belonging to the *Autographiviridae* family (last accessed April 23, 2020; **Supplementary Figure 3**). According to the phylogenetic tree, the vB_KpnP_Dlv622 phage belongs to the *Drulisvirus* genus of the family *Autographiviridae* and most closely related to the phage phiKpS2 (accession NC_047857.1, 82% query coverage and 92.6% identity according to BLASTn).

The genome of vB_KpnM_Seu621 was a linear dsDNA molecule of 142,896 bp with a G + C content of 44.64%. A total of 274 ORFs were identified. The complete genome of the KpS8 phage was also a linear dsDNA molecule of 143,800 bp (44.64% G + C content) containing 285 ORFs. Most of the predicted ORFs for both vB_KpnM_Seu621 and KpS8 phages were encoded on the positive strand. According to the Average Nucleotide Identity (ANI; Rodriguez-R and Konstantinidis, 2014) analysis, vB_KpnM_Seu621 and KpS8 phages had high ANI value of 99.48%. According to the BLAST analysis, phages belonged to the *Myoviridae* family. To verify the taxonomic position of the phages, the phylogenetic analysis was performed using multiple alignments of amino acid sequences of major capsid protein of vB_KpnM_Seu621 and KpS8 phages, 24 phages recommended by ICTV, and four the most related phages from the NCBI database. The results of the phylogenetic analysis showed that our phages are closely related to phage vB_KpnM_KB57 (accession NC_028659.1, 90% query coverage and 98.9% identity according to BLAST) and formed a distinct branch within the clade of *Mydovirus* genus, *Vequintavirinae* subfamily (**Supplementary Figure 4**).

Functional Annotation of *K. pneumoniae* Phages

According to functional analysis, the proteins of the vB_KpnP_Dlv622 phage could be attributed to five groups: (1) phage

structure (11 ORFs); (2) replication, regulation, transcription, and translation (20 ORFs); (3) DNA packaging (two ORFs); (4) host lysis (three ORFs); and (5) hypothetical protein (23 ORFs). vB_KpnP_Dlv622 had typical T7-related genome organization with the presence of lysis cassette composed of spanin-, holin-, and endolysin-encoding genes located next to each other, as well as phage DNA- and RNA-polymerases. No tRNA genes were identified with tRNAScan-SE and ARAGORN toolsets, as well as no significant similarities with known antibiotic resistance determinants, virulence or toxin proteins, and integrase genes were revealed (**Supplementary Table 1A**).

The genome of vB_KpnP_Dlv622 phage encoded two putative tail fiber and spike proteins dlv622_orf00051 and dlv622_orf00059. The dlv622_orf00051 was 317 aa long and was highly conserved among phages of the *Drulisvirus* genus. In contrast, dlv622_orf00059 showed more than 80% similarity only to a few phage proteins available in the NCBI database and encoded the potential pectate lyase domain with beta-helix structure characteristic of CPS depolymerases. According to a previous study, this structure of tail fiber and spike proteins means that phage vB_KpnM_Dlv622 belongs to Group A of KP34 viruses containing only one receptor-binding protein dlv622_orf00059 (**Table 1**; Latka et al., 2019).

For the vB_KpnM_Seu621 and KpS8 phages, a specific putative function (structural proteins, enzymes involved in the replication, regulation, transcription, and translation of DNA, host lysis) could be assigned to products of the same number of ORFs (N = 78). About 24 tRNA were detected in each bacteriophage by tRNAScan-SE and confirmed by ARAGORN. No genes related to phage lysogeny were predicted (**Supplementary Tables 1B,C**).

Based on the annotations of vB_KpnM_Seu621 and KpS8 phages, five ORFs are likely involved in tail fiber synthesis: (1) putative tail fiber protein (phage621_orf00040 and kps8_orf041), (2) putative tail fiber protein (phage621_orf00045 and kps8_orf046), (3) L-shaped tail fiber (phage621_orf00048 and kps8_orf049), (4) putative tail spike protein (phage621_orf00050 and kps8_orf051), and (5) putative tail spike protein (phage621_orf00052 and kps8_orf053). All the genes involved in tail fiber synthesis were either identical in both phages or had single amino-acid substitutions (phage621_orf00040 and kps8_orf041). It should be noted that among the ORFs described above phage621_orf00052/kps8_orf053 had a high score of similarity with dlv622_orf00059 (98% query coverage and 65.98% identity according to BLASTp; **Supplementary Figure 5**). In addition, it was revealed that these proteins possess the pectate lyase domain and beta-helix structure characteristic of CPS depolymerases (**Table 1**).

Host Range of the Three *Klebsiella pneumoniae* Phages

The panel of 83 *K. pneumoniae* strains was used to determine the host ranges of the phages. Antimicrobial susceptibility profiles revealed that 53 strains had a multidrug-resistant phenotype (resistance to three or more classes of antibiotics), including at least 19 carbapenem-resistant strains. Results of multilocus sequence typing and *wzi* gene sequencing showed that *K. pneumoniae* strains belong to 21 different sequence types and had 26 unique capsular types, respectively (**Supplementary Table 3**). The most common CPS-types were K2 (n = 14; 16.5%), K57 (n = 11; 12.9%), KL39 (n = 9; 10.6%), and K1 (n = 8; 9.4%).

Isolated phages had a narrow range of lytic activity against *K. pneumoniae* strains (**Supplementary Table 3**) and could only infect and lyse strains belonging to the K23 (4/4) capsular types. According to EOP analysis, *Myoviridae* phages vB_KpnM_Seu621 and KpS8 revealed a high productive infection for three of the four K23 strains, whereas phage vB_KpnP_Dlv622 showed similar effectiveness only on its original host strain (**Table 2**).

Activity of Phage Depolymerases

To confirm whether the predicted proteins have polysaccharide-degrading activity, we cloned genes kps8_053 (phage KpS8) and dlv622_00059 (phage vB_KpnP_Dlv622) into the pET22b+ expression vector. His-tag fusion proteins DepS8 and Dep622 were expressed and purified.

The activities of DepS8 and Dep622 were tested on four isolates showing sensitivity according to the spot test and four control non-sensitive isolates. Both DepS8 and Dep622 recombinant depolymerases were able to form translucent spots resembling the plaque halo on four K23 isolates and showed a lack of activity for other isolates under investigation (**Table 2**; **Figure 2**).

Depolymerases DepS8 and Dep622 Inhibit the Adsorption of Corresponding Bacteriophages

To study the interaction of bacterial viruses with surface receptors of a bacterial cell and determine whether the CPS depolymerases are the only key components to infect host cells, an adsorption inhibition assay was carried out. We used a competition assay to assess the role of DepS8 and Dep622 in

TABLE 1 | Polysaccharide depolymerase motifs identified in phage fiber and spike proteins.

Phage	Gene (Protein ID)	Protein size, aa	Motif, aa	Protein family	Analysis tool	Database identifier	E-value
vB_KpnP_Dlv622	Dlv622_orf00059 (QOI68577.1)	555	32–319	Pectin lyase fold	InterPro	IPR012334	3.87e-06
			24–445	Beta-helix, tailspike, Lyase	HHpred	1RMG_A	1.9e-16
vB_KpnM_Seu621 and KpS8	Seu621_orf00052 (QOI68629.1) and KpS8_053 (YP_009859099.1)	607	74–373	Beta-helix, tailspike, Lyase	HHpred	4RU5_B	4.3e-14
			80–364	Pectin lyase fold	InterPro	IPR012334	8.90e-05

TABLE 2 | The efficiency of plating and depolymerase activity for phages KpS8, vB_KpnM_Seu621, and vB_KpnP_Dlv622 phages and their recombinant depolymerases.

Strain	*cps*-type	MLST	Efficiency of plating			Dep-activity	
			KpS8	vB_KpnM_Seu621	vB_KpnP_Dlv622	DepS8	Dep622
Kp-9068*	K23	ST11	1.0	1.0	1.0	+	+
KPi4275**	K23	ST11	1.0	1.0	0.006	+	+
KPB2304-15	K23	ST11	1.0	1.0	0.006	+	+
KPB536-17-2	K23	ST1869	0.03	0.01	0.01	±	±
KPi1748	K2	ST65	–	–	–	–	–
KPi3014	K2	ST2174	–	–	–	–	–
KPi8289	K57	ST218	–	–	–	–	–
KPB2580	K1	ST23	–	–	–	–	–

*Host strain of vB_KpnP_Dlv622 and vB_KpnM_Seu621 phages.
**Host strain of KpS8 phage.

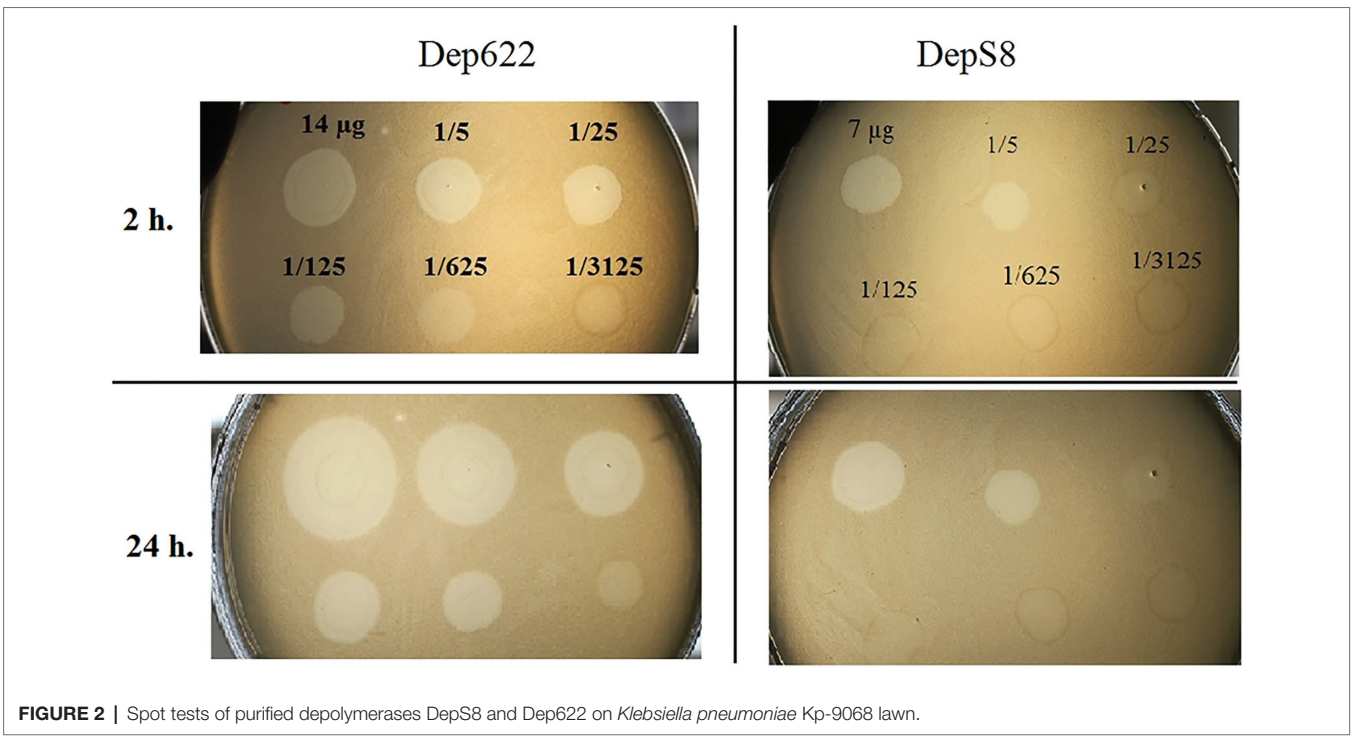

FIGURE 2 | Spot tests of purified depolymerases DepS8 and Dep622 on *Klebsiella pneumoniae* Kp-9068 lawn.

the KpS8 and vB_KpnP_Dlv622 phage-cell interaction at the initial stages of the infection process. The K1 specific depolymerase Dep_kpv71 (Solovieva et al., 2018) was used as a control (**Figure 3**).

The assay showed a 10-fold decrease in phage titer in the control experiments with SM-buffer and with treatment by K1-specific recombinant depolymerase. On the contrary, treating bacterial cells with K23-specific depolymerases DepS8 and Dep622 did not lead to decrease in the titer of free phage. Both DepS8 and Dep622 inhibit the phage adsorption to *K. pneumoniae* cells, indicating that the phage and depolymerases compete for the same moieties on the host cell surface, which are capsular polysaccharides. These results are consistent with that DepS8 and Dep622 proteins were *in silico* predicted as putative tail fibers/spikes, responsible for the host cells' recognition and reversible binding and subsequent degradation of *K. pneumoniae* cell capsular polysaccharides.

Depolymerase Application Increases the Survival Rate of *K. pneumoniae* Kp-9068 Infected *G. mellonella* Larvae

The influence of DepS8 and Dep622 depolymerases on *K. pneumoniae* Kp-9068 virulence was estimated on the *G. mellonella* model by two parameters: 50% lethal dose of bacterial cells and survival curves following injection of *G. mellonella* larvae with fixed doses of *K. pneumoniae* Kp-9068 (3×10^5 and 3×10^6 CFU per injection).

Experiments have shown a decrease in the virulence of *K. pneumoniae* Kp-9068 cells that were treated with depolymerases. The median lethal dose (LD_{50}) of untreated strain Kp-9068 was

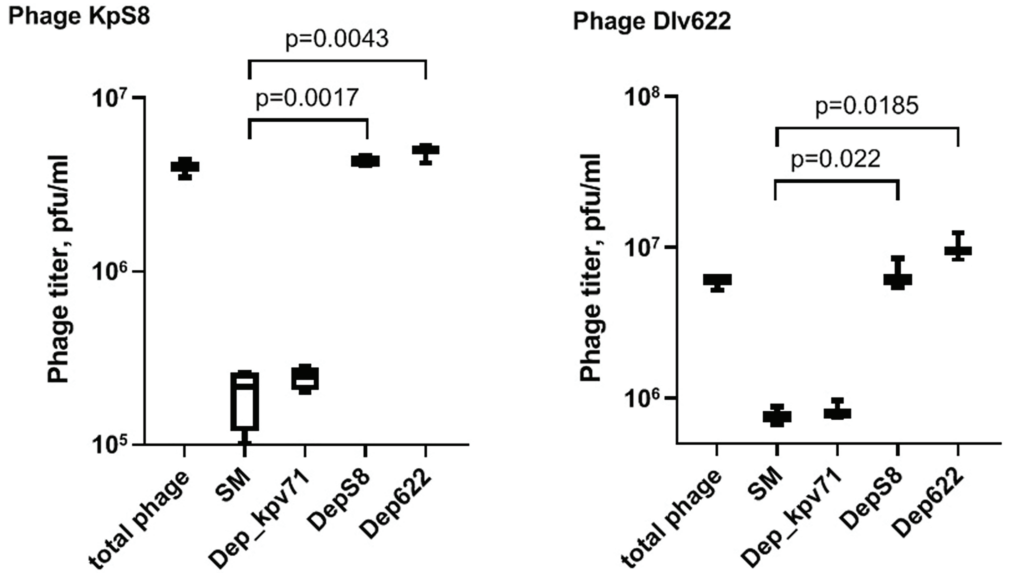

FIGURE 3 | Phage KpS8 and vB_KpnP_Dlv622 adsorption inhibition assay. From left to right, a titer of the total phage sample and titers of the free phage particles after the incubation with *K. pneumoniae* Kp-9068 cells in SM and in the presence of Dep_kpv71 (K1 specific depolymerase), DepS8, and Dep622 are shown.

estimated as $1.3 \times 10^5 \pm 5.8 \times 10^4$ CFU. At the same time, LD_{50} for bacteria Kp-9068 treated with depolymerase DepS8 or Dep622 was higher by 27.5 and 32.5 times, respectively (**Figure 4**).

Without the treatment, 100% of the larvae died within 48 h after inoculation of 3×10^6 CFU of *K. pneumoniae* Kp-9068 and 70% of the larvae died within 5 days after inoculation of 3×10^5 CFU (**Figure 5**). In contrast, a single dose of each enzyme injected together with bacteria significantly inhibited *K. pneumoniae*-induced death in a time-dependent manner. Only 10–30% mortality was recorded within 5 days after inoculation of *K. pneumoniae* Kp-9068 together with depolymerase DepS8 or Dep622 (**Figure 5**). No mortality of larvae was observed in the controls, upon injection of PBS buffer, DepS8, or Dep622 enzymes alone.

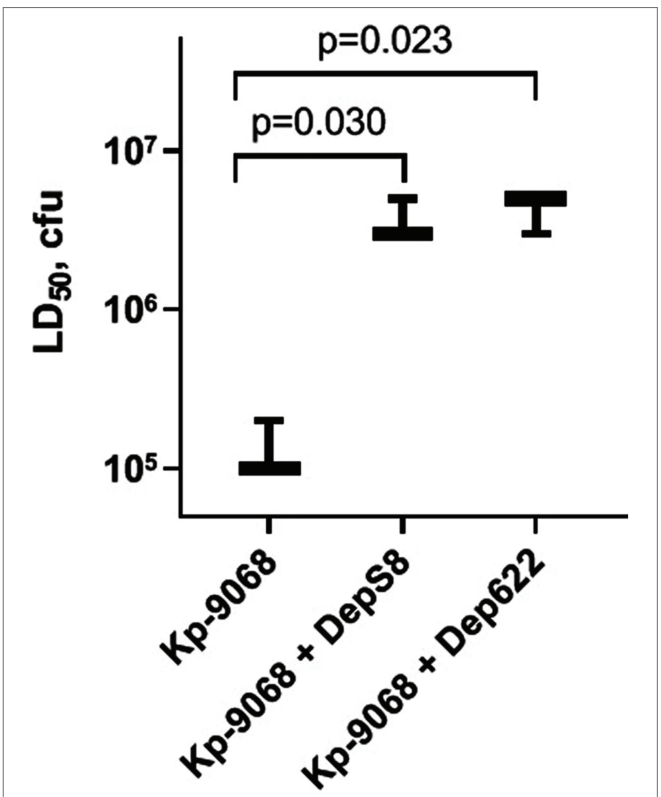

FIGURE 4 | A dose of bacteria *K. pneumoniae* Kp-9068 is sufficient to kill 50% of the *Galleria mellonella* larvae population (LD_{50}). From left to right, LD50 of the Kp-9068 untreated with depolymerase enzymes and LD_{50} of the Kp-9068 cells injected simultaneously with depolymerase DepS8 or Dep622. Average LD_{50} values from three independent experiments are shown and compared using Student's *t*-test analysis. Values of $p < 0.05$ were considered as statistically significant.

DISCUSSION

Multidrug-resistant *K. pneumoniae* strains belonging to ST11 were used as host strains for the isolation of bacteriophages. Such isolates are widespread and are often associated with nosocomial outbreaks caused by carbapenem-resistant and hypervirulent strains in China (Gu et al., 2018) and Greece (Voulgari et al., 2014). Furthermore, the K23 capsular type is one of the 10 most common capsular types typically associated with nosocomial *K. pneumoniae* infection provoked by carbapenem-resistant strains (Follador et al., 2016). Isolates with capsular type K23 are detected on average in 4% of cases; however, among *K. pneumoniae* associated with the production of carbapenemase, the percentage of such isolates can reach 9–17% (Satlin et al., 2017; Sonda et al., 2018).

Within the context of research for a possible antimicrobial therapeutic agent, three novel lytic K23-specific *K. pneumoniae*

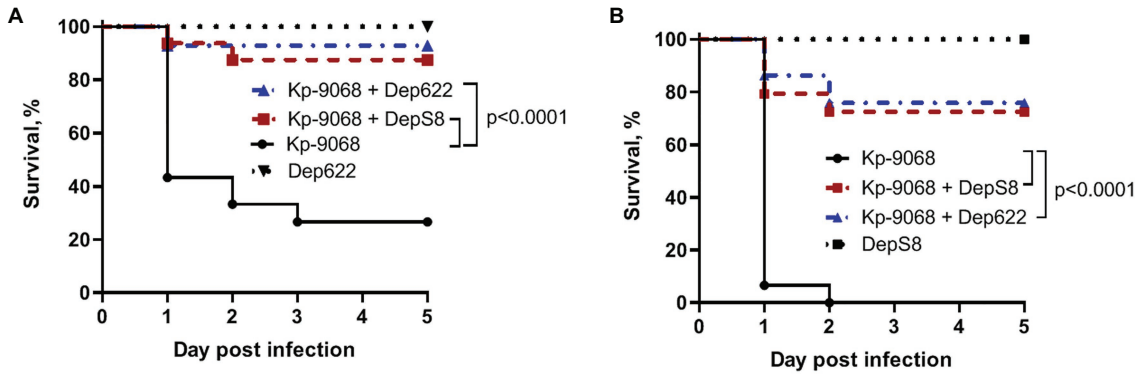

FIGURE 5 | Kaplan–Meier survival curves following injection of *G. mellonella* larvae with *K. pneumoniae* Kp-9068 and Kp-9068 simultaneously with depolymerase enzymes. **(A)** Larvae treatment with 3×10^5 CFU of *K. pneumoniae* Kp-9068; **(B)** Larvae treatment with 3×10^6 CFU of *K. pneumoniae* Kp-9068. Larvae ($n = 30$) were injected with either bacteria and bacteria simultaneously with enzyme DepS8 or Dep622 (2 μg per larva). The experiments were controlled by observation of phosphate-buffered saline (PBS)-injected larvae and larvae receiving the depolymerase only. Survival for each control group was 100%, so for simplicity, a group of PBS-injected larvae was not included in the figure. Statistically significant differences in survival between larvae infected with bacteria only and larvae infected with bacteria simultaneously with depolymerase DepS8 or Dep622 were estimated by the log-rank (Mantel-Cox) test.

phages were isolated. Phages KpS8 and vB_KpnM_Seu621 belonged to the *Myoviridae* family and had significant genetic similarities despite different times and sources of isolation (in 2016 from wastewater and in 2018 from river water). In turn, the vB_KpnP_Dlv622 phage belonged to the *Autographiviridae* family. Despite the considerable phylogenetic distance between the families, the bacteriophages possessed similar depolymerases and their corresponding recombinant proteins Dep622 and DepS8 exhibited the same rate of specificity and activity.

To search for similar cases, we analyzed proteins containing putative depolymerase domains for 76 *Klebsiella* phages, presented in NCBI (Volozhantsev et al., 2016, 2020; Labudda et al., 2017; Solovieva et al., 2018; Latka et al., 2019; Pan et al., 2019; Teng et al., 2019; Thiry et al., 2019; Wu et al., 2019; Domingo-Calap et al., 2020a,b; Gao et al., 2020; Horváth et al., 2020; Li et al., 2020; Zhang et al., 2020; **Supplementary Figure 6**). The depolymerase domains of our bacteriophages formed a separate cluster on the tree together with the BIS47_29 protein's domain (GenBank: YP_009832536.1). Given the fact that according to BLASTp the BIS47_29 protein was similar to kps8_orf053 (100% coverage and 92.09% identity) and dlv622_orf00059 (98% coverage and 65.9% identity), we can assume that BIS47_29 depolymerase also has specificity against capsule type K23.

Confirmed cases in the detection of homologous depolymerases in phages belonging to different families are quite rare (Volozhantsev et al., 2020). Apart from depolymerases specific against the K57 capsule, described in our previous study (Volozhantsev et al., 2020), and depolymerases described in the current article, no similar cases of depolymerases encoded by phages from different families have been reported. In addition to the cases mentioned above, we can assume based on the phylogenetic analysis that similar patterns are observed for at least four other types of depolymerases specific against capsule types K1, K30/K69, K63, and KN2 (**Supplementary Figure 6**). Although some authors suggest the theoretical possibility of lateral transfer of RBPs or depolymerase domains (Latka et al., 2019), for the time being, there are no reliable ways to distinguish between lateral transfer and convergent evolution.

Due to the dose-dependent effect and the standardizability of application protocols, therapy with phage derivatives is actively discussed on a par with the therapy with virulent bacteriophages (Górski et al., 2020; Volozhantsev et al., 2020). Recombinant tail spike proteins of phages vB_KpnP_Dlv622 and KpS8 significantly reduced the mortality of *G. mellonella* larvae infected with the host strain supporting infection by these phages (**Figure 5**). As can be seen from the spot-test data, depolymerases are not less effective than phages directly, and they behave as a potent tool in the treatment of antibiotic-resistant *K. pneumoniae* infection. Depolymerases cleave the polysaccharides of bacterial cells but, unlike phages, do not possess a lytic activity and do not kill host bacteria. Their therapeutic effect is due to the fact that by cleaving the capsular polysaccharides of *K. pneumoniae*, depolymerase eliminates the defense of the bacterium against the immune system, thus creating conditions for complement-mediated killing (Lin et al., 2014; Majkowska-Skrobek et al., 2018; Liu et al., 2020; Volozhantsev et al., 2020), and phagocytosis by macrophages (Majkowska-Skrobek et al., 2018).

CONCLUSION

Three new bacteriophages specific against *K. pneumoniae* with capsule type K23 were functionally characterized. Their depolymerases had significant similarity, despite the fact that bacteriophages belong to different families. Moreover, apart from the depolymerases specific against the K23 capsule, similar patterns were detected among K1-, K30/K69-, K57-, K63-, and KN2-specific depolymerases. Depolymerases derived from phages KpS8 and vB_KpnP_Dlv622 were equally efficient in cleaving capsular polysaccharides and also significantly reduced the mortality of *G. mellonella* larvae.

DATA AVAILABILITY STATEMENT

The datasets presented in this study can be found in online repositories. The names of the repository/repositories and accession number(s) can be found below: GenBank, MT939253, MT939252, and MT178275; BioProject, PRJNA705078.

AUTHOR CONTRIBUTIONS

RG, NV, and ES drafted the main manuscript and performed the data analysis. RG, NV, VK, IB, MK, NK, AP, GM, PS, VVV, ED, EK, MM, ID, EI, and ES planned and performed the experiments. RG, NV, AM, VAV, DB, and ES were responsible for bioinformatics analysis of data. All authors contributed to the article and approved the submitted version.

FUNDING

This work was supported by the State Assignment on the Development of a personalized approach to the therapy of infections using virulent bacteriophages (Code: Bacteriophage) and the Ministry of Science and Higher Education of the Russian Federation (grant number 075-15-2019-1671).

ACKNOWLEDGMENTS

We thank the Center for Precision Genome Editing and Genetic Technologies for Biomedicine, Federal Research and Clinical Center of Physical-Chemical Medicine of Federal Medical Biological Agency for the opportunity to use computational and sequencing resources. We are grateful to Nadezhda K. Fursova for providing data on antibiotic resistance and sequence types of *Klebsiella* strains from SCPM-Obolensk.

SUPPLEMENTARY MATERIAL

The Supplementary Material for this article can be found online at: https://www.frontiersin.org/articles/10.3389/fmicb.2021.669618/full#supplementary-material

REFERENCES

Ashmarin, I. P., and Vorobyev, A. A. (1962). *Statistical Methods in Microbiological Researches*. Leningrad: Medgiz.

Bankevich, A., Nurk, S., Antipov, D., Gurevich, A. A., Dvorkin, M., Kulikov, A. S., et al. (2012). SPAdes: a new genome assembly algorithm and its applications to single-cell sequencing. *J. Comput. Biol.* 19, 455–477. doi: 10.1089/cmb.2012.0021

Besemer, J., Lomsadze, A., and Borodovsky, M. (2001). GenemarkS: a self-training method for prediction of gene starts in microbial genomes. Implications for finding sequence motifs in regulatory regions. *Nucleic Acids Res.* 29, 2607–2618. doi: 10.1093/nar/29.12.2607

Brisse, S., Passet, V., Haugaard, A. B., Babosan, A., Kassis-Chikhani, N., Struve, C., et al. (2013). Wzi gene sequencing, a rapid method for determination of capsulartype for *Klebsiella* strains. *J. Clin. Microbiol.* 51, 4073–4078. doi: 10.1128/JCM.01924-13

Cantón, R., Akóva, M., Carmeli, Y., Giske, C. G., Glupczynski, Y., Gniadkowski, M., et al. (2012). Rapid evolution and spread of carbapenemases among *Enterobacteriaceae* in Europe. *Clin. Microbiol. Infect.* 18, 413–431. doi: 10.1111/j.1469-0691.2012.03821.x

Chan, P. P., and Lowe, T. M. (2019). "tRNAscan-SE: searching for tRNA genes in genomic sequences," in *Methods in Molecular Biology* ed. M. Kollmar (New York, NY: Humana Press), 1–14. doi: 10.1007/978-1-4939-9173-0_1

Chhibber, S., Kaur, S., and Kumari, S. (2008). Therapeutic potential of bacteriophage in treating *Klebsiella pneumoniae* B5055-mediated lobar pneumonia in mice. *J. Med. Microbiol.* 57, 1508–1513. doi: 10.1099/jmm.0.2008/002873-0

Ciacci, N., D'Andrea, M. M., Marmo, P., Demattè, E., Amisano, F., Di Pilato, V., et al. (2018). Characterization of vB_Kpn_F48, a newly discovered lytic bacteriophage for *Klebsiella pneumoniae* of sequence type 101. *Viruses* 10:482. doi: 10.3390/v10090482

Clark, J. R., and March, J. B. (2006). Bacteriophages and biotechnology: vaccines, gene therapy and antibacterials. *Trends Biotechnol.* 24, 212–218. doi: 10.1016/j.tibtech.2006.03.003

Clinical and Laboratory Standards Institute (2018). Performance Standards for Antimicrobial Susceptibility Testing M100. Wayne, PA: CLSI.

D'Andrea, M. M., Marmo, P., Angelis, L. H. D., Palmieri, M., Ciacci, N., Di Lallo, G., et al. (2017). φbO1E, a newly discovered lytic bacteriophage targeting carbapenemase-producing *Klebsiella pneumoniae* of the pandemic clonal group 258 clade II lineage. *Sci. Rep.* 7:2614. doi: 10.1038/s41598-017-02788-9

Darriba, D., Taboada, G. L., Doallo, R., and Posada, D. (2011). Prottest 3: fast selection of best-fit models of protein evolution. *Bioinformatics* 27, 1164–1165. doi: 10.1093/bioinformatics/btr088

Diancourt, L., Passet, V., Verhoef, J., Grimont, P. A. D., and Brisse, S. (2005). Multilocus sequence typing of *Klebsiella pneumoniae* nosocomial isolates. *J. Clin. Microbiol.* 43, 4178–4182. doi: 10.1128/JCM.43.8.4178-4182.2005

Domingo-Calap, P., Beamud, B., Mora-Quilis, L., González-Candelas, F., and Sanjuán, R. (2020a). Isolation and characterization of two *Klebsiella pneumoniae* phages encoding divergent depolymerases. *Int. J. Mol. Sci.* 21:3160. doi: 10.3390/ijms21093160

Domingo-Calap, P., Beamud, B., Vienne, J., González-Candelas, F., and Sanjuán, R. (2020b). Isolation of four lytic phages infecting *Klebsiella pneumoniae* K22 clinical isolates from Spain. *Int. J. Mol. Sci.* 21:425. doi: 10.3390/ijms21020425

European Centre for Disease Prevention and Control (2019). Surveillance of Antimicrobial Resistance in Europe Annual Report of the European Antimicrobial Resistance Surveillance Network (EARS-Net) 2018. Stockholm: ECDC.

Fang, F. C., Sandler, N., and Libby, S. J. (2005). Liver abscess caused by magA^{+} *Klebsiella pneumoniae* in North America. *J. Clin. Microbiol.* 43, 991–992. doi: 10.1128/JCM.43.2.991-992.2005

Follador, R., Heinz, E., Wyres, K. L., Ellington, M. J., Kowarik, M., Holt, K. E., et al. (2016). The diversity of *Klebsiella pneumoniae* surface polysaccharides. *Microb. Genom.* 2:e000073. doi: 10.1099/mgen.0.000073

Gao, M., Wang, C., Qiang, X., Liu, H., Li, P., Pei, G., et al. (2020). Isolation and characterization of a novel bacteriophage infecting carbapenem-resistant *Klebsiella pneumoniae*. *Curr. Microbiol.* 77, 722–729. doi: 10.1007/s00284-019-01849-8

Garneau, J. R., Depardieu, F., Fortier, L. C., Bikard, D., and Monot, M. (2017). Phageterm: a tool for fast and accurate determination of phage termini and packaging mechanism using next-generation sequencing data. *Sci. Rep.* 7:8292. doi: 10.1038/s41598-017-07910-5

Girmenia, C., Viscoli, C., Piciocchi, A., Cudillo, L., Botti, S., Errico, A., et al. (2015). Management of carbapenem resistant *Klebsiella pneumoniae* infections in stem cell transplant recipients: an Italian multidisciplinary consensus statement. *Haematologica* 100, e373–e376. doi: 10.3324/haematol.2015.125484

Górski, A., Międzybrodzki, R., Węgrzyn, G., Jończyk-Matysiak, E., Borysowski, J., and Weber-Dąbrowska, B. (2020). Phage therapy: current status and perspectives. *Med. Res. Rev.* 40, 459–463. doi: 10.1002/med.21593

Green, M., Hughes, H., Sambrook, J., and MacCallum, P. (2012). *Molecular Cloning: a Laboratory Manual*. New York: Cold Spring Harbor Laboratory Press.

Gu, D., Dong, N., Zheng, Z., Lin, D., Huang, M., Wang, L., et al. (2018). A fatal outbreak of ST11 carbapenem-resistant hypervirulent *Klebsiella pneumoniae*

in a Chinese hospital: a molecular epidemiological study. *Lancet Infect. Dis.* 18, 37–46. doi: 10.1016/S1473-3099(17)30489-9

Horváth, M., Kovács, T., Koderivalappil, S., Ábrahám, H., Rákhely, G., and Schneider, G. (2020). Identification of a newly isolated lytic bacteriophage against K24 capsular type, carbapenem resistant *Klebsiella pneumoniae* isolates. *Sci. Rep.* 10:5891. doi: 10.1038/s41598-020-62691-8

Hsieh, P. F., Lin, H. H., Lin, T. L., Chen, Y. Y., and Wang, J. T. (2017). Two T7-like bacteriophages, K5-2 and K5-4, each encodes two capsule depolymerases: isolation and functional characterization. *Sci. Rep.* 7:4624. doi: 10.1038/s41598-017-04644-2

Hung, C. H., Kuo, C. F., Wang, C. H., Wu, C. M., and Tsao, N. (2011). Experimental phage therapy in treating *Klebsiella pneumoniae*-mediated liver abscesses and bacteremia in mice. *Antimicrob. Agents Chemother.* 55, 1358–1365. doi: 10.1128/AAC.01123-10

Katoh, K., and Standley, D. M. (2013). MAFFT multiple sequence alignment software version 7: improvements in performance and usability. *Mol. Biol. Evol.* 30, 772–780. doi: 10.1093/molbev/mst010

Knecht, L. E., Veljkovic, M., and Fieseler, L. (2020). Diversity and function of phage encoded depolymerases. *Front. Microbiol.* 10:2949. doi: 10.3389/fmicb.2019.02949

Kornienko, M., Ilina, E., Lubasovskaya, L., Priputnevich, T., Falova, O., Sukhikh, G., et al. (2016). Analysis of nosocomial *Staphylococcus haemolyticus* by MLST and MALDI-TOF mass spectrometry. *Infect. Genet. Evol.* 39, 99–105. doi: 10.1016/j.meegid.2015.12.015

Kozlov, A. M., Darriba, D., Flouri, T., Morel, B., and Stamatakis, A. (2019). RAxML-NG: a fast, scalable and user-friendly tool for maximum likelihood phylogenetic inference. *Bioinformatics* 35, 4453–4455. doi: 10.1093/bioinformatics/btz305

Kropinski, A. M. (2009). "Measurement of the rate of attachment of bacteriophage to cells," in *Bacteriophages Methods and Protocols, Volume 1: Isolation, Characterization, and Interactions*. eds. M. R. J. Clokie and A. M. Kropinski (New York: Humana Press), 151–157.

Labudda, Ł., Strapagiel, D., and Karczewska-golec, J. (2017). Complete annotated genome sequences of four *Klebsiella pneumoniae* phages isolated from sewage in Poland. *Genome Announc.* 5, e00919–e01017. doi: 10.1128/genomeA.00919-17

Laslett, D., and Canback, B. (2004). ARAGORN, a program to detect tRNA genes and tmRNA genes in nucleotide sequences. *Nucleic Acids Res.* 32, 11–16. doi: 10.1093/nar/gkh152

Latka, A., Leiman, P. G., Drulis-Kawa, Z., and Briers, Y. (2019). Modeling the architecture of depolymerase-containing receptor binding proteins in *Klebsiella* phages. *Front. Microbiol.* 10:2649. doi: 10.3389/fmicb.2019.02649

Lee, C. R., Lee, J. H., Park, K. S., Kim, Y. B., Jeong, B. C., and Lee, S. H. (2016). Global dissemination of carbapenemase-producing *Klebsiella pneumoniae*: epidemiology, genetic context, treatment options, and detection methods. *Front. Microbiol.* 7:895. doi: 10.3389/fmicb.2016.00895

Li, M., Xiao, Y., Li, P., Wang, Z., Qi, W., Qi, Z., et al. (2020). Characterization and genome analysis of *Klebsiella* phage P509, with lytic activity against clinical carbapenem-resistant *Klebsiella pneumoniae* of the KL64 capsular type. *Arch. Virol.* 165, 2799–2806. doi: 10.1007/s00705-020-04822-0

Lin, T. L., Hsieh, P. F., Huang, Y. T., Lee, W. C., Tsai, Y. T., Su, P. A., et al. (2014). Isolation of a bacteriophage and its depolymerase specific for K1 capsule of *Klebsiella pneumoniae*: implication in typing and treatment. *J. Infect. Dis.* 210, 1734–1744. doi: 10.1093/infdis/jiu332

Liu, Y. C., Cheng, D. L., and Lin, C. L. (1986). *Klebsiella pneumoniae* liver abscess associated with septic endophthalmitis. *Arch. Intern. Med.* 146, 1913–1916. doi: 10.1001/archinte.1986.00360220057011

Liu, Y., Leung, S. S. Y., Huang, Y., Guo, Y., Jiang, N., Li, P., et al. (2020). Identification of two depolymerases from phage IME205 and their antivirulent functions on K47 capsule of *Klebsiella pneumoniae*. *Front. Microbiol.* 11:218. doi: 10.3389/fmicb.2020.00218

Liu, B., and Pop, M. (2009). ARDB—antibiotic resistance genes database. *Nucleic Acids Res.* 37, 443–447. doi: 10.1093/nar/gkn656

Liu, B., Zheng, D., Jin, Q., Chen, L., and Yang, J. (2019). VFDB 2019: a comparative pathogenomic platform with an interactive web interface. *Nucleic Acids Res.* 47, D687–D692. doi: 10.1093/nar/gky1080

Majkowska-Skrobek, G., Łątka, A., Berisio, R., Maciejewska, B., Squeglia, F., Romano, M., et al. (2016). Capsule-targeting depolymerase, derived from *Klebsiella* KP36 phage, as a tool for the development of anti-virulent strategy. *Viruses* 8:324. doi: 10.3390/v8120324

Majkowska-Skrobek, G., Latka, A., Berisio, R., Squeglia, F., Maciejewska, B., Briers, Y., et al. (2018). Phage-borne depolymerases decrease *Klebsiella pneumoniae* resistance to innate defense mechanisms. *Front. Microbiol.* 9:2517. doi: 10.3389/fmicb.2018.02517

Manohar, P., Tamhankar, A. J., Lundborg, C. S., and Nachimuthu, R. (2019). Therapeutic characterization and efficacy of bacteriophage cocktails infecting *Escherichia coli*, *Klebsiella pneumoniae*, and *Enterobacter* species. *Front. Microbiol.* 10:574. doi: 10.3389/fmicb.2019.00574

Mazzocco, A., Waddell, T. E., Lingohr, E., and Roger, J. P. (2009). "Enumeration of bacteriophages by the direct plating plaque assay," in *Bacteriophages Methods and Protocols, Volume 1: Isolation, Characterization, and Interactions*. eds. M. R. J. Clokie and A. M. Kropinski (New York: Humana Press), 77–81.

Meier-Kolthoff, J. P., and Göker, M. (2017). VICTOR: genome-based phylogeny and classification of prokaryotic viruses. *Bioinformatics* 33, 3396–3404. doi: 10.1093/bioinformatics/btx440

Mirzaei, M. K., and Nilsson, A. S. (2015). Isolation of phages for phage therapy: a comparison of spot tests and efficiency of plating analyses for determination of host range and efficacy. *PLoS One* 10:e0118557. doi: 10.1371/journal.pone.0118557

Munoz-Price, L. S., Poirel, L., Bonomo, R. A., Schwaber, M. J., Daikos, G. L., Cormican, M., et al. (2013). Clinical epidemiology of the global expansion of kpn carbapenemases. *Lancet Infect. Dis.* 13, 785–796. doi: 10.1016/S1473-3099(13)70190-7

Paczosa, M. K., and Mecsas, J. (2016). *Klebsiella pneumoniae*: going on the offense with a strong defense. *Microbiol. Mol. Biol. Rev.* 80, 629–661. doi: 10.1128/MMBR.00078-15

Pan, Y. J., Lin, T. L., Chen, Y. Y., Lai, P. H., Tsai, Y. T., Hsu, C. R., et al. (2019). Identification of three podoviruses infecting *Klebsiella* encoding capsule depolymerases that digest specific capsular types. *Microb. Biotechnol.* 12, 472–486. doi: 10.1111/1751-7915.13370

Pan, Y., Lin, T., Chen, C., and Tsai, Y. (2017). *Klebsiella* phage ΦK64-1 encodes multiple depolymerases for multiple host capsular types. *J. Virol.* 91, e02457–e02516. doi: 10.1128/JVI.02457-16

Payne, R. J. H., and Jansen, V. A. A. (2000). Phage therapy: the peculiar kinetics of self-replicating pharmaceuticals. *Clin. Pharmacol. Ther.* 68, 225–230. doi: 10.1067/mcp.2000.109520

Pires, D. P., Oliveira, H., Melo, L. D. R., Sillankorva, S., and Azeredo, J. (2016). Bacteriophage-encoded depolymerases: their diversity and biotechnological applications. *Appl. Microbiol. Biotechnol.* 100, 2141–2151. doi: 10.1007/s00253-015-7247-0

Podschun, R., and Ullmann, U. (1998). *Klebsiella spp*. as nosocomial pathogens: epidemiology, taxonomy, typing methods, and pathogenicity factors. *Clin. Microbiol. Rev.* 11, 589–603. doi: 10.1128/CMR.11.4.589

Rodriguez-R, L. M., and Konstantinidis, K. T. (2014). Bypassing cultivation to identify bacterial species. *Microbe* 9, 111–118. doi: 10.1128/microbe.9.111.1

Satlin, M. J., Chen, L., Patel, G., Gomez-Simmonds, A., Weston, G., Kim, A. C., et al. (2017). Multicenter clinical and molecular epidemiological analysis of bacteremia due to carbapenem-resistant *Enterobacteriaceae* (CRE) in the CRE epicenter of the United States. *Antimicrob. Agents Chemother.* 61, e02349–e02416. doi: 10.1128/AAC.02349-16

Scorpio, A., Tobery, S. A., Ribot, W. J., and Friedlander, A. M. (2008). Treatment of experimental anthrax with recombinant capsule depolymerase. *Antimicrob. Agents Chemother.* 52, 1014–1020. doi: 10.1128/AAC.00741-07

Shon, A. S., Bajwa, R. P. S., and Russo, T. A. (2013). Hypervirulent (hypermucoviscous) *Klebsiella pneumoniae*: a new and dangerous breed. *Virulence* 4, 107–118. doi: 10.4161/viru.22718

Solovieva, E. V., Myakinina, V. P., Kislichkina, A. A., Krasilnikova, V. M., Verevkin, V. V., Mochalov, V. V., et al. (2018). Comparative genome analysis of novel podoviruses lytic for hypermucoviscous *Klebsiella pneumoniae* of K1, K2, and K57 capsular types. *Virus Res.* 243, 10–18. doi: 10.1016/j.virusres.2017.09.026

Sonda, T., Kumburu, H., van Zwetselaar, M., Alifrangis, M., Mmbaga, B. T., Lund, O., et al. (2018). Molecular epidemiology of virulence and antimicrobial resistance determinants in *Klebsiella pneumoniae* from hospitalised patients in Kilimanjaro, Tanzania. *Eur. J. Clin. Microbiol. Infect. Dis.* 37, 1901–1914. doi: 10.1007/s10096-018-3324-5

Stewart, P. S. (1996). Theoretical aspects of antibiotic diffusion into microbial biofilms. *Antimicrob. Agents Chemother.* 40, 2517–2522. doi: 10.1128/AAC.40.11.2517

Tängdén, T., and Giske, C. G. (2015). Global dissemination of extensively drug-resistant carbapenemase-producing *Enterobacteriaceae*: clinical perspectives on detection, treatment and infection control. *J. Intern. Med.* 277, 501–512. doi: 10.1111/joim.12342

Teng, T., Li, Q., Liu, Z., Li, X., Liu, Z., Liu, H., et al. (2019). Characterization and genome analysis of novel *Klebsiella* phage Henu1 with lytic activity against clinical strains of *Klebsiella pneumoniae*. *Arch. Virol.* 164, 2389–2393. doi: 10.1007/s00705-019-04321-x

Thiry, D., Passet, V., Danis-wlodarczyk, K., Lood, C., Wagemans, J., De Sordi, L., et al. (2019). New bacteriophages against emerging lineages ST23 and ST258 of *Klebsiella pneumoniae* and efficacy assessment in *Galleria mellonella* larvae. *Viruses* 11:411. doi: 10.3390/v11050411

Turton, J. F., Englender, H., Gabriel, S. N., Turton, S. E., Kaufmann, M. E., and Pitt, T. L. (2007). Genetically similar isolates of *Klebsiella pneumoniae* serotype K1 causing liver abscesses in three continents. *J. Med. Microbiol.* 56, 593–597. doi: 10.1099/jmm.0.46964-0

Tzouvelekis, L. S., Markogiannakis, A., Psichogiou, M., Tassios, P. T., and Daikos, G. L. (2012). Carbapenemases in *Klebsiella pneumoniae* and other *Enterobacteriaceae*: an evolving crisis of global dimensions. *Clin. Microbiol. Rev.* 25, 682–707. doi: 10.1128/CMR.05035-11

Van Twest, R., and Kropinski, A. M. (2009). "Bacteriophage enrichment from water and soil," in *Bacteriophages Methods and Protocols, Volume 1: Isolation, Characterization, and Interactions* eds. M. R. J. Clokie and A. M. Kropinski (New York: Humana Press), 15–23.

Volozhantsev, N. V., Myakinina, V. P., Popova, A. V., Kislichkina, A. A., Komisarova, E. V., Knyazeva, A. I., et al. (2016). Complete genome sequence of novel T7-like virus vB_KpnP_KpV289 with lytic activity against *Klebsiella pneumoniae*. *Arch. Virol.* 161, 499–501. doi: 10.1007/s00705-015-2680-z

Volozhantsev, N. V., Shpirt, A. M., Borzilov, A. I., Komisarova, E. V., Krasilnikova, V. M., Shashkov, A. S., et al. (2020). Characterization and therapeutic potential of bacteriophage-encoded polysaccharide depolymerases with β galactosidase activity against *Klebsiella pneumoniae* K57 capsular type. *Antibiotics* 9:732. doi: 10.3390/antibiotics9110732

Voulgari, E., Gartzonika, C., Vrioni, G., Politi, L., Priavali, E., Levidiotou-Stefanou, S., et al. (2014). The Balkan region: NDM-1-producing *Klebsiella pneumoniae* ST11 clonal strain causing outbreaks in Greece. *J. Antimicrob. Chemother.* 69, 2091–2097. doi: 10.1093/jac/dku105

Wang, C., Li, P., Niu, W., Yuan, X., Liu, H., Huang, Y., et al. (2019). Protective and therapeutic application of the depolymerase derived from a novel KN1 genotype of *Klebsiella pneumoniae* bacteriophage in mice. *Res. Microbiol.* 170, 156–164. doi: 10.1016/j.resmic.2019.01.003

Wu, Y., Wang, R., Xu, M., Liu, Y., Zhu, X., Qiu, J., et al. (2019). A novel polysaccharide depolymerase encoded by the phage SH-KP152226 confers specific activity against multidrug-resistant *Klebsiella pneumoniae* via biofilm degradation. *Front. Microbiol.* 10:2768. doi: 10.3389/fmicb.2019.02768

Wyres, K. L., Wick, R. R., Gorrie, C., Jenney, A., Follador, R., Thomson, N. R., et al. (2016). Identification of *Klebsiella* capsule synthesis loci from whole genome data. *Microb. Genom.* 2:e000102. doi: 10.1099/mgen.0.000102

Yu, Z., Qin, W., Lin, J., Fang, S., and Qiu, J. (2015). Antibacterial mechanisms of polymyxin and bacterial resistance. *Biomed Res. Int.* 2015:679109. doi: 10.1155/2015/679109

Yu, G., Smith, D. K., Zhu, H., Guan, Y., and Lam, T. T. Y. (2017). Ggtree: an R package for visualization and annotation of phylogenetic trees with their covariates and other associated data. *Methods Ecol. Evol.* 8, 28–36. doi: 10.1111/2041-210X.12628

Zhang, K. Y., Gao, Y. Z., Du, M. Z., Liu, S., Dong, C., and Guo, F. B. (2019). Vgas: a viral genome annotation system. *Front. Microbiol.* 10:184. doi: 10.3389/fmicb.2019.00184

Zhang, R., Zhao, F., Wang, J., Pei, G., Fan, H., Zhangxiang, L., et al. (2020). Biological characteristics and genome analysis of a novel phage vB_KpnP_IME279 infecting *Klebsiella pneumoniae*. *Folia Microbiol.* 65, 925–936. doi: 10.1007/s12223-020-00775-8

Zhou, Y., Liang, Y., Lynch, K. H., Dennis, J. J., and Wishart, D. S. (2011). PHAST: a fast phage search tool. *Nucleic Acids Res.* 39, 347–352. doi: 10.1093/nar/gkr485

Conflict of Interest: The authors declare that the research was conducted in the absence of any commercial or financial relationships that could be construed as a potential conflict of interest.

Publisher's Note: All claims expressed in this article are solely those of the authors and do not necessarily represent those of their affiliated organizations, or those of the publisher, the editors and the reviewers. Any product that may be evaluated in this article, or claim that may be made by its manufacturer, is not guaranteed or endorsed by the publisher.

frontiers in Microbiology

ORIGINAL RESEARCH
published: 24 August 2021
doi: 10.3389/fmicb.2021.706700

Virulent *Drexlervirial* Bacteriophage MSK, Morphological and Genome Resemblance With Rtp Bacteriophage Inhibits the Multidrug-Resistant Bacteria

*Muhammad Saleem Iqbal Khan, Xiangzheng Gao, Keying Liang, Shengsheng Mei and Jinbiao Zhan**

Department of Biochemistry, Cancer Institute of the Second Affiliated Hospital (Key Laboratory of Cancer Prevention and Intervention, China National Ministry of Education), School of Medicine, Zhejiang University, Hangzhou, China

OPEN ACCESS

Edited by:
Krishna Mohan Poluri, Indian Institute of Technology Roorkee, India

Reviewed by:
Claudia Villicaña, Centro de Investigación en Alimentación y Desarrollo, Consejo Nacional de Ciencia y Tecnología (CONACYT), Mexico
Ping He, Shanghai Jiao Tong University, China

***Correspondence:**
Jinbiao Zhan
jzhan2k@zju.edu.cn

Specialty section:
This article was submitted to Virology, a section of the journal Frontiers in Microbiology

Received: *07 May 2021*
Accepted: *14 June 2021*
Published: *24 August 2021*

Citation:
Khan MSI, Gao X, Liang K, Mei S and Zhan J (2021) Virulent Drexlerviriial Bacteriophage MSK, Morphological and Genome Resemblance With Rtp Bacteriophage Inhibits the Multidrug-Resistant Bacteria. Front. Microbiol. 12:706700. doi: 10.3389/fmicb.2021.706700

Phage-host interactions are likely to have the most critical aspect of phage biology. Phages are the most abundant and ubiquitous infectious acellular entities in the biosphere, where their presence remains elusive. Here, the novel *Escherichia coli* lytic bacteriophage, named MSK, was isolated from the lysed culture of *E. coli* C (phix174 host). The genome of phage MSK was sequenced, comprising 45,053 bp with 44.8% G + C composition. In total, 73 open reading frames (ORFs) were predicted, out of which 24 showed a close homology with known functional proteins, including one tRNA-arg; however, the other 49 proteins with no proven function in the genome database were called hypothetical. Electron Microscopy and genome characterization have revealed that MSK phage has a rosette-like tail tip. There were, in total, 46 ORFs which were homologous to the Rtp genome. Among these ORFs, the tail fiber protein with a locus tag of MSK_000019 was homologous to Rtp 43 protein, which determines the host specificity. The other protein, MSK_000046, encodes lipoprotein (cor gene); that protein resembles Rtp 45, responsible for preventing adsorption during cell lysis. Thirteen MSK structural proteins were identified by SDS-PAGE analysis. Out of these, 12 were vital structural proteins, and one was a hypothetical protein. Among these, the protein terminase large (MSK_000072) subunit, which may be involved in DNA packaging and proposed packaging strategy of MSK bacteriophage genome, takes place through headful packaging using the pac-sites. Biosafety assessment of highly stable phage MSK genome analysis has revealed that the phage did not possess virulence genes, which indicates proper phage therapy. MSK phage potentially could be used to inhibit the multidrug-resistant bacteria, including AMP, TCN, and Colistin. Further, a comparative genome and lifestyle study of MSK phage confirmed the highest similarity level (87.18% ANI). These findings suggest it to be a new lytic isolated phage species. Finally, Blast and phylogenetic analysis of the large terminase subunit and tail fiber protein put it in Rtp viruses' genus of family *Drexlerviridae.*

Keywords: electron microscopy, rosette like tail, *Rtp_like* bacteriophage, *Drexlerviridae*, antibacterial activity

INTRODUCTION

Bacteriophages are the most abundant acellular biological entities, with an estimated 10^{31} phage particles in the biosphere (Keen, 2015). They are obligate intracellular parasites, present everywhere wherever bacteria live (Suttle, 2005). The roles of phages could not be ignored as they are used as vehicles in gene transfer (Gómez-Gómez et al., 2019), an alternative to antibiotics (Alvi et al., 2020), and antibody engineering using phage display technology (Kalim et al., 2019). Regarding benefits, bacteriophages also cause severe problems in industrial production and fermentation units. Previously identified bacteriophage Rtp and DTL were isolated from the lysed culture in the industrial firm. Furthermore, a recent study conducted by Pacífico et al. (2019) isolated 43 coliphages from the human body fluid specimens, including blood, urine, and tracheal aspirates. Maintaining a sterile laboratory and working environment exacerbates the problem because these entities are often less vulnerable to standard sterilization (Wietzorrek et al., 2006; Halter and Zahn, 2018; Sprotte et al., 2019).

Escherichia coli C, a significant Gram-negative bacterium primarily isolated from sour cow's milk by Ferdinand Hueppe in Germany. This *E. coli* strain was commonly used in the industrial fermentation process like propanol, butanol, and 3-hydroxypropanoate under anaerobic conditions (Monk et al., 2016; Pekar et al., 2018). To our best knowledge, only one temperate phage P2 of *E. coli* C has been reported by Bertani and coworkers to date (Wiman et al., 1970). The lytic single-stranded bacteriophage Phi X 174 was also isolated from *E. coli* C, having the smallest size and no tail. Phage X 174 is the first bacteriophage with the whole genome, sequenced by Sanger, belonging to the *Microviridae* family (Sanger et al., 1977; Zheng et al., 2009).

However, the number of the bacteriophage genomic world is incomplete and lags far behind their host bacteria (Clokie et al., 2011). Horizontal gene transfer between phage–host interactions contributes to the genetic diversity and evolution of the phage community (Chibani-Chennoufi et al., 2004). The emergence of antibiotic resistance against bacteria is a significant threat to public health due to the lack of new antimicrobial compound discovery. Colistin is a last-alternative defense against carbapenem-resistant bacterial infections (MCR1/4). So, a new executing strategy needs to be adopted. In this regard, phage therapy has opened new avenues for treating multidrug-resistant (MDR) and extensively drug-resistance (XDR) bacterial pathogens. For safety reasons, biosafety assessment of the phage should be done before use, as phages may act as a vehicle to carry the antibiotic resistance and virulence genes (Cui et al., 2017). A previous study was done by Granobles Velandia et al. (2012), who isolated a phage in which the genome contained Shiga toxins (*Stxs*). These findings suggested that genome sequencing is necessary for safety concerns.

Consequently, with the continuous development of Next Generation Sequencing (NGS) techniques, more than 8,000 phages have completed genome-wide sequencing (Salisbury and Tsourkas, 2019). Then classifying the bacteria based on shape, nucleic acid, size, and lifestyle as either temperate or lytic phages got attention; they played a crucial role in the horizontal gene transfer and combating antibiotic resistance in medicine (Ackermann, 2011; Cui et al., 2017). It is, therefore, immensely desired to explore and scratch the surface to determine the sequences of coliphages because phage genomics provides the evidence to trace phage and bacterial evolution.

Therefore, in this study, we report the isolation of a lytic phage of *E. coli* C named MSK bacteriophage from the lysed culture. MSK bacteriophage can cause rapid lytic infection of bacterial culture in less than 2 h. Numerous bacteriophages in modern industrial fermentation facilities or labs can be a severe problem, including quality and quantity of products and financial losses (Halter and Zahn, 2018). To better understand the lifestyle events, genome, critical investigations, and its possible therapeutic usage, we sequenced the genome of MSK bacteriophage.

This study is the first report of isolation, identification, and characterization of the virulent phage from *E. coli* C having double-stranded DNA and a rosette-like tail. Similar previous illustrations revealed that over 96% of phages are tailed and contain dsDNA (Ackermann, 2011). Furthermore, ViPTree, virfam, and comparative analysis showed that the phage MSK is a member of the *Drexlerviridae* family (*Siphoviridae*), *Braunvirinae* subfamily, and Rtp like viruses genus in terms of the genomic content capsid, tail structure, and protein composition. In addition, MSK phage possesses a tail fiber protein together with a series of 46 other ORF showing the recognizable homology with Rtp bacteriophage (T1 like bacteriophage) and also has morphological resemblance to the rosette-like tail morphology. Indeed, phage MSK was shown to have a narrow host range, infecting the *E. coli* strains (AMP, TCN, and Colistin), and is highly stable even at high temperatures (100°C) and pH. Overall, these studies in the future could provide detailed insights regarding phage therapeutic drugs, phage virulence, antibiotic gene finding, and tracing the phage evolution and diversity.

MATERIALS AND METHODS

Bacteriophage Enumeration and Purification

E. coli phage MSK was primarily isolated from lysed *E. coli* (Migula) Castellani and Chalmers ATCC®13706™, also called "*E. coli* C" which is the primary host of bacteriophage ΦX174 (Fujimura and Kaesberg, 1962). Phage MSK was subsequently propagated on *E. coli* C in Luria Bertani broth (0.5% salt). In detail, 250 mL of an *E. coli* culture was grown at 30°C until optical density (OD) 600 nm reached 0.4. Then phage suspension was inoculated for 4 h at 30°C at MOI 0.01 until the culture OD600 to 0.4. After the cell lysis, culture debris was pelleted by centrifugation at 7,155×g for 15 min at 4°C. The crude phage suspension was concentrated at 4°C with one-fifth of the lysate volume of 20% polyethylene glycol (PEG) 8,000 and 1.5 M NaCl for 4 h. Next, phage suspension with PEG was centrifuged (16,099 × g for 15 min at 4°C), and the phage pellet was suspended in 8 mL of phosphate buffer (pH = 7.4). Finally, phage was collected by centrifugation at 16,099 × g for 15 min, and residual cell debris was removed.

Phage concentration was done in the presence of a 12% sucrose bed by using ultracentrifugation (105,000 × g for 2 h at 4°C), and then the phage pellet was kept in PBS 300 μL overnight at 4°C. Further purification of phage particles was performed using discontinuous sucrose and iodixanol gradient ultracentrifugation (175,000 × g for 4 h at 4°C) which have been widely used to separate virus particles and vectors on a large scale (Zolotukhin et al., 1999). The purified band was separated and gradient media was removed using Amicon® Ultra-4 Centrifugal Filter Unit (100 kDa). The purified phage titer was determined by plaque-forming unit (*PFU/mL*), as already described (Clokie et al., 2009). This phage suspension (1.5×10^{10} *PFU*/mL) was stored at 4°C and used for subsequent experiments. Overall systematic representation of MSK bacteriophage enumeration and purification is shown (**Supplementary Figure 1**).

Electron Microscopy

A purified bacteriophage MSK sample was examined by transmission electron microscopy (TECNAI-Spirit 120 Kv) in The Center of Electron Microscopy, Zhejiang University School of medicine. Briefly, the carbon-supported grid was glow discharged using the PLECO EASI GLOW™ 91000 Glow discharge system. Then 10 times diluted sample (3 μL) was absorbed to the glow discharged grid for 30 s, and extra phage particles were swiped out with filter paper. Then the grid containing the phage was stained with 2% aqueous uranyl acetate (UA) with three times intervals of 10 s, 10 s, and 1 min. The grid was dried at room temperature for at least 1 min, and micrographs were taken at different magnification using 87 Kx and 105 Kx with FEI Tecnai G2 Transmission Electron Microscope.

Assessment of MSK Phage Potential to Reduce Bacterial Growth

A known reduction assay, as reported earlier, was used for bacterial growth retardation (Clokie et al., 2009). For this purpose, a known amount of bacterial culture of *E. coli* C (*CFU*/mL) was treated with phage MSK in three independent reactions at MOI 10, 1, and 0.1 incubated at 30°C with shaking for 4 h. One flask was considered as a control (without phage MSK) and incubated at 200 rpm. Growth was estimated by measuring the optical density (OD600) every 30 min for 4 h.

MSK Phage Stability Under Physiochemical Conditions

The different physiochemical conditions (pH, temperature, and UV light) affect the stability of bacteriophage, which directly affects the titer or MOI (Multiplicity of infection) of phage. For this purpose, the known phage titer (1.5×10^{10} *PFU*/mL) was treated at different pH values (4, 6, 7.4, 8, 10, and 12) and different temperatures (30, 37, 45, 60, 100, and 120°C) for 1 h and UV light (20 W) for an additional period (5, 10, 15, 25, and 60 min). Finally, the viral titer was determined by the double-layer plaque assay method.

Determination of Burst Size and Burst Time for MSK Bacteriophage

It is imperative for the bacteriophage analysis to measure the one-step growth curve, which helps us calculate the latent period and burst size. Briefly, the latent time was calculated from the single-stage growth curve. The burst size was calculated by the mean yield of phage used for a bacterial infection to the mean output of phage particles liberated after infection. This *in vitro* experiment was performed according to the method reported previously (Alvi et al., 2020). Briefly, bacterial host strain (1×10^{10} *CFU*) was harvested by centrifugation (1,789 ×g) for 5 min. Then, supernatant was discarded, and the pellet was mixed in 500 μL of LB broth. Further, bacterial culture was mixed with MSK (1×10^{10} *PFU/mL*) at MOI 1, followed by incubation for 1 min at 30°C. After that, free bacteriophage was removed from the mixture after centrifugation at 13,000 rpm for 30 s, and the titer in the supernatant was measured. Next, the pellet was dissolved in 100 mL of fresh sterile LB broth, followed by incubation at 30°C. After every 5 min interval, samples (1 mL) were collected for 1 h; subsequently, the phage titer was calculated by plating on an LB agar plate.

Genomic DNA Characterization and Library Generation

The genomic DNA of purified phage *E. coli* phage MSK was firstly extracted using the M13 DNA extraction kit (Omega) according to the manufacturer's protocol. Further, DNA was run on 0.8% agarose gel to get rid of other DNA contaminants. Then DNA was purified from a gel extraction kit (Omega). The concentration of the DNA sample was determined by Equalbit™ dsDNA High sensibility assay kit (Vanzyme, China, Cat No; EQ111-01/02) by using Qubit® 2.0 fluorometer and agarose gel electrophoresis to detect the quality of the DNA sample. Next, DNA was treated with *DNase I* and *RNase I* at 37°C overnight to make sure either DNA has single-stranded or double-stranded as previously described (Ma and Lu, 2008).

Initially, the size (base pair) of the genome was assessed through digestion with molecular scissors before sequencing. The phage MSK DNA was digested with a single and combination of enzymes. The single Fast-Digest enzymes included *EcoRI, NheI, XbaI, SacI, NdeI, BglII,* and *XhoI*. Similarly, the double digestion enzyme included these combinations: *XbaI + PacI and BamHI + PacI, PacI + SalI*. All enzymes were purchased from New England BioLabs® Inc. All the digestion were performed at 37°C with overnight incubation. The restriction fragments were mapped on 0.8% agarose gel and stained with red staining dye (Szymczak et al., 2020). For further characterization of DNA, electropherogram of *EcoRI* digested DNA was mapped with Agilent Fragment Analyzer Systems (Hangzhou Lianchuan Biotechnology Co., Ltd., China) to estimate the genome size (Lakha et al., 2016; Yu et al., 2016).

The genomic DNA of phage MSK was subjected to next-generation sequencing platforms (MGISEQ-2000 Beijing Genomics Institute) at the State Key Laboratory of agriculture science Zhejiang University, China. The DNA samples that have passed the electrophoresis detection were randomly broken into

pieces with a length of approximately 350 bp using a Covaris ultrasonic disruptor. Then the processed DNA fragments were repaired using an A-tail sequencing adapter at the end. After that constructed library was quantified using Agilent 2100 and also ensured the quality of the library. Finally, different libraries were pooled for sequencing.

Sequence Assembly and Genome Analysis

Raw data obtained from sequencing were cleaned to make it accurate and reliable for subsequent analysis. Before sequence assembly, 15 K-mer statistics were performed to estimate the size of the gnome. Sequence reads were assembled through SOAP denovo (version 2.04), SPAdes, ABySS, and finally use CISA software for integration. Gapclose (Version: 1.12) was used to fill the gap, Scaffold length greater than 500 bp was selected for further evaluation, and statistical analysis was performed. The genome annotation was performed utilizing different bioinformatics tools. Online RAST server, Gene MarkS (Version 4.17), and Gene Glimmer were used for the identification of open reading frames (ORFs) within the genome.

In addition, the Genome sequence was analyzed using RepeatMasker (Version open-4.0.5) software for scattered repetitive sequence prediction and Tandem Repeats Finder (Version 4.07b) for tandem repeats in DNA sequences. Furthermore, the genome was scanned by tRNAscan-SE software (Version 1.3.1) for tRNA prediction, rRNA was predicted by scrutinizing through rRNA library and rRNAmmer software (Version 1.2), and cmsearch program (Version 1.1rc4) was used to determine the final sRNA. The genome was also analyzed for gene island (genomics island, GIs) to ensure the transfer of horizontal gene transfer, which is predicted by comparative genome analysis and CRISPR-associated genes (Cas gene) in the genome was identified by using the CRISPR finder tool.[1] Finally, the sequence was analyzed using phiSpy software (Version 2.3) to predict prophage in the genome sequence.

Genome function annotation was done by comparing the ORFs with already reported genes using GO, KEGG, COG, NR, Pfam, TCDB, and swiss-port. Gene ontology (GO) was used to predict the cellular components, molecular function, and biological process in the genome. Metabolic pathways in the genome were predicted by KEGG[2] using multiple tools like KEGG pathway, KEGG drug, KEGG disease, KEGG module, KEGG Genes, KEGG genome, and KEGG orthology. NCBI COG protein database[3] was used to find the coding protein of the complete genome, which determined their features.

Transporter Classification Database (TCDB) was used to identify the membrane proteins in a sequence. Identifying of protein domains is particularly crucial for analyzing protein function done through the Pfam database.[4] Swiss-pro[5] provides a high level of annotation results like function, domain structure, post-translational modification, and variations. The enzyme family search was done by Carbohydrate-Active enZYmes Database (CAZy) was also utilized. Furthermore, comprehensive species information was obtained by using NR (non-redundant) Database. SignalP (Version 4.1) and TMHMM (Version 2.0c) were used to identify sequence elements involved in targeting the secretory pathway and transmembrane helices in annotated gene products, respectively.[6,7]

The genome sequence was also analyzed in seven different types (T1SS, T2SS, T3SS, T4SS, T5SS, T6SS, T7SS) of TNSS (type N secretion system), which are usually secreted into the extracellular environment and cause pathogenic response and cell death. For T3SS effector protein prediction, *EffectiveT3* software (Version 1.0.1) was used. The secondary metabolites play a role during specific growth periods, but these proteins have no apparent function. So, secondary metabolites prediction was made by using the antiSMASH program (version 2.0.2). Pathogen and host interaction database (PHI) was used to find the target genes responsible for the host infection.

The function of predicted ORFs and their similarity to other phage genes was analyzed using NCBI BLASTp,[8] HMMER,[9] and MPI Bioinformatics Toolkit, HHpred.[10] In addition the proteins were characterized for their theoretical molecular weight and isoelectric point (pI) using ProtParam (ExPASy—ProtParam tool). Finally, the genome map of the predicted ORFs and their GC percentage in the whole genome was drawn with the help of Snapgene.[11]

Genome Sequence Accession Number

The complete genome sequence of the *E. coli* phage MSK has been submitted in the NCBI GenBank (Bankit) nucleotide sequence database with accession number MW057918.

Safety Assessment of the Phage MSK

Lifestyle (lytic or temperate) of the *E. coli* phage MSK was predicted using the PHACTS program. Then all the interpreted ORFs were compared against the sequences in the comprehensive antibiotic resistance database (CARD),[12] which analyzed the sequences using BLAST and resistance gene identifier (RGI) software for prediction of resistome based on SNP and homology model. RGI uses a perfect, strict, and complete algorithm to identify the antimicrobial resistance (AMR) genes in the entire genome (Alcock et al., 2019). In addition to AMR genes determination, we also determine virulence factor by virulence Finder database,[13] for detection of *E. coli* virulence genes [verocytotoxin 1 (vtx1), verocytotoxin 2 (vtx2), and intimin (eae)] and subtypes (Joensen et al., 2014).

[1] http://crispr.i2bc.paris-saclay.fr/Server/

[2] http://www.genome.jp/kegg/

[3] http://www.ncbi.nlm.nih.gov/COG/

[4] http://pfam.xfam.org/

[5] http://www.ebi.ac.uk/uniprot

[6] http://www.cbs.dtu.dk/services/TMHMM/

[7] http://www.cbs.dtu.dk/services/SignalP/

[8] https://blast.ncbi.nlm.nih.gov/Blast.cgi?PAGE=Proteins

[9] https://www.ebi.ac.uk/Tools/hmmer/

[10] https://toolkit.tuebingen.mpg.de/tools/hhpred

[11] http://www.snapgene.com/

[12] http://arpcard.mcmaster.ca

[13] https://cge.cbs.dtu.dk/services/VirulenceFinder/

SDS PAGE and *in silico* Mass Fingerprinting

Phage MSK structural Protein profile was determined by Sodium Dodecyl Sulfate-Polyacrylamide Gel Electrophoresis (SDS-PAGE). The purified phage sample (20 μL) having phage particles was dissolved in 20 μL laemmli buffer, and the mixture was heated in boiling water (90°C) for 10 min. After heating, a medley of the sample was subjected to post cast, horizontal 12% SDS-PAGE gel electrophoresis with protein marker (pre-stained protein ladder, Thermo Fisher Scientific) and Tris-glycine as running buffer. The gel was stained with Coomassie Brilliant Blue R250 dye (Sigma), destained with the destaining solution for 30 min, and visualized under the camera. Peptide mass fingerprinting was performed *in silico* using Gel Molecular weight analyzer (Origin(Pro), 2021). The software calculated the peptide mass (kDa) by known molecular weight protein, a standard curve generated by a polynomial with order three and regression equation (R = 0.99927). Finally, the calculated molecular weight was compared against a feature table of MSK phage proteins manually, and then protein residues and molecular weight was calculated using Protein Molecular Weight (bioinformatics.org) and domains.

DNA Packaging Strategy and Comparative Genome Analysis

The identification of genome termini and prediction of the phage packaging mechanism was carried out using the PhageTerm application incorporated in Galaxy[14] (Garneau et al., 2017). The Classification of phage MSK major proteins (neck, head, and tail protein) was constructed using Virfam online automated tool, enabling us to predict the phage families. For this purpose, the annotated protein sequence of phage MSK was run online to predict the structural module (head, neck, and tail genes) and their function. Virfam can also predict the morphologic type and classify the phages based on the "head, neck, and tail" module. Primarily these analyses can be used to classify unknown viruses (Lopes et al., 2014).

Furthermore, the tree among *E. coli* phages MSK and other bacteriophages of different families were generated by ViPTree server version 1.9.[15] ViPTree (proteomics tree) was generated based on the genome wide sequence similarities computed by tBLASTx. The proteomics tree method is productive to scrutinize the genomes of the newly sequenced bacteriophages or viruses for the prediction of families.

Additionally, comparative genome analysis calculates the average nucleotide identity (ANI) using the ANI calculator (Yoon et al., 2017). Finally, the genome of MSK phage was compared with the *Drexlerviridae* family's four bacteriophages having (*Escherichia* phage vB_EcoS-2862V, *Escherichia* phage vB_Ecos_CEB_EC3a, *Escherichia* phage DTL and, Rtp bacteriophage) having ANI value greater than 83%. These bacteriophages have similar lengths (44–46 Kbp), the number of genes (67–75). The genome of the Rtp bacteriophage was downloaded in the in gene bank file (gb) as a reference genome, and the other three phage genome was downloaded in FASTA format. Comparative genomic analysis was done using multiple sequence alignment using MAUVE (Darling et al., 2004).

Antibacterial Activity of MSK Phage Against Multidrug-Resistant Bacteria

Antimicrobial activity of bacteriophage MSK was assessed on five clinical antibiotic resistance *E. coli* isolates acquired from the first affiliated hospital and Department of Pathogen Biology and Microbiology, Zhejiang University School of Medicine, China. These *E. coli* isolates were resistant to different antibiotics like ampicillin (AMP), Extended Spectrum Beta-Lactamase (ESBL), Tetracycline (TCN), Colistin (mcr-4), and Colistin (nmcr-1). The lytic activity of MSK was determined against these five *E. coli* pathogenic strains, *Pseudomonas syringae* and *Salmonella anatum,* using a spot test. Briefly, 100 μL of a log-phase culture of the test strain was mixed gently by avoiding bubble formation with 3 mL of LB semi-solid agar. The mixture was poured on the solidified LB agar plate and spread over the plate uniformly by swirling. Then 3 μL of purified, diluted phage (1.35×10^5 *PFU/mL*) was added to the solidified LB agar plate having different pathogenic strains. The appearance of clear zones after overnight incubation at 37°C was presumptive of positive lytic activity of MSK (Clokie et al., 2009).

RESULTS

MSK Bacteriophage Form Clear and Transparent Circular Plaque

The *Escherichia* phage MSK indicated a potent lytic activity against *E. coli* C. This phage, named MSK in recognition of its identifier, lysed the *E. coli* culture in the Gene and Antibody Engineering lab. The lysed culture was diluted and cultured to obtain transparent plaques on a double-layered plaque assay. Phage MSK produced circular and homogenous transparent plaques with a diameter of around 4–5 mm (**Figure 1**). The titer of the phage MSK was against host strain 10^8 *PFU*/mL. Finally, three times purified, a clear plaque was picked and propagated; lysate obtained was preserved at 4°C for further studies.

Characterization of Phage Morphology Through Electron Microscopy

Using the discontinuous sucrose and iodixanol gradient, three different negative staining results from each gradient media were obtained. The white strips corresponding to the location of particles were taken out from the gradient, and further negative staining of electron microscopy was performed for morphological characterization. From the results, the discontinuous sucrose gradient MSK particles were found to be broken non-infectious with opaque background having partial morphology. Most of the phage particles separated by this gradient always lost their DNA, tail and retained only capsid protein. Three different bands were separated during the discontinuous sucrose gradient. The first band micrograph

[14]https://galaxy.pasteur.fr/

[15]https://www.genome.jp/viptree/

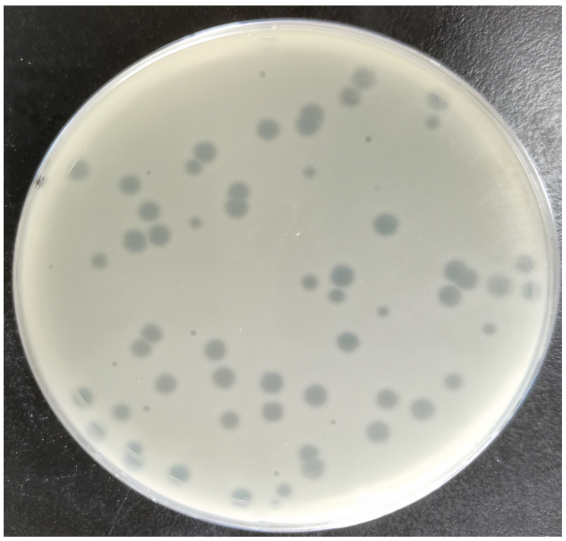

FIGURE 1 | Clear plaque fashioned by *Escherichia coli* phage MSK with *Escherichia coli C* host (primarily ΦX174 host) lawn on a double-layer agar plate.

represents the broken head from the tail and empty capsid with an opaque background (**Figure 2B**). The second micrograph depicts an intact particle with opaque background (**Figure 2C**). The third micrograph represents the particles which deformed and collapsed because of the centrifugation speed and gradient media (**Figure 2D**). Compared to sucrose gradient media, the iodixanol gave many essentially complete intact MSK phage particles and transparent background. The first micrograph represents some phage particles with empty shell, but many were intact compared to sucrose (**Figure 2E**). The second and third iodixanol EM micrograph found it to be a complete infectious particle containing DNA, capsid, and tail with transparent background (**Figures 2F,G**). The second and third bands obtained from iodixanol gradient with complete infectious and morphological features were used to further structure characterization.

Consequently, morphological characterization of phage MSK revealed a non-enveloped, long, non-contractile tail of approximately 151 nm in length and 8 nm in width, with four short linked rosette-like morphologies of the tail tip through electron micrographs. Moreover, it has an icosahedral head with an average diameter of 50 nm. Thus, MSK phage has a close morphological resemblance with Rtp bacteriophage based on the icosahedral head, tail morphology, and tail length.

MSK Lyse the Host Bacteria Growth for 4 h at Different MOI

Further, to check the lysing activity of the Phage MSK against host bacteria, we applied three MOIs (10, 1, and 0.1) along with control. Phage MSK completely inhibits the host bacterium growth *in vitro* for 4 h when different phage titers were applied in contrast to control. The differences between these groups become insignificant (**Figure 3**). The optical density of the phage inoculated group was much lower than that of a control group which indicated that MSK phage could completely lyse the host cell within 2 h of infection. After 2 h, the number of host cell OD becomes close to zero in growing media.

MSK Stability Under Different Physiochemical Conditions

Evaluation of the phage stability and its activity in different physiochemical conditions (pH, temperature, UV light) plays a significant role. Results in the pH range of 4–12 showed that phage MSK was less susceptible to all pH ranges, demonstrating MSK phage stability over a wide range. However, we were unable to identify the optimum pH range for MSK phage stability (**Supplementary Figure 2A**). Similarly, phage stability was evaluated at different temperatures ranging from (30°C to autoclave temperature. The plaque forming unit (PFU) showed that the phage was stable even at high temperatures (100°C). There was not a significant difference noted after applying different temperatures up to 100°C. The phage MSK did not make any plaques at a higher temperature of 120°C. One thing that was interesting to note was that phage MSK makes plaque with a smaller size at a higher temperature of 100°C. That shows that the phage was stable at 100°C (**Supplementary Figure 2B**).

Additionally, The UV light exposure for MSK phage stability also did not affect its stability. These findings demonstrated that phage is very stable even during the application of harsh conditions (**Supplementary Figure 2C**). In the last, we were unable to identify the reason behind this stability of the phage.

MSK Has a Short Latent Period and Burst Size

Moreover, to enumerate the phage latent period and burst size, we determined a one-step growth curve. The one-step growth curve showed that the phage MSK had a latent period of 25 min which produces more than 200 virions per cell. The burst time occurred between 25 and 45 min (**Figure 4**). Thus, the number of phage particles in the supernatant media increased rapidly, specifying that bacteria were lysed and phages were released into the environment.

MSK Phage DNA Quantification

Next, to determine the size of phage MSK, the DNA was purified (16.5 ng/μL) from the iodixanol purified bacteriophage and run on 0.8% agarose gel (**Figure 5A**). DNA was treated with *DNase I* and *RNase I* (**Figure 5B**), which confirmed that the genome is a linear double-stranded molecule. Firstly, before sequencing, the genomic size was estimated through single digestion with molecular scissors (**Figures 5C,D**), through which size estimation was indistinguishable. Then, DNA was digested with a combination of enzymes (**Figure 5E**), which also gave ambiguous band separation and size estimation. Further, the size and integrity of genomic DNA were quantified using the Agilent Fragment Analyzer Systems. Previously, single *EcoRI* digested with clear band of separation was brought to mapped electropherogram. Moreover, the appropriate size before preparing libraries for sequencing was also determined

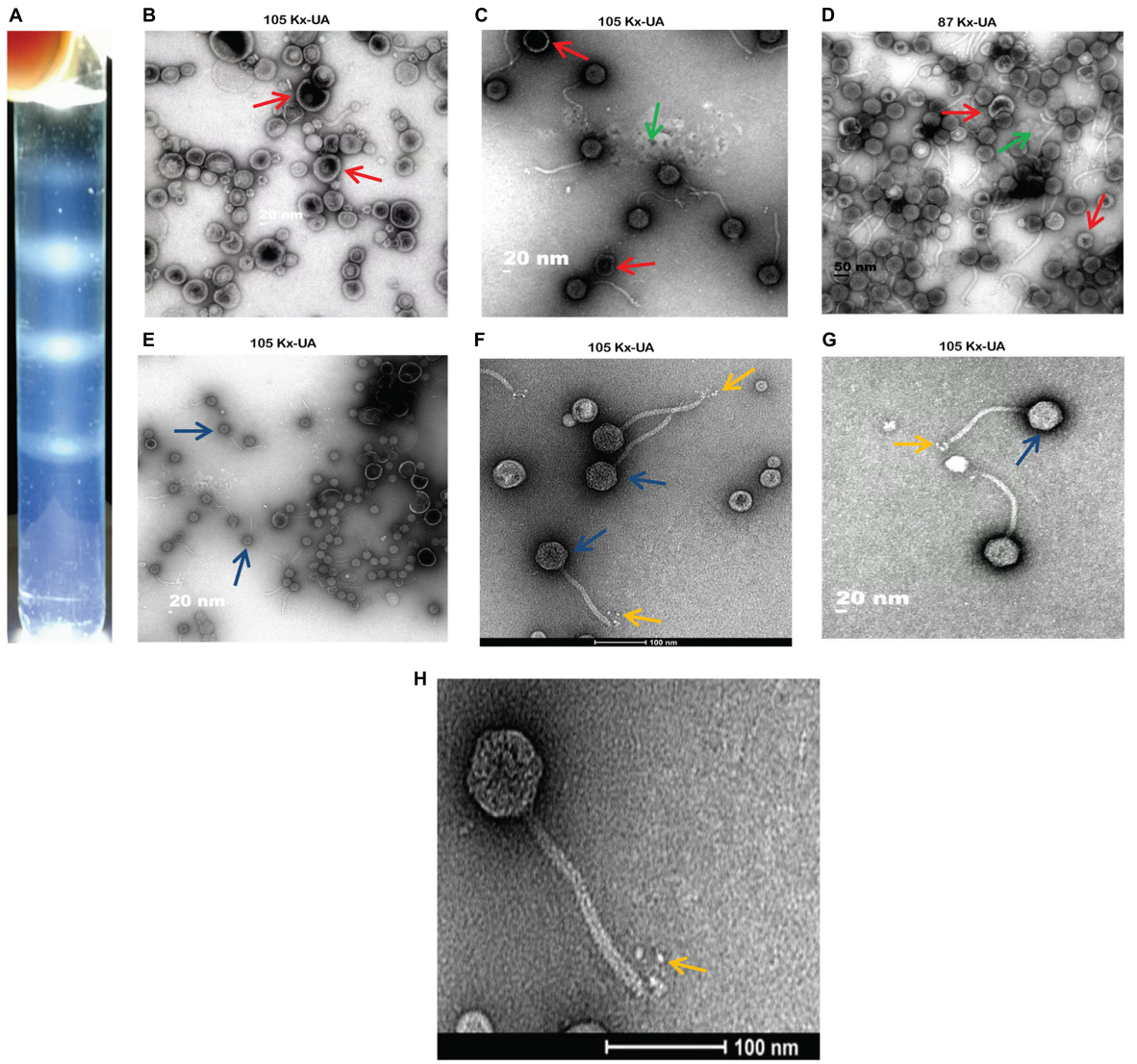

FIGURE 2 | A comparison between two density gradient media and Electron Micrograph of Escherichia phage MSK **(A)** cleared white band was observed in iodixanol gradient compared with sucrose gradient. **(B–D)** Three different bands separated during discontinuous sucrose density gradient. **(E–G)** Three various bands separated during discontinuous iodixanol density gradient. Red arrow: broken particles, blue arrow: intact particles, yellow arrow: rosette-like tail, green arrow: opaque background. **(H)** Electron micrograph of Escherichia phage MSK having a rosette-like tail with 100 nm bar line.

(**Figure 5I**). Finally, single, double enzyme digested, and electropherogram gave the estimation yield a contig of 40–43 kb in phage MSK genomic DNA.

Secondly, we sequenced the genomic DNA of *E. coli* phage MSK comprising 45,053 bp. Then, the DNA sequence was digested with the same enzyme in SanpGene to confirm the band pattern as shown (**Figures 5F–H**). These restriction digestion patterns *in silico* and *in vivo* assure the correct genome assembly.

Genome ORF Features Prediction and Module Formation

The assembled genome of *E. coli* phage MSK comprised 45,053 bp with a GC composition of 44.8%. During the sequence, NCBI blast analysis revealed that the phage genome was similar to previously sequenced *E. coli* phages with 88.44–90.36 percentage identities, including *Escherichia* phage vB_Ecos_CEB_EC3a, Enterobacteria phage vB_EcoS_ACG-M12, *Escherichia* phage DTL and Bacteriophage RTP. With the advancement of sequencing technology, a number of sequenced bacteriophages has been increasing continuously in the NCBI database. Assembled genome NCBI blast showed that the sequence was similar to previously sequenced 32 Escherichia phages displaying 90–91.18% identity during NCBI blast including *Escherichia* phage vB_EcoS-2862V (MK907276.1) and *Escherichia* phage vB_EcoS-2862IV (MK907275.1) revealed 91.18% nucleotide percentage identity and *E*-value = 0. These sequence similarity results suggest

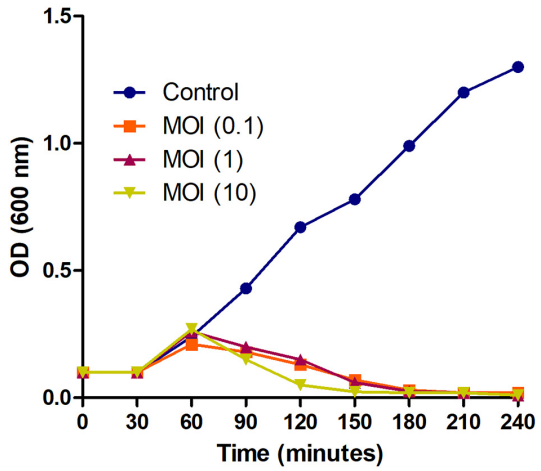

FIGURE 3 | Bacterial growth reduction assay of MSK bacteriophage at different MOI. Purified lytic bacteriophage *in vitro E. coli* C was infected with different phage MOIs (10, 1, and 0.1). *E. coli* C growth reduction assay of MSK at MOI = 10 showing a marked decrease in the bacterial growth within 2 hours as compared to MOI (0.1, 1) and non-treated *E. coli* C control. The bacterial growth was utterly suppressed till 3–4 hours, infecting with the MOI = 0.1,1,10.

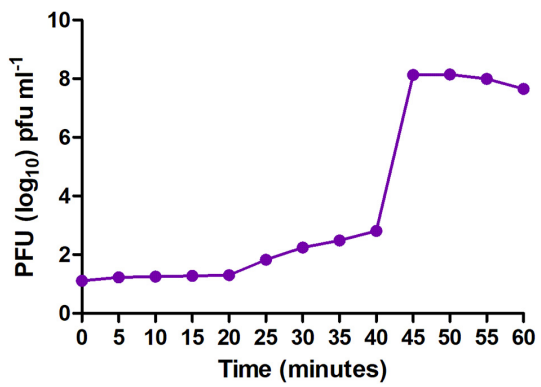

FIGURE 4 | One-step growth curve of MSK bacteriophage. The purified bacteriophage showed a latent period of 25 min, and burst time occurred between 25 and 45 min.

that the MSK phage is a member of the *Drexlerviridae* family (tail bacteriophage).

Gene annotation predicted a total of 73 open reading frames (ORFs). Gene Marks showed 71 (**Supplementary Figures 3A,B**), while gene glimmer and RAST sever predicted 73 ORFs, respectively (**Supplementary Table 1**). Each ORF had an average length of 564–600 bp, having 39.39% internal GC contents. The gene length distribution showed that ORF covers all the genome but is majorly distributed at the start of the genome (**Supplementary Figure 3C**). The persistence of repeat sequences has also been found in phage genomes like LTR/DNA/LINE, in different numbers like one, one, and two, respectively. Similarly, Tandem repeats (TR) sequence presence was also found in the genome, but analysis showed no single sequence of SINE, RC, minisatellite, and microsatellite (**Supplementary Figures 4A,B**).

Further, we also performed a tRNAscan program (version 2.0) analysis that showed only one Arg type tRNA of 78 bp in length, but no sRNA or rRNA presence was noticed in the genome (**Supplementary Figure 5A**). The genome analysis was also done by finding a CRISPR case-associated gene, but not a single sequence was identified. Finally, Phispy predicted that the genome has similarities with bacteriophages with an average length of 21,847 bp (16,781–38,627), which showed that our genome has all major structural and functional proteins for bacteriophage assembly (**Supplementary Figure 5B**).

Ahead, genome functional profile was predicted majorly by comparing the protein sequence with available databases with *e*-value $\leq$ 1e-5 and with the highest score value (default identity $\geq$ 40%) and for annotation coverage percentage should be higher than 40 (coverage $\geq$ 40%). Genome functional annotation was done using different algorithms. Using Gene Ontology, we predicted a total number of 22 proteins that are expected to be involved in molecular function, 16 in cellular components, and 38 in biological processes (**Supplementary Figure 6A**). Different KEGG systems were used for metabolic pathways prediction of gene products and compounds. Further, orthologous groups of proteins were predicted by protein database COG, which predicted eight functional genes (**Supplementary Figure 6B**).

Annotations were carried out by The NR (Non-Redundant), a protein database that gave us complete species information; the bacteriophage genome resembled about 14 different bacterial species (**Supplementary Figure 6C**). Then, TCBD functional classification showed that it has two proteins, one is holin (MSK_000044), and the other one is putative transport protein (MSK_000046) (**Supplementary Figure 6D**). Another classification showed it has one channel pores, and the other is an incomplete transport system (MSK_000044, MSK_000046) (**Supplementary Figure 6E**). The enzyme search through The CAZy database showed that there was only one major Glycoside Hydrolases (GH) enzyme member in the sequence (MSK_000045), which functioned as a Lysozyme RrrD as shown in **Supplementary Figure 6F**. Lysozyme is the hydrolyzing enzyme that causes the lysis of the 1–4 beta-linkages between N-acetylmuramic acid and N-acetyl-D-glucosamine residues in a peptidoglycan and between N-acetyl-D-glucosamine residues in chitodextrins. Particularly this enzyme helps the phage to release its progeny from the host cell by cytolysis. This enzyme can now also be used as an antimicrobial and bacteriolytic for therapeutic purposes because of its hydrolyzing ability against pathogenic bacteria (Srividhya and Krishnaswamy, 2007).

Proteins generally contain functional regions called domains, so predicting protein domains for analyzing protein function was done through Pfam (**Supplementary Table 1A**). Moreover, Pfam clan; Pfam families emerge from a single evolutionary origin (**Supplementary Table 1B**). After that high level of annotation, results like function, domain structure, post-translational modification, and variations are achieved through the swiss-pro database, which is mentioned in **Supplementary Table 2**.

The secreted protein synthesized in the cell and secreted out of the cell through the cell membrane under the guidance

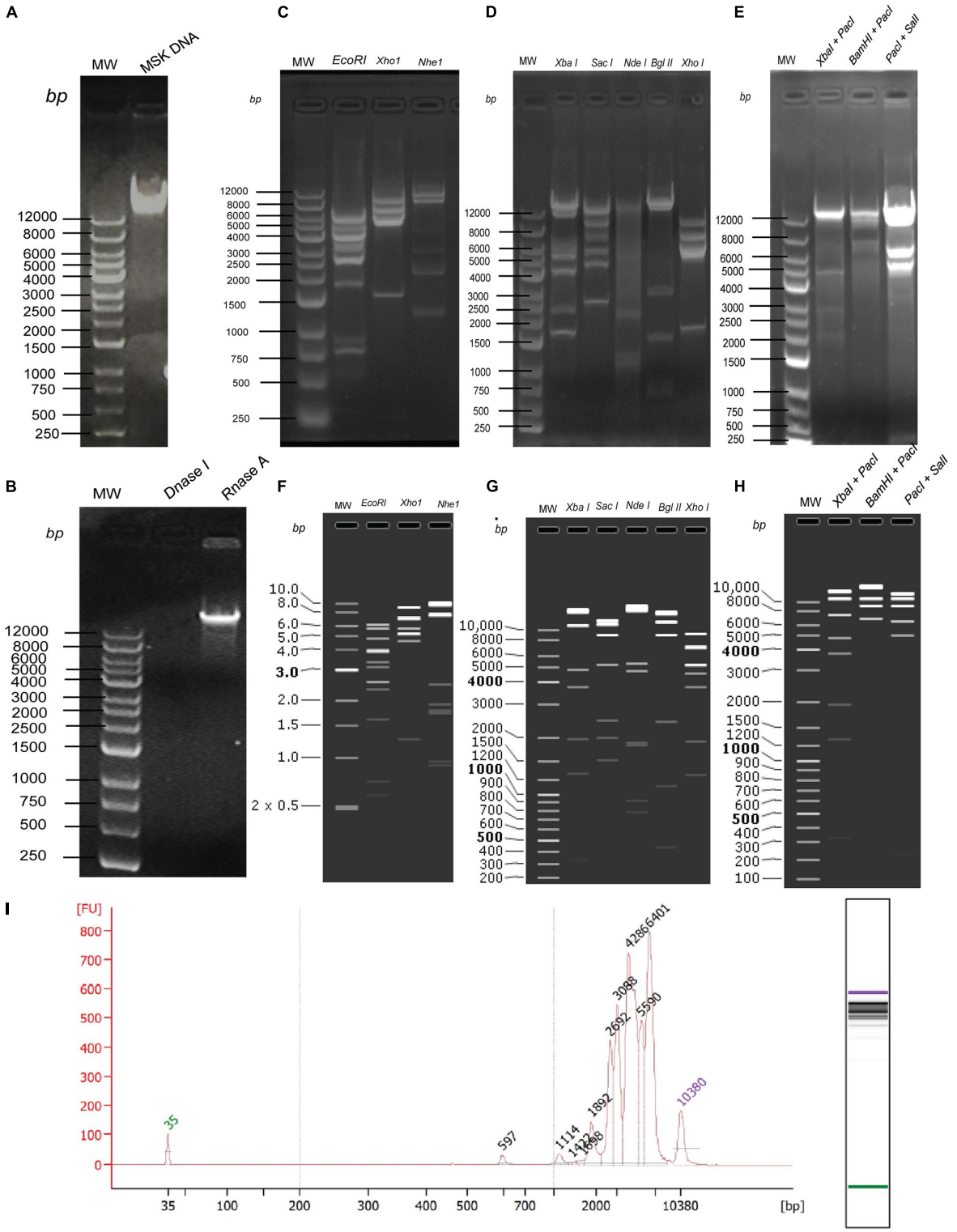

FIGURE 5 | *In vitro* and *in silico* phage MSK size estimation through restriction enzymes. **(A)** Purified DNA extracted from purified phage particles. **(B)** Phage genome confirmation using *DNase* I and *RNase* I. **(C)** Phage DNA digested with single enzymes digestion *Eco*RI, *Xho*I, and *Nhe*I. **(D)** Phage DNA digested with single enzymes digestion *Xba*I, *Sac*I, *Nde*I, *Bgl*II, *Xho*I. **(E)** Phage DNA digested with double enzymes digestion *Xba*I + *Pac*I and *BamH*I + *Pac*I, *Pac*I + *Sal*I. **(F)** *In silico* Phage DNA digested with single enzymes digestion *Eco*RI, *Xho*I, and *Nhe*I. **(G)** *In silico* Phage DNA digested with single enzymes digestion *Xba*I, *Sac*I, *Nde*I, *Bgl*II, *Xho*I. **(H)** *In silico* Phage DNA digested with double enzymes digestion *Xba*I + *Pac*I and *BamH*I + *Pac*I, *Pac*I + *Sal*I. **(I)** Phage DNA digested *Eco*RI and mapped with Agilent Fragment Analyzer Systems.

of a signal peptide composed of acid. Whereas the secreted protein N-terminus is composed of 15–30 amino groups. Six transmembrane helicase encoding regions predicted by TMHMM in some genes (MSK_000011, MSK_000018, MSK_000044, MSK_000046, MSK_000050, MSK_000067), while only two secretory signal peptide encoding genes were determined by SignalP in genome (MSK_000011, MSK_000046). The result obtained is also shown in the table (**Supplementary Figure 7A**).

Among the 73 predicted genes, no single gene was identified in the type N secretion system, which helps find a pathological response (**Supplementary Figure 7B**). EffectiveT3 software (Version 1.0.1) prediction shows that there only 4 true T3S effector proteins (MSK_000026, MSK_000028, MSK_000031, and MSK_000052) and 69 are false T3SS effector proteins (**Supplementary Figure 7C**). During the genome, annotation results showed no secondary metabolites, and pathogen-host interaction was founded.

Then, features analysis showed that there are 73 open reading frames in assembled MSK phage genome. Among these 73, 49 were called hypothetical proteins, as no homologous with proved function exists in the genome database. Twenty-four showed a close resemblance with identified functional proteins, divided into five putative functional protein modules; Morphogenesis proteins, metabolic enzymes, lysis cassette, additional phage feature proteins, and hypothetical proteins.

Genome analysis revealed that there were at least 16 ORFs involved in the morphogenesis of bacteriophage MSK. These proteins include major capsid protein, portal protein, lipoprotein, tail fiber, tail assembly and tail tap measure proteins, tRNA, and DNA packaging proteins (terminase large and small subunit); among these proteins, tail fiber protein and lipoprotein gave a close homology with Rtp bacteriophage. In addition, we identified seven ORFs that were involved in the metabolism, including primase and helicase, recombinase, DNA adenine methyltransferase, polynucleotide kinase/phosphatase; these enzymes aid in nucleotide metabolism. Due to the presence of the primase and helicase, the phage is independent of a host and uses its machinery for replication. In addition, phage MSK recombinase (MSK_000027) is considered to play a role in genome repair, replication, and recombination.

We also identified two ORFs encoding proteins associated with lysis cassette (holin and lysozyme), responsible for the host cell lysis. Among these, protein holin helped to form a pore and provide a channel for lysozyme to access and degrade the bacterial cell wall (peptidoglycan layer). Besides, two additional phage proteins helped the phage in morphogenesis or metabolism. Finally, these four feature modules and 24 hypothetical proteins are explained in the feature table (**Supplementary Table 3**). ORF with the locus tag MSK_000019 encodes the most significant protein (putative tail fiber proteins) with a size of ∼ 277 kDa. ORF with the locus tag MSK_000036 encodes the smallest protein (hypothetical protein) with a size of ∼10.13 kDa. The orientation of the genome shows that most of the genes (55) are on the plus strand, while 18 are on the reverse strand. The linear genome map of all hypothetical and functional proteins groups and their GC content percentage is presented in **Figures 6A,B**.

Analysis of Virulence and Antibiotic Resistance Genes

Another essential factor to be measured in bacteriophages is the virulence and the presence of antimicrobial-resistant genes. Nowadays, antimicrobial resistance (AMR) is becoming a global threat to public health and food security as it might cause about 10,000,000 deaths per year by 2050 (O'Neill, 2014). Besides, the world is looking for new antimicrobial referents that can substitute the old ones. To overcome this problem, bacteriophages are an auspicious choice against these superbugs (MDR and XDR). But, unfortunately, phages also act as a vehicle for resistance and virulence gene transmission, which further cause the spread of antibiotic resistance (Gómez-Gómez et al., 2019). Previously, in 2012, a phage with a Shiga toxin (*stx*) was confirmed to regulate the antibiotic resistance gene (Granobles Velandia et al., 2012).

Presently, the lifestyle of bacteria predicted that Phage MSK is a lytic phage and kills its host within 2 h at MOI = 10, with no lysogenic genes (**Supplementary File 3**). Temperate bacteriophages can share their genome with the host, which might cause the spread of antibiotic resistance and virulence gene transfer in phage therapy. Furthermore, bioinformatics analysis was done to find the antibiotic resistance gene, but there was no significant hit based on AMR (anti-microbial resistance) gene identified in the complete genome. Similarly, for virulence genes, the analysis VirulenceFinder 2.0 predicted that the MSK genome did not contain any virulence genes. Therefore, we assumed that MSK could be further used for phage therapy against drug resistance coliphages through these findings.

MSK Phage Protein Profile Prediction

Further, the structure profile of bacteriophages is determined by SDS-PAGE, enabling us to determine the individual protein, molecular weight, and size. These analyses can be used for the morphotyping and differentiation of distinct proteins even within the same species (Urban-Chmiel et al., 2018). ORF prediction revealed that fewer genes are encoding structural proteins. The structural protein of phage MSK was characterized by SDS-PAGE coupled with a gel molecular weight analyzer (Origin(Pro), 2021). Purified phage particle was heated and run on 2-D SDS-PAGE, and protein bands were analyzed using coomassie staining. Further, the protein SDS_PAGE picture was brought to the Gel molecular weight analyzer, which calculates thirteen bands using regression value (**Figure 7B**). That leads to the identification of morphogenesis, holin, metabolic enzymes, and additional phage feature protein (**Figure 7A**).

Molecular weight, calculated by Origin(Pro), 2021, was compared with a phage MSK coding region with the same molecular mass (kDa) calculated online predicted different function (**Figure 7B**). The molecular weight of 13 phage MSK structural proteins was depicted on SDS-PAGE ranging from 7 to 106 kDa representing MSK structural proteins. The most predominant protein was band #10, considering

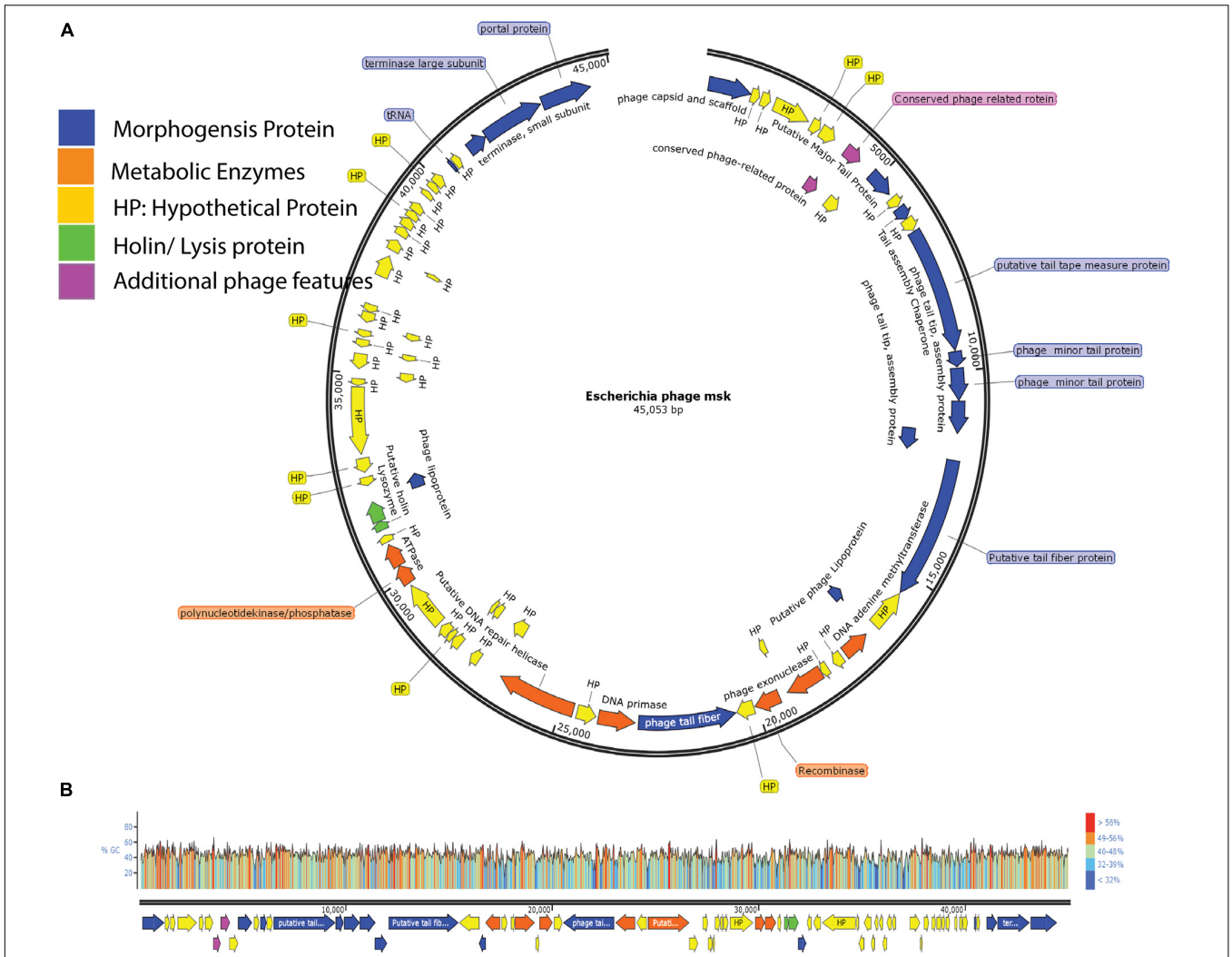

FIGURE 6 | Genome Map of *E. coli* phage MSK and GC content percentage lies in whole-genome. **(A)** The genome map of phage displays putative ORFs divided into five different modules with unique colors. Arrow direction of each ORF indicating the transcription direction, **(B)** G + C content of the phage genome lies between 40.8%, and colors in the GC content shows the percentage ratio.

the morphology of this phage, MSK_000010, which is the Major tail protein. Other proteins having the locus tags MSK_000017, MSK_000025, MSK_000042, and MSK_000044 were also detected with high coverage, but the number of detected peptides was less in comparison with MSK_000010. Overall, the molecular masses estimated by SDS-PAGE for most proteins were in agreement with the calculated masses from the gene sequence (**Figures 7A,B**).

Phage MSK structural profile possesses several features. The structural protein MSK_000014 is (tail tape measure protein) the most significant gene having 992 amino acid residues while MSK_000019 tail fiber protein is the subordinate structural gene having 816 a.a (amino acid), a characteristic shared by many tail fiber phages; these genes are located upstream of minor tail protein, tail assembly protein. Both of these proteins show amino acid sequence similarity to several tail phages. Thirteen MSK structural proteins were identified by SDS-PAGE analysis, including 12 major structural proteins. Among these proteins, terminase large subunit and others which were similar were involved in the pac-DNA packaging strategy encoded in the genomic region of MSK. This region is homologous to the terminase of the other *E. coli* phages suggesting a horizontal gene transfer between the phages and host and contributes to genetic diversity and evolution. Therefore, there is an immense desire to determine the sequences of phages because the phage genomics provides the phage and bacterial evolution tracing.

DNA Packaging Strategy and Phylogenetic Analysis

DNA packaging strategy is another most essential component of phage structural analysis. The terminase small and large protein units play a role in the initiation, termination, and translocation

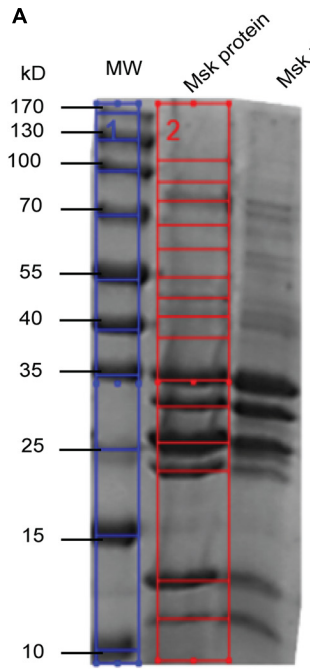

Band No.	Residues	Predicted function	Molecular mass (KD)	
			Calculated by online	Calculated Origin 2021
1	992	Tail tape measure	106.77	105.38
2	816	Phage tail fiber	87.53	88.23
3	664	DNA repair helicase	74.87	77.014
4	521	Terminase large subunit	59.21	57.28
5	422	Phage portal protein	46.84	44.94
6	376	-	41.88	41.64
7	361	phage capsid and scaffold	38.94	38.062
8	321	phage exonuclease	35.84	31.74
9	252	Phage tail tip protein	29.21	28.18
10	218	Major tail protein	23.4	23.43
11	183	ATPase	20.24	19.38
12	123	Conserved phage related protein	13.73	13.07
13	71	Holin	7.52	7.59

FIGURE 7 | SDS PAGE and *In silico* analysis of structural protein of phage MSK. **(A)** Coomassie blue staining of a 12% SDS–polyacrylamide gel showing structural proteins from phage MSK. (1) Blue line: The sizes (kDa) of different proteins from the broad-range weight marker (MW) are indicated on the left side (2) Red line on the right indicates the bands identified from the gel by Gel molecular weight analyzer tool [Origin(Pro), 2021] and verified by online molecular weight analyzer. **(B)** Identification of MSK various proteins and their predicted function from corresponding bands shown in the table.

of the phage DNA into proheads (Fujisawa and Morita, 1997). In this regard, MSK bacteriophage has two genes (MSK_00071 and MSK_00072) encoding terminase small and terminase large subunits; usually, both of these genes are adjacent like in Rtp and T1 (Roberts et al., 2004). The role of the small terminase is DNA-binding activity, and the large terminase provides ATP binding, prohead binding, and DNA cleavage activities (Wietzorrek et al., 2006). The phageTerm analysis showed that genome packaging of the *E. coli* phage MSK took place through headful packaging using pac-site on concatemeric precursor which lies in type unknown class; the exact mechanism was already identified in phage Rtp and T1 and phiC19 (Ramsey and Ritchie, 1983; Wietzorrek et al., 2006; Amarillas et al., 2016). From previous results, we can predict headful packaging in MSK bacteriophage occurring in the forwarded direction. The phageTerm method showed that it starts from position 36,862 in the genome, having a *p*-value ($1.62e^{-09}$), and Peaks localized 20 bases around the maximum. Li's method showed unique termini on the forwarding strand and no obvious termini on a reverse strand. The Phage genome does not have any termini and is either circular or completely permuted and terminally redundant, as shown (**Supplementary File 2**; Garneau et al., 2017).

In the same manner, NCBI blast results suggested that both large and small terminase have very close homology to Rtp and DTL bacteriophages which were previously isolated from industrial *E. coli* through a fermentation process in Germany and the United States. Further, finding the pac-site in the genome, MSK was compared with closely homolog bacteriophage Rtp. Wietzorrek et al. (2006) previously predicted five repeats of the ATATA sequence in T1 phage and closely related phage. However, genome analysis of phage MSK showed that these motifs were also not present in the genome, similar to Rtp.

The neck, head, and tail structure genome organization of phage MSK phage belong to *Siphoviridae* of type 1 (no cluster assigned) similar to Rtp. Interestingly, the TEM micrograph performed on the sample obtained by iodixanol gradient showed that structures compatible with Rtp phage head, tail, and tail fiber were witnessed (**Figure 2H**). We also observed that genome coverage of the sequencing was evenly distributed over the entire genome and share 47 ORF with Rtp bacteriophage. Along with Rtp, phage MSK closely resembles no other cluster assigned phages (T1, TLS, JK06, and ES18) (**Figure 8**). Phage MSK structural genes like (head, neck, and tail) have similar sequence and function with known Rtp phage and classify the phage with respect to other phages in Aclame (a classification of Mobile genetic Elements). These findings also support the phage tail module (terminase large protein) having close homology with Rtp bacteriophage and T1 bacteriophage, which has predicted the headful DNA packaging mechanism.

The Viral Proteomic tree analysis revealed that phage MSK protein sequences are almost similar to the bacteriophage RTP. ViPTree, dendrogram reveals global genomic similarity relationships between 579 bacteriophage sequences of different families. These relationships predict RTP bacteriophage and MSK falls in *Siphoviridae*. But according to the Rtp lineage information provided in the genome database (GenBank) the phage belongs

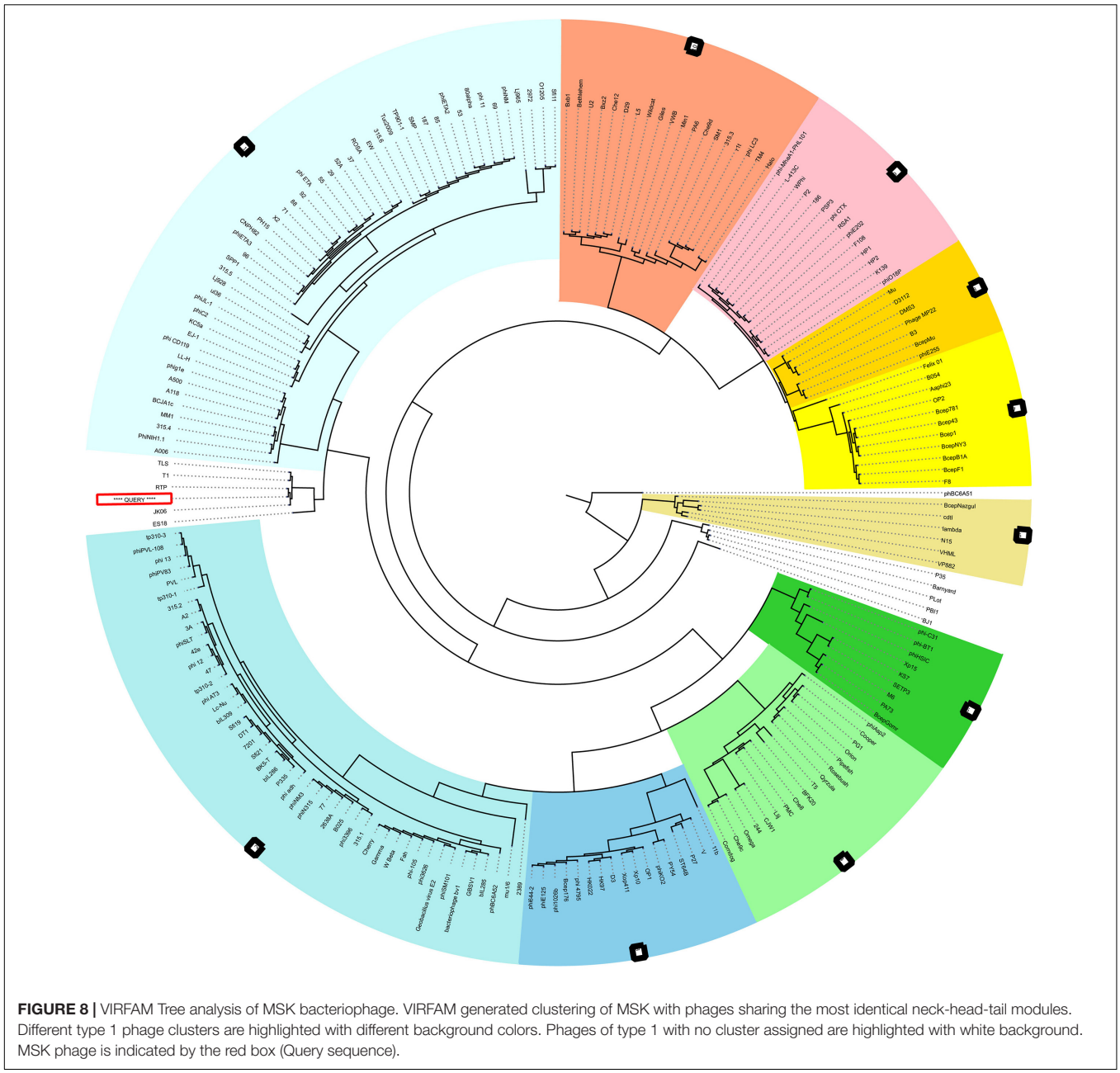

FIGURE 8 | VIRFAM Tree analysis of MSK bacteriophage. VIRFAM generated clustering of MSK with phages sharing the most identical neck-head-tail modules. Different type 1 phage clusters are highlighted with different background colors. Phages of type 1 with no cluster assigned are highlighted with white background. MSK phage is indicated by the red box (Query sequence).

to *Drexlerviridae* family. These findings concluded that phage MSK belongs to the *Drexlerviridae* and subfamily *Braunvirinae* (**Supplementary Figure 8**).

Comparative Genome Analysis of MSK Phage With Closely Related Phages

MSK comparative analysis was done with four *E. coli* phages [phage vB_EcoS-2862V (MK907276.1), *Escherichia* phage vB_Ecos_CEB_EC3a (NC_047812.1), *Escherichia* phage DTL (NC_047893.1) and, *Rtp* bacteriophage (AM156909.1)], by calculating the average nucleotide identity (ANI). ANI is widely used to compare the prokaryotic genome using USEARCH instead of BLAST. These four bacteriophages were isolated from different samples and shared ANI of 87.18, 85.32, 83.97, and 84.79 %, respectively. BLASTn of the phage MSK with Rtp showed that 89.60% of the MSK genome was homologous to the Rtp genome, covering almost entirely the functionally annotated region of the phage Rtp genome, the closest homology of the MSK genes are found in the Rtp phage as shown in the table (**Supplementary Table 3**).

The genome comparison with Rtp bacteriophage showed that it has 26 genes similar to MSK phage. Comparing the morphological features of the bacteriophage *Rtp* has a close resemblance to a rosette-like tail, and its tail fiber protein (MSK_000019) gave 95.92% homology with the MSK phage.

The custom database was used for subsequent comparative analysis. First, a multiple sequence alignment was performed; a comparison of the relatedness of the different nucleotides sequences was generated utilizing Mauve (Darling Lab). The genomic comparison of the phage MSK with *Escherichia* phage vB_EcoS-2862V, *Escherichia* phage vB_Ecos_CEB_EC3a, *Escherichia* phage DTL and, Rtp bacteriophages are shown (**Figure 9**). These results suggested that these phages have extensive synteny between genome structure with percentage identity 91.18, 88.44, 85.37, and 89.48% among these bacteriophage genomes. But it also shows some mosaicism in the genome, including ORF which encodes tRNA. The tRNA-Arg encoding gene was not present in bacteriophage *Rtp* and DTL but present in the *Escherichia* phage vB_EcoS-2862, *Escherichia* phage vB_Ecos_CEB_EC3a. These findings concluded that phage MSK belongs to the *Drexlerviridae* family and subfamily *Braunavirinae* and virus belong to *Rtp* viruses.

Antimicrobial Activity Against Multidrug-Resistant Coliphages

The prevalence of antibiotic resistance (AMP, TCN, and Colistin) and extended-spectrum beta-lactamase (ESBL) production has considerably escalated in all terrestrial regions. Infections due to these c bacteria are associated with high mortality across human beings. Phage MSK can kill pathogenic bacteria. That offers a novel approach with an unprecedented and orthogonal mechanism of action for the treatment of diseases.

A panel of five *E. coli* phages obtained from Zhejiang university hospital and labs mentioned in the table were used to test the infectivity of the newly discovered MSK phage using a spot test. Overall, MSK bacteriophage demonstrated a consistent narrow range; infecting 100% of clinical multidrug-resistant strains of *E. coli* were tested. But, this novel phage was unable to infect the *Salmonella* and *Pseudomonas* species. These findings concluded that this phage could only be used against drug resistance *E. coli* bacteria. All strains were susceptible to MSK phage gave plaques clear to evident plaques formation on LB agar plate (**Table 1**).

DISCUSSION

Bacteriophages are the most abundant biological entities present in all environments (natural and artificial) with their bacterial communities. These phages might have positive or negative ecological impact by eradicating recalcitrant bacteria from the natural environment (Meaden and Koskella, 2013; Batinovic et al., 2019). Several bacteriophages have been isolated previously from the natural environment (human) (Pacífico et al., 2019) and artificial environment (industrial units) (Wietzorrek et al., 2006; Halter and Zahn, 2018). This study characterizes the coliphage phage MSK, which explains the phages from the naturally occurring environment. Phage MSK can infect *E. coli* C, Previously temperate phage P2 and lytic phage X 174 have been isolated from the common host, despite no conserved proteins. Phage morphology and genome type were identified among these *E. coli* phage's genomes (Wiman et al., 1970; Barreiro and Haggård-Ljungquist, 1992; Zheng et al., 2009). Bacteriophage MSK shares identity features with the coliphages community, including morphological resemblance and genome size. These phages consist of a dsDNA genome with a size range of

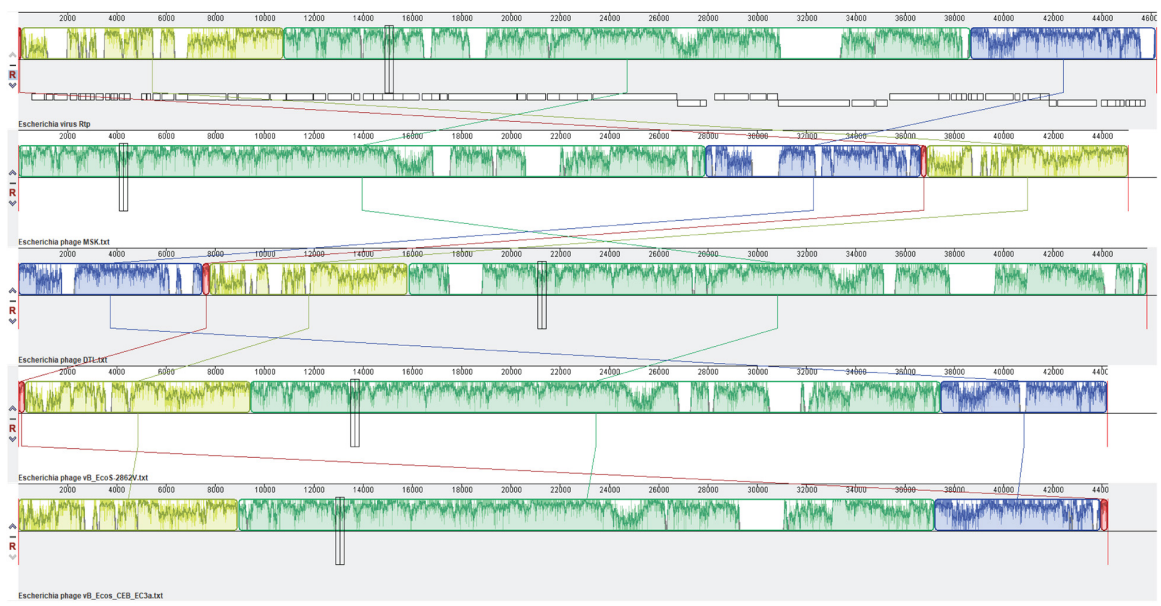

FIGURE 9 | Comparative genomic analysis of *Escherichia coli* phages of the *Drexlerviridae* family. The genome map of phage MSK displays putative ORFs shown with different colors and arrows indicating the transcription direction. The colored bars indicate homologous DNA regions between phages (Rtp, phage MSK, DTL, and B_EcoS-2862V). The connection lines indicate homologous regions between the genomes of four *Escherichia* coliphages. Rtp bacteriophage genome was downloaded from the NCBI genome database and used as a reference sequence.

TABLE 1 | Antimicrobial activity against multidrug resistant bacterial strains.

Name of bacterial strains	Source of strains	Activity/spot assay
E. coli (AMP)	Zhejiang University First Affiliated Hospital, Hangzhou	+
E. coli (ESBL)	Zhejiang University First Affiliated Hospital, Hangzhou	+++
E. coli (TCN)	Zhejiang University School of Medicine (C602)	+++
E. coli MG1655 (Colistin Resistant, NMCR-1	Department of Pathogen Biology and Microbiology	+++
E. coli MG1655 (Colistin Resistant, MCR-4	Department of Pathogen Biology and Microbiology Zhejiang University School of Medicine	+++
Salmonella anatum (Epsilon 15 host)	Department of Biochemistry and Genetic, Zhejiang University School of Medicine	–
Pseudomonas syringae (Phi-6 host)	Department of Biochemistry and Genetic, Zhejiang University School of Medicine	–

Escherichia coli, E. coli; AMP, Ampicillin; ESBL, Extended Spectrum Beta-Lactamase; TCN, Tetracycline; NMCR-1, Non-mobile Colistin Resistance; MCR-4, mobile colistin resistance; +, Clear plaque; +++, very clear plaque; –, No plaque formation.

45–50 kb bp and GC content of about 45–50% (Roberts et al., 2004; Pacífico et al., 2019). MSK bacteriophage showed 91% nucleotide sequence identity to 35 Rtp like Escherichia coliphages isolated from the clinical samples (Pacífico et al., 2019). Rtp phenotypes bacteriophages isolated from industrial and other animal sources also showed 85 to 90% nucleotide identity features (Wietzorrek et al., 2006; Ferreira et al., 2020). NCBI blast result showed that Escherichia phage vB_EcoS-2862II (MK907273.1) has the highest percentage identity (91.18%), Rtp bacteriophage (89.48%; AM156909.1), and DLT (85.37%; NC_047893.1).

Inevitably, there are many studies showing phages are present where bacteria reside. But, now, this hypothesis may not work because phages are isolated where bacterial abundance did not exist. Previous studies showed that these Rtp like phages could be isolated from the body fluid, as the human body is also not sterile (Pacífico et al., 2019) and many industrial units (Wietzorrek et al., 2006; Halter and Zahn, 2018) that can cause many problems in terms of quality, quantity, and an experimental result which further causes finical issues (Halter and Zahn, 2018). We noticed several others phage prevalence in the lab environment, including coliphages and *Pseudomonas* phage. Our lab isolated three morphological different pseudomonas phages (Data not shown here). We assume that some bacteriophages present in the lab environment, which might need to increase the host range, can further help to increase the number of phage identification.

The lifestyle of the phage MSK, like other T1 phages, demonstrates that it is a lytic phage with the ability to reduce the growth of *E. coli* C during 4 h of infection (**Figure 3**). Consequently, the genome of phage MSK has a holin gene (MSK_000044) right upstream of the lysozyme gene (MSK_000045). This constitutes its lytic cassette, indicating that the lytic activity of the lysozyme is holin-dependent and produces larger plaques and larger burst size (Abedon and Culler, 2007). In addition, our isolated phage MSK showed a latent period and burst time of 25 and 45 min, respectively. In comparison, *Drexlerviridae* family phage phiC119 showed a latent period of 20 min and burst size (210) 58 min (Amarillas et al., 2016). In contrast, T1 bacteriophage exhibit a latent period of 13 min and produces 100 virions per infected phage (Borchert and Drexler, 1980). Further, several factors like mutation, host cell size, host physiology, and culture condition might reflect the short burst size and the latent period during the propagation in the host (Sharaf et al., 2018). These results suggest that the latent period of the phage MSK is almost closed to other *Drexlerviridae* family bacteriophages, and this could be a potential candidate for phage therapy.

Physiochemical characteristics like temperature, pH, and UV might affect the activity and stability of phages (Jończyk-Matysiak et al., 2019). In this regard, bacteriophage MSK demonstrated stability to high temperature (100°C), pH, and UV exposure and did not adversely affect phage survival; yet, stability was not observed at 120°C. Maximum stability of phage MSK was observed at 100°C with a decrease in plaque size (**Supplementary Figure 2B**). Many studies reported that bacteriophages are commonly stable at the temperature range (60–70°C), and a temperature rise may decrease the number of plaque-forming units (Ramírez et al., 2018; Alvi et al., 2020). Similarly, phages are sensitive to acidic media; our results showed that phages are resistant over a wide range of pH. In general, the natures of phages make them sensitive to UV-irradiation by reducing their concentration or inactivating phage infectivity (Clark et al., 2012).

Interestingly, phage MSK infectivity was not decreased at various temperatures and UV exposure, as discussed earlier. On the contrary, previous studies reported where UV-light is used to cause mutation in bacteriophages to increase or decrease the host range (Kadavy et al., 2000). Conclusively, phage MSK showed stability against UV and heat treatment and did not show any alterations in plaque forming unit (*PFU*).

The genome of the phage MSK comprised 45,053 base pairs with a GC content of 44.8%. This GC content value was lower than its host which is consistent with previously reported phage phiC119 (Amarillas et al., 2016). Usually, lytic phages have lower GC content than their host, in contrast to temperate phages having an equal percentage to GC content (Rocha and Danchin, 2002; Amarillas et al., 2016). Furthermore, genome size determined 73 ORFs in phage MSK which are almost familiar with *Rtpvirus* (Rtp, DTL). The size of bacteriophage MSK is compared to those of the *Rtpvirus* genus bacteriophages Escherichia phage vB_EcoS-2862V (44,219 bp) and Escherichia phage vB_EcoS-2004IV (44,219 bp) (Pacífico et al., 2019). The phage MSK genome also shares a characteristic of overlapping ORFs with other phages, which enable the phage to minimize the genome size and play a role in regulating gene expression (Johnson and Chisholm, 2004; Pavesi, 2006).

Bioinformatics analysis of the bacteriophage MSK genome revealed that the genome is organized into five different functional components, showing the genome is arranged in a

compact manner (**Figure 2**). Like other tailed bacteriophages, these modules performed different biological functions in phage morphology, metabolism, lysis, DNA replication, and repair (Amarillas et al., 2016). Thus, the phage MSK has a mosaic genome structure and morphology similar to related phages, indicating the extensive genetic exchange and horizontal gene transfer within the phage community (Rohwer and Edwards, 2002). Furthermore, the phage genome also has the one tRNA-arg (78 bp), which also supports the hypothesis that bacteriophages with tRNA genes have larger burst size as a result of their virulence and propagation in their host increases (Delesalle et al., 2016; Sharaf et al., 2018).

MSK bacteriophage genomic region MSK_000019 encoding the module of the distal part of its tail that is over 90.99% identical to the gene segment of several Escherichia coliphages. This open reading frame is 90% homology with Rtp 43 protein (CAJ42247.1) involved in the host cell recognition (Wietzorrek et al., 2006). The metabolic module of the phage MSK consists of DNA primase and helicase, suggesting that phage replication is independent of the host machinery (**Figure 2**). Moreover, lipoproteins having N-terminal are also valuable contributors in sorting signals and playing roles in preventing superinfection by inactivation of receptors (Tokuda and Matsuyama, 2004). Interestingly, we also predicted a lipoprotein in the phage MSK genome which showed homology and had a conserved domain with Rtp 45 and T5 lipoproteins (Braun et al., 1994; Tokuda and Matsuyama, 2004; Wietzorrek et al., 2006).

Virulent and temperate bacteriophages have contained different recombinase families. There is six families of recombinases have been identified so far. Virulent and temperate bacteriophages contain two and four families of recombinases, respectively (Lopes et al., 2010). Virulent MSK phage genome might encode Gp2.5 recombinase (Erf), because similar recombinase has been identified in Rtp, T1, and T7 bacteriophage (Wietzorrek et al., 2006). MSK recombination gene (MSK_000027) is located (19403–20053) on the top strand, upstream of the phage exonuclease gene (MSK_000025). NCBI BLASTn analysis showed that MSK phage recombinase shares 97.69% homology with Rtp bacteriophage (Rtp49). These findings assumed that recombinase (MSK_000027) might play an essential role in replication, genome repair, and recombination facilitated by single-stranded DNA binding protein (Ssb) as experimentally verified in T7 bacteriophages (Kong and Richardson, 1998).

DNA packaging and its mechanism are also of prime importance in the lifestyle of a phage. In this regard, it is observed that phage MSK has a headful packaging strategy (pac-mechanism) of the type unknown already described for related bacteriophages, such as Rtp, phiC119 (Ramsey and Ritchie, 1983; Wietzorrek et al., 2006; Casjens and Gilcrease, 2009; Amarillas et al., 2016). Furthermore, a classification based on the structure modules (head, neck, and tail) was conducted, which indicates that the phage tail module (terminse large protein) was homolog with Rtp phage. These findings suggested that the phage MSK packages its DNA by headful packaging mechanism (pac-sites) similar to that of Rtp and T1, resulting in terminal redundancy and circular permutation. Furthermore, previous studies showed that phage phiC119 use the same packaging strategy as T1 based on homology (Ramsey and Ritchie, 1983; Wietzorrek et al., 2006).

Comparative analysis of the entire genome sequences of the *Escherichia* phages B_EcoS-2862V, B_Ecos_CEB_EC3a, RTP, DTL, and MSK was done to characterize the prophage. Among these phages, MSK bacteriophage revealed the highest correspondence (87.18% ANI) with Escherichia coli phage B_EcoS-2862V. As the Rtp bacteriophage is well studied in terms of the genome, phage MSK also showed higher diversity (84.79% ANI) in these phages. These identified sequences with the highest ANI values can be used in evolutionary and phylogenetic studies, particularly when the whole genome sequence is not available in the database. In addition to showing a robust evolutionary relationship, the whole-genome nucleotide MAUVE plot also showed a higher homology region among these phages of the same family. These local homology regions are supposed to be recombination sites and conserved regions among these lytic phages (**Figure 9**). Close comparative genome analysis of the phage suggested that it could be used in the antimicrobial resistance.

Like many other phages, MSK showed negligible intraspecies host range (*Salmonella, Pseudomonas*), while interspecies host range was 100%. This phage could infect the *E. coli* laboratory strains (DH5α and Rosetta and *E. coli* top 10). The presence of the specific host cell receptor provides the specificity in targeting the host, which can be further helpful for treating coliphage-related infections like ampicillin, tetracycline, and Colistin resistance (MCR-1 and MCR-2) *E. coli* bacteria (**Table 1**).

These observations highlight the importance of using phages in therapy. These findings ensure that the phage is strictly lytic and does not code any antibiotic-resistant and virulent genes. We know phages are a powerful tool for phage therapy, but if phages got resistant to bacteria, this might impede their potential application in phage therapy and biocontrol (Oechslin, 2018). Complete bioinformatics analysis revealed that bacteriophage MSK did not contain lysogeny proteins. Therefore, no undesirable antibiotic resistance genes and virulence genes were present but in the phage genome. These results suggested that phage MSK might be safe at the genome level and could be used in phage therapy.

In summary, genome analysis and electron microscopy revealed that phage MSK belongs to the *Derxivirdiae* family. Furthermore, phages exhibit a short latent period with a broad host range against coliphages, a narrow host range against other bacterial species, and stability at higher temperatures (100°C) and pH ranges. Genomic studies suggested that phage did not contain any antibiotic resistance and virulence genes. These results indicated that phage MSK might be suitable for phage therapy against antibiotic resistance of bacteria. In addition, phage MSK demonstrated strong lytic activity against Colistin resistance bacteria. However, further toxicity studies are required to ensure the safety of the phage. Therefore, our future research will be aimed at characterizing this phage for a better understanding of its potential as a biocontrol agent.

MSK bacteriophage belongs to the *Drexlerviridae* family of the *Caudovirales* order, *Rtpvirus* genus; it has a large icosahedral capsid and a long tail with four short linked rosette-like

morphology of the tail tip. This phage has a morphotype similar to Rtp bacteriophage, which we assume may be responsible for host recognition.

DATA AVAILABILITY STATEMENT

The datasets presented in this study can be found in online repositories. The names of the repository/repositories and accession number(s) can be found in the article/ **Supplementary Material**.

AUTHOR CONTRIBUTIONS

JZ acquired the funding and managed the project. JZ and MK conceived the study and designed the experiments. MK performed the experiments. SM, KL, and XG assisted with the experiments. MK analyzed the data, performed transmission electron microscopic analysis, prepared the initial draft, and wrote the manuscript. SM reviewed and edited the manuscript. All authors contributed to the article and approved the submitted version.

FUNDING

This work was supported by the National Natural Science Foundation of China (grant no. 81872784).

ACKNOWLEDGMENTS

We would like to thank Lou Y. F. and Zeeshan Umar, Department of Lab Medicine, The First Affiliated Hospital, Zhejiang University School of Medicine for providing us with drug-resistant bacteria. We are grateful to Muhammad Iqbal Alvi (Hazara University, Pakistan) for bioinformatics assistance. We are thankful to Kabeer Haneef (Tsinghua University, China) and Muhammad Sajid for critically reviewing and correcting the manuscript.

SUPPLEMENTARY MATERIAL

The Supplementary Material for this article can be found online at: https://www.frontiersin.org/articles/10.3389/fmicb.2021.706700/full#supplementary-material

REFERENCES

Abedon, S., and Culler, R. R. (2007). Optimizing bacteriophage plaque fecundity. *J. Theor. Biol.* 249, 582–592. doi: 10.1016/j.jtbi.2007.08.006

Ackermann, H. W. (2011). Bacteriophage taxonomy. *Microbiol. Aust.* 32, 90–94. doi: 10.1071/ma11090

Alcock, B., Raphenya, A. R., Lau, T. T. Y., Tsang, K. K., Bouchard, M., Edalatmand, A., et al. (2019). CARD 2020: antibiotic resistome surveillance with the comprehensive antibiotic resistance database. *Nucleic Acids Res.* 48, D517–D525.

Alvi, I., Asif, M., Tabassum, R., Aslam, R., Abbas, Z., and Réhman, S. (2020). RLP, a bacteriophage of the family Podoviridae, rescues mice from bacteremia caused by multi-drug-resistant *Pseudomonas aeruginosa*. *Arch. Virol.* 165, 1289–1297. doi: 10.1007/s00705-020-04601-x

Amarillas, L., Cháidez, C., González-Robles, A., Lugo-Melchor, Y., and León-Felix, J. (2016). Characterization of novel bacteriophage phiC119 capable of lysing multidrug-resistant Shiga toxin-producing *Escherichia coli* O157:H7. *PeerJ* 4, e2423. doi: 10.7717/peerj.2423

Barreiro, V., and Haggård-Ljungquist, E. (1992). Attachment sites for bacteriophage P2 on the *Escherichia coli* chromosome: DNA sequences, localization on the physical map, and detection of a P2-like remnant in *E. coli* K-12 derivatives. *J. Bacteriol.* 174, 4086–4093.

Batinovic, S., Wassef, F., Knowler, S. A., Rice, D. T. F., Stanton, C. R., Rose, J., et al. (2019). Bacteriophages in natural and artificial environments. *Pathogens (Basel, Switzerland)* 8:100. doi: 10.3390/pathogens8030100

Borchert, L. D., and Drexler, H. (1980). T1 genes which affect transduction. *J. Virol.* 33, 1122–1128. doi: 10.1128/jvi.33.3.1122-1128.1980

Braun, V., Killmann, H., and Herrmann, C. (1994). Inactivation of FhuA at the cell surface of *Escherichia coli* K-12 by a phage T5 lipoprotein at the periplasmic face of the outer membrane. *J. Bacteriol.* 176, 4710–4717. doi: 10.1128/jb.176.15.4710-4717.1994

Casjens, S., and Gilcrease, E. B. (2009). Determining DNA packaging strategy by analysis of the termini of the chromosomes in tailed-bacteriophage virions. *Methods Mol. Biol.* 502, 91–111. doi: 10.1007/978-1-60327-565-1_7

Chibani-Chennoufi, S., Bruttin, A., Dillmann, M.-L., and Brüssow, H. (2004). Phage-host interaction: an ecological perspective. *J. Bacteriol.* 186, 3677–3686. doi: 10.1128/jb.186.12.3677-3686.2004

Clark, E. M., Wright, H., Lennon, K.-A., Craik, V. A., Clark, J. R., and March, J. B. (2012). Inactivation of recombinant bacteriophage lambda by use of chemical agents and UV radiation. *Appl. Environ. Microbiol.* 78, 3033–3036. doi: 10.1128/aem.06800-11

Clokie, M. R., Millard, A. D., Letarov, A. V., and Heaphy, S. (2011). Phages in nature. *Bacteriophage* 1, 31–45. doi: 10.4161/bact.1.1.14942

Clokie, M. R. J., Clokie, M. R. J., and Kropinski, A. M. (2009). *Bacteriophages : Methods and Protocols, : Isolation, Characterization, and Interactions*. Berlin: Springer.

Cui, Z., Guo, X., Dong, K., Zhang, Y., Li, Q., Zhu, Y., et al. (2017). Safety assessment of Staphylococcus phages of the family Myoviridae based on complete genome sequences. *Sci. Rep.* 7:41259.

Darling, A. C., Mau, B., Blattner, F. R., and Perna, N. T. (2004). Mauve: multiple alignment of conserved genomic sequence with rearrangements. *Genome Res.* 14, 1394–1403. doi: 10.1101/gr.2289704

Delesalle, V. A., Tanke, N. T., Vill, A. C., and Krukonis, G. P. (2016). Testing hypotheses for the presence of tRNA genes in mycobacteriophage genomes. *Bacteriophage* 6:e1219441. doi: 10.1080/21597081.2016.1219441

Ferreira, A., Oliveira, H., Silva, D., Almeida, C., Burgan, J., Azeredo, J., et al. (2020). Complete genome sequences of eight phages infecting Enterotoxigenic *Escherichia coli* in swine. *Microbiol. Resour. Announc.* 9, e00858–20.

Fujimura, R., and Kaesberg, P. (1962). The adsorption of bacteriophage phi-X174 to its host. *Biophys. J.* 2, 433–449. doi: 10.1016/s0006-3495(62)86866-0

Fujisawa, H., and Morita, M. (1997). Phage DNA packaging. *Genes Cells* 2, 537–545. doi: 10.1046/j.1365-2443.1997.1450343.x

Garneau, J. R., Depardieu, F., Fortier, L. C., and Bikard, D. (2017). PhageTerm: a tool for fast and accurate determination of phage termini and packaging mechanism using next-generation sequencing data. *Sci. Rep.* 7:8292. doi: 10.1038/s41598-017-07910-5

Gómez-Gómez, C., Blanco-Picazo, P., Brown-Jaque, M., Quirós, P., Rodríguez-Rubio, L., Cerdà-Cuéllar, M., et al. (2019). Infectious phage particles packaging antibiotic resistance genes found in meat products and chicken feces. *Sci. Rep.* 9:13281.

Granobles Velandia, C. V., Krüger, A., Parma, Y. R., Parma, A. E., and Lucchesi, P. M. (2012). Differences in Shiga toxin and phage production among stx(2g)-positive STEC strains. *Front. Cell Infect. Microbiol.* 2:82. doi: 10.3389/fcimb.2012.00082

Halter, M., and Zahn, J. (2018). Characterization of a novel lytic bacteriophage from an industrial *Escherichia coli* fermentation process and elimination of virulence using a heterologous CRISPR Cas9 system. *J. Indu. Microbiol. Biotechnol.* 45, 153–163. doi: 10.1007/s10295-018-2015-7

Joensen, K. G., Scheutz, F., Lund, O., Hasman, H., Kaas, R., Nielsen, E., et al. (2014). Real-time whole-genome sequencing for routine typing, surveillance, and outbreak detection of verotoxigenic *Escherichia coli*. *J. Clin. Microbiol.* 52, 1501–1510. doi: 10.1128/jcm.03617-13

Johnson, Z., and Chisholm, S. (2004). Properties of overlapping genes are conserved across microbial genomes. *Genome Res.* 14, 2268–2272. doi: 10.1101/gr.2433104

Jończyk-Matysiak, E., Łodej, N., Kula, D., Owczarek, B., Orwat, F., Międzybrodzki, R., et al. (2019). Factors determining phage stability/activity: challenges in practical phage application. *Expert Rev. Anti Infect. Ther.* 17, 583–606. doi: 10.1080/14787210.2019.1646126

Kadavy, D. R., Shaffer, J., Lott, S., Wolf, T. A., Bolton, C., Gallimore, W. H., et al. (2000). Influence of infected cell growth state on bacteriophage reactivation levels. *Appl. Environ. Microbiol.* 66, 5206–5212. doi: 10.1128/aem.66.12.5206-5212.2000

Kalim, M., Liang, K., Khan, M. S., and Zhan, J.-B. (2019). Efficient development and expression of scFv recombinant proteins against PD-L1 surface domain and potency in cancer therapy. *Cytotechnology* 71, 705–722. doi: 10.1007/s10616-019-00316-3

Keen, E. C. (2015). A century of phage research: bacteriophages and the shaping of modern biology. *Bioessays* 37, 6–9. doi: 10.1002/bies.201400152

Kong, D., and Richardson, C. C. (1998). Role of the acidic carboxyl-terminal domain of the single-stranded DNA-binding protein of bacteriophage T7 in specific protein-protein interactions*. *J. Biol. Chem.* 273, 6556–6564. doi: 10.1074/jbc.273.11.6556

Lakha, W., Panteleeva, I., Squazzo, S., Saxena, R., Kroonen, J., Siembieda, S., et al. (2016). DNA fragmentation and quality control analysis using diagenode shearing systems and fragment analyzer. *Nat. Methods* 13, iii–iv.

Lopes, A., Amarir-Bouhram, J., Faure, G., Petit, M., and Guérois, R. (2010). Detection of novel recombinases in bacteriophage genomes unveils Rad52, Rad51 and Gp2.5 remote homologs. *Nucleic Acids Res.* 38, 3952–3962. doi: 10.1093/nar/gkq096

Lopes, A., Tavares, P., Petit, M.-A., Guérois, R., and Zinn-Justin, S. (2014). Automated classification of tailed bacteriophages according to their neck organization. *BMC Genomics* 15:1027. doi: 10.1186/1471-2164-15-1027

Ma, Y., and Lu, C. P. (2008). Isolation and identification of a bacteriophage capable of infecting *Streptococcus suis* type 2 strains. *Vet. Microbiol.* 132, 340–347. doi: 10.1016/j.vetmic.2008.05.013

Meaden, S., and Koskella, B. (2013). Exploring the risks of phage application in the environment. *Front. Microbiol.* 4:358–358. doi: 10.3389/fmicb.2013.00358

Monk, J. M., Koza, A., Campodonico, M., Machado, D., Seoane, J. M., Palsson, B., et al. (2016). Multi-omics quantification of species variation of *Escherichia coli* links molecular features with strain phenotypes. *Cell systems* 3, 238–251.e12.

Oechslin, F. (2018). Resistance development to bacteriophages occurring during bacteriophage therapy. *Viruses* 10:351. doi: 10.3390/v10070351

O'Neill, J. (2014). *Review on Antimicrobial Resistance: Tackling a Crisis for the Health and Wealth of Nations*. Available online at: http://amr-review.org/ (accessed January 15, 2015).

Origin(Pro) (2021). Origin(Pro) Version *Number* (e.g. "Version 2021b"). OriginLab Corporation, Northampton, MA, USA.

Pacífico, C., Hilbert, M., Sofka, D., Dinhopl, N., Pap, I.-J., Aspöck, C., et al. (2019). Natural occurrence of *Escherichia coli*-infecting bacteriophages in clinical samples. *Front. Microbiol.* 10:2484.

Pavesi, A. (2006). Origin and evolution of overlapping genes in the family Microviridae. *J. Gene. Virol.* 87(Pt 4), 1013–1017. doi: 10.1099/vir.0.81375-0

Pekar, J., Phaneuf, P. V., Szubin, R., Palsson, B., Feist, A., and Monk, J. M. (2018). Gapless, unambiguous genome sequence for *escherichia coli* c, a workhorse of industrial biology. *Microbiol. Resou. Announc.* 7, e00890–18.

Ramírez, K., Cazarez-Montoya, C., López-Moreno, H., and Campo, N. C.-D. (2018). Bacteriophage cocktail for biocontrol of *Escherichia coli* O157:H7: stability and potential allergenicity study. *PLoS One* 13:e0195023. doi: 10.1371/journal.pone.0195023

Ramsey, N., and Ritchie, D. A. (1983). Uncoupling of initiation site cleavage from subsequent headful cleavages in bacteriophage T1 DNA packaging. *Nature* 301, 264–266. doi: 10.1038/301264a0

Roberts, M. D., Martin, N., and Kropinski, A. (2004). The genome and proteome of coliphage T1. *Virology* 318, 245–266. doi: 10.1016/j.virol.2003.09.020

Rocha, E., and Danchin, A. (2002). Base composition bias might result from competition for metabolic resources. *Trends Genet. TIG* 18, 291–294. doi: 10.1016/s0168-9525(02)02690-2

Rohwer, F., and Edwards, R. (2002). The phage proteomic tree: a genome-based taxonomy for phage. *J. Bacteriol.* 184, 4529–4535. doi: 10.1128/jb.184.16.4529-4535.2002

Salisbury, A., and Tsourkas, P. K. (2019). A method for improving the accuracy and efficiency of bacteriophage genome annotation. *Int. J. Mol. Sci.* 20:3391. doi: 10.3390/ijms20143391

Sanger, F., Nicklen, S., and Coulson, A. (1977). DNA sequencing with chain-terminating inhibitors. *Proc. Natl. Acad. Sci. U.S.A.* 74, 5463–5467. doi: 10.1073/pnas.74.12.5463

Sharaf, A., Oborník, M., Hammad, A. M. M., El-Afifi, S., and Marei, E. (2018). Characterization and comparative genomic analysis of virulent and temperate Bacillus megaterium bacteriophages. *PeerJ* 6:e5687. doi: 10.7717/peerj.5687

Sprotte, S., Bockelmann, W., Brinks, E., Schleifenbaum, P., Cho, G.-S., Fiedler, G., et al. (2019). Genome analysis of the temperate bacteriophage PMBT6 residing in the genome of Bifidobacterium thermophilum MBT94004. *Arch. Virol.* 165, 233–236. doi: 10.1007/s00705-019-04448-x

Srividhya, K. V., and Krishnaswamy, S. (2007). Subclassification and targeted characterization of prophage-encoded two-component cell lysis cassette. *J. Biosci.* 32, 979–990. doi: 10.1007/s12038-007-0097-x

Suttle, C. (2005). Viruses in the sea. *Nature* 437, 356–361. doi: 10.1038/nature04160

Szymczak, M., Grygorcewicz, B., Karczewska-Golec, J., Decewicz, P., Pankowski, J., Országh-Szturo, H., et al. (2020). Characterization of a unique *Bordetella bronchiseptica* vB_BbrP_BB8 bacteriophage and its application as an antibacterial agent. *Int. J. Mol. Sci.* 21:1403. doi: 10.3390/ijms21041403

Tokuda, H., and Matsuyama, S.-I. (2004). Sorting of lipoproteins to the outer membrane in *E. coli*. *Biochim. Biophys. Acta* 1693, 5–13. doi: 10.1016/j.bbamcr.2004.02.005

Urban-Chmiel, R., Wernicki, A., Wawrzykowski, J., Puchalski, A., Nowaczek, A., Dec, M., et al. (2018). Protein profiles of bacteriophages of the family Myoviridae-like induced on *M. haemolytica*. *AMB Express* 8, 102–102. doi: 10.1186/s13568-018-0630-3

Wietzorrek, A., Schwarz, H., Herrmann, C., and Braun, V. (2006). The genome of the novel phage Rtp, with a rosette-like tail tip, is homologous to the genome of phage T1. *J Bacteriol.* 188, 1419–1436. doi: 10.1128/jb.188.4.1419-1436.2006

Wiman, M., Bertani, G., Kelly, B., and Sasaki, I. (1970). Genetic map of *Escherichia coli* strain C. *Mol. Gen. Genet.* 107, 1–31. doi: 10.1007/bf00433220

Yoon, S. H., Ha, S. M., Lim, J., Kwon, S., and Chun, J. (2017). A large-scale evaluation of algorithms to calculate average nucleotide identity. *Antonie Van Leeuwenhoek* 110, 1281–1286. doi: 10.1007/s10482-017-0844-4

Yu, J. G., Lim, J. A., Song, Y., Heu, S. G., Kim, G. H., Koh, Y., et al. (2016). Isolation and characterization of bacteriophages against *Pseudomonas* syringae pv. actinidiae causing bacterial canker disease in kiwifruit. *J. Microbiol. Biotechnol.* 26, 385–393. doi: 10.4014/jmb.1509.09012

Zheng, Y., Struck, D. K., and Young, R. (2009). Purification and functional characterization of phiX174 lysis protein E. *Biochemistry* 48, 4999–5006. doi: 10.1021/bi900469g

Zolotukhin, S., Byrne, B. J., Mason, E., Zolotukhin, I., Potter, M., Chesnut, K., et al. (1999). Recombinant adeno-associated virus purification using novel methods improves infectious titer and yield. *Gene. Ther.* 6, 973–985. doi: 10.1038/sj.gt.3300938

Conflict of Interest: The authors declare that the research was conducted in the absence of any commercial or financial relationships that could be construed as a potential conflict of interest.

Publisher's Note: All claims expressed in this article are solely those of the authors and do not necessarily represent those of their affiliated organizations, or those of the publisher, the editors and the reviewers. Any product that may be evaluated in this article, or claim that may be made by its manufacturer, is not guaranteed or endorsed by the publisher.

frontiers in Microbiology

ORIGINAL RESEARCH
published: 26 August 2021
doi: 10.3389/fmicb.2021.698962

Molecular Characteristics of Novel Phage vB_ShiP-A7 Infecting Multidrug-Resistant *Shigella flexneri* and *Escherichia coli*, and Its Bactericidal Effect *in vitro* and *in vivo*

Jing Xu[1,2†], Ruiyang Zhang[1,2†], Xinyan Yu[1,2†], Xuesen Zhang[3], Genyan Liu[4,5] and Xiaoqiu Liu[1,2]*

[1] Key Laboratory of Pathogen Biology of Jiangsu Province, Nanjing Medical University, Nanjing, China, [2] Department of Microbiology, Nanjing Medical University, Nanjing, China, [3] State Key Laboratory of Reproductive Medicine, Nanjing Medical University, Nanjing, China, [4] Department of Laboratory Medicine, The First Affiliated Hospital With Nanjing Medical University, Nanjing, China, [5] National Key Clinical Department of Laboratory Medicine, The First Affiliated Hospital With Nanjing Medical University, Nanjing, China

OPEN ACCESS

Edited by:
Krishna Mohan Poluri, Indian Institute of Technology Roorkee, India

Reviewed by:
Naveen Kumar Devanga Ragupathi, The University of Sheffield, United Kingdom
Anders S. Nilsson, Stockholm University, Sweden

***Correspondence:**
Xiaoqiu Liu
xiaoqiuliu2014@126.com

[†] *These authors have contributed equally to this work*

Specialty section:
This article was submitted to Virology, a section of the journal Frontiers in Microbiology

Received: *22 April 2021*
Accepted: *19 July 2021*
Published: *26 August 2021*

Citation:
Xu J, Zhang R, Yu X, Zhang X, Liu G and Liu X (2021) Molecular Characteristics of Novel Phage vB_ShiP-A7 Infecting Multidrug-Resistant Shigella flexneri and Escherichia coli, and Its Bactericidal Effect in vitro and in vivo. Front. Microbiol. 12:698962. doi: 10.3389/fmicb.2021.698962

In recent years, increasing evidence has shown that bacteriophages (phages) can inhibit infection caused by multidrug-resistant (MDR) bacteria. Here, we isolated a new phage, named vB_ShiP-A7, using MDR *Shigella flexneri* as the host. vB_ShiP-A7 is a novel member of *Podoviridae*, with a latency period of approximately 35 min and a burst size of approximately 100 phage particles/cell. The adsorption rate constant of phage vB_ShiP-A7 to its host *S. flexneri* was 1.405×10^{-8} mL/min. The vB_ShiP-A7 genome is a linear double-stranded DNA composed of 40,058 bp with 177 bp terminal repeats, encoding 43 putative open reading frames. Comparative genomic analysis demonstrated that the genome sequence of vB_ShiP-A7 is closely related to 15 different phages, which can infect different strains. Mass spectrometry analysis revealed that 12 known proteins and 6 hypothetical proteins exist in the particles of phage vB_ShiP-A7. Our results confirmed that the genome of vB_ShiP-A7 is free of lysogen-related genes, bacterial virulence genes, and antibiotic resistance genes. vB_ShiP-A7 can significantly disrupt the growth of some MDR clinical strains of *S. flexneri* and *Escherichia coli* in liquid culture and biofilms *in vitro*. In addition, vB_ShiP-A7 can reduce the load of *S. flexneri* by approximately 3–10 folds in an infection model of mice. Therefore, vB_ShiP-A7 is a stable novel phage with the potential to treat infections caused by MDR strains of *S. flexneri* and *E. coli.*

Keywords: bacteriophage vB_ShiP-A7, genome sequence, multidrug resistant, mass spectrometry, comparative genome, bactericidal ability

INTRODUCTION

A growing number of multidrug-resistant (MDR) bacteria have been reported, and the emergence of MDR bacteria leads to serious systemic and biofilm-associated infections (Shiferaw et al., 2012; Ahmed and Shimamoto, 2015; Klontz and Singh, 2015). For example, infections caused by MDR *Enterobacteriaceae*, especially β-lactam-resistant *Enterobacteriaceae*, are difficult to treat

(De Angelis et al., 2020). *Shigella* spp. and *Escherichia coli* are major members of the family *Enterobacteriaceae*, which comprises important enteric pathogens (The et al., 2016; Kotloff et al., 2018). *Shigella* spp. and *E. coli* can cause human infection through food contamination; in particular, a small number of cells of *Shigella* can cause diarrhea in humans (The et al., 2016). Globally, the morbidity and mortality rates of diarrhea caused by *Shigella* are high. In the era of antibiotic crisis, bacteriophages have been demonstrated to be effective alternative biocontrol agents for these members of *Enterobacteriaceae* (Kakasis and Panitsa, 2019).

Phages were first used to treat diarrhea caused by *Shigella* in the 1920s (D'Herelle, 1923). However, after antibiotics were discovered and widely used, only Eastern European countries insisted on phage treatment for infections (Nikolich and Filippov, 2020). In the 21st century, phages against MDR *Shigella* have been widely investigated (Tang et al., 2019; Kortright et al., 2019). Bernasconi et al. proved that three commercially available bacteriophage cocktails could suppress *Shigella* infections in the human intestine (Bernasconi et al., 2018). In a mouse model, Mai et al. prepared a new reagent composed of a phage cocktail and an antibiotic (ampicillin), named ShigActive^{TM}, to lyse *Shigella* (Mai et al., 2015). *Shigella* phages have also been successfully applied to food safety (Zhang et al., 2013). Soffer et al. characterized five lytic bacteriophages and combined them as a cocktail, ShigaShield^{TM}, to inhibit the growth of *S. sonnei* in food—the process of FDA and USDA assessment of the GRAS status (GRN672) (Soffer et al., 2017). Several phages have been reported to have the ability to infect both *E. coli* and *Shigella* (Chang and Kim, 2011; Lee et al., 2016; Sváb et al., 2019). Phages have been widely studied in the prevention and treatment of infections caused by *Shigella* spp. and *E. coli* in humans, suggesting that phages are promising for the treatment of infections caused by these *Enterobacteriaceae* members.

There are many limitations in phage therapy, such as phage pharmacology and infection kinetics, a narrow host range of phages, and phage resistance to bacteria. It has been shown that phage cocktails can overcome the limitations of the narrow host range of phages and phage resistance to bacteria (Matsuzaki et al., 2014; Kakasis and Panitsa, 2019). Cocktails of well-known lytic phages might open new perspectives in controlling infections caused by MDR bacteria. Therefore, isolating and characterizing more phages will allow us to obtain enough stock phages for the preparation of personalized phage cocktails against different clinical MDR bacterial strains. In addition, a comprehensive study of each novel phage is required to exclude a phage encoding toxic proteins or lysogen-related proteins in phage cocktails. It is also necessary to evaluate the effectiveness and safety of these new phages against MDR bacteria both *in vitro* and *in vivo*.

Phages have been isolated from different environmental sources and fecal samples of humans and animals (Kim et al., 2010; Sun et al., 2013; Jun et al., 2013; Schofield et al., 2015; Doore et al., 2018). In this study, we isolated a novel lytic phage named vB_ShiP-A7, using a clinically isolated MDR *S. flexneri* strain as a host, from wastewater in Nanjing, China. Phage vB_ShiP-A7 can also infect several clinically isolated MDR *E. coli* strains. The phage has a strong ability to lyse bacteria in liquid culture media and biofilms. Furthermore, phage vB_ShiP-A7 can significantly reduce the number of *S. flexneri* in mice. Thus, this phage may be used to monitor, diagnose, and control infections caused by MDR *S. flexneri* and *E. coli*.

MATERIALS AND METHODS

Bacterial Strains

All of the bacterial strains used in this study were grown in Luria-Bertani (LB) medium at 37°C (**Table 1**). *Escherichia coli* wild-type strain MG1655 was a stock of our lab, where as *S. flexneri* A7, *S. sonnei* A5, and 29 clinical strains of *E. coli* were isolated and cultured from different specimens of patients in the First Affiliated Hospital of Nanjing Medical University, Nanjing, China. Twenty-four clinical strains of *Shigella* spp. were tested at the Jiangsu Provincial Center for Disease Control and Prevention. *Shigella flexneri* A7 was deposited in the China Center for Type Culture Collection (CCTCC Number is PB 2020012) in Wuhan, China.

Isolation and Propagation of Bacteriophages

vB_ShiP-A7 was screened from wastewater in Nanjing (China) using an MDR strain *S. flexneri* A7 as a host. First, a wastewater sample was filtered through a 0.45-μm filter (Millipore, United States). Thereafter, the filtered liquid was added to the early-log-phase culture of *S. flexneri* A7 and cultured at 37°C for 4 h to enrich the phages. The cell culture was spun down to remove bacterial cells. Next, 10 μL of the supernatant, 100 μL of *S. flexneri* A7, and 3 mL of 0.6% (w/v) LB agar were mixed well, and the mixture was poured on the surface of an LB plate. After culturing at 37°C for approximately 12 h, plaques formed on the plate. A single clear plaque was selected to start a new round of screening. After several rounds of screening, the plaques appeared homogeneous on a double-layer agar plate. A single clear plaque was selected and inoculated in a liquid culture of the host strain. The supernatant of the culture with the phage was filtered through a 0.22 μm filter and used to start a new round of screening. We again obtained homogeneous plaques on a double-layer agar plate. The preliminary purified phage, named vB_ShiP-A7, from a single plaque was obtained and stored at 4°C.

Purification of Phage vB_ShiP-A7

Phage vB_ShiP-A7 was purified following the protocol of Yu et al. (2017). Briefly, phage vB_ShiP-A7 was added to the early-log-phase liquid culture of *S. flexneri* A7. After incubation at 37°C for 2 h, the culture medium was spun down at 14,000 × *g* for 10 min at 4°C. The supernatant was collected and passed through a 0.45 μm filter. The filtrate was concentrated using ultrahigh-speed centrifugation. The supernatant was removed, and the pellet was resuspended in SM buffer (10 mM Tris-HCl, pH 7.5; 100 mM NaCl; and 10 mM $MgSO_4$). The suspension was further separated using cesium chloride gradient ultrahigh-speed centrifugation. We collected approximately 1 mL of phage zone and diluted it 10 times in SM buffer. The sample was then

TABLE 1 | Host range spectrum of the bacteriophage vB_ShiP-A7.

Strains	Source	Subtype	Resistance	Lysis or not	Efficiency of Plating (EOP)
E. coli K-12 MG1655	ATCC 700926			N	N
Shigella flexneri A7			Ampicillin sulbactam, Aminoglycoside streptomycin, Spectinomycin	Clear plaque	100%
Shigella sonnei A5			Spectinomycin, Gentamycin, Streptomycin, Aminoglycoside, Ampicillin sulbactam	N	N
Shigella sonnei S20001			Amikacin, Azithromycin, Streptomycin	N	N
Shigella flexneri S20003		2b	Amikacin, Ampicillin, Ampicillin-Sulbactam, Azithromycin, Cefoxitin, Chloramphenicol, Ciprofloxacin, Nalidixic Acid, Streptomycin, Tetracycline	N	N
Shigella sonnei S20004			Amikacin, Ampicillin, Azithromycin, Cefotaxime, Cefoxitin, Nalidixic Acid, Streptomycin, Tetracycline, Trimethoprim-Sulfamethoxazole	N	N
Shigella flexneri S20005		2a	Amikacin, Ampicillin, Ampicillin-Sulbactam, Azithromycin, Aztreonam, Cefotaxime, Cefoxitin, Chloramphenicol, Ciprofloxacin, Nalidixic Acid, Streptomycin, Tetracycline, Trimethoprim-Sulfamethoxazole	N	N
Shigella flexneri S20006		2a	Amikacin, Ampicillin, Ampicillin-Sulbactam, Azithromycin, Aztreonam, Cefotaxime, Cefoxitin, Ceftazidime, Chloramphenicol, Ciprofloxacin, Nalidixic Acid, Streptomycin, Tetracycline	N	N
Shigella flexneri S20008		2a	Amikacin, Ampicillin, Ampicillin-Sulbactam, Azithromycin, Cefoxitin, Chloramphenicol, Ciprofloxacin, Nalidixic Acid, Streptomycin, Tetracycline	N	N
Shigella flexneri S20009		1a	Amikacin, Ampicillin, Ampicillin-Sulbactam, Azithromycin, Cefoxitin, Chloramphenicol, Ciprofloxacin, Nalidixic Acid, Streptomycin, Tetracycline	Clear plaque	26.5%
Shigella sonnei S20010			Amikacin, Azithromycin, Cefoxitin, Streptomycin, Tetracycline,	N	N
Shigella flexneri S20012		1a	Amikacin, Ampicillin, Ampicillin-Sulbactam, Azithromycin, Cefotaxime, Cefoxitin, Chloramphenicol, Ciprofloxacin, Nalidixic Acid, Streptomycin, Tetracycline, Trimethoprim-Sulfamethoxazole	Clear plaque	24.6%
Shigella flexneri S20013		2a		N	N
Shigella flexneri S20014		2b	Amikacin, Azithromycin, Cefoxitin, Streptomycin,	N	N
Shigella flexneri S20015		2b	Amikacin, Azithromycin, Cefoxitin, Streptomycin,	N	N
Shigella flexneri S20016		2b	Amikacin, Azithromycin, Meropenem, Streptomycin,	N	N
Shigella flexneri S20017		2b	Amikacin, Azithromycin, Cefoxitin, Streptomycin,	N	N
Shigella flexneri S20018		2b	Azithromycin, Cefoxitin, Streptomycin,	N	N
Shigella sonnei S20020			Amikacin, Ampicillin, Azithromycin, Cefotaxime, Cefoxitin, Nalidixic Acid, Streptomycin, Tetracycline, Trimethoprim-Sulfamethoxazole	N	N
Shigella flexneri S20022		1a	Amikacin, Ampicillin, Ampicillin-Sulbactam, Azithromycin, Cefoxitin, Chloramphenicol, Ciprofloxacin, Nalidixic Acid, Streptomycin, Tetracycline	Clear plaque	38.7%
Shigella flexneri S20023		1a	Amikacin, Ampicillin, Ampicillin-Sulbactam, Azithromycin, Aztreonam,Cefoxitin, Ceftazidime, Ciprofloxacin, Nalidixic Acid, Streptomycin, Tetracycline,Trimethoprim-Sulfamethoxazole	Clear plaque	45%
Shigella flexneri S20024		2a	Amikacin, Ampicillin, Ampicillin-Sulbactam, Azithromycin, Cefoxitin, Chloramphenicol, Ciprofloxacin, Nalidixic Acid, Streptomycin, Tetracycline	N	N
Shigella flexneri S20025		2b	Amikacin,Azithromycin, Cefoxitin, Streptomycin,	N	N
Shigella sonnei S20026			Amikacin, Ampicillin, Azithromycin, Cefotaxime,Cefoxitin, Nalidixic Acid, Streptomycin,Trimethoprim-Sulfamethoxazole	N	N

(Continued)

TABLE 1 | Continued

Strains	Source	Subtype	Resistance	Lysis or not	Efficiency of Plating (EOP)
Shigella flexneri S20027		1a	Amikacin,Azithromycin,Cefoxitin,Streptomycin	Clear plaque	38.9%
Shigella flexneri S20028	,	2a	Amikacin, Ampicillin, Ampicillin-Sulbactam, Azithromycin, Cefoxitin, Chloramphenicol, Ciprofloxacin, Nalidixic Acid, Streptomycin	N	N
Shigella flexneri S20029		1a	Amikacin,Azithromycin, Cefoxitin,Streptomycin	Clear plaque	41.1%
E. coli 393 D3	Urine	ESBL	Levofloxacin, Cefazolin, Cefepime, Cefotaxime, Ceftazidime	Clear plaque	0.03%
E. coli 395B5	Urine	ESBL	Gentamycin, Ampicillin sulbactam, Aztreonam, Cefepime, Cefazolin, Levofloxacin, Cefotaxime, Sulfamethoxazole and Trimethoprim	Clear plaque	4.1%
E. coli 397 D3	Urine	ESBL	Gentamycin、Ampicillin sulbactam、Levofloxacin、Cefotaxime, Cefepime, Aztreonam, Cefoxitin, Cefazolin, Sulfamethoxazole and Trimethoprim	Turbid plaque	N
E. coli 389 A6	Urine	ESBL	Sulfamethoxazole and Trimethoprim, Cefazolin, Aztreonam, Ceftazidime	N	N
E. coli 389G7	Urine	ESBL	Ampicillin sulbactam, Aztreonam, Cefazolin, Amikacin, Levofloxacin, Cefotaxime	N	N
E. coli 393B7	Urine	ESBL	Levofloxacin, Gentamycin, Cefazolin, Ampicillin sulbactam, Ceftazidime, Amoxicillin and Clavulanate, Amikacin, Aztreonam, Sulfamethoxazole and Trimethoprim, Minocycline, Cefotaxime, Cefepime, Cefoxitin	N	N
E. coli 393C8	Urine	ESBL	Sulfamethoxazole and Trimethoprim, Cefepime, Cefazolin, Cefotaxime, Levofloxacin	N	N
E. coli 395G6	Urine	ESBL	Gentamycin, Aztreonam, Cefazolin, Cefepime, Ceftazidime, Cefotaxime	N	N
E. coli 396J1	Urine	ESBL	Levofloxacin, Cefazolin, Imipenem, Cefepime, Cefotaxime	N	N
E. coli 394H7	Urine	ESBL	Cefotaxime, Levofloxacin, Ceftazidime, Aztreonam, Cefepime	N	N
E. coli 396J5	Urine	ESBL	Levofloxacin, Aztreonam, Imipenem Cefepime, Cefazolin, Cefotaxime	N	N
E. coli 389 G7	Urine	ESBL	Cefazolin, Ampicillin sulbactam, Levofloxacin, Aztreonam, Amikacin, Cefotaxime	N	N
E. coli 394F7	Urine	ESBL	Cefazolin, Aztreonam, Cefoxitin, Ceftazidime, Cefotaxime, Amoxicillin, and Clavulanate	N	N
E. coli 389D9	Urine	Non-ESBL	Sulfamethoxazole and Trimethoprim	N	N
E. coli 389G6	Urine	Non-ESBL	Levofloxacin	N	N
E. coli 389G4	Urine	Non-ESBL	Gentamycin, Cefazolin, Ampicillin sulbactam, Cefotaxime, Amikacin, Levofloxacin, Ceftazidime, cefoxitin	N	N
E. coli 390B6	Urine	Non-ESBL	Sulfamethoxazole and Trimethoprim	N	N
E. coli 390J2	Urine	Non-ESBL	Minocycline, Levofloxacin, Sulfamethoxazole, and Trimethoprim	N	N
E. coli 389E6	Urine	Non-ESBL	Levofloxacin	N	N
E. coli 390G7	Urine	Non-ESBL	Sulfamethoxazole and Trimethoprim, Gentamycin, Cefazolin, Ampicillin sulbactam, Levofloxacin	N	N
E. coli 390H2	Urine	Non-ESBL	Ampicillin sulbactam, Levofloxacin, Sulfamethoxazole and Trimethoprim, Gentamycin, Cefazolin	N	N
E. coli 391D3	Urine	Non-ESBL	Gentamycin, Cefazolin, Sulfamethoxazole and Trimethoprim	N	N
E. coli 389J4	Sputum	ESBL	Cefepime, Ceftazidime, Cefazolin, Aztreonam	N	N
E. coli 395J2	Sputum	ESBL	Gentamycin, Ampicillin, Minocycline, Levofloxacin	N	N
E. coli 397C8	Sputum	ESBL	Ceftazidime, Aztreonam, Cefepime, Ceftazidime	N	N
E. coli 396F3	Sputum	ESBL	Ampicillin, Gentamycin, Minocycline, Levofloxacin, Amikacin	N	N
E. coli 390A7	Sputum	Non-ESBL	Sulfamethoxazole and Trimethoprim	N	N
E. coli 391G4	Blood	ESBL	Cefepime, Cefazolin, Aztreonam, Ceftazidime	N	N
E. coli 393C1	Ascites	ESBL	Cefotaxime, Cefazolin, Cefepime, Ampicillin sulbactam, Aztreonam, Gentamycin, Ceftazidime, Sulfamethoxazole, and Trimethoprim	N	N

Negative results are indicated by "N."

centrifuged at 200,000× *g* for 3 h to remove cesium chloride. The pellets were resolved in SM buffer as the purified phage particles of vB_ShiP-A7.

Electron Microscopy

A drop of purified phage vB_ShiP-A7 particles (2×10^{11} PFU/mL) was dripped onto a copper grid. The phages on the copper grid were negatively stained using 2% (w/v) phosphotungstic acid. The morphology of phage vB_ShiP-A7was observed using an FEI Tecnai G2 Spirit Bio TWIN transmission electron microscope at 80 kV.

Analysis of the Phage Host Range

The infection ability of phage vB_ShiP-A7 on different strains was determined using standard spot tests (Kutter, 2009). Briefly, 100 μL of log-phase bacterial culture of each strain was mixed with 3 mL of melted soft agar (0.6% agar), which was poured over an LB plate. After preparing different concentrations of phagevB_ShiP-A7 suspensions (10^{10}–10^2 PFU/mL), 5 μL of each concentration of the phage suspension was dropped onto the surface of solidified plates containing different test strains. After overnight culture at 37 C, the inhibition of bacterial growth by different concentrations of vB_ShiP-A7 on each plate reflected the sensitivity of the strain to vB_ShiP-A7. All experiments were conducted in accordance with the ethical guidelines of Nanjing Medical University, the First Affiliated Hospital of Nanjing Medical University, and Jiangsu Provincial Center for Disease Control and Prevention (Nanjing, China), and informed consent was obtained from all patients.

Efficiency of Plating (EOP)

This method has been previously described by Kutter (2009). The positive clinical strains screened via standard spot tests were plated on double-layer agar plates with the phage. Plaques on each plate were counted, and the relative EOP was given as the ratio between the number of plaques on each clinical strain and the number of plaques on the host strain.

Temperature Stability

The thermal stability of phage vB_ShiP-A7 was determined at different temperatures. Five test tubes containing 10^9 phage particles were immersed in different temperature water baths for approximately 1 h (4, 25, 37, 45, and 50°C). Thereafter, the phage titers of all the samples were determined using the double-layer agar method (Yu et al., 2017).Three independent repeated experiments were performed. The average value was used to generate the figure, and the standard error of the mean (SEM) was marked.

Phage Adsorption Rate

The phage adsorption rate was determined using the protocol described by Zurabov and Zhilenkov (2021). Cells from an overnight culture of *S. flexneri* A7 were suspended in an LB broth to obtain a cell density of 10^8 CFU/mL. The phage suspension was added to 5 mL of the bacterial suspension to a final concentration of 10^7 PFU/mL. Thereafter, the mixture of phage and bacteria was diluted in 45 mL LB broth and incubated at 37°C and 100 rpm for 5 min. The supernatant was filtered through a 0.22 μm filter, and the concentration of the free phages was determined using the plaque assay described above. The reduction in phage titer was equal to the number of phages adsorbed to the cells. The phage titer did not change in the control phage filtrate. We calculated the adsorption constant of the phage using the formula shown below (Zurabov and Zhilenkov, 2021), where k is the adsorption rate constant, P is the concentration of free phage per mL, P0 is the initial concentration of phage, B is the bacterial density, and t is the time in minutes over which adsorption occurs.

$$k = -\ln\left(\frac{P}{P0}\right)/Bt$$

One-Step Growth Curve of Phage vB_ShiP-A7

A one-step growth curve of phage vB_ShiP-A7 was drawn following the protocol of Yang et al. (2015), with minor modifications. Phage vB_ShiP-A7 was added to the early-log-phase of the *S. flexneri* A7 culture (1×10^8 CFU/mL) at a multiplicity of infection (MOI) of 0.1 and incubated at 37°C for 5 min. The phages were then removed through centrifugation. Thereafter, the precipitate was put into 50 mL of LB medium and cultured at 37°C for 5 min. We obtained 1 mL cell cultures at different time points and centrifuged them at 14,000 rpm for 1 min (Eppendorf Centrifuge 5424) to remove the host bacteria. Free bacteriophages in these supernatants were counted using the double-layer agar plate method. Three independent experiments were performed to obtain the one-step growth curve of vB_ShiP-A7, in which the latency period, burst period, and burst size of the vB_ShiP-A7 were determined. The latency period refers to the time from the adsorption of bacterial cells by the phage to the release of new phages from the bacterial cells. The burst period refers to the period from the beginning of phage release to the end of phage release, which is just after the latency period. The burst size of the phage is equal to the amount of phage at the end of lysis divided by the initial number of bacterial cells at the time of infection.

Bacterial Challenge Assay

Overnight culture of *S. flexneri* A7 was added into the LB medium at a ratio of 1:100 and cultured for 2.5 h to the logarithmic phase. Phage vB_ShiP-A7 (MOI = 10, 1, or 0.1) was added to the log-phage cultures of *S. flexneri* A7. An equal volume of SM buffer was added to the negative control sample. We measured the optical density at 600 nm (OD600) of the bacterial culture medium every 15 min for a total of 300 min.

Genome Isolation and Sequencing of Phage vB_ShiP-A7

The ultra-purified particles of vB_ShiP-A7 (approximately10^{11} phage particles) were digested by DNase I (New England Biolabs) and RNase A (Tiangen Biotech) at 37°C for 2 h

to remove the residual genomic DNA and RNA of the host bacteria. Thereafter, the sample was treated with proteinase K (Tiangen Biotech) at 55°C for 15 min. This sample was further purified using a TIANamp Bacteria DNA Kit (Tiangen Biotech). The purified phage DNA concentration was measured using a spectrophotometer (Nanodrop Technologies, United States). The entire genome was sequenced on an Illumina platform (Illumina HiSeq 2500 sequencer, paired-end sequencing run, 2 × 150 bp). SOAPdenovov2.04 and GapCloser v1.12 were used to analyze the high-throughout sequencing results and assemble reads into a whole genome. The purified phage genome DNA was digested by the restriction endonuclease EcoRI or PstI at 37°C for 6 h. The enzyme digestion products were analyzed using 1% agarose gel.

Annotation and Comparison

Artemis software (Carver et al., 2005) and Glimmer 3 (Aggarwal and Ramaswamy, 2002) were used to predict the putative open reading frames (ORFs) in the genome of vB_ShiP-A7; each predicted protein length is more than 30 amino acids. Functional annotation of the genome of vB_ShiP-A7 was conducted using BLAST tools at NCBI[1] against the non-redundant protein sequence database. tRNAscan-SE was used to find transfer RNAs (tRNAs) in the genome of vB_ShiP-A7(v1.23[2]). RNAmmer was used to find ribosomal RNAs (rRNAs) in the genome of vB_ShiP-A7 (v1.2[3]). Molecular masses and isoelectric points of all the predicted phage proteins were calculated using DNAman. Using the NCBI database, we found that the whole-genome sequence of several phages had high homology with phage vB_ShiP-A7 sequence (>40%). The EMBOSS needle tool was used to compare the similarity of protein amino acid sequences (European Molecular Biology Laboratory-European Bioinformatics Institute). EasyFig was used to compare the annotated proteins of vB_ShiP-A7 with those of related phages[4] (Sullivan et al., 2011). The neighbor-joining algorithm in MEGA was used to analyze the phylogenetic relationships among the phages.

Analysis of Phage Particle Proteins

The particles of vB_ShiP-A7 were mixed with loading dye and boiled in a 100°C water bath for 5 min. The boiled sample was separated using 12% sodium dodecyl sulfate-polyacrylamide gel electrophoresis (SDS-PAGE). The gel was stained with silver according to the protocol of Shevchenko et al. (1996). Liquid chromatography-electrospray ionization tandem mass spectrometry (LC-ESI MS/MS) was used to analyze the proteins in the particles of vB_ShiP-A7. The virions of vB_ShiP-A7 were digested with trypsin first, and the tryptic peptides were then analyzed using a Q Exactive mass spectrometer (Thermo Scientific, United States). The MASCOT engine was used to find the corresponding peptides (Matrix Science, London, United Kingdom; version 2.2) against all putative ORFs predicted in the genome of vB_ShiP-A7.

[1]http://blast.ncbi.nlm.nih.gov/Blast.cgi

[2]http://lowelab.ucsc.edu/tRNAscan-SE

[3]http://www.cbs.dtu.dk/services/RNAmmer/

[4]http://mjsull.github.io/Easyfig/files.html

Biofilm Biomass Quantification Using Crystal Violet Staining

Overnight bacterial cultures of *S. flexneri* A7 and *E. coli* 395B5were subcultured into LB medium separately until the early mid-logarithmic phase with approximately 10^8 CFU/mL. The bacterial culture was diluted to 10^7 CFU/mL using LB medium, and 200 μL of the diluted bacterial culture (10^7 CFU/mL) was added to each well in a 96-well plate (Corning Corp., United States). After incubation at 37°C for 24 h, 100 μL of the culture medium was removed from each well. At the same time, 100 μL of fresh LB medium with phage vB_ShiP-A7 (10^9 PFU/mL) was added to the sample wells, and 100 μL of LB was added to the control wells. After culture for another 24 h, the culture medium of each well was gently removed. The wells were then washed twice using 1 × phosphate-buffered saline (PBS). Biofilms attached to the wells were stained with 0.5% (w/v) crystal violet (200 μL/well) for 20 min at 37°C. To remove the excess crystal violet stain, the wells were washed 3 times with PBS. Pictures of the different wells were taken under a 20 × objective lens using a Zeiss (Axio Vert A1) microscope. Finally, the prestained biofilm was dissolved using 30% (v/v) acetic acid in water for biomass quantification at an absorbance of 560 nm using a plate reader (BioTek-Synergy HT).

Inhibitory Effect of the Phage on *S. flexneri* in a Mouse Infection Model

Forty C57BL/6 mice (6 weeks old) were randomly divided into four groups: "control group," "phage group," "*Shigella* infection group," and "*Shigella* infection plus phage treatment group," with 10 mice in each group. Before infection with *S. flexneri* A7, the mice were fed drinking water containing broad-spectrum antibiotics (metronidazole 215 μg/L, colistin 0.85 U/mL, gentamicin 35 μg/L, and vancomycin 45 μg/L) for 3 days. On the fourth day, we started to feed these mice without antibiotics, and each mouse was weighed and recorded as the initial weight. On the fifth day, the day of mouse infection, *S. flexneri* A7 was grown to the exponential growth phase in an LB broth before being pelleted via centrifugation and washed 2 times in PBS. The bacteria were resuspended in the requisite volume of PBS to yield the desired in oculum (10^8 CFU/mL). The mice in the "*Shigella* infection group" and "*Shigella* infection plus phage treatment group" were given 200μL bacterial suspension by gavage. The mice in the "control group" and "phage group" were given 200 μL of PBS by gavage. Five hours after bacterial infection, the purified phages were administered through drinking water to the mice in the "phage group" and "*Shigella* infection plus phage treatment group" (10^{11}purified phage particles in SM buffer were added to 200 mL drinking water). The mice in the "control group" and "*Shigella* infection group" only received 200 mL drinking water with the same amount of SM buffer. After bacterial infection, the activity and defecation of these mice were observed. The feces of the mice were harvested, dissolved, and diluted. For the feces of each mouse, *S. flexneri* A7 was quantified via colony counts, and the phages was quantified using the plaques on the double-layer agar plates.

Nucleotide Sequence Accession Number

The whole assembled genome sequence of vB_ShiP-A7 is deposited in the GenBank database under accession number MK685668.

RESULTS

Morphology of Phage vB_ShiP-A7

Using *S. flexneri* A7 as the host strain, a novel phage vB_ShiP-A7 was isolated from wastewater in Nanjing, China. After overnight incubation with *S. flexneri* A7 at 37°C, phage vB_ShiP-A7 formed large clear round plaques of approximately13 ± 0.60 mm in diameter on a double-layer agar plate (**Figure 1A**). We observed the morphology of this phage under an electron microscope. Phage vB_ShiP-A7 has an isometric head with a diameter of approximately 61.42 ± 1.23 nm and a noncontractile short tail of approximately 13 nm in length (**Figure 1B**). Phage vB_ShiP-A7 is a member of the family *Podoviridae*. This phage was named vB_ShiP-A7 following the phage nomenclature defined by Kropinski et al. (2009).

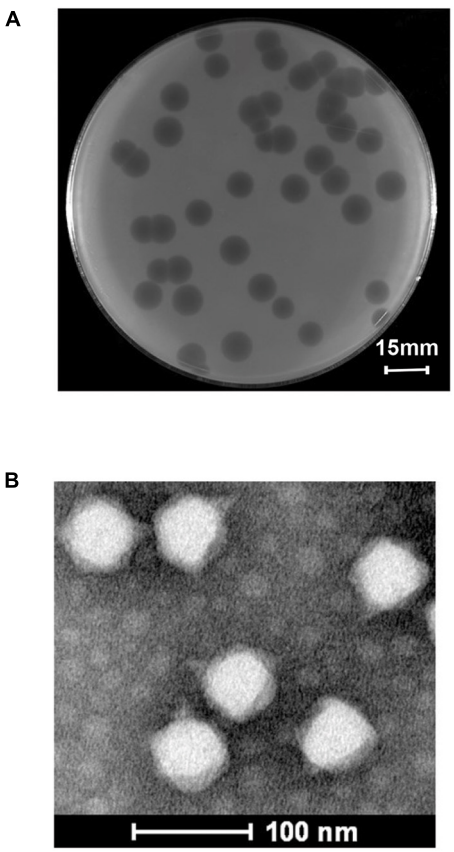

FIGURE 1 | Isolation and morphological analysis of phage vB_ShiP-A7. **(A)** Plaques of phage vB_ShiP-A7 on the top agar plate. The bar indicates 15 mm. **(B)** The morphology of phage vB_ShiP-A7 under transmission electron microscopy. The bar indicates 100 nm.

Thermal Stability and Population Dynamics of Phage vB_ShiP-A7

The activity of vB_ShiP-A7 was measured after incubation at different temperatures (4°C, 25°C, 37°C, 45°C, and 50°C) for 1 h (**Figure 2A**). The activity of phage vB_ShiP-A7 did not change from 4 to 37°C. When the temperature increased up to 45°C, the phage began to lose its activity rapidly (**Figure 2A**). These data suggest that vB_ShiP-A7 is stable over a relatively wide temperature range from 4 to 37°C. Therefore, it can be preserved well at 4°C in the laboratory as well as in the body of mammals at 37°C. A one-step growth experiment was conducted to assess the population kinetics of phage vB_ShiP-A7 using *S. flexneri* A7 as a host (**Figure 2B**). Phage vB_ShiP-A7 was released 35 min after infection, with a burst size of approximately 100 phage particles/infected cell (**Figure 2B**). The adsorption rate constant at 5 min post-infection was determined to be 1.405×10^{-8} mL/min (**Supplementary Table 1**). Approximately 91.97% of the phage particles were adsorbed on the *S. flexneri* A7 cells in 5 min at an MOI = 0.1.

Bacteriophage vB_ShiP-A7 Inhibits Planktonic Bacterial Growth

The efficacy of phage vB_ShiP-A7 on planktonic bacterial growth was assessed by inoculating a bacterial broth culture of *S. flexneri* A7 in the logarithmic period with phage vB_ShiP-A7 at different MOIs of 0.1, 1, and 10. Our results showed that the growth of the host strain *S. flexneri* A7 was completely disrupted within 90 min by phage vB_ShiP-A7 at different MOIs, and this growth inhibition lasted until 300 min after infection. The speed of bacterial lysis was accelerated by the increase in the phage titer (**Figure 2C**).

Host Range and EOPs of Phage vB_ShiP-A7

The ability of phage vB_ShiP-A7 to infect different bacterial strains was estimated using standard spot tests (Kutter, 2009). Phage vB_ShiP-A7 can infect and form clear plaques on the MDR strain of *S. flexneri* A7 and on the 6 clinical MDR strains of *S. flexneri* serotype 1a but not the MDR strains of *S. Sonnei* (**Table 1**). In addition, vB_ShiP-A7 at low titers can form clear plaques on 2 of the MDR *E. coli* strains (393D3 and 395B5) and turbid plaques on 1 MDR *E. coli* strain (397D3); however, it cannot infect the wild-type *E. coli* strain MG1655 (**Table 1**). The EOPs of phage vB_ShiP-A7 on different clinical MDR strains are shown in **Table 1**. The results showed that the phage could specifically infect some serotypes of *Shigella* and also recognize some strains of *E. coli*, but it had a better lytic effect on strains of *Shigella flexneri* serotype 1a (**Table 1**). Thus, vB_ShiP-A7 may be used as a biocontrol agent to prevent or treat infections caused by MDR *S. flexneri* or *E. coli*.

Basic Characteristics of the Genome of vB_ShiP-A7

To exclude the possibility that vB_ShiP-A7 contains any virulent proteins, it is necessary to identify the complete genome sequence of vB_ShiP-A7. Next-generation sequencing results showed

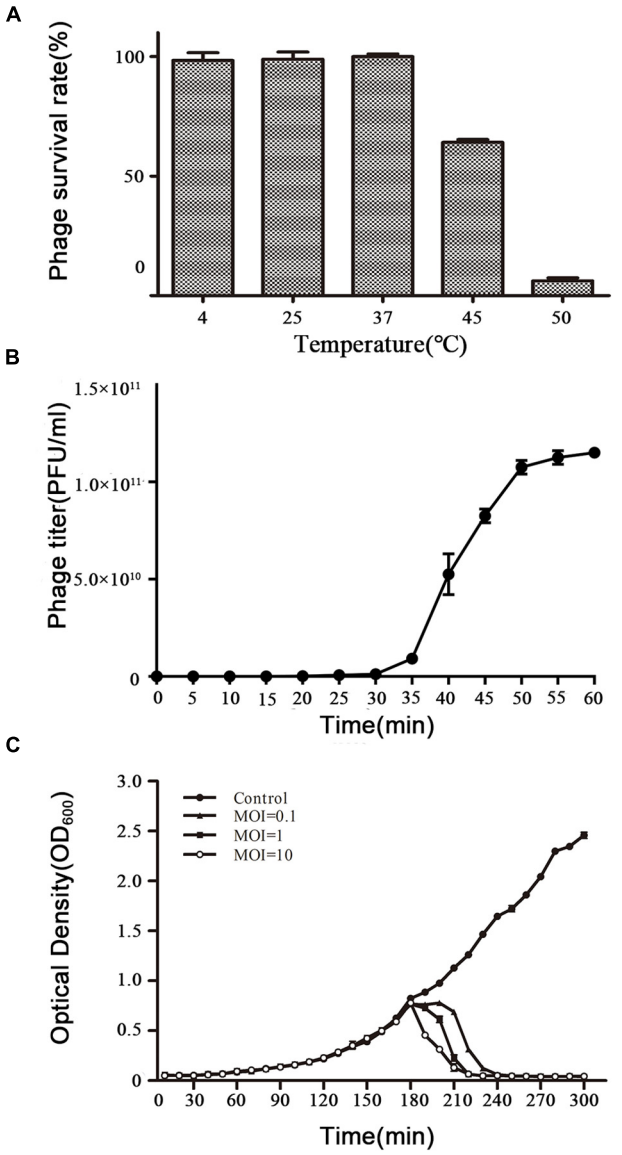

FIGURE 2 | Biological characteristics of phage vB_ShiP-A7. **(A)** The survival rate of vB_ShiP-A7 after treatment at different temperatures for 1 h. **(B)** One-step growth curve of vB_ShiP-A7 on strain *Shiglla flexneri* A7 at 37°C. **(C)** Bacterial challenge assay with phage vB_ShiP-A7 to *Shiglla flexneri* A7. vB_ShiP-A7 was added at MOIs of 0.1 (close triangles), 1 (close squares), and 10 (open circles) to different bacterial cultures after 2 h incubation (OD600 = 0.25). SM buffer instead of vB_ShiP-A7 was inoculated into a bacterial culture and used as the negative control (close circles). The light absorption value at OD600nm of each bacterial culture was recorded at 15 min intervals over a period of 300 min. In **(B,C)**, data from 3 independent experiments are combined and presented as the mean with the Standard Error of Mean (SEM).

that the complete genome of phage vB_ShiP-A7 is a linear double-stranded DNA of approximately 39,881 bp. To verify the nucleotide sequence obtained, the genomic DNA of phage vB_ShiP-A7 was further digested with EcoRI (2 sites at 28,588 and 37,095), PstI (1 site at 9333) (**Supplementary Figure 1**). However, 2 unexpected 2.9 kb and 9.3 kb fragments were identified after digestion, indicating that phage vB_ShiP-A7 is likely linear but not circular. To determine the terminal sequences of the vB_ShiP-A7 genome, the 2.9 kb and 9.3 kb fragments obtained by EcoRI and PstI digestion were recovered and directly sequenced with outward-pointing primers. As expected, the sequencing reaction terminated at the end of the genome. Thus, the vB_ShiP-A7 genome is indeed linear and has identical direct terminal repeats (DTRs) of 177 bp. We proved that the genomic DNA of vB_ShiP-A7 contains 177 bp terminal repeats located in the genome from nucleotides 1–177 and 39,882–40,058 (**Figure 3**). Therefore, the final genome length of phage vB_ShiP-A7 is 40,058 bp with 49.4% GC content (**Table 2** and **Figure 3**). The general organization of the genome of vB_ShiP-A7 follows that of the T7-like phages, in which 43 putative ORFs were predicted in the complementary strand, as summarized in **Table 2**. We did not find tRNA or rRNA genes in the genome of vB_ShiP-A7. Thirty-one ORFs (72.1%) were highly homologous to known functional genes, which were predicted to have similar functions with related genes (**Table 2**) and are labeled in different colors in **Figure 3**. The predicted functional proteins encoded by vB_ShiP-A7 can be divided into five categories: DNA/RNA replication/modification (DNA polymerase, DNA primase/helicase, ssDNA-binding protein, DNA ligase, RNA polymerase, bacterial RNA polymerase inhibitor, nucleotide kinase, exonuclease, and endonuclease), host lysis (lysin protein and endopeptidase Rz), packaging (DNA packaging protein and DNA packaging protein A), structural proteins (tail fiber protein, internal virion protein D, internal core protein, DNA injection channel protein A, internal virion protein A, tail tubular protein A, tail tubular protein B, major capsid protein, capsid and scaffold protein, head-to-tail joining protein, tail assembly protein, and host range protein), and additional functions (carbohydrate ABC transporter permease, N-acetylmuramoyl-L-alanine amidase, dGTP triphosphohydrolase inhibitor, putative protein kinase, putative S-adenosyl-L-methionine hydrolase, and predicted antirestriction protein) (**Table 2**, **Figure 3**). Twelve hypothetical proteins were also predicted in the genome of vB_ShiP-A7, and their potential functions in the life cycle of vB_ShiP-A7 need to be determined in future studies. In addition, lysogen-related proteins, such as integrase, recombinase, repressor, and excisionase, were not present in the genome of vB_ShiP-A7. We conclude that phage vB_ShiP-A7 is a lytic bacteriophage. We did not observe any known toxic proteins encoded by the genome of vB_ShiP-A7. The characteristics of this lytic phage lacking genes encoding harmful factors make it an effective and promising candidate as an antibacterial agent.

Comparative Genome Analysis of vB_ShiP-A7 With Its Related Phages

The whole-genome sequence of vB_ShiP-A7 was analyzed using BlastN analysis against the NCBI nonredundant DNA database. The highest similarity throughout the whole vB_ShiP-A7 genome was observed with 15 phages (coverage 74%–88%, identity 86%–93%), including *Escherichia* phage P483 (Chen et al., 2016), *Escherichia* phage P694 (Chen et al., 2016), *Enterobacteria*

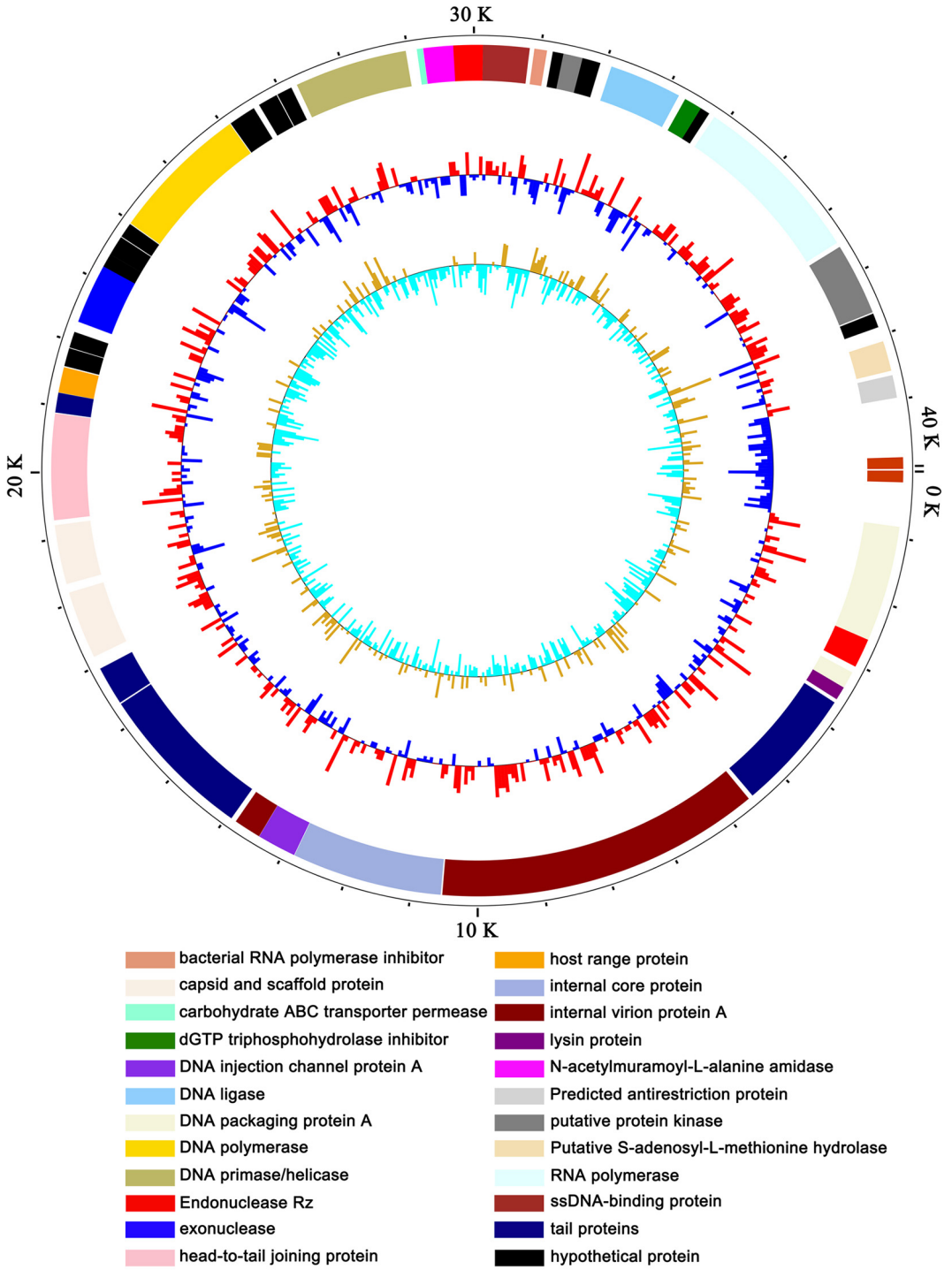

FIGURE 3 | Map of the genome organization of bacteriophage vB_ShiP-A7. The predicted ORFs of vB_ShiP-A7 are indicated in different colors in the outermost ring. All of the ORFs predicted in the vB_ShiP-A7 genome were in negative strand. ORFs with predicted functions are marked in different colors. Hypothetical proteins are labelled in black. The second ring represents the GC content. Red outward indicates that the GC content is above average, and blue inward indicates that the GC content is below average. The innermost ring represents the GC skew.

phage BA14 (Mertens and Hausmann, 1982), *Escherichia* phage vB EcoP S523, *Enterobacteria* phage 285P,*Pectobacterium* phage PP74 (Kabanova et al., 2018), *Kluyvera* phage Kvp1 (Lingohr et al., 2008), *Erwinia* phage FE44 (Faidiuk and Tovkach, 2014), *Salmonella* phage BSP161, *Salmonella* phage BP12A, *Yersinia* phage PYPS50, *Yersinia* phage Yepe2,*Yersinia* phage

TABLE 2 | Predicted ORFs and genes encoded by the vB_ShiP-A7 genome (GenBank database under accession number MK685668).

ORFs	Start	Stop	Directions	No of residues	MW(da)	pI	Predicted molecular function
ORF1	848	2608	-	586	66236.1	5.35	DNA packaging protein
ORF2	2608	3054	-	148	16740.9	7.51	endopeptidase Rz
ORF3	3153	3419	-	88	10113.7	4.38	DNA packaging protein A
ORF4	3412	3618	-	68	7337.2	6.72	lysin protein
ORF5	3675	5540	-	621	68063.2	6.34	tail fiber protein
ORF6	5612	10546	-	1644	179456.2	7.02	internal virion protein D
ORF7	10570	12849	-	759	85637.0	5.78	internal core protein
ORF8	12856	13449	-	197	21320.4	10.26	DNA injection channel protein A
ORF9	13452	13865	-	137	15747.5	8.71	internal virion protein A
ORF10	13946	16342	-	798	89101.9	6.35	tail tubular protein B
ORF11	16365	16955	-	196	21966.7	4.22	tail tubular protein A
ORF12	17154	18188	-	344	36520.6	6.63	major capsid protein
ORF13	18321	19220	-	299	32722.7	3.91	capsid and scaffold protein
ORF14	19295	20902	-	535	58734.0	4.35	head-to-tail joining protein
ORF15	20916	21218	-	100	10201.8	10.64	tail assembly protein
ORF16	21221	21607	-	128	14558.0	6.78	host range protein
ORF17	21626	21904	-	92	9895.3	10.26	hypothetical protein
ORF18	21914	22159	-	81	9134.7	4.40	hypothetical protein
ORF19	22322	23236	-	304	34816.3	4.79	exonuclease
ORF20	23233	23442	-	69	7319.0	9.87	hypothetical protein
ORF21	23442	23744	-	100	11218.9	8.50	hypothetical protein
ORF22	23756	23983	-	75	9410.1	6.24	hypothetical protein
ORF23	23997	26111	-	704	79084.7	6.33	DNA polymerase
ORF24	26124	26540	-	138	15743.3	9.66	hypothetical protein
ORF25	26632	26934	-	100	10943.6	10.65	hypothetical protein
ORF26	26948	27181	-	77	8715.8	11.71	hypothetical protein
ORF27	27273	28985	-	570	63571.7	4.89	DNA primase/helicase
ORF28	29153	29245	-	30	3665.0	7.53	carbohydrate ABC transporterpermease
ORF29	29250	29705	-	151	16950.3	8.10	N-acetylmuramoyl-L-alanine amidase
ORF30	29702	30148	-	148	17215.9	9.80	endonuclease
ORF31	30148	30852	-	234	26229.4	4.24	ssDNA-binding protein
ORF32	30922	31113	-	63	6972.6	4.93	bacterial RNA polymerase inhibitor
ORF33	31201	31374	-	57	6888.7	4.55	hypothetical protein
ORF34	31364	31657	-	97	11374.1	5.21	nucleotide kinase
ORF35	31657	31935	-	92	10188.1	11.30	hypothetical protein
ORF36	32108	33208	-	366	41577.2	4.68	DNA ligase
ORF37	33316	33588	-	90	10648.3	7.51	dGTP triphosphohydrolase inhibitor
ORF38	33588	33737	-	49	6078.8	11.37	hypothetical protein
ORF39	33829	36480	-	883	98990.8	7.32	RNA polymerase
ORF40	36554	37651	-	365	41750.0	7.61	putative protein kinase
ORF41	37673	37891	-	72	8446.1	11.76	hypothetical protein
ORF42	38113	38571	-	152	17040.3	6.74	putative S-adenosyl-L-methioninehydrolase
ORF43	38640	38984	-	114	13287.4	3.71	predicted antirestriction protein

YpP-G (Rashid et al., 2012), *Yersinia* phage Berlin and *Yersinia* phage Yep-phi (Zhao et al., 2011) (**Figure 4**). Except for *Escherichia* phage vB EcoP S523, *Salmonella* phage BSP161, *Salmonella* phage BP12A, and *Yersinia* phage PYPS50, all the other 11 related phages are known T7-like phages. To further explore the evolutionary position of vB_ShiP-A7, a phylogenetic analysis was performed with MEGA using the neighbor-joining method for the genomes of phage T7, phage vB_ShiP-A7, and its related 15 different phages. The phylogenetic tree based on the whole genomes of these phages shows 2 major branches (**Figure 4**). vB_ShiP-A7 is closely related to phages *Escherichia* phage P483, *Escherichia* phage vB EcoP S523, *Yersinia* phage PYPS50, and *Salmonella* phage BSP161 (**Figure 4**). We also built a phylogenetic tree based on one of the conserved proteins (major capsid protein) of these phages. The result suggested that phage vB_ShiP-A7 is most closely related to *Pectobacterium* phage PP74 and *Escherichia* phage P694 and is relatively close to phage T7 (**Supplementary Figure 2**). In addition, the genome organization

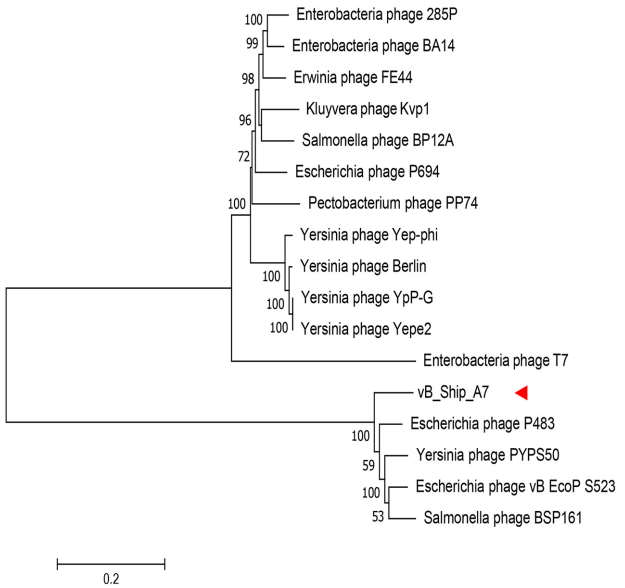

FIGURE 4 | Phylogenetic tree based on the whole genome sequence of vB_ShiP-A7 and its related phages. After comparing the genome sequences of these phages using the ClustalW program, a phylogenetic tree was generated using the neighbour-joining method with 1000 bootstrap replicates.vB_ShiP-A7 was marked by a red arrow.

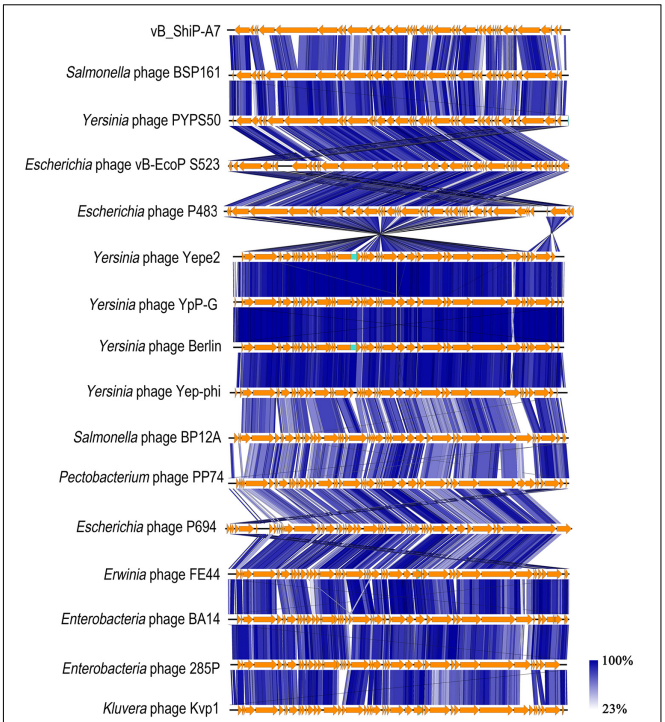

FIGURE 5 | Schematic genomic alignment of phage vB_ShiP-A7 with its related phages. Homologous ORFs or genes are present in brown, and amino acid identities of different proteins are indicated by different shades of blue.

of vB_ShiP-A7 follows that of the T7-like phages. The genomic information indicates that phage vB_ShiP-A7 is a novel member of the unclassified T7-like phages. Currently, this group of phages is highly variable. vB_ShiP-A7 and its related phages are isolated from different places in the world, and they can infect different species of bacteria, suggesting that the evolutionary relationships among these phages are complicated.

The DTRs of vB_ShiP-A7 are very similar to the DTRs of Berlin, Yepe2, Yep-phi, and Kvp1 (Lingohr et al., 2008; Zhao et al., 2011; Chen et al., 2016). The diversity of packaging mechanisms of phages, leading to various types of DNA termini, i.e., 5′cos (Lambda), 3′cos (HK97), pac (P1), headful without a pac site (T4), DTR (T7), and host fragment (Mu), has been described (Garneau et al., 2017). The vB_ShiP-A7 genome has DTRs of 177 bp, and similar DTRs were also found in its genetic relatives and the T7 phage, indicating that phage vB_ShiP-A7 uses a similar packaging mechanism as in the T7 phage.

We compared proteins encoded by phage vB_ShiP-A7 with that of its 15 related phages using EasyFig. Most of the proteins encoded by vB_ShiP-A7 and its 15 related phages are highly similar (**Figure 5**). Several dissimilar proteins among the genomes of these phages are shown as colorless or in light colors in **Figure 5**. DNA ligase encoded by ORF36 of vB_ShiP-A7 shows divergence with related phages (100% coverage, 65%–74% identity). The tail assembly protein encoded by ORF15 of vB_ShiP-A7 is very different from the homologous proteins of the other related phages (45%–96% coverage and 57%–89% identity). The tail fiber protein encoded by ORF5 of vB_ShiP-A7 also has a relatively low homology with that of its related phages (37%–46% coverage and 54%–60% identity) (**Figure 5**). The similarity of the tail fiber protein of vB_ShiP-A7 with other homologs is only found at the N-terminus, which is associated with the tail structure (Lingohr et al., 2008). The C-terminus of this tail fiber protein of vB_ShiP-A7, involved in ligand interactions, exhibits relatively large variability from tail fiber proteins of related phages (**Figure 5**). We built a phylogenetic tree based on the tail fiber proteins of different phages (**Supplementary Figure 3**). The tail fiber protein of this phage is most similar to that of *Yersinia* phage VB_YenP-AP5 and *Serratia* phage 2050H2, and it is relatively close to the tail fiber protein of *Escherichia* phage P694. The variation in tail fiber protein is relatively large, and it is very different from the major capsid protein in evolution.

Structural Proteins of vB_ShiP-A7

Purified phage vB_ShiP-A7 particles were denatured and separated using SDS-PAGE. At least six distinct protein bands were shown in the silver-stained SDS-PAGE gel, which were speculated to be structural proteins of vB_ShiP-A7 by their estimated molecular weights (internal virion protein D, internal core protein, tail fiber protein, head-to-tail joining protein, major capsid protein, capsid, and scaffold protein) (**Figure 6**). To further confirm these structural proteins, the proteins of the phage particles were analyzed using mass spectrometry (**Table 3**). A total of 18 proteins were identified, including all the proteins shown on the SDS-PAGE gels (**Table 3**, **Figure 6**). Nine of them are known structural proteins, and DNA primase/helicase was also identified in the phage particles. In

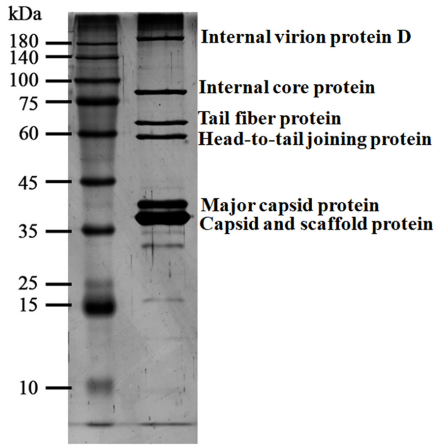

FIGURE 6 | Particle proteins of vB_ShiP-A7 separated by SDS-PAGE gel. The purified vB_ShiP-A7 particles were separated by SDS-PAGE and stained with silver. The six bands from top to bottom corresponding to different particle proteins of vB_ShiP-A7 are internal virion protein D, internal core protein, tail fiber protein, head-to-tail joining protein, major capsid protein, capsid, and scaffold protein. Protein molecular mass markers are indicated on the far left.

addition, some hypothetical proteins (ORF17, ORF18, A7_225, A7_120, A7_146, A7_426, A7_68, and A7_88) were detected using mass spectrometry, but their functions need to be determined further. The hypothetical proteins encoded by A7_225, A7_120, A7_146, A7_426, A7_68, and A7_88 were only found when we used all of the possible ORFs predicted with Artemis in the genome of vB_ShiP-A7 as a reference. However, they were omitted from the annotation file of vB_ShiP-A7 (uploaded to NCBI under assigned number MK685668) since they do not have similar sequences to any predicted proteins at NCBI (see text footnote 1) or these ORFs may exist in the interior of known genes. Interestingly, some of these peptides (A7_225, A7_120, A7_146, A7_68, and A7_88) were encoded by antisense RNAs on known genes of the late operon of vB_ShiP-A7 (**Table 3**). In addition, proteins that were similar to the known toxic proteins through a comparative analysis were not identified *via* mass spectrometry in vB_ShiP-A7 particles.

The Ability of vB_ShiP-A7 to Destroy Bacterial Biofilms

Biofilm removal is the key to treating chronic infectious diseases. We tested the effects of phage vB_ShiP-A7 on biofilms formed by *S. flexneri* A7 and *E. coli* 395B5. Approximately 24 h after the addition of 100 μL of phage vB_ShiP-A7 (10^9 PFU/mL), the log reduction in biofilm biomasses of strains *S. flexneri* A7 and *E. coli* 395B5 due to phage treatment is shown in **Figure 7A**, indicating that this phage could inhibit biofilm formation. The biofilm formation on the surface of the plate wells of strains *S. flexneri* A7 and *E. coli* 395B5 in the phage-treated samples was significantly lesser than that of the untreated controls (**Figure 7B**). This result suggests that vB_ShiP-A7 can reduce biofilm formation on clinical strains of *S. flexneri* A7 and *E. coli* 395B5, indicating the possibility of using phage vB_ShiP-A7 as a biofilm disruption agent.

vB_ShiP-A7 Administration Significantly Reduces *S. flexneri* A7 Colonization

The mouse infection model results showed that the mice developed diarrhea symptoms on the first day after infection with *Shigella*. Three days after infection, the weight of the mice in the "*Shigella* infection group" was lower than that of the "control group," which was consistent with the time of diarrhea symptoms. Phage vB_ShiP-A7 ("phage group") had no effect on the health of the mice (**Figure 8A**). Compared with the "control group," the weight of the mice in the "*Shigella* infection plus phage treatment group" had no significant change, indicating that phage vB_ShiP-A7 had a protective effect on *Shigella* infection in mice (**Figure 8A**).Next, 10^{11} purified vB_ShiP-A7 particles were added to drinking water to treat *Shigella* infection in mice. By counting the number of bacteria, we observed that the number of *Shigella* cells in the feces of the "*Shigella* infection plus phage treatment group mice" was significantly (3–10 folds) reduced compared to that in the "*Shigella* infection group"(**Figure 8B**), suggesting that the phage had a certain bactericidal effect on mice *in vivo*.

DISCUSSION

Shigella spp. and *E. coli* belong to the family *Enterobacteriaceae*, which can cause intestinal infections (The et al., 2016). Previous studies have demonstrated that bacteriophages can be used to treat these infections (Soffer et al., 2017; Tomat et al., 2018). In this study, a new lytic phage, vB_ShiP-A7, was isolated and characterized, with lytic activity against several MDR clinical strains of both *S. flexneri* and *E. coli* (**Table 1**). Several phages have been reported to have the ability to infect both *E. coli* and *Shigella* (Chang and Kim, 2011; Lee et al., 2016; Sváb et al., 2019). Since *E. coli* and *Shigella* are genetically similar, it is reasonable to expect some similar phages to target both strains. However, not all phages can lyse *Shigella* and *E. coli* at the same time. Phage SSE1 against *S. dysenteriae* has the highest identity with *Escherichia* phage ST0, but it cannot infect *E. coli* ST100 strains (Lu et al., 2020). Lytic phages are relatively specific and usually infect a subgroup of strains within one bacterial species or across closely related species, which causes less disruption to the gut flora than antibiotic treatment (Zhang et al., 2013). Phage vB_ShiP-A7 can infect some specific strains of *S. flexneri* and *E. coli* (**Table 1**). The EOPs of this phage for all the test strains are shown in the last column of **Table 1**, indicating that the phage can infect and lyse some serotypes of *S. flexneri* clinical strains more efficiently than *E. coli* clinical strains. However, phage vB_ShiP-A7 does not recognize the wild-type *E. coli* strain MG1655.

Phage vB_ShiP-A7 belongs to the family *Podoviridae*, based on its morphology under an electron microscope (**Figure 1**). vB_ShiP-A7 has a large burst size, suggesting that the concentration of bacteriophage vB_ShiP-A7 increased rapidly and effectively lysed bacteria (Nilsson, 2014). Next-generation sequencing demonstrated that the genome of phage vB_ShiP-A7

TABLE 3 | Phage vB_ShiP-A7 particle proteins identified in mass spectrometry.

First protein	Unique peptides	Unique sequence coverage [%]	Mol. weight [kDa]	Sequence length	Start	End	Location
ORF6	111	72.9	179.52	1644	10546	10546	ORF6
ORF7	56	69.7	85.783	760	12852	12852	ORF7
ORF12	34	92.6	37.502	351	18188	18188	ORF12
ORF14	25	56.6	58.744	535	20902	20902	ORF14
ORF13	15	42.5	33.488	306	19220	19220	ORF13
ORF8	11	65.2	22.545	207	13449	13449	ORF8
ORF15	7	66	10.875	106	21218	21218	ORF15
ORF17	4	51.1	9.8971	92	21904	21904	ORF17
A7_225	3	25.4	7.7616	67	29770	29970	Antisense of ORF30
A7_120	2	28.1	10.122	89	16521	16787	Antisense of ORF11
A7_146	2	39	6.5657	59	19923	20099	Antisense of ORF14
ORF27	2	5.3	64.9	582	28985	27273	ORF27
ORF18	2	43.9	9.2674	82	22159	21914	ORF18
A7_426	2	46.7	3.5044	30	19069	18980	Antisense of ORF13
ORF11	2	18.4	21.97	196	16955	16365	ORF11
ORF5	2	4.7	68.075	621	5540	3675	ORF5
	2	93	4.7304	43	9639	9767	Antisense of ORF6
A7_88	2	34.8	7.6992	69	11963	12169	Antisense of ORF7

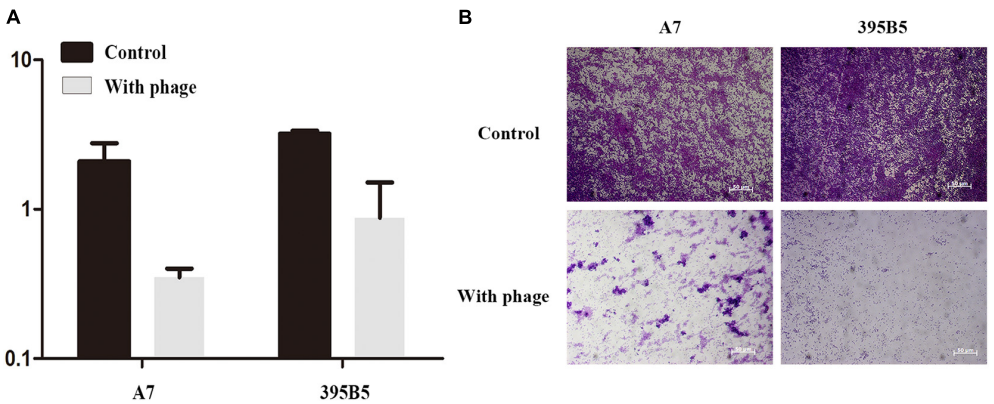

FIGURE 7 | Crystal violet assay showing the biofilm biomass of *Shiglla flexneri* A7 and *E. coli*395B5 grown in the presence or absence of phage vB_ShiP-A7. **(A)** We measured optical density readings in replicates to evaluate the inhibition of biofilm by phage vB_ShiP-A7. **(B)** The 2 above pictures are *Shiglla flexneri* A7 strain and *E. coli* 395B5 strain without phage; The bottom 2 pictures are *Shiglla flexneri* A7 and *E. coli* 395B5 exposured to phage vB_ShiP-A7.

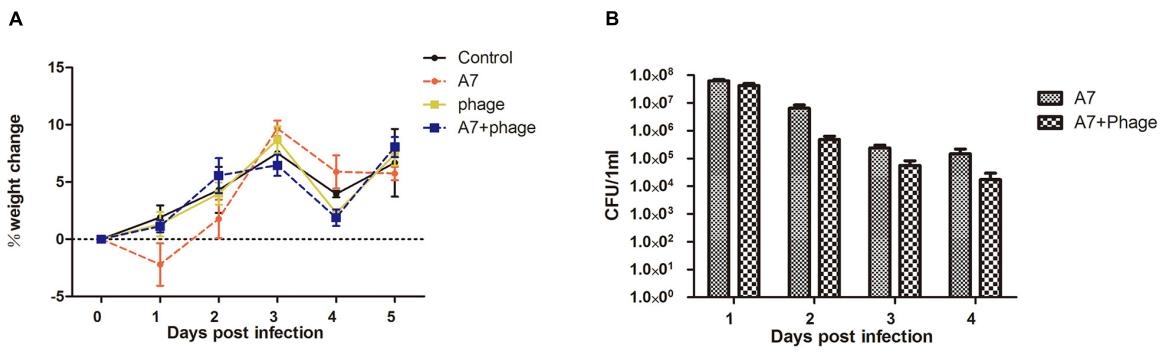

FIGURE 8 | Inhibitory effect of phage vB_ShiP-A7 on *Shiglla flexneri* A7 infection in mice. **(A)** Changes of body weight of mice in different treatment groups, Control (control group), A7 (*Shiglla flexneri* A7infection group), phage (phagevB_ShiP-A7 group), and A7+phage (*Shiglla flexneri* A7 infection plus phage vB_ShiP-A7 treatment group). **(B)** Killing effect of the phage on *Shiglla flexneri* A7 in mice at different days after infection, A7 (*Shiglla flexneri* A7infection group) and A7+phage (*Shiglla flexneri* A7 infection plus phage vB_ShiP-A7 treatment group).

does not encode integrases, recombinases, or harmful gene products (**Table 2**, **Figure 3**). In addition, phage vB_ShiP-A7 showed promising effects against bacterial growth in liquid and biofilm (**Figures 2**, **6**), suggesting that it may be used as an anti-infective agent.

The general genome organization of phage vB_ShiP-A7 is similar to that of T7-like phages, which encode RNA polymerase. Comparative genomic analysis demonstrated that phage vB_ShiP-A7 is highly similar to 15 related phages, among which 11 phages are unclassified T7-like phages (**Figures 4**, **5**). The three considerably different phylogenetic trees based on whole-genome sequences of phages, major capsid proteins, and tail fiber proteins suggest that phage vB_ShiP-A7 is closely related to T7-like phages (**Figure 4**, **Supplementary Figures 2, 3**). Therefore, this phage can be assigned as a novel virulent phage of the T7-like family. Several proteins of this phage are different from those of other phages, especially the tail fiber protein (**Figure 5**, **Supplementary Figure 3**). The tail protein of phages is the key protein that recognizes host bacteria. Different tail proteins of phages can cause phages to infect different host bacteria (Steven et al., 1988). Yosef et al. (2017) reported that a small change in the tail protein sequence of a phage can lead to changes in the host range. The different C-terminus of the tail fiber protein of vB_ShiP-A7, involved in ligand interactions, may allow this phage to infect some specific hosts. The phage could be used as a component of a phage cocktail. Most of the genes of vB_ShiP-A7 and the 15 related phages are highly homologous. High homology of the same functional phage genes was found in different phage species, indicating that horizontal gene transfer between phages is a component of evolution (Chen et al., 2016; Yosef et al., 2017). The gene arrangement of phage vB_ShiP-A7 is different from that of its related phages (**Figure 5**). Gene rearrangement was also observed in other *Escherichia* phages (Xu et al., 2018). vB_ShiP-A7 and its relatives may have evolved through horizontal exchange and rearrangement of their genes, which is a common phenomenon in the evolution of tailed phages (Zhao et al., 2011; Dekel-Bird et al., 2013; Chen et al., 2016).

Eighteen proteins were identified in vB_ShiP-A7 phage particles using mass spectrometry, including known structural proteins and hypothetical proteins (**Table 3**, **Figure 6**). Interestingly, some of these hypothetical proteins were encoded by antisense RNA on late operon-encoded structure proteins (A7_225, A7_120, A7_146, A7_68, and A7_88) (**Table 3**). Anne et al. found that PAK_P3 expressed antisense RNA elements targeting its structural region during the early stage of infection (Chevallereau et al., 2016), which might be used to shut down the expression of late structural genes during the early stage of infection. An antisense RNA was also found in the lambda phage genome, which was transcribed from the paQ promoter and did not encode proteins or peptides (Nejman-Faleńczyk et al., 2015). We found several small peptides/proteins encoded by antisense RNAs in *E. coli* phage vB_EcoP-EG1 (Gu et al., 2019). These small peptides/proteins encoded by antisense RNAs in the late operon may exist in different phages and are involved in phage infection processes, and their detailed functions remain to be determined.

In terms of controlling bacterial food source pollution, some bacteriophage products have been certified by FDA, such as ListShield^{TM}, EcoShield^{TM}, and SalmoFresh^{TM} (Tang et al., 2019). Currently, ShigaShield^{TM} against *Shigella* is undergoing FDA and USDA reviews for their safety (Soffer et al., 2017). There is no mature commercial phage for the treatment of *Shigella dysentery* (Tang et al., 2019). A large number of *Shigella* phages with clear properties are needed for the preparation of phage cocktails with clinical application value. Before a new phage is used in human infection treatment, its safety, antibacterial effect, phage pharmacology, and infection kinetics must be tested in animal models, which will improve our understanding of the pharmacology, immunology, safety, and potential for bacterial resistance (Romero-Calle et al., 2019). *Shigella* spp. infection in mice cannot completely simulate human dysentery (Mai et al., 2015), but it can still give us some useful information on evaluation of phage lysis efficiency against *Shigella* and the toxicity of phages *in vivo*. We found that *Shigella* only caused transient diarrhea in mice. Phage vB_ShiP-A7 treatment reduced the number of *Shigella* cells in the intestines of these mice, and the mice in the phage treatment group neither suffered transient diarrhea nor experienced weight loss. The results showed that phage vB_ShiP-A7 had a therapeutic effect on mice infected with MDR *Shigella*, and no adverse reactions were observed. The phage may be used to treat infections caused by drug-resistant *Shigella* spp. Animal infection models can provide reference data for phage therapy, but the frequency and duration of phage treatment, route of administration, and optimal dose need to be verified through preclinical trials (Wittebole et al., 2014). Thus, vB_ShiP-A7 can be used to treat human infectious diseases only after human preclinical trials.

CONCLUSION

In this study, a novel phage, vB_ShiP-A7, was isolated and fully characterized. The phage was stable and could rapidly lyse its host bacteria. The phage genome lays a foundation for studying the interaction between phages and their hosts. Comparative genomic analysis of this phage with related phages sheds light on the mechanisms of evolutionary changes in these T7-like family phage genomes. *In vitro* and *in vivo* experiments showed that the phage could effectively control the number of drug-resistant bacteria. Given bacteriophages have been utilising gradually in the food processing industry, or in human disease treatment (Tang et al., 2019), this phage we isolated and characterized may become an alternative treatment for infections caused by MDR *Shigella* and *Escherichia*, hence reducing the pressure to find new antibiotics.

DATA AVAILABILITY STATEMENT

The datasets presented in this study can be found in online repositories. The names of the repository/repositories and accession number(s) can be found below: https://www.ncbi.nlm.nih.gov/genbank/, MK685668.

ETHICS STATEMENT

The studies involving human participants were reviewed and approved by the ethical rules of Nanjing Medical University (Nanjing, China), The First Affiliated Hospital of Nanjing Medical University, and Jiangsu Provincial Center for Disease Control and Prevention (Nanjing, China), and informed consent was obtained from all patients. The patients/participants provided their written informed consent to participate in this study. The animal study was reviewed and approved by the ethical rules of Nanjing Medical University. Written informed consent was obtained from the individual(s) for the publication of any potentially identifiable images or data included in this article.

AUTHOR CONTRIBUTIONS

JX, RZ, XY, and XL conceived, designed, and coordinated the study. JX, RZ, and XY carried out the experimentation. JX and XL analyzed the data. GL, JX, XY, and XL contributed to the reagents, materials, and analysis tools. XZ helped to edit the manuscript. All authors read and approved the manuscript.

FUNDING

This work was supported by the National Natural Science Foundation of China (81501797 to XL and 31800156 to XY) and the Natural Science Foundation of Jiangsu Province (BK20171044 to XY). The role of the funders consisted of financial support for all experimental realizations.

ACKNOWLEDGMENTS

We appreciate the bioinformatics platforms (http://mjsull.github.io/Easyfig/files.html and http://www.sanger.ac.uk/science/tools/artemis) and stations (http://lowelab.ucsc.edu/tRNAscan-SE and http://www.cbs.dtu.dk/services/RNAmmer) for providing computing and storage resources.

SUPPLEMENTARY MATERIAL

The Supplementary Material for this article can be found online at: https://www.frontiersin.org/articles/10.3389/fmicb.2021.698962/full#supplementary-material

Supplementary Figure 1 | The terminal sequence of Phage vB_ShiP-A7 were determined by genomic digestion and sequencing.

Supplementary Figure 2 | Phylogenetic tree based on the major capsid proteins' sequence of vB_ShiP-A7 and its related phages.

Supplementary Figure 3 | Phylogenetic tree based on the tail fiber proteins' sequence of vB_ShiP-A7 and its related phages.

Supplementary Table 1 | We determined the adsorption rate of this phage.

REFERENCES

Aggarwal, G., and Ramaswamy, R. (2002). Ab initio gene identification: prokaryote genome annotation with GeneScan and GLIMMER. *J. Biosci.* 27, 7–14. doi: 10.1007/BF02703679

Ahmed, A. M., and Shimamoto, T. (2015). Molecular characterization of multidrug-resistant *Shigella* spp. of food origin. *Int. J. Food Microbiol.* 194, 78–82. doi: 10.1016/j.ijfoodmicro.2014.11.013

Bernasconi, O. J., Donà, V., Tinguely, R., and Endimiani, A. (2018). In vitro activity of 3 commercial bacteriophage cocktails against *salmonella* and *shigella* spp. isolates of human origin. *Pathog. Immun.* 3, 72–81. doi: 10.20411/pai.v3i1.234

Carver, T. J., Rutherford, K. M., Berriman, M., Rajandream, M. A., Barrell, B. G., and Parkhill, J. (2005). ACT: the artemis comparison tool. *Bioinformatics* 21, 3422–3423. doi: 10.1093/bioinformatics/bti553

Chang, H. W., and Kim, K. H. (2011). Comparative genomic analysis of bacteriophage EP23 infecting *Shigella* sonnei and *Escherichia coli*. *J. Microbiol.* 49, 927–934. doi: 10.1007/s12275-011-1577-0

Chen, M., Xu, J., Yao, H., Lu, C., and Zhang, W. (2016). Isolation, genome sequencing and functional analysis of two T7-like coliphages of avian pathogenic *Escherichia coli*. *Gene* 582, 47–58. doi: 10.1016/j.gene.2016.01.049

Chevallereau, A., Blasdel, B. G., De Smet, J., Monot, M., Zimmermann, M., Kogadeeva, M., et al. (2016). Next-generation "-omics" approaches reveal a massive alteration of host rna metabolism during bacteriophage infection of *Pseudomonas Aeruginosa*. *PLoS Genet.* 7:e1006134. doi: 10.1371/journal.pgen

D'Herelle, F. (1923). Autolysis and bacteriophages. *J. State Med.* 31, 461–466.

De Angelis, G., Del Giacomo, P., Posteraro, B., Sanguinetti, M., and Tumbarello, M. (2020). Molecular mechanisms, epidemiology, and clinical importance of β-lactam resistance in *Enterobacteriaceae*. *Int. J. Mol. Sci.* 21:5090. doi: 10.3390/ijms21145090

Dekel-Bird, N. P., Avrani, S., Sabehi, G., Pekarsky, I., Marston, M. F., Kirzner, S., et al. (2013). Diversity and evolutionary relationships of T7-like podoviruses infecting marine cyanobacteria. *Environ. Microbiol.* 15, 1476–1491. doi: 10.1111/1462-2920.12103

Doore, S. M., Schrad, J. R., Dean, W. F., Dover, J. A., and Parent, K. N. (2018). *Shigella* phages isolated during a dysentery outbreak reveal uncommon structures and broad species diversity. *J. Virol.* 92, e2117–e2117. doi: 10.1128/JVI.02117-17

Faidiuk, I. V., and Tovkach, E. I. (2014). Exclusion of polyvalent T7-like phages by prophage elements. *Mikrobiol Z.* 76, 42–50.

Garneau, J., Depardieu, F., Fortier, L., Bikard, D., and Monot, M. (2017). PhageTerm: a tool for fast and accurate determination of phage termini and packaging mechanism using next-generation sequencing data. *Sci. Rep.* 7:8292. doi: 10.1038/s41598-017-07910-5

Gu, Y., Xu, Y., Xu, J., Yu, X., Huang, X., Liu, G., et al. (2019). Identification of novel bacteriophage vB_EcoP-EG1 with lytic activity against planktonic and biofilm forms of uropathogenic *Escherichia coli*. *Appl. Microbiol. Biotechnol.* 103, 315–326. doi: 10.1007/s00253-018-9471-x

Jun, J. W., Kim, J. H., Shin, S. P., Han, J. E., Chai, J. Y., and Park, S. C. (2013). Characterization and complete genome sequence of the *Shigella* bacteriophage pSf-1. *Res. Microbiol.* 164, 979–986. doi: 10.1016/j.resmic.2013.08.007

Kabanova, A., Shneider, M., Bugaeva, E., Ha, V. T. N., Miroshnikov, K., Korzhenkov, A., et al. (2018). Genomic characteristics of vB_PpaP_PP74, a T7-like Autographivirinae bacteriophage infecting a potato pathogen of the newly proposed species *Pectobacterium parmentieri*. *Arch. Virol.* 163, 1691–1694. doi: 10.1007/s00705-018-3766-1

Kakasis, A., and Panitsa, G. (2019). Bacteriophage therapy as an alternative treatment for human infections. A comprehensive review. *Int. J. Antimicrob. Agents* 53, 16–21.

Kim, K. H., Chang, H. W., Nam, Y. D., Roh, S. W., and Bae, J. W. (2010). Phenotypic characterization and genomic analysis of the *Shigella* sonnei bacteriophage SP18. *J. Microbiol.* 48, 213–222. doi: 10.1007/s12275-010-0055-4

Klontz, K. C., and Singh, N. (2015). Treatment of drug-resistant *Shigella* infections. *Expert. Rev. Anti. Infect. Ther.* 13, 69–80. doi: 10.1586/14787210.2015.983902

Kortright, K. E., Chan, B. K., Koff, J. L., and Turner, P. E. (2019). Phage therapy: a renewed approach to combat antibiotic-resistant bacteria. *Cell Host Microbe* 25, 219–232. doi: 10.1016/j.chom.2019.01.014

Kotloff, K. L., Riddle, M. S., Platts-Mills, J. A., Pavlinac, P., and Zaidi, A. M. (2018). Shigellosis. *Lancet* 391, 801–812. doi: 10.1016/S0140-6736(17)33296-8

Kropinski, A. M., Prangishvili, D., and Lavigne, R. (2009). Position paper: the creation of a rational scheme for the nomenclature of viruses of Bacteria and Archaea. *Environ. Microbiol.* 11, 2775–2777. doi: 10.1111/j.1462-2920.2009.01970.x

Kutter, E. (2009). "Bacteriophage therapy: past and present," in *Encyclopedia of Microbiology*, ed. M. Schaecter (Oxford: Elsevier), 258–266.

Lee, H., Ku, H. J., Lee, D. H., Kim, Y. T., Shin, H., Ryu, S., et al. (2016). Characterization and genomic study of the novel bacteriophage HY01 infecting both *Escherichia coli* O157:H7 and *Shigella flexneri*: potential as a biocontrol agent in food. *PLoS One* 11:e0168985. doi: 10.1371/journal.pone.0168985

Lingohr, E. J., Villegas, A., She, Y. M., Ceyssens, P. J., and Kropinski, A. M. (2008). The genome and proteome of the Kluyvera bacteriophage Kvp1–another member of the T7-like Autographivirinae. *Virol. J.* 5:122. doi: 10.1186/1743-422X-5-122

Lu, H., Liu, H., Lu, M., Wang, J., Liu, X., and Liu, R. (2020). Isolation and Characterization of a Novel myovirus Infecting *Shigella* dysenteriae from the Aeration Tank Water. *Appl. Biochem. Biotechnol.* 192, 120–131. doi: 10.1007/s12010-020-03310-0

Mai, V., Ukhanova, M., Reinhard, M. K., Li, M., and Sulakvelidze, A. (2015). Bacteriophage administration significantly reduces *Shigella* colonization and shedding by *Shigella*-challenged mice without deleterious side effects and distortions in the gut microbiota. *Bacteriophage* 5:e1088124. doi: 10.1080/21597081.2015.1088124

Matsuzaki, S., Uchiyama, J., Takemura-Uchiyama, I., and Daibata, M. (2014). Perspective: the age of the phage. *Nature* 509:S9. doi: 10.1038/509S9a

Mertens, H., and Hausmann, R. (1982). Coliphage BA14: a new relative of phage T7. *J. Gen. Virol.* 62, 331–341. doi: 10.1099/0022-1317-62-2-331

Nejman-Faleńczyk, B., Bloch, S., Licznerska, K., Felczykowska, A., Dydecka, A., Wêgrzyn, A., et al. (2015). Small regulatory RNAs in lambdoid bacteriophages and phage-derived plasmids: Not only antisense. *Plasmid* 78, 71–78.

Nikolich, M. P., and Filippov, A. A. (2020). Bacteriophage therapy: developments and directions. *Antibiotics (Basel)* 9:135. doi: 10.3390/antibiotics9030135

Nilsson, A. S. (2014). Phage therapy–constraints and possibilities. *UPS J. Med. Sci.* 119, 192–198. doi: 10.3109/03009734.2014.902878

Rashid, M. H., Revazishvili, T., Dean, T., Butani, A., Verratti, K., Bishop-Lilly, K. A., et al. (2012). A Yersinia pestis-specific, lytic phage preparation significantly reduces viable *Y. pestis* on various hard surfaces experimentally contaminated with the bacterium. *Bacteriophage* 2, 168–177.

Romero-Calle, D., Guimarães Benevides, R., Góes-Neto, A., and Billington, C. (2019). Bacteriophages as alternatives to antibiotics in clinical care. *Antibiotics (Basel)* 8:138. doi: 10.3390/antibiotics8030138

Schofield, D. A., Wray, D. J., and Molineux, I. J. (2015). Isolation and development of bioluminescent reporter phages for bacterial dysentery. *Eur. J. Clin. Microbiol. Infect. Dis.* 34, 395–403. doi: 10.1007/s10096-014-2246-0

Shevchenko, A., Wilm, M., Vorm, O., and Mann, M. (1996). Mass spectrometric sequencing of proteins from silver-stained polyacrylamide gels. *Anal. Chem.* 68, 850–858.

Shiferaw, B., Solghan, S., Palmer, A., Joyce, K., Barzilay, E. J., Krueger, A., et al. (2012). Antimicrobial susceptibility patterns of *Shigella* isolates in foodborne diseases active surveillance network (FoodNet) sites, 2000-2010. *Clin. Infect. Dis.* 54,Suppl 5, S458–S463. doi: 10.1093/cid/cis230

Soffer, N., Woolston, J., Li, M., Das, C., and Sulakvelidze, A. (2017). Bacteriophage preparation lytic for *Shigella* significantly reduces *Shigella* sonnei contamination in various foods. *PLoS One* 12:e0175256. doi: 10.1371/journal.pone.0175256

Steven, A. C., Trus, B. L., Maizel, J., Unser, M., Parry, D. A., Wall, J. S., et al. (1988). Molecular substructure of a viral receptor-recognition protein. The gp17 tail-fiber of bacteriophage T7. *J. Mol. Biol.* 200, 351–365. doi: 10.1016/0022-2836(88)90246-X

Sullivan, M. J., Petty, N. K., and Beatson, S. A. (2011). Easyfig: a genome comparison visualizer. *Bioinformatics* 27, 1009–1010. doi: 10.1093/bioinformatics/btr039

Sun, Q., Lan, R., Wang, Y., Wang, J., Wang, Y., Li, P., et al. (2013). Isolation and genomic characterization of SfI, a serotype-converting bacteriophage of *Shigella* flexneri. *BMC Microbiol.* 13:39. doi: 10.1186/1471-2180-13-39

Sváb, D., Falgenhauer, L., Rohde, M., Chakraborty, T., and Tóth, I. (2019). Complete genome sequence of C130_2, a novel myovirus infecting pathogenic *Escherichia coli* and *Shigella* strains. *Arch. Virol.* 164, 321–324. doi: 10.1007/s00705-018-4042-0

Tang, S. S., Biswas, S. K., Tan, W. S., Saha, A. K., and Leo, B. F. (2019). Efficacy and potential of phage therapy against multidrug resistant *Shigella* spp. *PeerJ.* 7:e6225. doi: 10.7717/peerj.6225

The, H. C., Thanh, D. P., Holt, K. E., Thomson, N. R., and Baker, S. (2016). The genomic signatures of *Shigella* evolution, adaptation and geographical spread. *Nat. Rev. Microbiol.* 14, 235–250. doi: 10.1038/nrmicro.2016.10

Tomat, D., Casabonne, C., Aquili, V., Balagué, C., and Quiberoni, A. (2018). Evaluation of a novel cocktail of six lytic bacteriophages against Shiga toxin-producing Escherichia coli in broth, milk and meat. *Food Microbiol.* 76, 434–442. doi: 10.1016/j.fm.2018.07.006

Wittebole, X., De Roock, S., and Opal, S. M. (2014). A historical overview of bacteriophage therapy as an alternative to antibiotics for the treatment of bacterial pathogens. *Virulence* 5, 226–235. doi: 10.4161/viru.25991

Xu, Y., Yu, X., Gu, Y., Huang, X., Liu, G., and Liu, X. (2018). Characterization and genomic study of phage vB_EcoS-B2 infecting multidrug-resistant *Escherichia coli*. *Front. Microbiol.* 9:793. doi: 10.3389/fmicb.2018.00793

Yang, M., Du, C., Gong, P., Xia, F., Sun, C., Feng, X., et al. (2015). Therapeutic effect of the YH6 phage in a murine haemorrhagic pneumonia model. *Res. Microbiol.* 166, 633–643. doi: 10.1016/j.resmic.2015.07.008

Yosef, I., Goren, M. G., Globus, R., Molshanski-Mor, S., and Qimron, U. (2017). Extending the host range of bacteriophage particles for DNA transduction. *Mol. Cell* 66, 721–728. doi: 10.1016/j.molcel.2017.04.025

Yu, X., Xu, Y., Gu, Y., Zhu, Y., and Liu, X. (2017). Characterization and genomic study of "phiKMV-Like" phage PAXYB1 infecting *Pseudomonas aeruginosa*. *Sci. Rep.* 7:13068. doi: 10.1038/s41598-017-13363-7

Zhang, H., Wang, R., and Bao, H. (2013). Phage inactivation of foodborne *Shigella* on ready-to eat spiced chicken. *Poult. Sci.* 92, 211–217. doi: 10.3382/ps.2011-02037

Zhao, X., Wu, W., Qi, Z., Cui, Y., Yan, Y., Guo, Z., et al. (2011). The complete genome sequence and proteomics of Yersinia pestis phage Yep-phi. *J. Gen. Virol.* 92, 216–221. doi: 10.1099/vir.0.026328-0

Zurabov, F., and Zhilenkov, E. (2021). Characterization of four virulent *Klebsiella pneumoniae* bacteriophages, and evaluation of their potential use in complex phage preparation. *Virol. J.* 18:9. doi: 10.1186/s12985-020-01485-w

Conflict of Interest: The authors declare that the research was conducted in the absence of any commercial or financial relationships that could be construed as a potential conflict of interest.

Publisher's Note: All claims expressed in this article are solely those of the authors and do not necessarily represent those of their affiliated organizations, or those of the publisher, the editors and the reviewers. Any product that may be evaluated in this article, or claim that may be made by its manufacturer, is not guaranteed or endorsed by the publisher.

Advantages of publishing in Frontiers

OPEN ACCESS
Articles are free to read for greatest visibility and readership

FAST PUBLICATION
Around 90 days from submission to decision

HIGH QUALITY PEER-REVIEW
Rigorous, collaborative, and constructive peer-review

TRANSPARENT PEER-REVIEW
Editors and reviewers acknowledged by name on published articles

Frontiers
Avenue du Tribunal-Fédéral 34
1005 Lausanne | Switzerland

Visit us: www.frontiersin.org
Contact us: frontiersin.org/about/contact

REPRODUCIBILITY OF RESEARCH
Support open data and methods to enhance research reproducibility

DIGITAL PUBLISHING
Articles designed for optimal readership across devices

FOLLOW US
@frontiersin

IMPACT METRICS
Advanced article metrics track visibility across digital media

EXTENSIVE PROMOTION
Marketing and promotion of impactful research

LOOP RESEARCH NETWORK
Our network increases your article's readership